Identification of a microRNA therapy targeting sFlt-1 in preeclampsia

Milda Bartkeviciute-Grubliauskiene

Doctor of Philosophy

Aston University

February 2021

Identification of microRNA therapy targeting sFlt-1 in preeclampsia

Milda Bartkeviciute-Grubliauskiene
Aston University
Doctor of Philosophy
2021

Summary

Preeclampsia is a multifactorial disease of the pregnancy contributing to maternal and neonatal morbidity and mortality worldwide. Typically, preeclampsia is characterised by the onset of new hypertension at or after 20 weeks' gestation and can be accompanied by proteinuria and/or multiple organ failure. Despite decades of research, the only effective method to relieve preeclamptic symptoms is the removal of the placenta and the baby, which if not addressed in time, will progress to a potentially fatal end-stage disease - eclampsia with convulsion and eventual death.

Anti-angiogenic soluble vascular endothelial growth factor (VEGF) receptor-1 (sFlt-1)-dependent loss of VEGF activity has been linked with the pathogenesis of preeclampsia. Abnormally high levels of sFlt-1 detected in maternal circulation and the placenta in women with preeclampsia falls dramatically postpartum, highlighting placenta as the main source of maternal sFlt-1. The protective heme oxygenase-1 (HO-1) enzyme acts as an inhibitor of sFlt-1 with low expression found in preeclamptic placenta. The exact mechanism behind this negative regulation is unknown, however it has been suggested that restoration of HO-1 expression and/or activity in preeclampsia may offer a therapeutic approach to regulate sFlt-1.

MicroRNAs (miRNAs) are increasingly recognised as major gene regulators involved in pregnancy. We hypothesised that HO-1 regulates sFlt-1 via miRNA-dependent gene silencing. This could be employed as a strategy to treat abnormally high sFlt-1 levels associated with preeclampsia. We identified miR-122 to act downstream of HO-1 and inhibit sFlt-1 release in human endothelial cells. Adenovirus-mediated miR-122 overexpression in HO-1 compromised pregnant mice reduced maternal sFlt-1, improved fetal weight and inhibited the resorption rate without having any negative observational effects on the pregnancy.

Viral-based delivery is known to induce immune response. To minimise health risks associated with off-target miR-122 overexpression, we also employed targeted liposomes to deliver the miR-122. Liposomes have been shown to successfully encapsulate nucleic acids, provide stable protection against degradation and facilitate cellular uptake. To minimise off-target effects and deliver miR-122 specifically to placenta, we designed the CGKRK surface-modified neutral PC liposomes and loaded it with miR-122. Intravenous administration of the decorated liposomes provided efficient miR-122 delivery to the placenta and resulted in effective down-regulation of placental ischaemia-induced sFlt-1 and reduction in fetal death rate.

Based on these findings, exogenous miR-122 overexpression limits sFlt-1 release and improves poor fetal outcome in HO-1 compromised pregnancy. Surface functionalised liposomes present a novel therapeutic strategy to deliver miR-122 specifically to the placenta and limit sFlt-1 release observed in preeclampsia.

This thesis is dedicated to my late and beloved mother Rozita.

She was my inspiration, my strength, my everything.

I carry her loving memory in my heart with honour and hope she is proud of the woman and the scientist I have become.

Acknowledgements

Firstly, I would like to express my deepest gratitude to Dr Tim Watts, who believed in me and funded my PhD journey. I am also eternally grateful to Professor Asif Ahmed without whom I would never be where I am today. I am indebted to him for his mentorship, guidance and unconditional support that helped me to build my confidence and allowed me to prove to myself that I am capable of achieving great goals. I am truly thankful for the advice, supervision, encouragement and for the help with the thesis.

I would like to express my gratefulness to Dr Shakil Ahmad for his supervision and scientific guidance during my studies that allowed me to excel in my PhD. Also, I am grateful to Dr Keqing Wang for her continuous support and advice that helped me to stay on track and find solutions to scientific problems. I feel truly blessed to have been surrounded by world-class scientists that are my everyday inspiration and motivation.

Besides my mentors and supervisors, I would like to thank Dr Mandeep Marwah for her expertise in the liposome formulation as presented in Chapter 5. I am grateful for her dedication to the project and a life-long friendship that evolved over the many tireless hours spent together in the laboratory. Special thanks to Dr Jaimy Saif for the help and assistance with the *in vivo* experiments and Dr Meng Cai for the early support and introduction to the field of microRNAs.

I would like to express my appreciation to my fellow PhD colleagues Sophie, May, Hala, Lorena, Yolanda, Re Ea, Sarah and Alina for their help, support and friendship that made my PhD journey so much more interesting and fun. Countless hours of conversations, scientific problem solving, laughter and unforgettable adventures allowed me to grow as person and a scientist.

I will always be grateful to my father Vytas, who gave me the strength in the moments of weakness, believed in me unconditionally and encouraged me to never give up. Also, I am thankful to my sister Inga, niece Urte and the rest of the family for continuous emotional support and motivation.

Finally, a million thanks to my lovely husband Aidas, who stood by me every single step of the way, who patiently listened and cared for me as well as cheered me up on the sad or happy days.

Table of Contents

List of abbreviations

λex	Excitation wavelength
λem	Emission wavelength
6-FAM	6-carboxyfluorescein (CF)
ACOG	American College of Obstetricians and Gynecologists
Ad	Adenovirus
AF	Amniotic Fluid
AGO	Argonaute
ANOVA	Analysis of Variance
BMI	Body Mass Index
BSA	Bovine Serum Albumin
C12E8	Octaethylene glycol monododecyl ether
Cat. #	Catalogue number
CMV	Cytomegalovirus
cDNA	Complementary Deoxyribonucleic Acid
CO	Carbon monoxide
COX	Cyclooxygenase
C_T	Cycle Threshold
CVD	Cardiovascular Disease
DAPI	4',6-diamidino-2-phenylindole
DBP	Diastolic Blood Pressure
DGCR8	DiGeorge syndrome chromosomal [or critical] region 8
DLS	Dynamic Light Scattering
DMSO	Dimethyl sulfoxide
DNA	Deoxyribonucleic Acid
dNTPs	deoxyribonucleotide triphosphate
DOTAP	1,2-dioleoyl-3-trimethylammonium-propane
DSPE	1, 2-Distearoyl-sn-glycero-3-phosphoethanolamine
E	Embryonic day
E	Efficiency
EDTA	Ethylenediaminetetraacetic Acid
EDVs	EnGeneIC Delivery Vehicles
EGFR	Epidermal Growth Factor Receptor
EGM	Endothelial Growth Media
ELISA	Enzyme Linked Immunosorbent Assay
EphA2	Ephrin type-A receptor 2
EVT	Extravillous Trophoblasts
FACS	Fluorescence activated Cell Sorting
FBS	Fetal Bovine serum
FDA	Food and Drug Administration
Flt-1	Fms-like tyrosine kinase -1 (VEGFR-1)
GFP	Green Fluorescent Protein
GWAS	Genome Wide Association Studies
HCV	Hepatitis C Virus

HELLP	Hemolysis, Elevated Liver enzymes and Low Platelet count
HET	Heterozygous
HO-1, 2, 3	Heme Oxygenase 1, 2
HPMA	N-(2-hydroxypropylmethacrylamide)
HRP	Horseradish peroxidase
hsp	Heat Shock Protein
HUVECs	Human Umbilical Vein Endothelial Cells
IGF-1, -2	Insulin Growth Factor -1, -2
IL-1β	Interleukin -1 beta
IL-10	Interleukin -10
IP	Intraperitoneal
ISSHP	International Society for the Study of Hypertension in Pregnancy
IUGR	Intra-uterine Growth Restriction
IV	Intravenous
kDa	Kilodalton
KDR/Flk-1	Kinase insert domain receptor/ Fetal Liver Kinase -1 (VEGFR-2)
KO	Knockout
LNA	Locked Nucleic Acid
LNP	Lipid Nanoparticles
LPH	Lipid-Polymer Hybrid
$MgCl_2$	Magnesium Chloride
$MgSO_4$	Magnesium sulfate
MicroRNA	Micro Ribonucleic Acid (miRNA)
MOI	Multiplicity of Infection
mRNA	Messenger Ribonucleic Acid
MTT	3-(4,5-dimethylthiazol-2-yl)-2,5-diphenyl tetrazolium bromide
MWCO	Molecular Weight Cut Off
NC3RS	National Centre for the Replacement, Refinement & Reduction
NO	Nitric Oxide
NOS	Nitric Oxide Synthase
OD	Optical Density
PBS	Phosphate Buffered Saline
PCR	Polymerase Chain Reaction
PC	Phosphatidylcholine
PDGF	Platelet-derived Growth Factor
PEG	Poly(ethylene glycol)
PEI	Polyethylenimine
PFU	Plaque forming Unit
PGE	Prostaglandin E
PI	Polydispersity
PlGF	Placenta Growth Factor
PLAC1	Placenta Enriched 1
PLGA	Poly(lactic-co-glycolic acid)
PNA	Peptide Nucleic Acid
Pol II	Polymerase II
PPARγ	Peroxisome proliferator-activated receptor gamma
pre-mRNA	Precursor Messenger Ribonucleic Acid
pre-miRNA	Precursor Micro Ribonucleic Acid

pri-miRNA	Primary Micro Ribonucleic Acid
RD	Reagent Diluent
RIPA buffer	Radioimmunoprecipitation Assay Buffer
RISC	RNA-induced silencing complex
RNA	Ribonucleic Acid
RNase III	Ribonuclease III
RNU6	Ribonucleic Acid, U6 Small Nuclear
RNU44	Ribonucleic Acid, U6 Small Nuclear (SNORD44)
RNU48	Ribonucleic Acid, U48 Small Nuclear (SNORD48)
ROS	Reactive oxygen species
ROUT	Robust regression and outlier removal
RPM	Rotation Per Minute
RT-qPCR	Real Time Quantitative Polymerase Chain Reaction
RUPP	Reduced Uterine Perfusion Pressure
SBP	Systolic Blood Pressure
SDS-PAGE	Sodium Dodecyl Sulfate Polyacrylamide Gel Electrophoresis
SEM	Standard Error of the Mean
sFlt-1	Soluble fms-like tyrosine kinase -1
sFlt1-e15a	Soluble fms-like tyrosine kinase 1 -exon 15a
sFlt1-i13	Soluble fms-like tyrosine kinase 1 -intron 13
siRNA	Silencing Ribonucleic Acid
SNP	Single Nucleotide Polymorphisms
SOD	Superoxide dismutase
StAmP	Statins to Ameliorate early-onset Pre-eclampsia
T	Thymine
TAMRA	Carboxytetramethylrhodamine
TB	Trypan Blue
TBS	Tris Buffered Saline
TBS-T	Tris Buffered Saline with Tween
TNF-α	Tumour Necrosis Factor -alpha
TOP-1	Topoisomerase -1
U	Uracil
UAB	University of Alabama
UK	United Kingdom
UTR	Untranslated region
VAR2CSA	Variant surface antigen 2-CSA
VEGF	Vascular Endothelial Growth Factor
VEGFR-1	Vascular Endothelial Growth Factor -1 (Flt-1)
VEGFR-2	Vascular Endothelial Growth Factor -2 (KDR/Flk-1)
WGA	Wheat Germ Agglutinin
WHO	World Health Organisation
WT	Wild-type
YWHAZ	14-3-3 Protein Zeta/Delta

List of figures

Chapter 1

Chapter 2

Chapter 3

Chapter 4

Chapter 5

Appendix

List of tables

Chapter 1

Chapter 3

Chapter 5

List of Equations

Chapter 3

Chapter 1

Introduction

1.1 Preeclampsia

Preeclampsia is a major contributor to the maternal and neonatal mortality and morbidity. It is one of the leading causes of preterm birth and significant maternal morbidity (Tang et al., 1997), affecting 5% to 7% of pregnant women worldwide (preeclampsia.org). This means that over half a million women die each year from pregnancy-related causes. Sadly, 99% of these deaths occur in developing countries (Huppertz, 2008, MacKay et al., 2001, World Health Organisation, 2005). There is no definite treatment to prevent, treat or cure preeclampsia. Induced preterm delivery of the fetus and placenta is the only solution of preventing life-threatening complications (Brown et al., 2018a, National Guideline, 2019, National Collaborating Centre for and Children's, 2010). If the solution is not addressed in time, mother acquires enhanced risk to develop eclampsia with the onset of seizures, HELLP syndrome (Hemeolysis, Elevated Liver enzymes and Low Platelet count), multiple systemic organ failure, aspiration pneumonia, cerebral haemorrhage, coma and finally cardiac arrest (Uzan et al., 2011).

Systematic review identified that 12% of maternal deaths are attributed to eclampsia globally (Khan et al., 2006) and 1 in 50 of the women who have eclampsia in the UK die (World Health Organisation, 1988, Duley, 1992, Douglas and Redman, 1994, Kullberg et al., 2002, Duley, 2009). Moreover, pregnant women who were affected by preeclampsia/eclampsia at some point in their lives, are subjected to increased risk for cardiovascular related diseases (CVD) including 4-fold increased risk of hypertension, 2-fold increased risk of fatal and nonfatal ischemic heart disease, cerebrovascular and peripheral arterial diseases, stroke, and venous thromboembolism, which result in early mortality rates (Bellamy et al., 2007). A systematic review estimated that women with a history of more severe preeclampsia, particularly those who experienced preterm delivery, poor fetal growth, or fetal death possess a higher risk of CVD in “dose-dependent” manner (McDonald et al., 2008).

1.2 Clinical symptoms of preeclampsia

According to International Society for the Study of Hypertension in Pregnancy (ISSHP) guidelines, preeclampsia is characterised by the onset of gestational hypertension (BP ≥140 mmHg systolic or ≥90 mmHg diastolic) at or after 20 weeks' gestation and accompanied by ≥1 of the following new-onset conditions including proteinuria and/or acute kidney injury, liver failure, neurological complications, haematological complications, uteroplacental dysfunction and intrauterine fetal growth restriction (IUGR) (Brown et al., 2018a, National Guideline, 2019, National Collaborating Centre for and Children's, 2010, Tranquilli et al., 2013, 2014).

Early onset preeclampsia differs phenotypically from preeclampsia occurring at term depending on the adaptation of maternal cardiovascular development. Early onset preeclampsia, defined as <34 weeks of gestation, appears to be more frequent in patients with lower high body mass (BMI) and with bilateral notching of the uterine artery, whereas late-onset preeclampsia (>34 weeks of gestation) is more frequent in patients with higher BMI index and low total vascular resistance (Valensise et al., 2008).

Despite many years of interest and ongoing research, the only effective method to relieve preeclamptic symptoms to date is the removal of the baby and the placenta. Depending on the severity of the preeclamptic features and gestational age, preeclamptic patients are closely monitored and receive extensive management of the symptoms until the progression of the pregnancy becomes a risk to maternal and fetal status, which is usually followed by the premature delivery induction (Brown et al., 2001, Phipps et al., 2019).

1.3 Pathology of preeclampsia disease

1.3.1 "Disease of theories"

Despite great scientific advances, preeclampsia is still defined as a "disease of theories". It reflects the unknown aetiology and a great confusion between the cause and consequence. Generally, preeclampsia is characterised by the widespread endothelial dysfunction, systemic inflammation and impaired placental development

(Ramma and Ahmed, 2011, Ahmed and Ramma, 2015a). Insufficient placental development including abnormal spiral artery remodelling, placental hypoxia, oxidative stress, impaired angiogenesis and insufficient placental perfusion contribute to the development of preeclampsia (Ahmed and Ramma, 2015a, Young et al., 2010, Ramma and Ahmed, 2011). Many of these attributes have been proposed as a cause of preeclampsia, however neither of the theories *per se* are sufficient to generate preeclampsia and therefore do not fit the Bradford Hill causation criteria (Table 1.1) (Lyall et al., 2013, Ahmed et al., 2016). In addition, characteristics of preeclampsia are non-specific and defined to more than one disease (Brown et al., 2001, Huppertz, 2008). In 1991, a two-stage theory has been proposed by Redman (1991). Stage one was defined by the hypoxic stress and damage within the developing placenta, which is caused by inefficient utero–placental circulation. Factors released by damaged placenta enter maternal circulation where they sensitise maternal endothelium causing widespread endothelial dysfunction and inflammation. This pathological process leads to clinical manifestation of the preeclampsia disease and was defined as stage two (Redman, 1991). However, the theory remains unconfirmed.

Table 1. 1. Bradford-Hill causation criteria.

Criterion	Explanation
Temporality	The cause always precedes the effect
Dose response	An increase in exposure results in an increase in the risk
Strength	The stronger the association, the more likely it is that there is a causal relationship between the associated factors
Consistency	The results can be replicated by different people or in different studies
Specificity	A single cause will result in a specific effect
Coherence	There must be coherence between the epidemiology and the experimental findings
Plausibility	The cause can be linked to the effect through a plausible mechanism

1.3.2 Placenta contribution to clinical preeclampsia symptoms

It was thought that, systematic symptoms and tragic complications of preeclampsia are caused by the mother being immunocompromised to the fetus (Huppertz, 2008). Also, it was proposed in 1996 that, the maternal immunologic response of hypertensive disorder of pregnancy can be caused by the antigen presented in sperm (Robillard et al., 1994). The response may be reduced by prolonged exposure to paternal antigen, which might explain why women that already experienced successful pregnancy are at lower risk for developing preeclampsia than women on their first pregnancy (Trupin et al., 1996, Tubbergen et al., 1999). However, based on the evidence, it is now widely accepted that placenta has a major role in the development of preeclampsia. In a case of extrauterine pregnancy, which later developed into preeclampsia, delivery of the fetus alone was not sufficient and the symptoms persisted until the placenta was removed (Piering et al., 1993). Furthermore, cases of postpartum preeclampsia have been associated with retained placental fragments and sudden improvement after uterine curettage (Young et al., 2010). Serum from women with hydatidiform moles (in which fetus is absent) and preeclampsia patients had a negative correlation between anti- and pro-angiogenic factors concentrations when compared to matched control pregnant patients. The condition improved after the curettage and removal of the mole (Koga et al., 2010). Thus, placenta is a central target in preeclampsia, responsible for the symptoms and disease-related complications.

1.3.3 Risks associated with preeclampsia development

Several pre-existing maternal characteristics have been shown to increase the risk of developing preeclampsia by rendering the maternal endothelium more sensitive to the circulating placenta-derived components (Roberts and Cooper, 2001), including previous history of preeclampsia, family history of preeclampsia, nulliparity, advanced maternal age, high BMI, multiple (twin) pregnancy, obesity, renal disease, pre-existing

diabetes, underlying hypertension, autoimmune disease and antiphospholipid antibodies (Roberts and Cooper, 2001, Young et al., 2010, Duckitt and Harrington, 2005, Bramham et al., 2014). However, whether preeclampsia is a heritable disease, remains debatable. Understanding preeclampsia heritability has proved challenging due to the heterogeneous nature of the disease, combined complex genetic and environmental risk factors and the contribution of at least two genomes (maternal and fetal) to each pregnancy outcome. Nevertheless, it has a substantial heritable component estimated to 55-60%, of which 30-35% is attributed to a maternal genetic effect and 20% to fetal effect (Gray Kathryn et al., 2018). The risk of getting preeclampsia is heritable as it has been shown that children born to mothers with preeclampsia have an increased maternal risk of developing preeclampsia or paternal risk of contribution to preeclampsia during their pregnancy (Esplin et al., 2001).

Gene predisposition also may play a role in developing preeclampsia (Roberts and Cooper, 2001, Williams and Broughton Pipkin, 2011, Buurma et al., 2013). Genome-wide association studies (GWAS) for preeclampsia have identified several SNPs linked with increased risk of preeclampsia development (Zhao et al., 2013). More than 648,000 SNPs were genotyped in 538 preeclampsia cases and 540 normal pregnancy controls from unrelated Australian individuals of Caucasian ancestry. Two SNP associations (rs7579169 and rs12711941) were found significantly associated with preeclampsia. Both SNPs reside in an intergenic region less than 15 kb downstream from the 3′ terminus of the Inhibin, beta B (*INHBB*) gene on 2q14.2 (Johnson et al., 2012). Interestingly, decreased levels of inhibin beta were found in preeclamptic serum (Petraglia et al., 1997). In a separate study, 50,000 SNPs were genotyped in 877 preeclampsia cases and 3004 controls from multi-ethnic individuals. SNP (rs9478812) in the pleiotropic *PLEKHG1* gene was identified to have a study-wide statistically significant association with the preeclampsia development (Gray Kathryn et al., 2018). *PLEKHG1* is a large gene (232 kb) with 15 exons that encodes the PLEKHG1 protein, a Rho guanine nucleotide exchange factor expressed across a wide range of tissues. *PLEKHG1* variants have previously been implicated in GWAS of hypertensive diseases (Franceschini et al., 2013), therefore SNPs in *PLEKHG1* locus may predispose women to develop hypertensive disease in pregnancy. In addition to these studies, a GWAS performed in 2017 tested nearly 7,5 mln sequence variants from 2,658 offspring from preeclamptic pregnancies and 308,292 controls of European descent from Iceland and UK. Three SNPs

(rs4769613, rs12050029 and rs149427560) had a genome-wide significant association with preeclampsia and were located on the chromosome 13 near the *FLT1* gene (McGinnis et al., 2017). Soluble fms-like tyrosine kinase-1 (Flt-1) is a culprit protein implicated in the pathogenesis of preeclampsia and discussed in more detail in Section 1.4.2. Systematic review provided by Kleinrouweler et al. (2013) overviewed nearly 40 annotated gene transcripts and 17 microRNAs of which angiogenesis-related cluster Flt-1, vascular endothelium growth factor-A (VEGF-A), and placental growth factor (PlGF) were significantly overexpressed during preeclampsia. Identification of the differential expression of these genes in normotensive and preeclampsia placentas is essential to understand molecular mechanisms involved in preeclampsia and larger studies are required to further define maternal preeclampsia heritability.

1.4 Imbalance between pro- and anti-angiogenic factors in preeclampsia

Normal human placental development consists of vasculogenesis and certain elements of tumorigenesis. Ectodermally derived cytotrophoblasts (placental cells), invade the uterus where they reside in the interstitial compartment and line uterine arteries and veins. They undergo pseudovasculogenesis, switching their adhesion molecule repertoire from epithelia cell origin to mimic that of vascular cells (Zhou et al., 1997b, Powe et al., 2011). In preeclampsia, differentiating/invading cytotrophoblasts fail to express adhesion molecules such as integrin or cadherin, thereby compromising blood flow to the maternal-fetal interface leading to abnormal placentation (Zhou et al., 1993, Zhou et al., 1997a). Angiogenesis is essential for normal mammalian development and is tightly controlled by the local balance of pro- and anti-angiogenic factors. Implication of angiogenic balance results in failed angiogenesis, which may be the cause of preeclampsia (Powe et al., 2011).

1.4.1 Vascular growth factor (VEGF)

Vascular endothelial growth factor (VEGF) is a secreted factor that promotes angiogenesis and maintains the integrity of the endothelium. It is known that proliferation of endothelial cells is crucial for many physiological processes, which include normal growth and differentiation, reproductive angiogenesis, embryonic development, wound healing (Ferrara et al., 2003). It is also involved in many pathological cases such as intraocular neovascular syndromes, neovascularisation of cancerous tumours, endometriosis and etc (Ferrara and Davis-Smyth, 1997). Therefore, it has to be tightly regulated. VEGF-A (often referred in literature as VEGF), -B, -C, -D, -E and placental growth factor (PlGF) are members of the platelet-derived growth factor (PDGF) family. VEGF is known to be expressed in different transcripts encoding polypeptides 206, 189, 145, 165 and 121. $VEGF_{165}$ is the most abundant form of all transcripts, both $VEGF_{121}$ and $VEGF_{165}$ are secreted as a soluble form of VEGF, whereas $VEGF_{189}$ and $VEGF_{206}$ are membrane bound (Ahmed et al., 1997). VEGF, VEGF-B and PlGF bind to 180 kDa kinase domain-containing, high-affinity VEGFR-1 receptor, also known as fms-like tyrosine kinase-1 (Flt-1). VEGF, VEGF-C, VEGF-D and parapoxvirus-derived VEGF-E (Ogawa et al., 1998) bind to 200–230 kDa receptor VEGFR-2, also known as kinase insert domain receptor/fetal liver kinase 1 (KDR/Flk-1) (Ferrara et al., 2003, Karkkainen and Petrova, 2000). Unlike VEGFR-1, VEGFR-2 is highly expressed on many different types of cells and mediates mitogenic, angiogenic and permeability-enhancing effects (Ferrara et al., 2003). Interestingly, VEGF-A binds VEGFR-1 with at least 10-fold higher affinity than VEGFR-2 and even though the crystal structure of human PlGF is structurally similar to VEGF-A, PlGF binds VEGFR-1, but not VEGFR-2 (Ferrara and Davis-Smyth, 1997).

VEGF-A and its receptors are expressed during various stages of human placentation and mainly expressed by endothelial and trophoblast cells (Sharkey et al., 1993, Charnock-Jones et al., 1994, Ahmed et al., 1997). VEGF-dependent signalling through VEGFR-2 mediates mitogenic, angiogenic, migration, cell adhesion and permeability-enhancing effects. On the other hand, VEGF signalling through VEGFR-1, inhibits VEGFR-2-dependent endothelial cell proliferation resulting in negative regulation of VEGF effects (Dunk and Ahmed, 2001, Ferrara, 2004, Cudmore et al., 2012).

VEGFR-1 suppressed proliferation occurs via nitric oxide (NO) and leads to endothelial differentiation and promotion of vascular integrity (Bussolati et al., 2001, Dunk and Ahmed, 2001). VEGFR-1 possess higher affinity to VEGF and weaker kinase signalling properties, whereas VEGFR-2 binds to VEGF with low affinity but initiates much stronger signalling magnitude (Ferrara, 2004). Therefore, it seems that VEGFR-2 is responsible for main proliferative functions and VEGFR-1 is a regulatory component preventing VEGFR-2 dependent VEGF signalling. VEGF receptors are expressed on different type of cells, including endothelial cells, trophoblast cells, blood monocytes, etc. and the signalling properties can be different depending on the developmental stage and the cell type (Ahmed et al., 1997, Ferrara, 2004). VEGF is critical for embryonic development and it has been shown that a loss of a single allele results in embryonic lethality (Ferrara et al., 1996).

VEGF, which is responsible for growth, differentiation and migration of trophoblasts in placental villi and the maternal decidua, was found to be significantly increased during pregnancy complicated by preeclampsia (Sharkey et al., 1996). More importantly, increasing VEGF levels correlated with the severity of hypertension (Kupferminc et al., 1997). However, other studies showed that VEGF in preeclampsia is decreased (Tsatsaris et al., 2003). Due to inconsistency and discrepancies in methods measuring VEGF, it was confirmed that, free levels of circulating VEGF are decreased, whereas the total VEGF, circulating free or bound to soluble VEGFR-1 (sFlt-1), levels are increased. Also interestingly VEGF levels increase in parallel to sFlt-1 (Tsatsaris et al., 2003). The mechanism behind that involves VEGF dependent endothelial VEGFR-1 and VEGFR-2 heterodimer complex formation where, VEGFR-1 negatively regulates some of the VEGFR-2 mediated functions (Figure 1.1) (Cudmore et al., 2012, Cai et al., 2017b). In that way, VEGF is able to mediate its own bioactivity and sFlt-1 receptor release via VEGFR-2 (Ahmad et al., 2011). Taking into account that VEGFR-1 is relatively under-expressed in normal physiological conditions, forming a heterodimer with VEGFR-2 is very rare and presents a regulatory mechanism for angiogenesis and endothelial cell turnover homeostasis. Increased pathological expression of VEGFR-1 or VEGF-dependent heterodimerisation with VEGFR-2 may lead to dysregulated levels of VEGF and sFlt-1 as seen in preeclampsia.

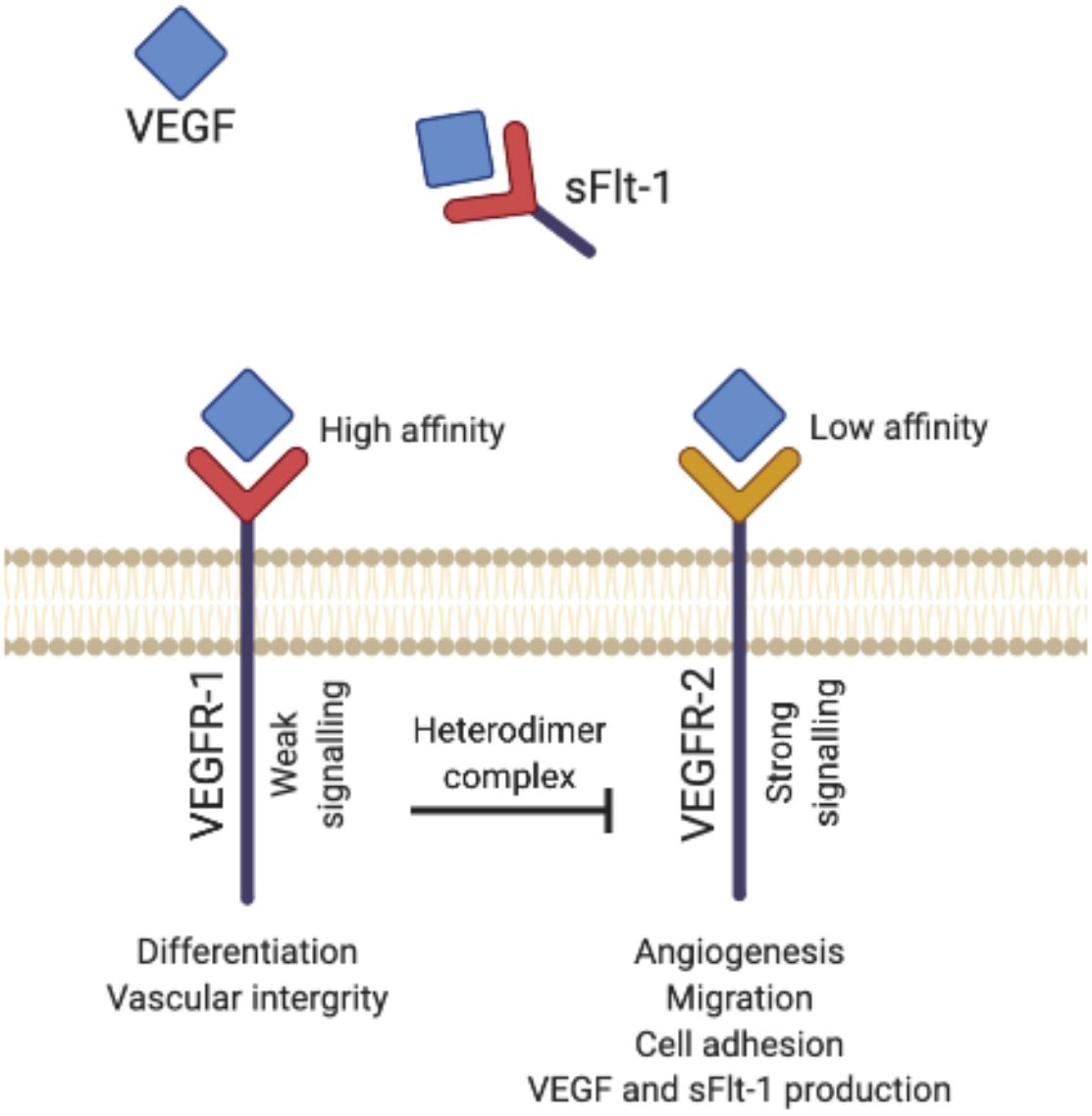

Figure 1. 1. VEGF-dependent signalling in endothelial cells.

VEGF signalling promotes VEGFR-1 and VEGFR-2 heterodimer complex formation, which is responsible for the negative regulation of VEGFR-2 mediated functions.

1.4.2 Soluble fms-like tyrosine kinase-1 (sFlt-1)

FLT pre-mRNA can be alternatively spliced into two distinct products encoding the full-length membrane-bound receptor VEGFR, that mediates VEGF mitogenic activity or the truncated soluble Flt-1 (sFlt-1) lacking the seventh Ig-like domain, transmembrane sequence and the cytoplasmic domain (Thomas et al., 2010). The novelty of soluble Flt-1 has been described in the late 90's when cDNA sequence encoding sFlt-1 has been shown to be increased in pregnancy (He et al., 1999). Soluble Flt-1 binds to free circulating VEGF with high affinity preventing VEGF-dependent signalling (Kendall and Thomas, 1993, Kendall et al., 1996). Normal pregnancy and advancing gestational age are associated with healthy increase of sFlt-1, which in balance with other factors regulating angiogenic responses, provides a limiting and protective barrier for potentially unhealthy VEGF-dependent over signalling (Chen and Khalil, 2017, Sela et al., 2008).

Gene encoding human *FLT* is highly expressed in the cytotrophoblast shell/columns and extravillous trophoblasts (EVT) in the maternal decidua in the first trimester and at term (Charnock-Jones et al., 1994). The presence of *FLT* gene in non-endothelial cells indicates that VEGF is responsible for the growth and differentiation of cytotrophoblast at the site of implantation (Charnock-Jones et al., 1994). In fact, many studies showed that not only vascular endothelial cells are able to express VEGF receptors and sFlt-1. Blood monocyte cells express VEGFR-1 but not VEGFR-2 as a cell surface molecule and neutralisation of VEGFR-1 results in suppression in VEGF-induced migration (Barleon et al., 1996, Clauss et al., 1996, Sawano et al., 2001). In addition to expressed surface VEGFR-1, Barleon et al. (2001) showed that, activation of both human umbilical vein endothelial cells (HUVEC) and isolated blood monocytes produced high levels of sFlt-1 (Barleon et al., 2001). Thus, not only endothelial and trophoblast cells but blood monocytes also are able to secrete sFlt-1, which is detectable in males and healthy pregnant female donors. Equal regulation of membrane bound VEGFR-1 and sFlt-1 mRNA and protein levels suggest important homeostatic angiogenesis in normal pregnancy (Clark et al., 1998, Barleon et al., 2001).

Many studies identified increased circulating plasma sFlt-1 as a pivotal anti-angiogenic factor involved in preeclampsia in addition to endothelial dysfunction,

hypertension, and proteinuria (Ahmed, 1997, Maynard et al., 2003, Bergmann et al., 2010). It was proposed that the sFlt-1-dependent loss of VEGF activity is the prominent event linked to the pathogenesis of preeclampsia (Ahmed, 1997). Soluble Flt-1 has been found increased in amniotic fluid (Vuorela et al., 2000) and >6-fold higher in circulation of preeclampsia-complicated pregnancies (Koga et al., 2003). Case-control longitudinal study within the Calcium for Preeclampsia Prevention Trial, which involved healthy nulliparous women showed that preeclampsia patients develop increased sFlt-1 and decreased PlGF levels earlier when compared to normotensive pregnancies (Levine et al., 2006). Serum sFlt-1 levels were found increased in preeclampsia as soon as five weeks before the onset of the disease. At the onset of clinical disease, the mean serum level of sFlt-1 in the women with preeclampsia was 2.5 times higher than normotensive controls. (Levine et al., 2004). *In vivo* studies showed that, exogenously induced sFlt-1 overexpression resulted in hypertension and glomerular endotheliosis (Maynard et al., 2003), whereas reduced circulating levels of free sFlt-1 below critical threshold rescued damaging effects of sFlt-1 (Bergmann et al., 2010). In addition, removal of circulating plasma sFlt-1 by apheresis with a plasma-specific dextran sulfate showed significant reduction in proteinuria, improved blood pressure and prolonged pregnancy (Thadhani et al., 2011, 2016). This highlights sFlt-1 as a potent anti-angiogenic factor, which is able to cause preeclampsia-like symptoms on its own and presents a good indicative measure for preeclampsia.

sFlt-1 can be spliced differently into three main isoforms (Sela et al., 2008). Two isoforms encode the short and long versions (Thomas et al., 2007, Thomas et al., 2009, Thomas et al., 2010) of the ordinary sFlt-1 protein (also known as sFlt1-i13 or sFLT_v1), first described by Kendall and Thomas (1993) terminating within intron 13 by skipped splicing and upstream polyadenylation (Huckle and Roche, 2004, Heydarian et al., 2009, Thomas et al., 2009). Both short and long isoforms of sFlt-1 encode the same 687 amino acid long sFlt1 protein, however due to the alternative polyadenylation at different sites in intron 13, mRNAs consist of a 17 or 4146 nucleotides 3'-UTR, respectively (Ashar-Patel et al., 2017). The third variant of sFlt-1 arises by alternate splicing and polyadenylation within an Alu sequence (also known as sFlt1-e15a, sFLT1_v2 or sFlt1-14). Originally, sFlt1-e15a was found to be largely expressed in vascular smooth muscle and sFlt1-i13 in the endothelium (Sela et al., 2008). Soluble Flt1-i13 is largely expressed by multiple organs including placenta, whereas sFlt1-e15a is highly specific only to human placenta

(Jebbink et al., 2011). Both sFlt1-i13 and sFlt1-e15a were found to be elevated in preeclampsia (Jebbink et al., 2011).

Quantification in normal and preeclamptic placentas showed that the expression of sFlt1-e15a is higher than sFlt1-i13 and is more specific to trophoblasts cells rather than endothelial or vascular smooth muscle cells or macrophages (Thomas et al., 2009). In fact, splice variant sFlt1-i13 makes up 15 % of total placental sFlt-1 and it is thought to be endothelium-specific, whereas, sFlt1-e15a makes up at least 80 % of placental sFlt-1 (Jebbink et al., 2011), which is thought to be placenta-specific and considered as the main isoform responsible for the preeclampsia phenotype (Palmer et al., 2016). Generated specific sFlt1-e15a ELISA in Palmer et al. (2015) study identified increasing serum sFlt1-e15a levels across pregnancy and especially high levels in severe early-onset preeclampsia (Palmer et al., 2015). It was demonstrated that sFlt1-e15a is biologically active and competes with VEGF to block VEGFR-2 signalling thereby inhibiting endothelial cell migration, invasion, tube formation, and angiogenesis. Interestingly, sFlt1-e15a is a human specific variant and is not expressed in rodents. It might be the reason why rodents do not develop preeclampsia (Palmer et al., 2015).

1.4.3 Heme oxygenase-1 (HO-1)

Heme oxygenase (HO) is a rate-limiting oxidation reaction enzyme converting heme into biliverdin, carbon monoxide (CO) and free iron (Fe^{2+}) (Keyse and Tyrrell, 1989). Three isoforms of HO have been identified, HO-1, HO-2 and HO-3. HO-1, also known as heat shock protein (hsp), is inducible form of the enzyme, which is stimulated by various forms of stress and plays a role in maintaining antioxidant/oxidant homeostasis during cellular injury (Soares and Bach, 2009, Gozzelino et al., 2010). It is highly sensitive to all kinds of stimuli including oxidative stress caused by pathological conditions such as ischemia, GSH-depletion, hypoxia, cellular transformations and various disease states (Rossi et al., 2017, André and Felley-Bosco, 2003, Hettiarachchi et al., 2014). When stressed, HO-1 expression was demonstrated to increase in the heart, kidneys and vasculature (Maines et al., 1993, Raju and Maines, 1996). Many studies show that, HO-1 provides anti-oxidative defence mechanism against post-ischemic

tissue injury (Ito et al., 1997, Katori et al., 2002). HO-2 on the other hand, is a constitutive form of the enzyme, which is found in brain, testis, endothelial and smooth cells from cerebral vessels (Muñoz-Sánchez and Chánez-Cárdenas, 2014). Although, HO-3 is related to HO-2, both of these enzymes are less well characterized in the literature (McCoubrey et al., 1997, Muñoz-Sánchez and Chánez-Cárdenas, 2014).

HO-1 system is well known for its antioxidant properties. Heme molecule, which promotes lipid peroxidation and oxygen free radical formation, is sequestered by HO-1 to protect the cell from deleterious effects (Kim et al., 2011). Fe^{2+} released in oxidation reaction is rapidly converted to Fe^{3+} by redox enzyme ferritin to reduce the bioavailability of Fe^{2+} and promote iron storage. Simultaneous expression of HO-1 and ferritin allows safe disposal of Fe^{2+} and inhibition of its pro-oxidant potential (Berberat et al., 2003, Balla et al., 1992). Bilirubin, which is reduced from biliverdin by the cytosolic enzyme biliverdin reductase is a potent antioxidant (Stocker et al., 1987, McGeary et al., 2003). Carbon monoxide (CO), the by-product of oxidation reaction, is cytoprotective anti-inflammatory signalling molecule and potent endothelium-dependent vasodilator regulating vascular tone (Brouard et al., 2000, Otterbein et al., 2000b). It also prevents anti-aggregation of the platelets and inhibits both apoptotic and proliferation pathways (Dennery, 2014). It has been reported that low concentrations of CO selectively down-regulate the expression of pro-inflammatory cytokines TNF-α, IL-1β, and MIP-1 as well as increase anti-inflammatory cytokine IL-10 both *in vivo* and *in vitro* (Otterbein et al., 2000a). Even though endogenous CO is protective, exogenous CO is odourless gas, a product of incomplete combustion that can be lethal upon toxic inhalation (Kim et al., 2011).

The first known human case of HO-1 deficiency was a six-year-old boy presented with severe growth retardation, persistent haemolytic anaemia, abnormal coagulopathy and persistent endothelial damage. Also, iron deposition was noted in renal and hepatic tissues. Sequence analysis revealed that *Hmox1* gene had a complete loss of exon-2 of the maternal allele and a two-nucleotide deletion within exon-3 of the paternal allele (Yachie et al., 1999a). Although HO-1 deficiency in humans is very rare, few more cases since then were identified. A fifteen-year-old girl, previously well, was presented with congenital asplenia, inflammation, lymphadenopathy, severe intravascular haemolysis, nephritis, hypertension and haemoglobinuria. After five months of hospitalisation, the

condition deteriorated further followed by death due to fungal sepsis. Mutation analysis revealed a homozygous mutation in the HO gene and absence of functional HO protein (Radhakrishnan et al., 2009). A ten-year-old-boy presented with fever, pallor, severe hypertension, asplenia, proteinuria and haemolysis. Mutation analysis showed homozygous missense in the HO gene, which usually results in the absence of the functional HO-1 protein. The condition was successfully treated with non-myeloablative matched sibling donor allogeneic stem cell transplant (Yadav et al., 2018). A seventeen-month-old female presented with fever, tachypnoea, signs of respiratory distress, pericardial effusion and hepatomegaly. Laboratory findings showed leukocytosis, thrombocytosis, haemolytic anaemia, elevated inflammatory markers, increased levels of the hepatic transferase, triglycerides and ferritin as well as decreased level of fibrinogen. The condition progressively deteriorated followed by death caused by recurrent fever, bleeding, heart failure, and ascites. Post-mortem sequencing analysis revealed a homozygous mutation in the *Hmox1* gene (Tahghighi et al., 2019).

HO-1 deficiency in animals equates to nearly all the clinical and biological HO-1 deficiency-like symptoms observed in humans. Genetically modified HO-1 knockout (KO) mice experienced growth retardation, anaemia, iron deposition and vulnerability to stressful injury and accumulation of free radicals (Poss and Tonegawa, 1997b, Mamiya et al., 2008). In contrast, transgenic mice overexpressing HO-1 were protected against hypoxia-induced inflammatory cell infiltration and suppressed production of pro-inflammatory cytokines and chemokines (Minamino et al., 2001).

1.4.4 Role of HO-1 in pregnancy and preeclampsia

Multiple studies in rodents revealed that HO-1 is crucial for the maintenance of healthy pregnancy. Genetically modified HO-1 heterozygous (*Hmox1*$^{+/-}$) and HO-1 null (*Hmox1*$^{-/-}$) mice placenta exhibit poor trophoblast survival and differentiation into a mature phenotype when compared to wild-type littermates (Zenclussen et al., 2011). It leads to thinner junctional zone and deficiency in vascular remodelling (Zhao et al., 2009, Zhao et al., 2011a). In addition, *Hmox1*$^{+/-}$ and *Hmox1*$^{-/-}$ implantations are associated with diminished pro-angiogenic VEGF and PlGF mRNA expression at the fetomaternal interface as well as lower numbers of uterine natural killer cells, which are necessary for

the correct spiral artery remodelling (Linzke et al., 2014). As a result, insufficient blood supply (Robson et al., 2012) causes increased blood pressure (Linzke et al., 2014, Zhao et al., 2009) leading to severe growth restriction of *Hmox1*$^{+/-}$ fetuses (Zenclussen et al., 2011, Linzke et al., 2014, Zhao et al., 2009), whereas *Hmox1*$^{-/-}$ females are unable to sustain a pregnancy and suffer intrauterine death (Zenclussen et al., 2011, Zenclussen et al., 2012, Poss and Tonegawa, 1997a, Zhao et al., 2009). HO-1 also plays a crucial role in the development of fetal tolerance as inhibition of HO-1 has been demonstrated to attenuate adaptive T-regulatory cell-dependent protective effects in the abortion prone *in vivo* model (Schumacher et al., 2012).

Increased expression or activity of HO-1 was demonstrated to be protective against miscarriage in a well-established abortion prone mouse model (Sollwedel et al., 2005, Zenclussen et al., 2006). Alternative infection-dependent mouse abortion model revealed that infections themselves downregulate HO-1 expression in the placenta, and that induction of HO-1 dramatically increased fetal survival in the infected animals (Tachibana et al., 2011, Tachibana et al., 2008). It was demonstrated that HO-1 inhibition provokes hypertension (George et al., 2013), whereas HO-1 induction normalises blood pressure in rats (George et al., 2011b). Moreover, it was demonstrated that HO-1 metabolite, CO, could restore HO-1 deficiency-dependent damaging effects. *Hmox1*$^{-/-}$ animals treated with CO normalised uterine natural killer cell numbers, increased the expression of VEGF and PlGF at the fetomaternal interface which resulted in restored spiral artery remodelling (Linzke et al., 2014). Inhalation of low-dose CO improved both fetal weight and fetal survival, suggesting that CO is at least partially responsible for the protective effects of HO-1 during pregnancy (Zenclussen et al., 2011). Most importantly, CO treatment rescued *Hmox1*$^{-/-}$ fetuses from the fatality that would die otherwise *in utero* (Zenclussen et al., 2011). In addition, application of CO compensates for HO-1 deficiency and was demonstrated to improve hypertension *in vivo* (Linzke et al., 2014). Based on the gathered data *in vivo*, the expression of HO-1 is important for the optimal placental development and fetal growth. Dysregulation of the HO-1 pathway is likely to play a part in the pathology of pregnancy complications.

Reduced HO-1 expression in human placenta has been associated with idiopathic recurrent miscarriage (Denschlag et al., 2004), normotensive IUGR and preeclampsia (Ahmed et al., 2000, Lyall et al., 2000). The end-tidal breath CO level measurements

were significantly lower in the pregnancy-induced hypertension and preeclampsia patients when compared to healthy pregnant women (Baum et al., 2000, Kreiser et al., 2004). Cellular component of blood from preeclampsia patients contained decreased levels of HO-1, which correlated with the severity of preeclampsia-induced symptoms such as proteinuria and high blood pressure (Nakamura et al., 2009). Ahmed et al. (2000) demonstrated that the induction of HO-1 attenuates TNF-α-mediated cellular damage in placental villous explants and reduces vascular tension in pre-constricted placental arteries (Ahmed et al., 2000). Based on these observations in addition to decreased HO-1 expression in preeclamptic placenta, authors suggested that HO-1 offers protection against cytotoxic damage in the placenta during normal pregnancy and that the impairment of HO-1 activation may compromise the protective mechanism and predispose the placenta to cellular injury and subsequent maternal endothelial cell activation (Ahmed et al., 2000).

Cigarette smoking in pregnancy has been reported to increase HO levels in the placentas and in the trophoblasts following an *in vitro* exposure to cigarette smoke extract (Sidle et al., 2007). Placental villous explants from pregnant women exposed to cigarette smoke extract exhibited reduced sFlt-1 production (Mehendale et al., 2007). Moreover, cigarette smoking during pregnancy has been reported to correlate positively with a marked decrease in maternal serum sFlt-1 levels (Jeyabalan et al., 2008, Belgore et al., 2000) and reduced risk of developing preeclampsia (Conde-Agudelo et al., 1999, England and Zhang, 2007). Study performed by Cudmore et al. (2007) demonstrated that HO-1 inhibition leads to increased sFlt-1 production from endothelial cells, whereas adenoviral overexpression of HO-1 or treatment with CO-releasing compound inhibits VEGF-induced sFlt-1 release (Cudmore et al., 2007). This study established that HO-1/CO axis is capable of negatively modulating sFlt-1 in pregnancy. Placental explants from rats exposed to hypoxia led to significant downregulation in HO-1 levels and increase in sFlt-1, whereas treatment with HO-1 inducer or CO-releasing compound markedly reduced hypoxia-induced sFlt-1 *ex vivo* (George et al., 2012). The evidence further suggests that HO-1 acts as a negative sFlt-1 regulator. As HO-1/CO axis presents a therapeutic pathway to reduce pathological sFlt-1 levels and treat or prevent preeclampsia. The exact mechanism by which HO-1 inhibits sFlt-1 is needed to identify a potential therapeutic strategy.

1.5 Preeclampsia treatment

Although many therapeutic approaches have been proposed to treat preeclampsia, none of them are approved for clinical use. Preeclampsia remains an unmet medical need disorder. Combination of clinical tests including maternal risk factors, blood pressure, placental growth factor (PlGF), uterine artery Doppler and history of previous pregnancy complications may indicate a need for advanced prenatal care. Aspirin (150 mg/day) supplementation is prescribed to prevent preterm (before 37 weeks' gestation) but not term preeclampsia (Brown et al., 2018a, National Guideline, 2019, National Collaborating Centre for and Children's, 2010). Patients presented with the hypertensive disorder of pregnancy are immediately treated with antihypertensives to reduce the likelihood of developing preeclampsia and other complications including low platelets and elevated liver enzymes; and MgSO4 for convulsion prophylaxis (Brown et al., 2018a, National Guideline, 2019, National Collaborating Centre for and Children's, 2010). Induction of preterm delivery depends on the severity of the preeclampsia, gestational age, maternal and fetal status. It is recommended for patients with preeclampsia to receive (Brown et al., 2001, Phipps et al., 2019):

- induction of delivery at ≥ 37 weeks' gestation if the patient presents severe preeclamptic features
- expectant management at < 37 weeks' gestation if the patient presents no severe preeclamptic features
- induction of delivery irrespective of the gestational age if the patient presents one of the following:
    - repeated episodes of severe hypertension despite the antihypertensive treatment
    - progressive thrombocytopenia
    - abnormal renal or liver enzyme tests
    - pulmonary oedema
    - abnormal neurological features
    - stillbirth
- Induction of delivery and maternal stabilisation at ≥ 34 weeks' gestation if the patient presents severe preeclamptic features

- Corticosteroids treatment to accelerate fetal lung maturity, management of the symptoms and maintenance of the pregnancy with intensive maternal and neonatal care at < 34 weeks' gestation if the patient presents severe preeclamptic features
- Counselling and possible termination of pregnancy at < 24 weeks' gestation

It has been suggested that therapeutics directed at decreasing circulating levels of sFlt-1 could be a possible treatment for preeclampsia (Ramma and Ahmed, 2014, Ahmed and Cudmore, 2009). Since HO-1 has been identified as a negative sFlt-1 regulator *in vitro* (Cudmore et al., 2007) and that low HO-1 levels and high sFlt-1 levels may be linked with the preeclampsia pathogenesis (Ahmed et al., 2000, Gozzelino et al., 2010, Otterbein et al., 2000a, Soares and Bach, 2009), a good fraction of potential therapeutic candidates relies on restored HO-1 expression and/or activity (Muchova et al., 2007). These include resveratrol, a naturally produced phenol (Hannan et al., 2017) and statins such as pravastatin (Costantine et al., 2010, Kumasawa et al., 2011, Redecha et al., 2009, Saad et al., 2014, Brownfoot et al., 2015, Brownfoot et al., 2016), simvastatin (Lee et al., 2004a, Grosser et al., 2004, Cudmore et al., 2007, Brownfoot et al., 2016) and rosuvastatin (Brownfoot et al., 2016).

Statins have been shown to increase HO-1 system *in vitro* and *in vivo* (Muchova et al., 2007), and to lower sFlt-1 levels in HUVECs and human placental explants (Cudmore et al., 2007). Simvastatin acts, in part, through HO-1 and exerts anti-inflammatory and anti-oxidative properties (Lee et al., 2004a). It upregulates HO-1 mRNA (Grosser et al., 2004) and protein (Cudmore et al., 2007) in placenta and most importantly decreases VEGF-induced sFlt-1 release from normal term placental villous explants (Cudmore et al., 2007). Mice injected with Ad-sFlt-1 and exposed to pravastatin in drinking water, led to lowered maternal plasma sFlt-1 levels (Costantine et al., 2010). Simvastatin, rosuvastatin and pravastatin all reduced sFlt-1 secretion from endothelial cells, trophoblasts and preterm preeclamptic placental explants (Brownfoot et al., 2016). In addition, all statins induced HO-1 in endothelial cells, however, only simvastatin increased HO-1 expression leading to potent inhibition of sFlt-1 secretion from endothelial cells, trophoblast cells and placental explants (Brownfoot et al., 2016).

Statin therapy is currently contraindicated during pregnancy as the recent evidence provided so far is limited and inconclusive (Ofori et al., 2007). Food and Drug

Administration categorises statins as category X drugs (Kazmin et al., 2007, Edison and Muenke, 2004) as statins exhibit a risk of reaching the embryo and downregulating biosynthesis of cholesterol as well as other important metabolic intermediates, crucial for developing fetal unit (Ofori et al., 2007). A small number of cases exploring teratogenic effects of the original statins used at the time observed adverse birth outcomes associated with lipophilic statins use (Edison and Muenke, 2004). However, a number of recent studies showed that use of statins did not cause any fetal or maternal adverse effects during pregnancy in animal models of preeclampsia (Costantine et al., 2010, Bauer Ashley et al., 2013, Kumasawa et al., 2011, Saad et al., 2014, Brownfoot et al., 2015, Fox et al., 2011) and human preeclamptic patients (Brownfoot et al., 2015, Costantine et al., 2016, Lefkou et al., 2016, Ofori et al., 2007). Although, researchers reported the benefits of statins use in treating or preventing preeclampsia, the conclusions are limited and inconclusive due to small sample sizes, incomplete outcomes and exclusion of statin effect on non-live births. Recently, Ahmed and colleagues completed the world's first randomised control clinical trial on pravastatin in early-onset preeclampsia (Ahmed et al., 2020). They demonstrated that pravastatin *per se* had no adverse effects during pregnancy and all recorded fetal deaths occurred in the control arm of the study. No differences were detected in maternal plasma sFlt-1 levels or sFlt-1:PlGF ratio, however, preeclamptic patients who received pravastatin experienced prolonged pregnancy by up to 4 days and less common adverse neonatal outcomes (Ahmed et al., 2020). Although, the study confirms that statins are safe to use in pregnancy, treatment approach equates to a "shotgun" approach lacking tissue specificity and increased risk of off-target effects. Future strategies exploring and developing tissue-targeted therapeutics are required to treat or prevent preeclampsia.

1.6 MicroRNA role in pregnancy

Most scientists considered non-coding regions of DNA that form 95% of human genome as a junk DNA. Now, it is widely accepted that RNAs produced from non-coding regions of DNA possess a regulatory role in almost every physiologically important process within the human body (Bartel, 2004, 2009). Study conducted in 2010 revealed that nearly 50% of human mRNAs are regulated by more that 2000 human microRNAs

(miRNAs) (Krol et al., 2010). Mature miRNA is a small single-stranded molecule consisting of approximately 22 nucleotides, which is found in the cytoplasm. Biogenesis of miRNA is complicated multi-step process that starts in the nucleus and involves multiple enzymes and processing factors. MicroRNA genes are usually found in clusters and are transcribed by RNA polymerase II (Pol II) in the animal cell nucleus. Primary transcripts of miRNA genes (pri-miRNA) form a double stranded hairpin stem-loop structures (Treiber et al., 2019) and contain two flanking ends containing 5'- cap and polyadenylated tail (Cai et al., 2004, Lee et al., 2004b). Pri-miRNA transcripts are recognised by DiGeorge Syndrome Critical Region 8 (DGCR8) protein which associates with the RNase III enzyme Drosha to form a microprocessor complex in order to initiate the cleavage of flanked ends and to liberate the hairpin stem-loop structure (Lee et al., 2003). After this step pri-miRNA becomes precursor miRNA (pre-miRNA) and is transported to the cytoplasm by nuclear export receptor exportin-5 (Lund et al., 2004, Yi et al., 2003, Zeng and Cullen, 2004). In the cytoplasm, double-stranded pre-miRNA is cleaved from hairpin loop by RNase III-type enzyme Dicer to form a double-stranded miRNA duplex (Bernstein et al., 2001). The next step involves argonaute (AGO) protein, which is crucial in determining the significance of the mature miRNA sequence. AGO selectively retains the guiding strand based on the stability of the 5' end, while the passenger strand is discarded (Schwarz et al., 2003). AGO proteins loaded with mature single-stranded miRNA sequence dissociate from the Dicer followed by the formation of the miRNA-induced silencing complex (miRISC). MicroRNA-RISC complex enables endonuclease activity directed against target mRNA strands that are complementary to miRNA fragment called "seed" sequence (Hammond, 2005, Treiber et al., 2019). Using "seed" sequence alignment by partial or perfect complementary of just 6-7 nucleotides miRNA binds to the 3' untranslated region (3'-UTR) of target mRNA. Perfect match initiates degradation of the mRNA by cleavage (Yekta et al., 2004, Mansfield et al., 2004), whereas imperfect alignment results in the translational inhibition (Figure 1.2) (Bartel, 2004, Cai et al., 2017a, Treiber et al., 2019).

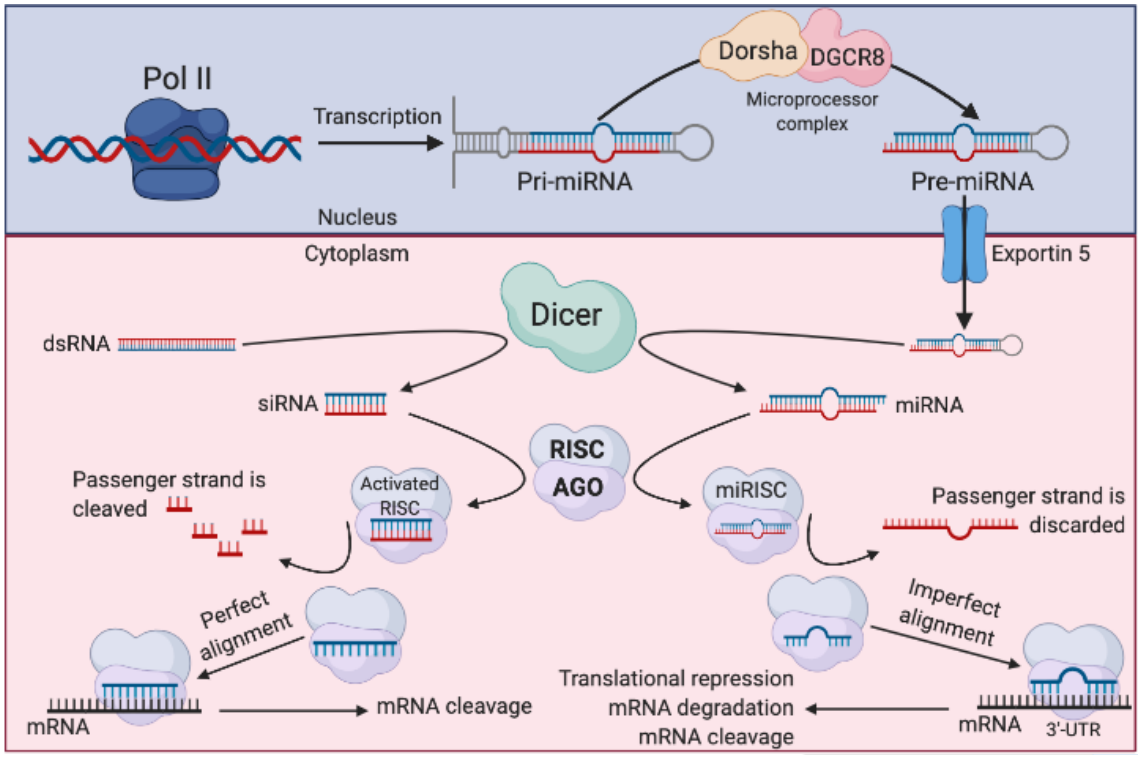

Figure 1. 2. MicroRNA and siRNA dependent gene regulation mechanism.

MicroRNA genes are transcribed by RNA polymerase II (Pol II) in the nucleus. Primary miRNA (Pri-miRNA) transcripts are recognised by DiGeorge Syndrome Critical Region 8 (DGCR8) protein which associates with Drosha to cleavage the hairpin stem-loop structure and form precursor miRNA (pre-miRNA). It is transported to the cytoplasm by nuclear export receptor exportin-5 where pre-miRNA and dsRNA are cleaved by Dicer to form miRNA duplex and siRNA. AGO retains the guiding strand and the passenger strand is destined for destruction (miRNA) or cleavage (siRNA). AGO proteins dissociate from the Dicer and form RNA-induced silencing complex (RISC). MicroRNA-RISC (miRISC) or activated RISC enables endonuclease activity directed against mRNA. Depending on the nature of the alignment, miRNA initiates either translational repression, miRNA degradation or mRNA cleavage. Perfect alignment of siRNA initiates mRNA cleavage.

MicroRNA presents an important fine-tuned gene silencing regulation. It is estimated that miRNAs regulate target mRNA translation of approximately one-third of human protein-coding genes and have a central role in wide range of processes including cellular development, apoptosis, fat metabolism, neuronal gene expression, brain morphogenesis, muscle differentiation, stem cell division (Mattick and Makunin, 2006, Kim and Nam, 2006), angiogenesis and vascular inflammation (Urbich et al., 2008). Substantial amount of miRNAs are expressed in the human placenta (Pineles et al., 2007b). This organ has the capability of miRNA synthesis, as all key components of miRNA biogenesis pathway are expressed in placenta (Mouillet et al., 2011). AGO2, a central component of the RNA-induced silencing complex (RISC) has been shown to be essential for early stages of embryogenesis (Lykke-Andersen et al., 2008), embryonic survival and placental development (Cheloufi et al., 2010). MicroRNA-221, miR-222 (Poliseno et al., 2006) and miR-29 (Yang et al., 2013) play an important role in HUVEC cell cycle regulation, proliferation and angiogenesis, whereas miR-126 and miR-21 have been shown to regulate angiogenic signalling (Sabatel et al., 2011, Fish et al., 2008, Dews et al., 2006). MicroRNA-210 is known to have a significant role in endothelial cell migration, invasion and vascularisation via regulation of receptor protein-tyrosine kinases Ephrin-A3 (Fasanaro et al., 2008, Pulkkinen et al., 2008, Zhang et al., 2012). MicroRNA-126 knockout mice experienced severely delayed vascularization during cranial vessel and retina development, embryonic lethality, loss of vascular integrity and defective angiogenesis (Wang et al., 2008, Kuhnert et al., 2008). In trophoblast, miR-19b and miR-106a have been associated with impaired syncytiotrophoblast differentiation (Kumar et al., 2013). It has been shown that miR-155 inhibits CYR61-mediated expression of VEGF leading to impaired trophoblast migration (Zhang et al., 2010). MicroRNA-155 also directly binds to Cyclin D1 and therefore is directly involved in trophoblast cell cycle progression, migration and invasion (Dai et al., 2012). In addition to miR-210 having a significant role in endothelial function, miR-210 has been shown to regulate migration and invasion capability of trophoblast cells via *in vivo* and *in vitro* validated targets (Zhang et al., 2012). Let-7a, miR-377, miR-145, miR-155, miR-34, miR-141 and miR-200a have been associated with placental development by inhibiting genes regulating trophoblast survival, invasion and proliferation (Forbes et al., 2012, Doridot et al., 2013). Collectively, evidence suggests that multiple miRNAs regulate endothelial and trophoblast phenotype important for placental development.

1.6.1 Dysregulation of miRNA expression may be implicated in preeclampsia pathogenesis

Alterations in the miRNA expression have been linked with many human diseases (Christopher et al., 2016) including cardiovascular disease, liver disease, immune dysfunction, metabolic disorders and cancer (Zhang, 2008, Chai et al., 2013). HIF-1α is known to promote miR-210 expression (Kulshreshtha et al., 2007), which in a hypoxia-induced environment regulates endothelial cell survival, migration and tube formation (Fasanaro et al., 2008, Pulkkinen et al., 2008). Since placental development in early stages is reminiscent of the invasive properties of malignant tumours (Keniry et al., 2012) a good amount of research has been dedicated to explore miRNA-dependent gene regulation during pathological pregnancy.

Many groups investigated miRNA expression profiles in preeclampsia (Table 1.2). The first global transcriptomic analysis of miRNA expression revealed that not only independent miRNAs but also several miRNA clusters are differently expressed in preeclamptic placenta (Zhu et al., 2009a). In addition, several miRNAs were found dysregulated in the preeclamptic serum (Munaut et al., 2016, Xu et al., 2014) highlighting the novelty of them being a promising biomarker for preeclampsia detection (Wu et al., 2012). Serum miR-152, miR-183 and miR-210 were found higher in the second and third trimester of the preeclamptic patients when compared to healthy controls (Li et al., 2015b). Computerised algorithms and alignment programs identified that potential target genes regulated by these miRNAs participate in several signalling pathways, focal adhesion, regulation of the actin cytoskeleton (Choi et al., 2013), placental development, cell differentiation, cell junction, expression of membrane components and cellular response elements (Biró et al., 2017).

Table 1. 2. Major miRNAs reported in preeclampsia.

Upregulated miRNA	Downregulated miRNA	Reference
Preeclamptic placenta		
miR-195, miR-223, miR-218, miR-17, miR-18a, miR-19b1, miR-92a1, miR-379, and miR-411	miR-210, miR-30a-3p, miR-518b, miR-524, miR-17-3p, miR-151, and miR-193b	(Xu et al., 2014)
miR-92b, miR-197, miR-342-3p, miR-296, miR-26b, miR-25, miR-296-3p, miR-26a, miR-198, miR-202, miR-191, miR-95, miR-204	miR-21, miR-223	(Choi et al., 2013)
miR-181a, miR-584, miR-30a-3p, miR-210, miR-152, miR-517*, miR-518b, miR-519e*, miR-638, miR-296, miR-362	miR-101, miR-10b, miR-218, miR-590, miR-204, miR-32, miR-126*, miR-18a, miR-19a, miR-411, miR-377, miR-154*, miR-625, miR-144, miR-195, miR-150, miR-1, miR-18b, miR-363, miR-542-3p, miR-450, miR-223, miR-374	(Zhu et al., 2009a)
miR-3941, miR-155*, miR-455, miR-3143, miR-3928, miR-1204, miR-1183, miR-302c, miR-3186, miR-3616, miR-3670, miR-3200, miR-219-2-3p, miR-423-3p, miR-3157, miR-130b, miR-1915, miR-1197, miR-431, miR-500a, miR-518a, miR-124*, miR-875, miR-1914, miR-383, miR-367*, miR-1305	miR-542-3p, miR-126*, miR-412, miR-544b, miR-3942, miR-3652, miR-548o, miR-516a-3p, miR-885-3p, miR-663b, miR-1248, miR-631, miR-19a*, miR-3943, miR-548w, 103-2*, miR-30a	(Lykoudi et al., 2018)
miR-187, miR-210, miR-1181, miR-943, miR-33b*, miR-466, miR-1238	miR-202, miR-628, miR-488, miR-548u, miR-603, miR-200b*, miR-450b	(Biró et al., 2017)
miR-16, miR-29b, miR-195, miR-26b, miR-181a, miR-335, miR-222		(Hu et al., 2009)
	miR-328, miR-584, miR-139, miR-500, miR-1247, miR-34c, miR-1	(Enquobahrie et al., 2011)
let-7b, miRNA-302*, miRNA-104, miRNA-128a, miRNA-182*, miRNA-133b		(Noack et al., 2011)
miR-26a		(Müller-Deile et al., 2018)
miR-155		(Pineles et al., 2007b, Yang et al., 2017b, Li et

		al., 2014b, Zhang et al., 2012)
miR-210		(Korkes et al., 2017, Pineles et al., 2007b) (Enquobahrie et al., 2011)
miR-431		(Yang and Meng, 2019).
miR-182		(Pineles et al., 2007b)
miR-106a, miR-19b		(Kumar et al., 2013)
miR-122		(Lasabová et al., 2015, Bai et al., 2017)
miR-496	miR-15b, miR-181, miR-210, miR-483	(Mayor-Lynn et al., 2011)
miR-17, miR-20a, miR-20b		(Wang et al., 2012c)
Human umbilical vein endothelial cells from preeclamptic patients		
miR-146a	miR-29a-3p, miR-29c-3p, miR-155	(Zhou et al., 2017) (Cheng et al., 2011)
Preeclamptic plasma or serum		
miR-1304, miR-320a, miR-5002	miR-188-3p, miR-211, miR-4498, miR-4432, miR-3184, miR-92a-2, miR-424-3p, miR-5582-3p, miR-1273c, miR-3171, miR-203a-3p, 5009-3p, miR-892b, miR-5000, miR-107, miR-3649, miR-4482-3p, miR-506, miR-2392, miR-642b-3p, miR-4758, miR-369-3p, miR-4329, miR-3064, miR-188-3p	(Zhong et al., 2019)
miR-1233, miR-650, miR-520a, miR-215, miR-210 miR-25, miR-518b, miR-193a-3p, miR-32, miR-296, miR-204, miR-152	miR-126, miR-335, miR-144, miR-204, miR-668, miR-376a, miR-15b	(Ura et al., 2014)
miR-215, miR-155, miR-650, miR-210, miR-21, miR-518b, miR-29a	miR-18a, miR-19b1, miR-144, miR-15b	(Jairajpuri et al., 2017)
miR-885	miR-376c-3p, miR-19a-3p, miR-19b-3p	(Sandrim et al., 2016)
miR-141 and miR-29a	miR-144	(Li et al., 2013)
miR-155		(Yang et al., 2017b)
miR-210		(Zhang et al., 2012)

The most extensively researched miRNAs in preeclampsia are miR-210 and miR-155. MicroRNA-210 was found upregulated in human severe preeclamptic plasma (Zhang et al., 2012) and placenta (Zhu et al., 2009a). Studies showed that miR-210 is upregulated in murine placenta from mice experiencing preeclampsia-like symptoms (Kopriva et al., 2013). Ephrin-A3 mRNA (Fasanaro et al., 2008, Pulkkinen et al., 2008, Zhang et al., 2012) and transcription factor homeobox-A9 (HOXA9) mRNA (Zhang et al., 2012) have been proposed as miR-210 targets that are known to have a significant role in cellular migration, invasion and vascularisation (Zhang et al., 2012). MicroRNA-210 also plays an important role in the regulation of mitochondrial function (Chen et al., 2010b). It has been shown that metabolic imbalance, excessive ROS production and cell damage caused by mitochondrial dysfunction are associated with the increased miR-210 expression in preeclampsia (Lee et al., 2011, Muralimanoharan et al., 2012). High miR-155 expression was found in isolated HUVECs (Cheng et al., 2011) and maternal plasma (Yang et al., 2017b, Shen et al., 2018) from preeclamptic patients. It was shown that miR-155 binds to CYR61 and Cyclin D1, which regulate trophoblast cell cycle progression, migration and invasion (Zhang et al., 2010, Dai et al., 2012). MicroRNA-155 also plays an important role in the maintenance of vascular integrity via endothelial nitric oxide synthase (eNOS) (Sun et al., 2012, Shen et al., 2018), cGMP-dependent protein kinase 1 (PKG1) (Choi et al., 2018) and angiotensin II receptor 1 (AT1R) (Cheng et al., 2011), which are implicated in pathogenesis of preeclampsia (Li et al., 2014b, Shan et al., 2008). Several other functional studies revealed that miR-26a was found upregulated in preeclamptic placenta and overexpression of miR-26a in zebrafish caused proteinuria, oedema and glomerular endotheliosis (Müller-Deile et al., 2018). MicroRNA-19b and miR-106a have been associated with impaired syncytiotrophoblast differentiation and were overexpressed in preeclamptic placentas (Kumar et al., 2013). Different miR-29 isoforms were found downregulated in HUVECs isolated from preeclamptic pregnancies (Yang et al., 2013, Zhou et al., 2017). Vast amount of evidence suggest that miRNA has a direct impact on physiological pathways involved in pregnancy and that the dysregulation at a molecular lever may be associated with the pathological development of preeclampsia.

1.6.2 MicroRNA as a potential therapeutic strategy

Endogenous miRNA regulates protein expression by targeted gene-silencing (Cai et al., 2017a) and dysregulation of certain miRNAs have been found associated with multiple diseases (Mishra et al., 2016, Christopher et al., 2016, Zhang, 2008, Chai et al., 2013). MicroRNA or small interfering RNA (siRNA)-induced RNA interference (RNAi) mechanism regulates endogenous levels of mRNA and have been proposed for the treatment of many diseases (Lam et al., 2015) including preeclampsia (Turanov et al., 2018, Li et al., 2020).

MicroRNAs and siRNAs have similar physiochemical properties but distinct functions. Both are short RNA duplexes that target mRNA to produce a gene silencing effect. Small interfering RNA is a 21-23 nucleotide duplex having perfect complementarity to one specific target mRNA (Lam et al., 2015). Intracellularly siRNA is loaded to the RISC complex where the passenger strand of the duplex is cleaved by AGO2 with the guide strand remaining in the complex. RISC complex facilitates siRNA attachment to target mRNA and induces endonucleolytic cleavage (Figure 1.2) (Lam et al., 2015). MicroRNA duplex on the other hand, has a partial complementarity to multiple mRNA targets (100 or more at the same time) inducing translational repression and only very rarely degradation or endonucleolytic cleavage of the target mRNA (Kim and Rossi, 2007, Ha and Kim, 2014). These separate properties of miRNA and siRNA distinguishes the therapeutic mode of action and clinical application.

MicroRNA and siRNA have been used for numerous studies to manipulate gene expression and explore therapeutic effect by using many *in vitro* (Justiniano et al., 2013, Li et al., 2020) and *in vivo* models (Koo and Kwon, 2018, Turanov et al., 2018). Synthetically designed siRNA sequence has one mode of action. Intracellularly siRNA elicits RNAi and prevents translation of target mRNA by cleavage (Lam et al., 2015). MicroRNA on another hand, has two modes of action including target miRNA replacement or miRNA inhibition. MicroRNA replacement uses synthetically designed double-stranded miRNA mimics, which are complementary to the target mRNA sequence and replaces abolished endogenous miRNA. This type of miRNA therapeutic allows to restore loss-of-function and mimic the function of endogenous miRNA. MicroRNA inhibition uses synthetically designed single-stranded miRNA inhibitor, which

is complementary to mature miRNA target sequence. It uses the perfect complementarity of the sequence and initiates cleavage of the miRNA sequence resulting in endogenous miRNA function loss (Lam et al., 2015).

MicroRNA therapeutic application has a broader application when compared to siRNA. It has an advantage over siRNA as it is able to simultaneously target multiple mRNAs at once and regulate mRNA expression involved in complex multigenic diseases such as cancers (Mack, 2007) and neurogenerative disorders (Junn and Mouradian, 2012). By targeting multiple genes, miRNA has the ability to regulate a gene network that often works together in the same cellular pathway and change the whole disease phenotype required for effective treatment. In contrast, the therapeutic potential of siRNA is limited to one specific gene. Therefore, siRNA is not fit for purpose to modulate complex diseases, unless multiple siRNA sequences in a single formulation are used to have a clinical significance (Li et al., 2014a).

Specifically designed siRNAs have been shown to target sFlt-1 mRNA and induce effective gene downregulation in pregnant mice (Li et al., 2020, Turanov et al., 2018) and baboon model of preeclampsia (Turanov et al., 2018). Small interfering RNA designed to target sFlt-1 mRNA significantly reduced sFlt-1 levels in the preeclamptic *in vivo* model (Turanov et al., 2018). In addition, siRNA treatment also reduced sFlt-1 levels during normal murine pregnancy (Li et al., 2020, Turanov et al., 2018). It has been suggested that increasing sFlt-1 levels during normal pregnancy may be required for the advancing placental development (Clark et al., 1998, He et al., 1999). Only levels above the certain threshold cause damage associated with high sFlt-1 levels (Bergmann et al., 2010). In addition, RNAi induced by using siRNA-dependent gene silencing has been shown to cause significant target downregulation sustained for at least several months (Nair et al., 2017, Foster et al., 2018). Although, siRNA-dependent inhibition of sFlt-1 translation might be reversed by using synthetic, high-affinity antisense oligonucleotides complementary to the siRNA guide strand (Zlatev et al., 2018), the process requires additional step in the whole process and constant monitoring of time sensitive siRNA-induced toxic side effects (Janas et al., 2018). Further studies are needed to confirm siRNA therapeutic potential in treating abnormal sFlt-1 levels in preeclampsia. MicroRNA mimics on the other hand, offer a reversible one-step gene regulation resulting in transient translational inhibition. Fine-tuned regulatory nature of

miRNA might be more suitable for targeting threshold-sensitive sFlt-1 levels during preeclamptic pregnancy. However, no miRNA to date has been identified to target sFlt-1 *in vivo*.

MicroRNA can be delivered either locally or systematically. Local delivery of miRNAs by injection or topical application allows easy access of the target region and shows reduced toxicity and reduced side effects when compared with systemic delivery (Lam et al., 2015). Systemic administration is associated with poor miRNA delivery (Layzer et al., 2004) as it subjects naked miRNA to poor cellular uptake due to their negative charge and limited stability in blood due to their rapid degradation or inactivation by nucleases (Lee et al., 2019). This results in inefficient intracellular delivery, short half-life in systemic circulation, multiple off-target side effects and innate immune response activation (Fabbri et al., 2013, Krutzfeldt, 2016, Deng et al., 2014c, Chen et al., 2015b). For miRNA to be considered as a therapeutic tool for clinical development, a specific delivery system is required. Viral delivery of miRNAs was shown to be useful in providing overexpression or downregulating properties of target miRNA (Couto and High, 2010, Kumar et al., 2008, Liu et al., 2010). The virus is stripped of all viral proteins (Amalfitano, 1999) to reduce toxicity and prolong transgene expression (Crettaz et al., 2009, Maione et al., 2001). However, viral vectors are known to initiate innate and adaptive immune response (Marshall, 1999). Several chemical modifications to the nucleic acid sequence have been proposed to increase the stability, lower immune response and reduce off-target effects (Watts et al., 2008). Modifications include ribose 2'- OH group modification, locked and unlocked nucleic acids, phosphorothioate modification (Bramsen and Kjems, 2013). For miRNA to be properly loaded to RISC complex to induce effective gene silencing chemical modifications are usually applied to the passenger strand. However, these modifications still possess a risk of poor delivery due to the challenging intrinsic properties of the miRNA including hydrophilic nature, negative charge and high molecular weight.

1.6.3 MicroRNA treatment using nanoparticle-based delivery system

Nanomedicine is the application of the nanomaterials for medical purposes including diagnosis, monitoring, control, prevention and treatment (Tinkle et al., 2014). Nanoparticles refer to a natural or synthetically manufactured material comprising from particles in the size range of 1–100 nm (Bleeker et al., 2013). Nanoparticles can be applied in nanomedicine for controlled drug delivery (nanotherapy), imaging and regenerative medicine (Soares et al., 2018). Continuous development of the nanoparticles allowed advanced treatment strategies to treat various cancers, fungal infections, chronic pain, rheumatoid arthritis, atopic dermatitis, hepatitis and many others approved in EU clinical market (Hafner et al., 2014, Choi and Han, 2018).

The most important attribute of the nanoparticles is their small size and flexibility to modifications. Clinically applicable nanoparticle while in circulation should be stable and inert towards the blood components, protect the payload from systemic degradation, promote controlled release, display reasonable circulation half-life with reduced renal and hepatic clearance rate, should be non-immunogenic and exhibit no or limited toxicity to normal tissues (Baumann and Winkler, 2014, Chen et al., 2015b). Nanoparticles have been shown to protect the nucleic acids from premature nuclease degradation, increase circulation time, reduce the need for chemical modifications, which may affect the specificity and functionality of the RNA molecules, facilitate the cellular uptake and reduce off-target side effects (Yin et al., 2014). Currently there are several types of nanoparticles proposed for miRNA delivery to treat variety of diseases (Lee et al., 2019):

- Synthetic polymers (poly(ethylene imine)s (PEIs), Poly-(lactic-co-glycolic acid) (PLGA), poly(ε-caprolactone) (PCL), and polyurethanes (PUs)). Synthetic polymers are often water-soluble and positively charged allowing easy conjugation with negatively charged miRNA molecules. However, their positive charge and non-biodegradability can affect cell viability.
- Natural polymers that can be obtained from animal or vegetal sources (chitosan, hyaluronic acid). Chitosan is a non-cytotoxic, non-immunogenic, and highly biocompatible. At acidic pH chitosan acquires positive charge and attracts

opposite-charged miRNA molecules, with high loading efficiency. However, their strong interaction with the miRNA results in inefficient unpacking of the complex in the cytoplasm. Hyaluronic acid is a highly hydrophilic anionic natural polysaccharide, which is recognised by hyaluronic acid receptors on the surface of the cells. It is often used as surface modification of the nanoparticles to mask their overall positive charge to reduce cytotoxicity and increase targeted uptake.

- Inorganic nanoparticles (gold, calcium phosphate, silica, iron oxides). Inorganic nanoparticles offer biocompatibility, controllable size and morphology. Iron oxide nanoparticles have been proposed for imaging purposes, as contrast agents for magnetic resonance imaging (MRI) and thermal therapy. Silica nanoparticles exhibit high biocompatibility and stability. Calcium phosphate nanoparticles are nontoxic, bio-resorbable and easily synthesised nanocarriers. Gold nanoparticles offer biocompatibility, easy functionalization, and customisable size and shape. However, a specific surface modification of inorganic nanoparticles is required to provide a linker between the particle and miRNA, which presents a separate set of challenges.
- Lipid-based nanoparticles (liposomes). Liposomes consist of amphoteric lipid molecules (phospholipids) that form spherical, self-closed structures in aqueous media to minimise the entropically unfavourable interaction between hydrophobic chains and aqueous medium. They are thus capable of incorporating both hydrophilic and hydrophobic drugs. Depending on the payload, liposomes can be synthesised as having neutral, positive or negative overall charge by incorporating certain anchor lipid. Liposomes offer flexibility and can be easily customised based on the size, charge and payload preferences. Since, lipids are the main components of the cellular membrane, liposomes are capable of interaction-dependent cellular uptake of their contents. Neutral or cationic liposomes that contain miRNA in the aqueous core, offer protection against degradation, increased stability in blood circulation, prolonged circulation half-life and minimal immune response.

Flexibility and customisation of the nanoparticles make them very attractive nanomaterial for the clinical use. Surface modification and functionalisation optimise and stabilise nanocarriers to fit specific needs associated with miRNA encapsulation (Lee et al., 2019):

- surface modification with poly-arginine is known to enhance cellular uptake
- addition of cationic polymer chitosan, has been shown to promote the retention of miRNAs
- protamine sulfate coating has been used to enhance complexation of miRNAs on the nanoparticle surface
- negatively charged lipids, bile acids or polymers, have been combined with highly positive nanoparticles to facilitate miRNA release and enhance cytoplasmic drug delivery
- surface modification using polyethylene glycol (PEG) is used to increase nanocarrier half-life, biodistribution, reduce toxicity and avoid immune response
- surface functionalisation using specific ligands has been shown to guide nanoparticle to target tissue and reduce off-target side effects

Surface functionalisation using targeting moieties is a very important part of the nanoparticle composition. It allows targeted delivery of miRNA with minimal off-target side effects reducing potentially detrimental consequences (Riehemann et al., 2009). Nanoparticles decorated with guiding/targeting surface moieties allow specific binding to the target cells and facilitate the internalisation via receptor-mediated endocytosis (Scherer et al., 2002). Some most commonly used moieties include:

- antibodies (Meissner et al., 2015)
- nanobodies, which are synthetic proteins that are derived from and possess functional properties of an antibody (Meissner et al., 2015)
- aptamers, which are relatively non-immunogenic short (15 kDa) oligonucleotide sequences that bind to a target with high affinity and specificity
- affibodies, which are small alpha-helical polypeptide ligands that function as inert antibody mimetics (Babu et al., 2014)
- natural polymers such as Chitosan or hyaluronic acid (Lee et al., 2019)
- receptor-specific peptides (Zhou et al., 2016, Zhang et al., 2018b, Cureton et al., 2017)

MicroRNA based nanomedicine is widely used in tissue engineering, cancer therapy and neurodegenerative disorders summarised in Table 1.2. As of 2019, there are seven miRNAs involved in pre-clinical, phase 1 and phase 2 clinical trials including miR-34, miR-92, miR-16, miR-122, miR-29, miR-21 and miR-155 (Hanna et al., 2019). Two

miRNAs are used for direct application, which does not require any modifications or specific delivery to inhibit endogenous miRNA expression and function. Direct intradermal injection to the specific site is used for miR-92 inhibitor (MRG 110) to accelerate wound healing and for miR-29 (MRG-201) to prevent keloid and fibrous scar tissue formation. Other three miRNAs submitted for clinical trials are chemically modified to stabilise nucleic acid sequence when administered intravenously. Modified 15-nucleotide locked nucleic acid–modified antisense oligonucleotide complementary to the 5′ region of mature miR-122 (Miravirsen) is used to treat Hepatitis C. Chemically modified single-stranded oligonucleotide inhibitor is used to inhibit endogenous miR-21 (RG-012) to treat Aport syndrome and to inhibit endogenous miR-155 (Cobomarsen MRG-106) to treat T-cell lymphoma/mycosis fungoides. Two out of seven miRNAs involved in clinical trials are packaged using nanocarrier. Liposomal formulation is used to load miR-34 (MRX34) to treat liver cancer, lymphoma and melanoma. EnGeneIC delivery vehicles (EDV's), which are non-living bacterial minicells (nanoparticles) are used to load miR-16 (MesomiR-1) and treat mesothelioma and lung cancer (Hanna et al., 2019)ClinicalTrials.gov).

Table 1. 3. A summary of nanoparticles used for delivering miRNA for tissue engineering, cancer therapy and neurodegenerative disorders.

Delivery System	Disease	miRNA	Animal Model	Reference
Polyethyleneimine	Colon cancer	miR-145 miR-33a	Mouse xenograft tumour	(Ibrahim et al., 2011)
Polyurethane-polyethyleneimine	Lung cancer	miR-145	Mouse xenograft tumour	(Chiou et al., 2012)
Polyurethane-polyethyleneimine	Glioblastoma	miR-145	Mouse xenograft tumour	(Yang et al., 2012)
Pamam-folic acid	Glioma	miR-7	Mouse xenograft tumour	(Liu et al., 2013)
Hyaluronic acid-chitosan	Breast cancer	miR-34a	Mouse xenograft tumour	(Deng et al., 2014a)
Atelocollagen	Metastatic prostate cancer	miR-16	Mouse xenograft tumour	(Takeshita et al., 2010)
Porous silica nanoparticles with disialoganglioside$_2$ antibody	Neuroblastoma	miR-34a	Mouse xenograft tumour	(Tivnan et al., 2012)
Cationic liposomes	Colon cancer	miR-143	Mouse xenograft tumour	(Akao et al., 2010)
Cationic liposomes	Non-small-cell lung cancer	miR-29b	Mouse xenograft tumour	(Wu et al., 2013)
Neutral lipid emulsion	Non-small-cell lung cancer	miR-34a let-7	Mouse xenograft tumour	(Trang et al., 2011)
Solid lipid nanoparticle	Lung cancer	miR-34a	Mouse xenograft tumour	(Shi et al., 2013)
Solid lipid nanoparticle	Melanoma with lung metastasis	miR-34a	Mouse with lung cancer induced by murine melanoma cells	(Shi et al., 2014)

Lipid protamine hyaluronic	Melanoma with lung metastasis	Combined miR-34a therapy	Mouse with lung cancer induced by murine melanoma cells	(Chen et al., 2010a)
Chitosan	Bone regeneration	miR-199	Rat tibia defect animal model	(Chen et al., 2015a)
Hyaluronan sulfate	Myocardial infarction	miR-21	MI mouse model	(Bejerano et al., 2018)
Poly (lactic-co-glycolic acid) Plga	Bone regeneration	miR-26a	Ovariectomy-induced osteoporotic mouse model	(Zhang et al., 2016b)
Polyketal	Myocardial infarction	miR-106b miR-148b miR-204	MI mouse model	(Yang et al., 2017a)
Gold nanoparticles	Glioblastoma	miR-182	Mouse xenograft tumour	(Kouri et al., 2015)
Cationic liposomes	Hepatic carcinoma	miR-101	Mouse xenograft tumour	(Xu et al., 2017)
Neutral liposomes	Glioblastoma	miR-21 inhibitor	Mouse xenograft tumour	(Costa et al., 2015)
Cationic liposomes	Hepatic carcinoma	miR-122	Mouse xenograft tumour	(Hsu et al., 2013)
Neutral liposomes	Breast cancer	miR-10b inhibitor with paclitaxel	Mouse xenograft tumour	(Zhang et al., 2015)
Neutral liposomes	Angiogenesis	miR-126	Hind limb ischaemia	(Endo-Takahashi et al., 2014)

1.7 Nanoparticle-based treatment for pregnancy complications

More than 60 years ago, over the counter thalidomide use in early pregnancy to treat anxiety, sleeping disturbances and morning sickness caused what is now known a "Thalidomide Disaster". Thalidomide was first released in 1957, West Germany, which was deemed safe and recommended for the use in pregnancy (Miller, 1991). However, its initial enter to the USA market was failed by the FDA due to the lack of anti-teratogenic evidence and was refused for clinical use. Only in 1961 the medication was removed from the European market based on severe teratogenic effects leaving 10,000 children born with severe birth defects of which about 40% died during birth (Miller, 1991, Webster and Freeman, 2001). After this devastating disaster more stringent testing of adverse teratogenic, reproductive and developmental effects were put in place. However, extra testing and strict control over the medication used during pregnancy, left the market severely deprived of the therapeutics required for pregnancy complications, including preeclampsia (Fisk and Atun, 2008). Furthermore, pregnancy complications have detrimental effects on maternal and neonatal health, which presented in the short and long term, place NHS under a massive financial burden (Fisk and Atun, 2008, Goldenberg and Jobe, 2001). Although, therapeutics required to treat pregnancy complications are urgently needed to improve the pregnancy care and to reduce NHS costs, therapeutic gap in the market may sustain for some time due to vigorous testing of potential teratogenic side effects (Fisk and Atun, 2008, Goldenberg and Jobe, 2001) and severely underfunded research (Hahn, 2015).

The biggest challenge in designing a therapeutic to target pregnancy complications is feto-placental transfer. Currently, majority of the drugs that are used to treat nonpregnant patients, are not suitable for use in pregnancy. Some of the drugs are known to cause fetal abnormalities and are categorised as FDA category X. These drugs have potential ability to cross placental barrier, accumulate within the fetal tissues and cause detrimental effects associated with poor fetal development or even fetal death (Black and Hill, 2003). Only handful of medications where maternal benefit outweighs a potential risk for fetal abnormalities are clinically approved and allowed to use in pregnancy. This is because the medication most likely crosses the placental barrier

but possess no to very little risk for the fetal transfer and fetal abnormalities (Black and Hill, 2003). Therefore, successfully designed therapeutic strategy to treat pregnancy-related complications not only has to address the pathological culprit, but also has to be safe for use in pregnancy.

Nanomedicine offers a potentially safe therapeutic strategy to treat pregnancy complications. Depending on the nanoparticle selection, characterisation and surface modifications, treatment using nanocarriers as a delivery system to carry potentially teratogenic agents exhibit very little or no incidental fetal exposure. Valproic acid, an antiepileptic drug, is well-known for its ability to cause fetal malformations when administered freely (Nau et al., 1981). Liposomes encapsulating valproic acid showed no placental transfer to the fetal compartment in an *ex vivo* system of dual placenta model using perfusion of an isolated lobule of term human placenta with maternal and fetal circuits (Barzago et al., 1996). In general transferability of the nanoparticles from placenta to fetal compartment is poor (Menezes et al., 2011) and by using surface functionalised nanoparticles, drugs can be safely delivered specifically to the placenta minimising the side effects associated with off-target organ delivery (Zhang et al., 2019, Figueroa-Espada et al., 2020).

Several surface-functionalised nanoparticles including antibody, aptamer or peptide conjugated liposomes, gold nanoparticles, nanocells and polymers (Zhang et al., 2019, Figueroa-Espada et al., 2020) have been proposed to address placenta-targeted therapeutic shortfall observed in pregnancy complications (Kaitu'u-Lino et al., 2013, Zhang et al., 2018b). One of the first studies exploring targeted nanoparticle delivery used bacterially derived nanocellular EnGeneIC Delivery Vehicles (EDVs). Nanoparticles were conjugated with EGFR antibody due to the high EGFR expression on the placental surface and loaded with chemotherapeutic doxorubicin. Placenta-targeted nanoparticles significantly inhibited trophoblastic tumour growth *in vivo* (Kaitu'u-Lino et al., 2013). Other study used synthetic chondroitin sulfate A binding protein derived from VAR2CSA to decorate the surface of the lipid-polymer nanoparticles. Modified nanoparticles showed trophoblast-specific binding when compared to other cell types in the placenta and other chondroitin sulfate A – expressing cells in other tissues (Salanti et al., 2004, Salanti et al., 2003, Resende et al., 2008). Chondroitin sulfate A decorated lipid-polymer nanoparticles loaded with doxorubicin significantly increased the anti-

cancer activity *in vitro* and inhibited primary tumour growth as well as metastasis *in vivo* (Zhang et al., 2018a). Same nanoparticles loaded with methotrexate significantly impaired placental and fetal development in mouse required for ectopic pregnancy management (Zhang et al., 2018b). Short-chain peptides have proven to be effective in guiding nanoparticles to the placenta. Synthetic peptide CNKGLRNK (Cys-Asn-Lys-Gly-Leu-Arg-Asn-Lys) decorated liposomes showed selective binding to the endothelium of the uterine spiral arteries and placental labyrinth. When loaded with nitric oxide donor and administered to pregnant eNOS null mice, it increased fetal weight and mean spiral artery diameter, improved placental efficiency and diminished placental oxidative stress (Cureton et al., 2017). REDV (Arg-Glu-Asp-Val) peptide modified trimethyl chitosan polyplex was shown to selectively bind to vascular endothelial cells. Due to the cationic charge, biodegradability, biocompatibility and permeability-enhancing properties, polyplex conjugated with miR-126 through a bifunctional PEG provided an efficient vehicle to deliver miRNA-126 specifically to the vascular endothelial cells and enhance cellular proliferation. Therefore, REDV decorated polyplex conjugated with miR-126 could potentially be used to induce rapid endothelialisation required for cardiovascular diseases (Zhou et al., 2016).

Tumour-homing peptides including CGKRK (Cys-Gly-Lys-Arg-Lys) and cyclic peptide iRGD (Cys-Arg-Gly-Asp-Lys-Gly-Pro-Asp-Cys) have been used to modify nanoparticle surface and facilitate anti-cancer drug delivery to the tumour. CGKRK decorated golden nanoparticles conjugated with STAT3 siRNA have been shown to accumulate within the tumour *in vivo* resulting in increased survival of melanoma-bearing mice (Gulla et al., 2018). CGKRK decorated polymers loaded with paclitaxel also showed accumulation within the tumour tissue *in vivo* resulting in reduced tumour size (Hu et al., 2013). iRGD peptide decorated lipid-polymer hybrid nanoparticles linked with doxorubicin and sorafenib reduced tumour weight in hepatocellular carcinoma mouse model (Zhang et al., 2016a).

Growing placenta resembles several characteristics presented by tumours (Ferretti et al., 2007, Keniry et al., 2012). During placental development villous placental cells undergo rapid proliferation, produce a variety of growth factors and cytokines, evade immune surveillance (Ferretti et al., 2007) in addition to migration and invasion of extravillous trophoblasts causing remodelling of the uterine spiral arteries

(Pijnenborg et al., 2006). CGKRK and iRGD tumour-homing peptides bind to calreticulin and integrin α_V receptors, respectively (King et al., 2016, Sugahara et al., 2009), which are highly expressed by the placental tissue (Højrup et al., 2001, Bilban et al., 2009). When administered intravenously, CGKRK and iRGD peptides rapidly accumulated within the mouse and human placenta (King et al., 2016, Beards et al., 2017) showing that the targeting properties exhibited by tumour-homing peptides may be used for placenta-homing delivery. Liposomes decorated with CGKRK or iRGD peptides provided a placental-targeted delivery of the internal liposomal cargo. IGF-2 was then loaded to these placenta-targeted liposomes and used to treat poor fetal outcome in mice bearing *igf-2* knockout. Placenta targeted IGF-2 treatment significantly enhanced placental growth in healthy mice and improved fetal weight distribution in growth-restricted mice with minimal off-target side effects (King et al., 2016). These findings highlight the advantages of placenta-specialised delivery using peptide conjugated liposomes.

Surprisingly, with a huge success rate of the nanoparticle delivery platform, not many studies explored miRNA therapy for pregnancy related diseases. The main focus has been shifted towards miRNA profiling during compromised pregnancy, including identification of certain biomarkers used for potential diagnosis. Multiple studies reported increased miRNA levels associated with the pregnancy complications and the severity of the disease, which was then used to explore potential mRNA target expression mainly using *in vitro* models. It is clear that a research gap exists exploring reduced miRNA expression profiles, which potentially may have a significant contribution towards the pathogenesis of the disease. Surface functionalised nanoparticles have been utilised to deliver miRNA to specialised tissues and proved to have a significant therapeutic effect. Moreover, emergence of placenta-targeted nanoparticles created new opportunities for designing potential treatment strategies to target pregnancy complications. Although, few placenta-targeted nanoparticles were identified, placenta-specific miRNA therapeutics used to treat pregnancy-related complications are still lacking.

Chapter 2

Hypothesis and Aims

2.1 Rationale for the thesis

Therapeutic drugs to prevent or treat preeclampsia are urgently required. The main aim of the thesis is to identify a potential therapeutic strategy to target high sFlt-1 levels observed in preeclampsia. It has been known for over a decade that HO-1 negatively regulates sFlt-1 (Cudmore et al., 2007, Farina et al., 2008, Zhao et al., 2009, George et al., 2011c, McCarthy et al., 2011, Kaartokallio et al., 2014, Zenclussen et al., 2014). Also, several miRNAs dysregulated in preeclampsia (Pineles et al., 2007b, Zhu et al., 2009, Hu et al., 2009) were identified to target sFlt-1 mRNA (Justiniano et al., 2013, Hassel et al., 2012, Korkes et al., 2017). Based on this evidence, we propose that HO-1 regulates sFlt-1 via miRNA-dependent gene silencing. Endothelial cells will be exposed to HO activator and analysed using miRNA array to identify miRNAs directly regulated by HO-1 activity. Upregulated miRNAs will be screened using multiple target alignment softwares to identify miRNAs with a complementary sequence to the sFlt-1 mRNA. Having identified a specific sFlt-1-targeting miRNA, we aim to explore its function and therapeutic effect *in vivo*. Pregnant HO-1 compromised mice will be treated with adenovirus carrying miRNA to determine miRNA-dependent sFlt-1 inhibition and whether it improves fetal outcome. To reduce potential negative effects associated with adenovirus use, we aim to design a placenta-specific liposomal nanocarrier to deliver miRNA with minimal off target-organ accumulation. A surgically induced preeclampsia mouse model (mRUPP) will be treated with placenta-targeted liposomes loaded with the miRNA. It will help to determine therapeutic effect of placenta-specialised miRNA delivery to inhibit pathological sFlt-1 release and improve pregnancy outcome *in vivo* (Figure 2.1).

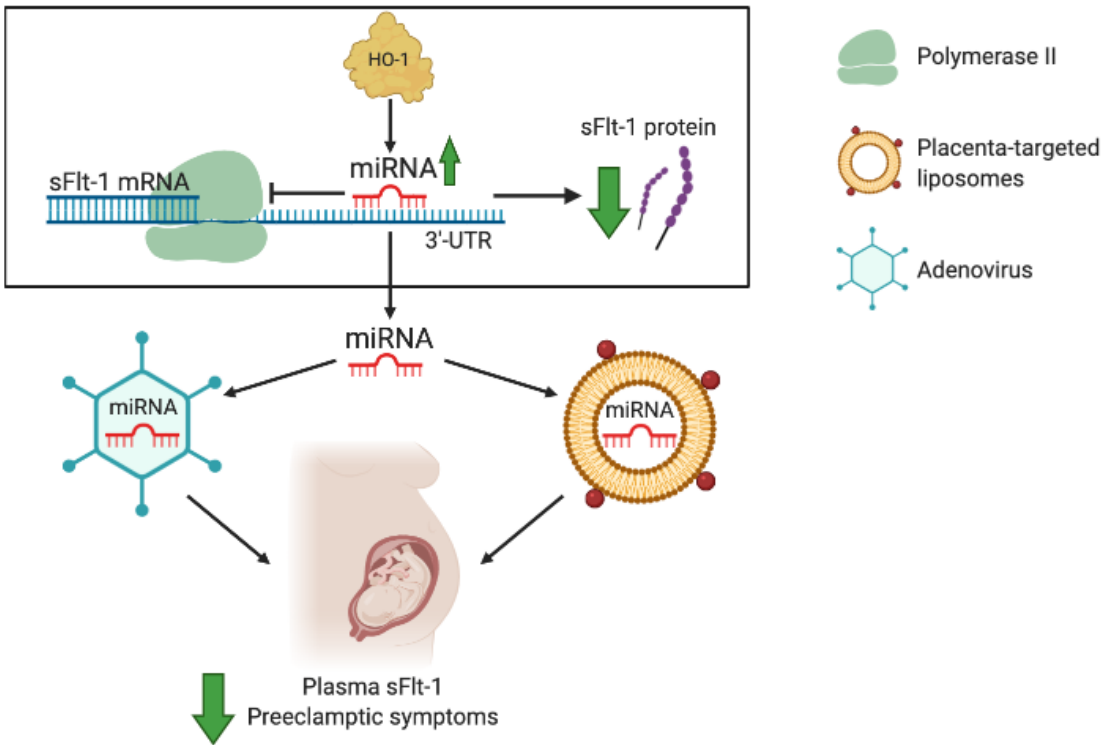

Figure 2. 1. Rationale for the thesis.

Placenta-specific liposomal delivery of miRNA as a potential treatment or prevention for preeclampsia.

2.2 Hypothesis

1. During pregnancy HO-1 negatively regulates sFlt-1 directly via miRNA-dependent gene silencing. Dysregulation of this miRNA may lead to increased sFlt-1 levels observed in preeclampsia.

2. Replacement therapy using adenovirus vector encoding miRNA presents a therapeutic strategy to target high sFlt-1 levels in HO-1 compromised pregnancy.

3. Placenta-specialised nanoparticle delivery of miRNA presents a novel therapy to inhibit abnormal sFlt-1 in preeclampsia.

2.3 Aims

1. To identify miRNA, which is directly upregulated by the induction of HO-1 and has a complementary “seed” sequence to sFlt-1 mRNA.

2. To explore miRNA-dependent sFlt-1 inhibitory effect in human endothelial cells *in vitro* and HO-1 compromised pregnancy *in vivo*.

3. To design placenta-targeted liposomes suitable to encapsulate miRNA and explore its sFlt-1 targeting abilities in human endothelial cells.

4. To determine placental targeting abilities and off-target maternal organ accumulation *in vivo* by using our designed placenta-targeted liposomes.

5. To assess a potential therapeutic effect of placenta-specialised delivery of miRNA to inhibit abnormal sFlt-1 levels and improve pregnancy outcome in preeclamptic model in mouse.

Chapter 3

Materials and Methods

3.1 Materials and reagents

Lipids: L-α-phosphatidylcholine (PC, Avanti Polar Lipids Inc., Cat. # 840051P), 1,2-distearoyl-*sn*-glycero-3-phosphoethanolamine-N-[amino (polyethylene glycol)-2000] (ammonium salt) (DSPE-PEG (2000) Amine, Avanti Polar Lipids Inc., Cat. # 880128P), 1,2-distearoyl-*sn*-glycero-3-phosphoethanolamine-N-[maleimide (polyethy-lenene glycol)-2000] (ammonium salt) (DSPE-PEG (2000) Maleimide, Avanti Polar Lipids Inc., Cat. # 880126P), 3β-Hydroxy-5-cholestene (cholesterol, Sigma-Aldrich, Cat. # C8667).

Nucleic acid sequences and primers: miR-122 mimic (miScript miRNA mimic, hsa-miR-122-5p, Qiagen, Cat. # 219600), AllStars Negative Control siRNA (Qiagen, Cat. # 1027281), siRNA against HO-1 (FlexiTube siRNA, Qiagen, Cat. # 1027420), 6FAM fluorescent miR-122 (Dharmacon, Horizon Discovery, Cat. # CTM-451897), 6FAM fluorescent cel-miR-67 scrambled control sequence (Dharmacon, Horizon Discovery, Cat. # CTM-510607) (Tabl3 3.1). Genotyping primers qPCR primers (IDT, Integrated DNA technologies) (Table 3.3 and 3.7).

Adenovirus and plasmids: control empty adenovirus (Ad-CMV, Vector Biolabs, Cat. # 1300), miR-122 adenovirus (Ad-miR-122, Vector Biolabs), HO-1 adenovirus (Ad-HO-1, Vector Biolabs). Plasmid containing 3'-UTR of sFlt-1 (pmiR-Flt1) and mutant plasmid (pmiR-Flt1-M1) (GeneCopoeia, Cat. # HmiT054531-MT01, MD, USA).

Materials: Primary Human Umbilical Vein Endothelial cells (PromoCell, Cat. # C-12203), Pur-A-Lyzer™ Maxi Dialysis tubing (12-14 kDa MWCO, Sigma-Aldrich, Cat. # PURX12050), 4cm^2 cylindrical cell culture insert (ThincertTM, Greiner Bio-One, Cat. # 662160), positively charged slides (SuperFrost ™, VWR Cat. # 631-0108), QIAshredder spin columns (Qiagen, Cat. #79656), LightCycler® 384-well qPCR multiwell plate (Roche, Cat. # 04729749001), Microvettes CB 300 K2E (Sarstedt, Cat. # 16.444),

Kits: Human miFinder RT2 miRNA PCR Array (Qiagen, Cat. # 331211), Dual-Luciferase® reporter assay system (Promega, Cat. # E1910), P5 Primary Cell 4D-Nucleofector™ X Kit (Lonza, Cat. # V4XP-5024), DuoSet Elisa Kit for mouse VEGFR1/Flt1 (R&D Systems, Cat. # DY471), DuoSet Elisa Kit for human VEGFR1/Flt1 (R&D Systems, Cat. # DY321B), miRNeasy Kit (Qiagen, Cat. #217004), qScript microRNA cDNA Synthesis Kit (Quanta, Cat. NO: 95107-025).

Reagents: RNase-free phosphate-buffered saline (PBS, Invitrogen™, Cat. # AM9624), PBS (Lonza, Cat. No LZBE17-517Q), octaethylene glycol monododecyl ether (C12E8, Sigma-Aldrich, Cat. # P8925), Endothelial Cell Growth Medium 2 (PromoCell, Cat. # C-22211), Endothelial Cell Growth Medium 2 supplement pack (Promocell, Cat. # C-39211), M199 media (Lonza, Cat. # LZBE12-119F), Fetal Bovine Serum (FBS, Gibco, Cat. # 11550356), recombinant ov-Vascular Endothelial Growth Factor-E (VEGF-E, Reliatech, GmbH Cat. # 300-045), QIAzol (Qiagen, Cat. #79306), Thiazolyl Blue Tetrazolium Bromide powder (MTT, Sigma-Aldrich, Cat. # M5655), dimethyl sulfoxide (DMSO, Sigma-Aldrich, Cat. # D4540), 6-carboxyfluorescein (6FAM, Sigma, Cat. # C0662), Trypan Blue (TB, Sigma Cat. # T6146), poly-L-lysine hydrobromide (Sigma-Aldrich, Cat. # P6282), RIPA lysis buffer (Millipore, Merk, Cat. # 20-188), protease inhibitor cocktail (Sigma-Aldrich, Cat. # P8340), phosphatase inhibitor cocktail 3 (Sigma-Aldrich, Cat. # P0044), paraformaldehyde powder (Sigma-Aldrich, Cat. # 158127), wheat germ agglutinin unconjugated (WGA, Vector Laboratories, Cat. # L-1020), VECTASHIELD Antifade Mounting Medium with DAPI (Vector Laboratories, Cat. # H-1200), 1X Reagent Diluent (RD, R&D Systems, Cat. # DY995), Tween® 20 (Sigma-Aldrich, Cat. # P9416), 2% Normal Goat Serum (R&D Systems, Cat. # DY005), sulfuric acid (Sigma-Aldrich, Cat. # 339741), LightCycler® 480 SYBR Green I Master probe (Roche, Cat. # 04707516001), tissue lysis buffer (DirectPCR, Viagen Biotech, Cat. # 102-T), proteinase K (Bioline, Cat. # BIO-37084), GoTaq® Green Master Mix (Promega, Cat. # M7122), agarose powder (Bioline, Cat. # BIO-41025), Nucleic Acid Gel Stain (GelRed®, Biotium, Cat. # 41008), OCT embedding matrix (CellPath, Cat. # KMA-0100-00A), isopentane (Sigma-Aldrich, Cat. # M32631), hemin (Sigma, Cat No. H9039).

Table 3. 1. MicroRNA mimics and siRNA sequences.

Name	Product	Forward (Active)	Reverse (Passenger)
hsa-miR-122-5p	miR-122 mimic	5′-UGGAGUGUGACAAUGGUGUUUG-3′	Not disclosed
hsa-miR-122-5p fluorescent	miR-122 mimic fluorescent	5′-P-UGGAGUGUGACAAUGGUGUUUG-3′	5′-6FAM-AACACCAUUGUCACACUCCA-3′
AllStars Negative Control siRNA	Scrambled	Not disclosed	Not disclosed
Cel-miR-67 fluorescent	Scrambled fluorescent	5′-P-UCACAACCUCCUAGAAAGAGUAGA-3′	5′-6FAM-UACUCUUUCUAGGAGGUUGUGA UU-3′
Cel-miR-39-3p	Spike-in control	Not disclosed	5′-UCACCGGGUGUAAAUCAGCUUG-3′
siHO-1	siRNA against HO-1	5′-GGCAGAGGGUGAUAGAAGAUU-3′	5′-UCUUCUAUCACCCUCUGCCUU-3′

3.2 Equipment

Avanti Mini-Extruder (Avanti Polar Lipids Inc., Alabama, USA), ZetaPlus analyser (Brookhaven Instruments, USA), Particle Solutions V.3.0 software (Brookhaven Instrument, USA), fluorescence spectrophotometer (Tecan Spark Control 10M plate reader, Switzerland), stability cabinet (Firlabo Thermostatic cabinet, France), Amaxa™ 4D-Nucleofector™ electroporator (Amaxa GmbH, Cologne, Germany), flow cytometer (BD Accuri C6, Becton Dickinson Biosciences, USA), Mikro-Tip pressure catheter (Millar, Houston, Texas), LabChart software (ADInstruments Ltd, Oxford, UK), Leica CM1950 cryostat (Leica Biosystems, UK), Nikon Eclipse Ti-E inverted microscope (Nikon Instruments Europe B.V.), NIS-Elements imaging software (Nikon Instruments Europe B.V.), automatic VelociRuptor V2 Microtube Homogeniser (SLS, Cat # SLS1401), NanoDrop™ 2000 spectrophotometer (ThermoFisher, USA), NanoDrop ™ 2000 software 1.6 (ThermoFisher, USA), LightCycler® 480 II Instrument (Roche Molecular Systems, Switzerland), LightCycler® 480 II Software (Roche Molecular Systems, Switzerland), G:Box (Gel Image Analysis Systems, Syngene, India), Syngene software (Gel Image Analysis Systems, Syngene, India).

3.3 Preparation of the liposomes

Neutral PC liposomes were prepared by the ethanol injection method established by Batzri and Korn (1973). To design PC liposomes 8 mM of PC was combined with 0.5 mM DSPE-PEG (2000) Amine, 0.08 mM DSPE-PEG (2000) Maleimide and 4 mM cholesterol dispersed in 0.2 ml ethanol. The combination of lipids was injected to 1 ml of RNase-free PBS buffer with or without 1 nmol of 6FAM fluorescently tagged miR-122 mimics. Liposomes were then extruded through polycarbonate membranes 32 times using Avanti Mini-Extruder. In order to achieve 100 nm sized liposomes and produce evenly sized population, formulation was extruded eight times through a polycarbonate membrane in the order of descending pore size (800 nm × 8; 400 nm × 8; 200 nm × 8; 100 nm × 8). To formulate targeted liposomes, 0.3 µM of fluorescently tagged peptides bearing the N-terminal cysteine moiety TAMRA-CGGGCGKRK (CGKRK) were incubated with the extruded liposomes for 4 hours at room temperature (Figure 3.1). The

incubation allows strong conjugation of free thiol groups on the cysteine residues to maleimide groups on the liposomal surface via a Michael-type addition reaction (King et al., 2016). Ethanol, unencapsulated miR-122 and unconjugated CGKRK peptides were removed via dialysis (Maurer et al., 2001) using Pur-A-Lyzer™ Maxi Dialysis tubes against PBS buffer for 18 hours.

Based on the addition of the peptides and miR-122, four different formulations were produced:

1. empty undecorated PC liposomes (PC-empty)
2. undecorated liposomes loaded with 6FAM (green) labelled fluorescent miR-122 (PC-miR-122)
3. TAMRA (red) fluorescently labelled CGKRK decorated empty PC liposomes (CGKRK-PC-empty)
4. TAMRA (red) fluorescently labelled CGKRK decorated PC liposomes loaded with 6FAM (green) labelled fluorescent miR-122 (CGKRK-PC-miR-122)

Liposomal formulations were transferred to glass vials and stored in the dark at room temperature for further assessments.

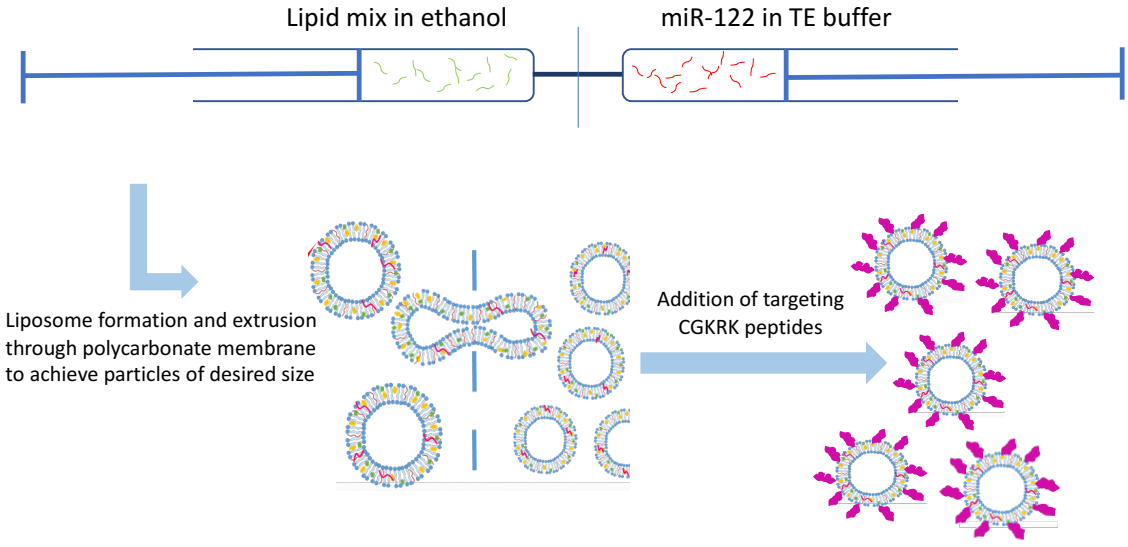

Figure 3. 1. Preparation of the liposomes.

Neutral PC liposomes were prepared by the extrusion method. PC, DSPE-PEG-Amine, DSPE-PEG-Maleimide and cholesterol dissolved in ethanol, dispersed into miR-122 and PBS buffer mix and extruded through multiple membranes. Following extrusion, CGKRK peptides were added to the liposome preparation to design placenta-targeted CGKRK-PC-miR-122 liposomes.

3.4 Characterisation of the liposomes

The relative surface charge of the particles was quantified using zeta potential (ζ), which measures a relative potential difference between cathode and anode probes in the liposomal solution. A clear cuvette was filled with 2 ml of filtered water followed by the addition of the liposomes at 1:100 liposomes to water ratio. Zeta potential was measured using ZetaPlus analyser, which was repeated 3 times and recorded using Particle Solutions V.3.0 software.

Mean particle size (nm) and polydispersity index (PI) of the liposomes were measured by dynamic light scattering. PI measurement is used to determine the homogeneity of the liposomal formulation. PI<0.3 indicates a homogenous liposomal population, whereas PI>0.3 indicates heterogenous liposomal population (Song and Kim, 2006). A clear cuvette was filled with 3 ml of filtered water followed by the addition of the liposomes at 1:50 liposomes to water ratio. Mean liposome size and PI were measured using ZetaPlus analyser, which was repeated 3 times and recorded using Particle Solutions V.3.0 software.

To evaluate the stability of the liposomal formulation, liposomes were stored in stability cabinet (temperature 25°C; humidity 60%) for 21 days. Repeated measurements of mean liposome size and PI were performed on days 1, 7, 14 and 24 using ZetaPlus analyser, which was repeated 3 times and recorded using Particle Solutions V.3.0 software.

3.4.1 CGKRK peptide conjugation efficiency

CGKRK standard curve for the assay was prepared by diluting fluorescently labelled CGKRK (TAMRA-CGGGCGKRK) peptides in serial dilutions in PBS buffer at the range of 0 - 10 µg/ml. To determine CGKRK peptide conjugation, after dialysis 100 µl of CGKRK-PC and CGKRK-PC-miR-122 liposomes in addition to CGKRK standards were added to the black 96-well plate in triplicates. Peptide conjugation efficiency was determined by the TAMRA fluorescence reading at λex 546 nm and λem 579 nm using

fluorescence spectrophotometer. The percentage of conjugated peptides was calculated using the linear equation generated from the calibration curve.

3.4.2 Liposomal entrapment of miR-122

3.4.2.1 MicroRNA-122 encapsulation

MicroRNA-122 standard curve for the assay was prepared by diluting fluorescently labelled miR-122 (miR-122-6FAM) mimics in serial dilutions in PBS buffer at the range of 0 – 1 nmol/ml. To determine miR-122 entrapment efficiency, after dialysis 6 mM of octaethylene glycol monododecyl ether (C12E8) detergent was added to the PC-miR-122 and CGKRK-PC-miR-122 liposomes in 1:1 ratio to disrupt liposomal lipid bilayer and release internal payload. Liposomes were then centrifuged at 16,100 RCF for 30 min to separate and remove the lipids. After the spin, 100 µl of the supernatant in addition to miR-122 standards were added to the black 96-well in triplicates. MicroRNA-122 entrapment efficiency was determined by the 6FAM fluorescence reading at λex 495 nm, λem 517 nm using fluorescence spectrophotometer.

3.4.2.2 MicroRNA-122 retention

To evaluate the liposomal retention of miR-122, after dialysis liposomes were stored in stability cabinet (temperature 25 ± 2°C; humidity 60% ± 5%) for 21 days. At days 1, 7, 14 and 21 a volume of 250 µl of the PC-miR-122 and CGKRK-PC-miR-122 liposomes were transferred to Pur-A-Lyzer™ Maxi Dialysis tubes and dialysed against PBS buffer for 18 hours to remove free miR-122. After dialysis 6 mM of C12E8 detergent was added to the liposomes in 1:1 ratio and then centrifuged at 16,100 RCF for 30 min. After the spin, 80 µl of the supernatant in addition to miR-122 standards were added to the black 96-well in triplicates. To represent miR-122 retention, miR-122 encapsulation was calculated on days 1, 7, 14 and 21 after continuous measurement of 6FAM fluorescence was read at λex 495 nm, λem 517 nm using fluorescence

spectrophotometer. The percentage of miR-122 encapsulated to the PC liposomes was calculated using Equation 3.1.

$$E = \frac{Mt - Ms}{Mt} \times 100\%$$

Equation 3. 1. Formula to calculate the percentage of the liposomal encapsulation efficiency.
E – encapsulation efficiency; *Mt* – total added miR-122 content (nmoles); *Ms* – miR-122 content in supernatant (nmoles).

3.4.3 MicroRNA-122 release from the liposomes

A permeable insert model system was used to assess miR-122 release from PC-miR-122 and CGKRK-PC-miR-122 liposomes over the period of 24 hours. A 4 cm^2 cylindrical cell culture insert lined with a 50 nm pore size membrane was placed in 6-well plate. The insert was filled with 0.3 ml of PC-miR-122 or CGKRK-PC-miR-122 liposomal formulation (donor compartment) followed by 9 ml addition of PBS to the plate (receiver compartment). The plate was incubated at 37°C on a shaker. To determine miR-122 release from the liposomes, 0.5 ml of the solution from the well was transferred to black 96-well plate in triplicates and fresh 0.5 ml PBS was added to the 6-well plate to replace the volume. In addition, miR-122 standards were added to the same black 96-well plate in triplicates. MicroRNA-122 release was calculated at 0.5, 1, 2, 3, 4, 5, 6 and 24 hours after continuous measurement of 6FAM fluorescence was read at λex 495 nm, λem 517 nm using fluorescence spectrophotometer. The percentage of miR-122 release to the receiver compartment was calculated using Equation 3.2.

$$R = \frac{\left(\frac{a \times V}{a+b-c} \times 100\%\right) + \left(\frac{b \times V}{a+b-c} \times 100\%\right) + \left(\frac{c \times V}{a+b-c} \times 100\%\right)}{3}$$

Equation 3. 2. Formula to calculate the percentage of the miR-122 release (R).
V – vessel volume (ml); V_R – replacement volume (ml); a – previous time point cumulative miR-122 release (nmoles); b – observed concentration x V (nmoles); c – previous time point concentration x (V-V_R) (nmoles).

3.5 Cell culture

3.5.1 Human Umbilical Vein Endothelial Cells

Primary Human Umbilical Vein Endothelial cells (HUVECs) were cultured in full growth media supplemented with Fetal Calf Serum (0.02ml/ml), Epidermal Growth Factor (5ng/ml), Basal Fibroblast Growth Factor (10ng/ml), Insulin-like Growth Factor (20ng/ml), Vascular Endothelial Growth Factor 165 (0.5ng/ml), Ascorbic Acid (1µg/ml), Heparin (22.5µg/ml), Hydrocortisone (0.2µg/ml) and 5ml of 1X Penicillin/Streptomycin. Culture medium was changed every 48 hours and cells were incubated at 37°C in a 5% CO_2 humidified atmosphere incubator. Cells were sub-cultured at 70-80% confluency and used for experiments up to passage 5. Cells that reached 70-80% were washed, trypsinised, counted using haemocytometer, centrifuged at 200 x G for 5 minutes at room temperature and plated depending on the treatment. Before each treatment cells were starved using M199 media supplemented with 5% Fetal Bovine Serum and antibiotics for 2 hours. To maintain quiescent state of the cells and ensure consistent results, treatments were diluted in the starvation media unless stated otherwise.

3.5.2 MicroRNA PCR array

MicroRNA expression profiling was performed by Dr Meng Cai using qPCR-based array. HUVEC cells were starved for 2 hours followed by the 10 µM hemin treatment for 24 hours. After the treatment cells were washed, lysed and total RNA was isolated using previously described method (section 3.10.3). Human miFinder RT2 miRNA PCR Array kit was used to identify array of downregulated and upregulated miRNAs. Differentially expressed miRNAs after hemin treatment were demonstrated as a heat map. By using a combination of online bioinformatic tools, miRNA target prediction websites (microRNA.org, miRWalk, miRTarBase) and online database libraries (GeneCards.org and miRbase.org), upregulated miRNAs were scanned against mature sFlt-1 (NM_001159920.2) mRNA sequence to identify complementary miRNA.

3.5.3 Luciferase reporter assay

Luciferase reporter assay was performed by Dr Meng Cai. Firefly luciferase cDNA was fused with 3'-UTR of sFlt-1 (pmiR-Flt1) with the control renilla luciferase gene driven by CMV promoter in the same plasmid. Mutant plasmid (pmiR-Flt1-M1) was generated using site directed mutagenesis technique where two binding sites for miR-122 were mutated from GTCAAAATAGATTATTATAA to GTCAAGAGCAAGGCGCA and from TACAATATTTGTACTATTATAT to TACAATATTTAGACGCGCT. Normal pmiR-Flt1 and mutated pmiR-Flt1-M1 plasmids were used for luciferase assay to confirm miR-122 targeting to 3'-UTR of sFlt-1 mRNA. HUVEC cells were transfected with pmiR-Flt1 or pmiR-Flt1-M1 plasmids with or without miR-122 mimic using previously described method (section 3.5.4.1) and incubated for 24 hours at 37°C in a 5% CO_2 humidified atmosphere incubator. The relative firefly luciferase activity was measured and normalised to the renilla activity according to the manufacturer's protocol of Dual-Luciferase® reporter assay system.

3.5.4 Transfection by electroporation

3.5.4.1 MicroRNA-122 transfection

The transfection protocol for primary HUVEC cells was optimised by the Lonza team specifically for the electroporation using Amaxa™ 4D-Nucleofector™ equipment. HUVEC cells upon being 70% confluent were trypsinised and counted using haemocytometer. To evaluate the most optimal miR-122 amount to induce sFlt-1 inhibition *in vitro*, 1×10^6 cells were counted, aliquoted and centrifuged at 200 x G for 5 minutes at room temperature. Supernatant was removed leaving only the cell pallet. Electroporation was performed using Amaxa electroporator and P5 Primary Cell 4D-Nucleofector™ X Kit. Cell pellet was resuspended with the transfection solution consisting of 18 µl of supplement and 82 µl nucleofection solution. A range of 0 nmoles, 0.25 nmoles, 0.5 nmoles and 1 nmoles of miR-122 mimic were added to the transfection solution, which was then transferred to the cuvette and electroporated using CA-167 program. Cells were immediately transferred to fresh pre-warmed full growth media

and transferred to 12-well plate for overnight incubation at 37°C in a 5% CO_2 humidified atmosphere incubator. Followed by 2 hours starvation, cells were stimulated with VEGF-E (10 ng/ml) for 24 hours at 37°C in a 5% CO_2 humidified atmosphere incubator. In addition, as a positive control for miR-122 treatment, HUVEC cells were treated with hemin (10 µM) in combination with or without VEGF-E (10 ng/ml) and incubated for 24 hours at 37°C in a 5% CO_2 humidified atmosphere incubator. Conditioned media was collected for sFlt-1 ELISA analysis. Cells were washed with PBS and lysed with QIAzol lysis buffer for total RNA (including miRNA) extraction and subsequent RT-qPCR analysis.

3.5.4.2 Heme oxygenase-1 knockdown using siRNA

HUVEC cells upon being 70% confluent were trypsinised and counted using haemocytometer. To determine miR-122 expression in the absence of HO-1, 1×10^6 cells were counted, aliquoted and centrifuged at 200 x G for 5 minutes at room temperature. Supernatant was removed and cells resuspended with the transfection solution followed by the addition of 0.5 nmol of scrambled sequence or 0.5 nmol of siHO-1. The mixture was electroporated, plated as described above (section 3.5.4.1) and incubated for 24 hours at 37°C in a 5% CO_2 humidified atmosphere incubator. Cells were washed with PBS and lysed with QIAzol lysis buffer for total RNA (including miRNA) extraction and subsequent RT-qPCR analysis.

3.5.4.3 Combination of miR-122 and siHO-1 transfection

HUVEC cells upon being 70% confluent were trypsinised and counted using haemocytometer. To determine whether miR-122 acts downstream of HO-1, 1×10^6 cells were counted, aliquoted and centrifuged at 200 x G for 5 minutes at room temperature. Supernatant was removed and cells resuspended with the transfection solution followed by the addition of either: (1) 0.5 nmol of scrambled sequence, (2) 0.5 nmol of siHO-1, (3) 0.25 nmol of miR-122 mimic or (4) combination of 0.5 nmol of siHO-1 and 0.25 nmol of miR-122 mimic (siHO-1/miR-122). The mixture was electroporated, plated and stimulated with VEGF-E (10 ng/ml) as described above followed by incubation for

24 hours at 37°C in a 5% CO_2 humidified atmosphere incubator. Conditioned media was collected for sFlt-1 ELISA analysis.

3.5.5 Adenoviral gene transfer

HUVEC cells upon being 70% confluent were trypsinised and counted using haemocytometer. For adenoviral transduction, 2.5 x 10^5 cells/well were plated to 6-well plate followed by overnight incubation at 37°C in a 5% CO_2 humidified atmosphere incubator. Concentration of the virus amount required for the infection was calculated using Equation 3.3. Serum-starved HUVECs were infected either with control adenovirus (Ad-CMV) or HO-1 adenovirus (Ad-HO-1) at a multiplicity of infection (MOI) of 50 (Table 3.2). Infected cells were incubated for 24 hours at 37°C in a 5% CO_2 humidified atmosphere incubator. Cells were washed with PBS and lysed with QIAzol lysis buffer for total RNA (including miRNA) extraction and subsequent RT-qPCR analysis.

$$V = \frac{MOI \times cells}{stock\ titre}$$

Equation 3. 3. Formula to calculate volume of the virus required for the *in vitro* transduction.
V – volume (ml/well in 6-well plate or ml/ml); MOI – multiplicity of infection; cells – number of cells required for infection (cells/well in 6-well plate or cells/ml); stock titre – stock concentration of the supplied virus (PFU/ml).

Table 3. 2. Adenovirus titre and volume for *in vitro* transduction study.

Adenovirus	Titre	MOI	Cell Density	Volume
Ad-CMV	1 x 10^{11} PFU/ml	50	2.5 x 10^5 cells/well	0.125 µl/well
Ad-HO-1	9 x 10^{10} PFU/ml	50	2.5 x 10^5 cells/well	0.139 µl/well

3.5.6 Cell viability assay (MTT)

HUVEC cells upon being 70% confluent were trypsinised and counted using haemocytometer. For cellular viability assay, 1.5×10^4 cells/well were plated to 96-well plate and incubated for 24 hours at 37°C in a 5% CO_2 humidified atmosphere incubator. Cells were starved for 2 hours followed by the treatment with (1) CGKRK-PC-empty, (2) CGKRK-PC-scrambled and (3) CGKRK-PC-miR-122 liposomes at 1:2, 1:5, 1:10 and 1:100 dilution liposomes to starvation media ratio for 24 hours at 37°C in a 5% CO_2 humidified atmosphere incubator. After incubation, cells were washed with PBS followed by the addition of 80 µl/well serum free M199 media and 20 µl/well of MTT (0.2 mg/ml diluted in sterile PBS) for 4 hours at 37°C in a 5% CO_2 humidified atmosphere incubator. After the incubation the MTT was aspirated and 200 µl/well of DMSO was added for 5 min. Absorbance was measured at 590nm using spectrophotometer. Optical density (OD) reading of "no MTT" blank control was averaged and subtracted from all other values.

3.5.7 Evaluation of liposomal internalization by flow cytometry

To confirm the cellular internalisation of the nanoparticles, PC liposomes were loaded with 12.5µM of 6-carboxyfluorescein (6FAM). HUVEC cells that reached 70-80% confluency were washed, trypsinised and counted. For the flow cytometry analysis, 2.5×10^5 cells/well were aliquoted, centrifuged at 200 x G for 5 minutes at room temperature and seeded in 6-well plate and left overnight. Cells were starved for 2 hours followed by (1) PC-empty, (2) CGKRK-PC-empty, (3) PC-6FAM and (4) CGKRK-PC-6FAM PC liposomal treatment at 1:10 liposomes to starvation media ratio for 6 hours. After the treatment, medium was removed and cells were washed in PBS, trypsinised and resuspended in 3 ml ice-cold FACS buffer (5% FBS in PBS). Clear flow cytometry cuvettes were filled with 1 ml of the cell suspension and analysed using flow cytometer. In order to distinguish internalised microparticles from those attached to the cell membrane, Trypan Blue (TB, 2mg/ml) was added to the already analysed cells suspension to quench the extracellular fluorescence (Patiño et al., 2015). Preselected 1×10^4 events were

analysed before and after the addition of TB. Baseline of the FITC fluorescence was set using untreated control group before and after the addition of TB. Obtained information about microparticle internalization efficiency was expressed as a percentage (%) of the gated cells population.

3.5.8 Cellular uptake studies

3.5.8.1 Cellular localisation of the liposomes

Sterile round coverslips in 18mm diameter were placed in 12-well plate and coated with 200 µl poly-l-lysine (1mg/ml) for 30 min at room temperature. After 30 min, solution was removed by aspiration and rinsed with PBS. To assess the cellular localisation of the liposomes, HUVEC cells that reached 70-80% confluency were washed, trypsinised and counted. For fluorescent imaging, 1×10^5 cells/well were aliquoted, centrifuged at 200 x G for 5 minutes at room temperature, seeded on coverslips and incubated overnight at 37°C in a 5% CO_2 humidified atmosphere incubator. Cells were starved for 2 hours followed by (1) PC-6FAM and (2) CGKRK-PC-6FAM PC liposomal treatment at 1:10 liposomal to starvation media ratio for 6 hours at 37°C in a 5% CO_2 humidified atmosphere incubator. After the treatment cells were washed with 1 x PBS and fixed using 4% paraformaldehyde solution (w/v in PBS) for 15 min at 37°C. After fixing, cells were washed with 3 x PBS and incubated with WGA (5 µg/ml in PBS) to stain the cellular membrane for 10 min at room temperature. After staining, cells were washed with 2 x PBS and one drop of VECTASHIELD Antifade Mounting Medium with DAPI was added to stain nuclei. Coverslip was transferred onto the glass slide and fixed. To preserve the fluorescence all the steps were performed in the darkened environment and slides were stored in the dark at 4°C.

3.5.8.2 Cellular uptake of liposomal miR-122

To assess the cellular uptake of the liposomes, HUVEC cells that reached 70-80% confluency were washed, trypsinised and counted. For the cellular uptake study, 1×10^5 cells/well were aliquoted, centrifuged at 200 x G for 5 minutes at room temperature, seeded to 12-well plate and incubated overnight at 37°C in a 5% CO_2 humidified atmosphere incubator. CGKRK-PC liposomes were loaded with 0.5, 1, 5, 10 and 25 nmoles of 6FAM fluorescently labelled miR-122. Cells were starved for 2 hours followed by the PC liposomal treatment at 1:10 liposomes to starvation media for 6 hours at 37°C in a 5% CO_2 humidified atmosphere incubator. After the treatment, the medium was removed, cells were washed in PBS and lysed with 90 µl ice-cold RIPA lysis buffer supplemented with protease and phosphatase inhibitor cocktail (1:1 ratio) at 1:100 inhibitors to buffer ratio. In order to break down any internalised intact liposomes, 90 µl of C12E8 detergent was added to the cell lysate. A 50 µl of the cell lysate was aliquoted into a black 96-well plate along with previously described miR-122 standards (section 3.4.2.1) in triplicates. Measurement of 6FAM fluorescence was read at λex 495 nm, λem 517 nm using fluorescence spectrophotometer.

3.5.8.3 Functional effect of internalised liposomal miR-122

Following cellular localisation and internalisation studies, CGKRK-PC liposomes were loaded with 1 nmole of non-fluorescently labelled miR-122. HUVEC cells that reached 70-80% confluency were washed, trypsinised and counted. To analyse sFlt-1 release, 1×10^5 cells/well were aliquoted, centrifuged at 200 x G for 5 minutes at room temperature and seeded in 12-well plate and incubated overnight at 37°C in a 5% CO_2 humidified atmosphere incubator. Cells were starved for 2 hours followed by the (1) CGKRK-PC-empty-PC, (2) CGKRK-PC-scrambled or (3) CGKRK-PC-miR-122 PC liposomal treatment at 1:10 liposomes ratio to starvation media for 24 hours hours at 37°C in a 5% CO_2 humidified atmosphere incubator. After the treatment, the medium was collected for sFlt-1 ELISA, cells were washed in PBS and lysed with QIAzol lysis buffer for total RNA (including miRNA) extraction and subsequent RT-qPCR analysis.

3.6 Animal procedures

Animal studies carried out in this study were approved and regulated by United Kingdom Government Home Office in accordance with the "Guidance on the operation of Animals" (Scientific Procedures) Act, 1986, in agreement with Aston University institutional guidelines and regulations for ethical animal use and care. All aspects of animal use and care took into account NC3RS (Replacement, Reduction and Refinement) guidelines and were covered by the Home Office project licence awarded to Dr Shakil Ahmad (PPL number 30/3453) and Home Office personal licence (PL number I634F8EFF). Mice were housed with suitable nesting material and provided with standard pellet chow diet and water ad libitum. Animals were caged under a 12-hour light/dark cycle at 21-23°C with 65 % humidity. Mice were euthanised in accordance with United Kingdom Home Office Animal Act, 1986 with the use of procedures approved by the Aston University Ethical Review Committee.

3.6.1 Genotyping

Maternal ear notches and fetal tail samples were collected and immersed in lysis buffer containing 1:100 Proteinase K (v/v) followed by overnight incubation at 55°C. Enzyme was inactivated at 85°C for 45min and samples centrifuged at 13,000 RPM for 1 min. DNA template was mixed with primers (Table 3.3) and GoTaq® Green Master Mix already containing optimal concentration of GoTaq® DNA Polymerase, dNTPs, $MgCl_2$ and reaction buffer for efficient amplification by PCR (Table 3.4). Amplified DNA together with positive, negative and reagent controls were loaded to 1.5% agarose gel (w/v) in 0.5X TBS containing 1X Nucleic Acid Gel Stain, followed by separation by electrophoresis at 110V. The image of the bands present in the gel was captured by G:Box and analysed with Syngene software. Genotype of the pups was determined by the number and position of the bands (Figure 3.2).

Table 3. 3. Genotyping primer sequences.

Target	Direction	Sequence
Wild-type 1 (WT1)	Forward	GTACACTGACTGTGGGTGGGGGAG
Wild-type 2 (WT2)	Reverse	AGGGCCGAGTAGATATGGTAC
Mutant 1 (MT1)	Forward	GCTTGGGTGGAGAGGCTATTC
Mutant 2 (MT2)	Reverse	CAAGGTGAGATGACAGGAGATC

Table 3. 4. Components of PCR reaction.

PCR Mix	1 Reaction	PCR Running Conditions		
Distilled water	7 µl	1. Denature	95°C	2 min
GoTaq® Green Master Mix	10 µl	2. Denature	94°C	25 sec
Primers: WT1 + WT2	0.5 µl	3. Anneal	54°C	25 sec
Primers: MT1 + MT2	0.5 µl	4. Extension	72°C	1.15 min
DNA template	2 µl	Repeat steps 2 – 4 for 35 cycles		
Final volume	20 µl	5. Final extension	72°C	5 min

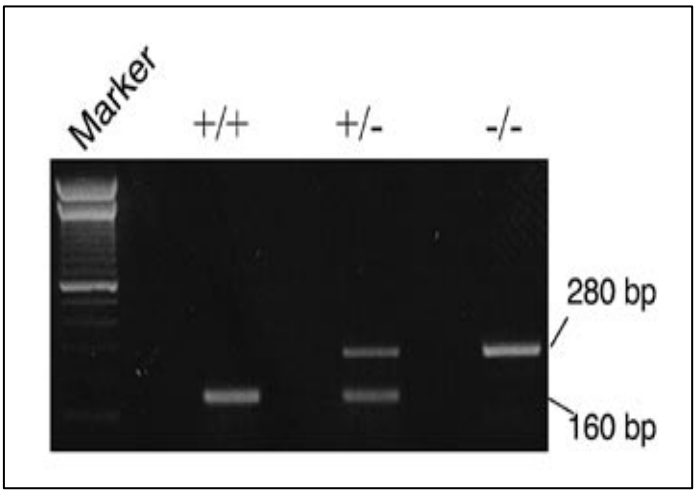

Figure 3. 2. Identification of the fetal genotype.

Wild-type pups present one 160bp band (+/+), HO-1 heterozygous pups present two bands at 160bp and 280bp (+/-) and HO-1 knockout pups (mutant) present one 280bp band (-/-).

3.6.2 Murine reduced uterine perfusion pressure (mRUPP) model

Reduced uterine perfusion pressure (RUPP) surgery is widely used in mice (mRUPP) and rats (rRUPP) to obstruct the blood flow to the fetal arcade which leads to increased blood pressure and placental ischaemia (Granger et al., 2006, Walsh et al., 2009). There are few different types of obstruction including ovarian, uterine and abdominal which may be ligated separately or combined depending on the desired effect and severity of the ischaemia (McCarthy et al., 2011). Based on the validation and optimisation of the mRUPP model in our laboratory, double ovarian ligation was selected for this project. Mice were randomly selected for the mRUPP surgery and at E11.5 were anaesthetised with 2% isoflurane. A mid-abdominal incision was made, and internal organs were taken out and placed on a saline soaked cotton gauze and covered to maintain sterility. Embryonic horn was pulled out and stretched to the sides in order to observe the number and position of the foetuses. The number of live and dead embryos was counted and noted. Using sharp forceps ovarian branch was carefully isolated and silk suture (7/0) was tied around the arterial and venous ovarian vessels distal to the branches of the ovaries. The same ligation was performed on the opposite side (Figure 3.3). Uterine horn together with internal organs were placed back to the original position. The abdominal incision was sutured using Vicryl 6.0 sutures followed by intraperitoneal injection of analgesic buprenorphine (0.05mg/kg). Mice were transferred to a post-operative area and placed on the heated matt. Analgesic injection was repeated every 12 hours for 3 days. Recovery period of 4 days was closely monitored using scoring system.

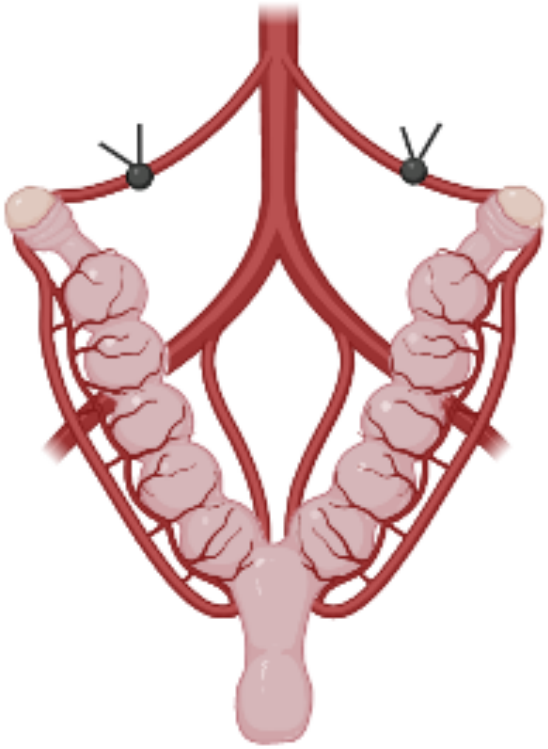

Figure 3. 3. Representative image of the double ovarian mRUPP procedure.

Silk suture was used to tie a double knot on the ovarian branch around the arterial and venous ovarian vessels distal to the branches of the ovaries. The procedure was performed on both sides.

3.6.3 Arterial blood pressure measurement

At E17.5 mice were anesthetised using 2% isoflurane. Arterial blood pressure was measured using Mikro-Tip pressure catheter according to Zhao et al. (2011b) method, which was optimised and adapted for this specific procedure. A 1 to 2 cm incision was made just below the mandible to the thoracic inlet along midline neck. The right carotid artery was then exposed and separated from neighbouring structures, including the vagus nerve. First silk suture (7/0) was used to ligate distal part (towards the head) of the isolated carotid artery. Second silk suture was placed proximally (towards the heart) and tied very loosely to allow temporary blood flow obstruction. Third silk suture was placed in the middle of two ligatures with a loose knot. Small incision was made do the distal part of the artery. Pressure and temperature calibrated Mikro-Tip pressure catheter was inserted via the incision towards the heart and secured with the middle suture. The proximal ligature was then loosened to alleviate the obstruction and catheter was lightly pushed 10mm into the ascending aorta (Figure 3.4). Mean arterial blood pressure (MAP, mmHg), systolic blood pressure (SBP, mmHg), diastolic blood pressure (DBP, mmHg), core body temperature (°C) and heartrate (BPM beats/min) were monitored in real time and recorded using LabChart software. Five minutes were allowed for the arterial blood pressure to stabilise before the actual recording was made over an additional 10 minutes. When the recording was completed, the catheter was pushed back past by proximal suture which was then tightly ligated. Catheter was carefully taken out and submerged in enzyme active tergazyme solution (Alconox). Total blood was collected via the cardiac puncture followed by Schedule 1. Plasma, amniotic fluid and placental tissue were collected and snap-frozen in dry-ice for protein and RNA analysis. Viable births and resorptions were counted followed by fetal and placental weights. Fetal tail clips were collected for the genotypic assessment.

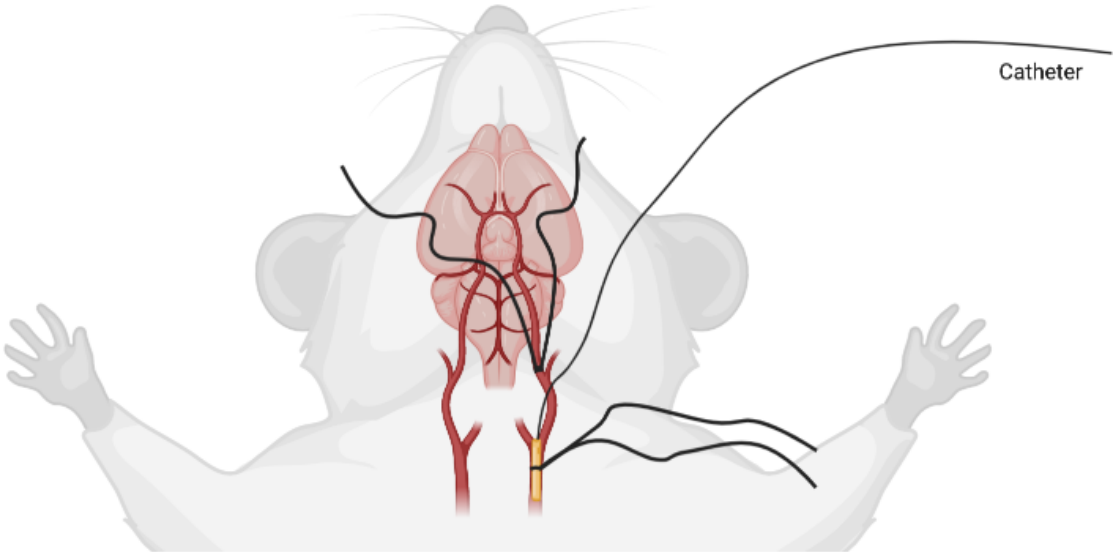

Figure 3. 4. Representative image of carotid artery isolation and arterial blood pressure measurement.

Silk suture was used to ligate distal part of the isolated carotid artery. Small incision was made do the distal part of the artery. Mikro-Tip pressure catheter was inserted via the incision towards the heart and secured with the suture. Once the catheter was secured and operating, it was lightly pushed 10mm into the ascending aorta.

3.6.4 Ad-miR-122 overexpression

HO-1 genetically modified mice were generated according to protocol established by Poss and Tonegawa (1997a). HO-1 heterozygous *Hmox1*$^{+/-}$ (HET) and HO-1 null mice *Hmox1*$^{-/-}$ (KO) possessing loss of both *Hmox1* alleles were sourced by Anupam Agarwal, M.D., The University of Alabama at Birmingham (UAB), USA. HET female mice between the age of 8 – 24 weeks were time-mated with age-matched HET males. The first day of HET pregnancy (E0.5) was defined by the presence of a vaginal plug the following morning. HET pregnancy generates mixed genotypic progeny, which includes *Hmox1*$^{+/+}$, *Hmox1*$^{+/-}$ and *Hmox1*$^{-/-}$ pups.

C57BL/6 wild-type mice (WT) were either bred in house or sourced from Charles River Laboratories. WT female mice between the age of 8 – 24 weeks were time-mated with age-matched WT males. The first day of WT pregnancy (E0.5) was defined by the presence of a vaginal plug the following morning. WT pregnancy generates one genotypic progeny, identified as *Hmox1*^{wt}.

Pregnant WT and HET mice were subjected to the tail bleeds at E5.5, E10.5 and E15.5. No more than 3.5% of total blood volume was collected at the single occasion. Blood was collected using Microvettes and centrifuged at 10000 RPM for 10min at 4°C and stored in -80°C. At E10.5 mice received 100 µl intraperitoneal injection of either empty vector adenovirus (control group, Ad-CMV) or miR-122 expressing adenovirus (Ad-miR-122) diluted in saline at 5 x 10^9 PFU (Table 3.5). For the purpose of clarity, Ad-CMV was highlighted as purple and Ad-miR-122 as green with a theme that remains constant throughout the chapter. On day E17.5 mice were anaesthetised using 2% isoflurane and arterial blood pressure was measured. Total blood was collected via the cardiac puncture followed by Schedule 1. Plasma and placental tissues were collected and snap-frozen in dry-ice for protein and RNA analysis. Fetal outcome was assessed using viable births and resorptions count in addition to fetal and placental weights. *Hmox1*$^{+/+}$ genotype served as an internal control and *Hmox1*^{wt} genotype as an external control. To identify the effect of the treatment, multiple comparisons were statistically performed to *Hmox1*$^{+/+}$ genotypic group.

Table 3. 5. Adenovirus titre and injection volume for *in vivo* treatment study.

Adenovirus	Stock Titre	Injection Titre	Amount in 100 µl Saline	Virus Concentration
Ad-CMV	1 x 10^{11} PFU/ml	5 x 10^{9} IFU	50 µl	5 x 10^{10} IFU/ml
Ad-miR-122	1.7 x 10^{11} PFU/ml	5 x 10^{9} IFU	30 µl	5 x 10^{10} IFU/ml

3.6.5 Placenta-targeted liposomal miR-122 treatment

WT female mice between the age of 8 – 24 weeks were time-mated with age-matched WT males. The first day of WT pregnancy (E0.5) was defined by the presence of a vaginal plug the following morning. To assess CGKRK peptide placenta-targeting properties and off-target maternal organ accumulation of the liposomes, pregnant WT mice received 100µl tail-vein injection of the liposomes on E17.5. Treatment groups included undecorated PC-6FAM and CGKRK-PC-6FAM liposomes. Six hours post treatment mice were anaesthetised using 2% isoflurane and total blood was collected via the cardiac puncture followed by Schedule 1. Placental tissues were collected and snap-frozen using OCT embedding matrix in ice-cold isopentane for the fluorescence imaging.

To assess a potential therapeutic effect of placenta-specialised miR-122 liposomal treatment, mRUPP (section 3.6.2) with the satisfactory post-surgery recovery score (0-3) were randomly selected to receive CGKRK-PC-scrambled or CGKRK-PCmiR-122 liposomal treatment. Twenty-four hours post-surgery mice were restrained followed by 100µl tail-vein injection of the liposomes on E12.5, which was then repeated every second day at E14.5 and E16.5. On day E17.5 mice were anaesthetised using 2% isoflurane and arterial blood pressure was measured (section 3.6.3). Total blood was collected via the cardiac puncture followed by Schedule 1. Plasma and placental tissues were collected and snap-frozen in dry-ice for protein and RNA analysis. Fetal outcome was assessed using viable births and resorptions count in addition to fetal and placental weights.

3.7 Human placental tissue collection and preparation

Institutional Ethics Committee approved the placental tissue collection and written informed consent was obtained for the study: Research into Pregnancy Complications (REC reference: 15/WM/0284; Protocol number: RGP001; IRAS project ID: 171356). All women were followed prospectively from enrolment until delivery. Placental biopsies and blood samples were obtained from pregnancies complicated with preeclampsia (27–34 weeks of gestation) and after elective Caesarean sections from normal pregnancies at third trimester (27–35 weeks of gestation). Samples obtained from preeclamptic pregnancies were age-matched with control healthy pregnancies. Preeclampsia was defined as blood pressure >140/90 mmHg on at least two consecutive measurements and maternal proteinuria of at least 300 mg/24 hours, platelet count <150,000/ml and urate >350 mmol/l. All subjects in the preeclampsia group were investigated in the puerperium to ensure that they were normotensive with no significant proteinuria at 20 weeks postdelivery. Placental tissues were taken from a central location, lying between the basal and chorionic plates and snap-frozen in liquid nitrogen immediately after collection for RNA analysis. Plasma and placental tissues were stored at -80°C for further assessments.

3.8 Fluorescence imaging

Mouse placenta and maternal organs including liver, kidney, spleen, lung and heart embedded in OCT were cross sectioned using cryostat at 5 µm thickness and mounted onto positively charged slides. Mounted slides were fixed using ice-cold methanol for 15 min and washed 3 x times with PBS. One drop of VECTASHIELD Antifade Mounting Medium with DAPI was added to stain nuclei. Slides were covered with cover slip and fixed. To preserve the fluorescence all the steps were performed in the darkened environment and slides were stored in the dark at 4°C.

Tissue cross-section slides and coverslip slides with HUVECs were examined on a Nikon Eclipse Ti-E inverted microscope and images were captured using NIS-Elements imaging software using the same gain and exposure times so that the comparisons

across different treatment groups could be made. GFP filter was used to identify 6FAM fluorescence, mCherry filter was used to identify WGA in coverslips or TAMRA in mouse tissue cross-sections and DAPI filter was used to identify nuclei. All three channels were merged to create an overlay images for localisation studies. Representative images were selected using random sampling from independent areas in the coverslips and placental and maternal organ tissues.

3.9 Enzyme-linked immunosorbent assay (ELISA)

Conditioned media from the cells and serum collected from mice and human patients were used to measure sFlt-1 protein levels. DuoSet Elisa Kits for mouse or human sFlt-1 were used. Stock of capture antibody, detection antibody and recombinant sFlt1 protein were diluted in PBS and the latter two in 1X Reagent Diluent (RD) (Table 3.6).

Table 3. 6. Components of the ELISA assay.

ELISA Kit	**Mouse sFlt-1 ELISA**		**Human sFlt-1 ELISA**	
Dilution	Stock concentration	Working concentration	Stock concentration	Working concentration
Capture Antibody	288 µg/ml	1.6 µg/ml	360 µg/ml	2 µg/ml
Detection Antibody	58.5 µg/ml	0.325 µg/ml	90 µg/ml	0.5 µg/ml
sFlt-1 Standards	140 ng/ml	10 ng/ml	300 ng/ml	8 ng/ml

Half-area 96-well plates were coated with 50 µl/well working concentration of capture antibody and left overnight at room temperature. Standards were prepared by serial dilutions of recombinant sFlt-1 protein in RD. The plate was washed with wash buffer 3 x 0.05% Tween® 20 (v/v in PBS) and blocked with 50 µl/well of RD for 1 hour on a shaker. After incubation the plate was washed with wash buffer 3 x times and loaded with 50 µl/well of standards, plasma or conditioned media samples diluted 1:10 (human plasma 1:50) in RD in triplicates and left for 2 hours in room temperature on a shaker. Mouse detection antibody was prepared 15 minutes prior the incubation in 2% Normal Goat Serum (v/v in RD). Plate washed with wash buffer 3 x times and incubated with 50

µl/well of detection antibody for another 2 hours at room temperature on a shaker. Incubation was followed by the wash with wash buffer 3 x times and 50 µl/well of 1:200 streptavidin-HRP (v/v in RD) was loaded to the plate for 20 min incubation in the dark. Plate was washed with wash buffer 3 x times and incubated with 50 µl/well of substrate reagent (Reagent A and Reagent B at 1:1 ratio) for 20 min on a shaker. The reaction was stopped with 25 µl/well of sulfuric acid and the absorbance was measured at 450 nm with the background correction at 540 nm using spectrophotometer. Optical density (OD) reading of RD was averaged and subtracted from all other values. Concentration of the samples was interpolated from the standard curve non-linear regression ($0.98 < r^2$) using GraphPad Prism software.

3.10 RNA isolation and Reverse Transcription-Quantitative Polymerase Chain Reaction (RT-qPCR)

3.10.1 Tissue preparation for extraction

Human and mouse placental tissues in were weighed (≤30mg) and immersed in QIAzaol lysis buffer containing ceramic beads. Tissues were homogenised using automatic homogeniser in a room temperature. Extended homogenization was performed using QIAshredder spin columns to increase RNA yield from the tissues and incubated in room temperature for 5 min.

3.10.2 Amniotic fluid exosome preparation for extraction

Amniotic fluid (AF) was extracted individually from amniotic sacks at E17.5. To extract exosomes and determine miR-122 expression, AF samples were diluted in equal volume of PBS and centrifuged at 12,000 g x 30 min at 4°C. Supernatant was filtered through 0.22mm sterile filter and filtrate was further centrifuged at 100,000 g x 2 hours. The pellet was resuspended in 200 µl of PBS and spiked with 10 µl of cel mir-39 (5 mol/µl stock).

3.10.3 Total RNA extraction

Total RNA from placental tissue lysates, HUVEC cell lysates and exosomes extracted from amniotic fluid, were extracted using miRNeasy kit. Tissue homogenates, cellular lysates and amniotic fluid exosomes were mixed with 140 µl/sample of chloroform and vortexed. To separate RNA into clear phase homogenates were centrifuged at 12,000 x g for 15 min at 4°C. After separation, the clear phase was transferred into fresh tubes and pure ethanol was added at a volume of 1.5 and thoroughly mixed. Ethanol and RNA mix was transferred to mini spin columns followed by the series of washes with RWT (700 µl/column centrifuged at 8000 g x 15 s) and RPE (500 µl/column centrifuged at 800 g x 15 s and 2 min) buffers. The membrane was dried by centrifuging the column at full speed for 1 min. Total RNA including small non-coding RNAs were eluted with 50 µl/column of RNase-free water in RNase and Nuclease free tubes. Total RNA (ng/µl) concentration was determined by the NanoDrop 2000 spectrophotometer. Total mRNA including small miRNA were reverse transcribed into cDNA using qScript microRNA cDNA Synthesis Kit. For one polyadenylation reaction reagents were mixed and subjected to the first PCR step and immediately incubated on ice (Table 3.7). For one reverse transcription reaction polyadenylation reaction mixture was supplemented with reverse transcriptase and subjected to the second PCR step and incubated on ice (Table 3.7). Complementary DNA (cDNA) was diluted 40X with nuclease-free water and either stored at -80°C or used for real-time qPCR.

3.10.4 cDNA synthesis

Specific forward and reverse primer sequences for mRNA amplification were generated based on the sequences found in the literature. Specific forward primer sequences for miRNA amplification were designed based on the mature miRNA sequence. Reverse primer for miRNA amplification was included within the qScript microRNA cDNA synthesis kit and named as Universal primer. For one qPCR reaction LightCycler® 480 SYBR Green I Master probe was mixed with PCR-grade water and primers to prepare primer master mix (Table 3.8). Forward and Reverse primer (in miRNA case universal primer) are described in Table 3.9. LightCycler® 384-well qPCR

multi-well plate was loaded with primer master mix and cDNA. Real-time qPCR was performed with LightCycler® 480 II Instrument with the pre-defined parameters for optimal amplification and SYBR Green detection. Amplification and melting curve data were generated using LightCycler® 480 II Software.

Table 3. 7. Reagents required for one polyadenylation and reverse transcription reaction.

Polyadenylation Reaction		**PCR Running Conditions**
RNA (ng/µl)	1 µg	1. 60 min at 37°C 2. 5 min at 70°C 3. Immediate incubation on ice
Poly (A) Tailing Buffer (5X)	2 µl	
Poly (A) Polymerase	1 µl	
Nuclease-Free Water	Calculated amount	
Final Volume	10 µl	
Reverse Transcription Reaction		**PCR Running Conditions**
cDNA Reaction Mix	9 µl	1. 20min 42°C 2. 5min 85°C 3. Incubation on ice
qScript Reverse Transcriptase	1 µl	
Total Volume	20 µl	

Table 3. 8. Reagents required for one real-time qPCR reaction.

Real Time - qPCR		**PCR Running Conditions**
LightCycler® 480 SYBR Green I Master probe	5 µl	Automatically predefined by the LightCycler® 480 II Instrument
PCR-Grade Water	3.8 µl	
Forward Primer	0.5 µl	
Reverse Primer (or Universal Primer for miRNA)	0.5 µl	
Final Volume	9 µl	
cDNA	1 µl	
Total Volume	10 µl	

Table 3. 9. Real-time qPCR primer sequences.

Gene	Forward	Reverse
Species	**HUMAN**	
sFlt-1	GGCTGTTTTCTCTCGGATCTC	CCGAGCCTGAAAGTTAGCAA
HO-1	GGGTGATAGAAGAGGCCAAGACT	GCAGAATCTTGCACTTTGTTGCT
Actin	CATGTACGTTGCTATCCAGGC	CTCCTTAATGTCACGCAGGAT
YWHAZ	CCTGCATGAAGTCTGTAACTGAG	GACCTACGGGCTCCTACAACA
TOP-1	TCGAAGCGGATTTCCGATTGA	CTTTGTGCCGGTGTTCTCGAT
Species	**MOUSE**	
sFlt-1	ATGCGTGCAGAGCCAGGAAC	GGTACAATCATTCCTCCTGC
HO-1	CGCCTTCCTGCTCAACATT	TGTGTTCCTCTGTCAGCATCAC
Actin	GCTCGTCGTCGACAACGGCTCCGGC	CAAACATGATCTGGGTCATCTTCTCGCGG
YWHAZ	TGAGCTGTCGAATGAGGAGAG	CCTCCACGATGACCTACGG
TOP-1	GACCATCTCCACAACGATTCC	ATGCCGGTGTTCTCGATCTTT
Species	**HUMAN / MOUSE miRNA**	
miR-122	TGGAGTGTGACAATGGTGTTTG	Universal
RNU6	GCAAATTCGTGAAGCGTTCC	Universal
RNU48	AGTGATGATGACCCCAGGTAACTC	Universal
RNU44	GCAAATGCTGACTGAACATGAA	Universal

3.10.5 Relative expression analysis

Primer-specific target amplification was verified by melt curve analysis (Figure 3.5). Optimization of reaction conditions including annealing temperatures and the concentration of the qPCR reaction components were performed in-house to ensure optimal qPCR reaction and consistent results. Efficiency of the amplification (*E*) reaction was calculated automatically by the software using standard curve method (Equation 3.4), which is usually represented in percentage (Equation 3.5). Standard curve with an efficiency as close as possible to *E* = 2 (number of target molecules doubles with every amplification PCR cycle), slope between -3.9 and -2.9 (optimal slope for standard curve -3.32) and $r^2 \geq 0.98$ (Figure 3.6) were used as standard parameters.

$$E = 10^{-1/slope}$$

Equation 3. 4. The formula is used to calculate amplification efficiency (*E*) from the slope of the standard curve.

$$\%\, Efficiency = (E - 1) \times\ 100\%$$

Equation 3. 5. The formula used to calculate percentage of amplification efficiency (*E*).

The noise band was adjusted manually, whereas the threshold line was set automatically by the software based on standards to minimize error calculations. Cycle threshold (C_T) values were calculated using Absolute Quantification – Fit Points method by the LightCycler® 480 II Software. Relative expression was calculated using basic $\Delta\Delta C_T$ method and expressed as fold-change ($2^{-(\Delta\Delta CT)}$) using Equation 3.6.

$$\Delta C_T = C_T\,(gene\ of\ interest) - C_T(reference\ gene)$$

$$\Delta\Delta C_T = C_T\,(test\ samples) - C_T\,(control\ sample)$$

$$Relative\ expression = 2^{-(\Delta\Delta C_T)}$$

Equation 3. 6. Calculations used to determine relative expression of the gene of interest.
ΔC_T is calculated to determine the change between the gene of interest and the reference gene. $\Delta\Delta C_T$ is calculated to determine the change between the experimental samples including test sample and control sample. Assuming 100% amplification efficiency (E = 2), $2^{-(\Delta\Delta CT)}$ calculation is used to determine the relative expression of the change.

Actin, TOP-1 and YWHAZ reference genes (Cleal et al., 2009, Drewlo et al., 2012, Kaitu'u-Lino et al., 2014, Meller et al., 2004, Patel et al., 2002) for mRNA and RNU6, RNU44 and RNU48 (Enquobahrie et al., 2011) for miRNA expression were tested each time for a different set of experiments. Most stable and consistent candidate was used for calculations and specified in figure legends.

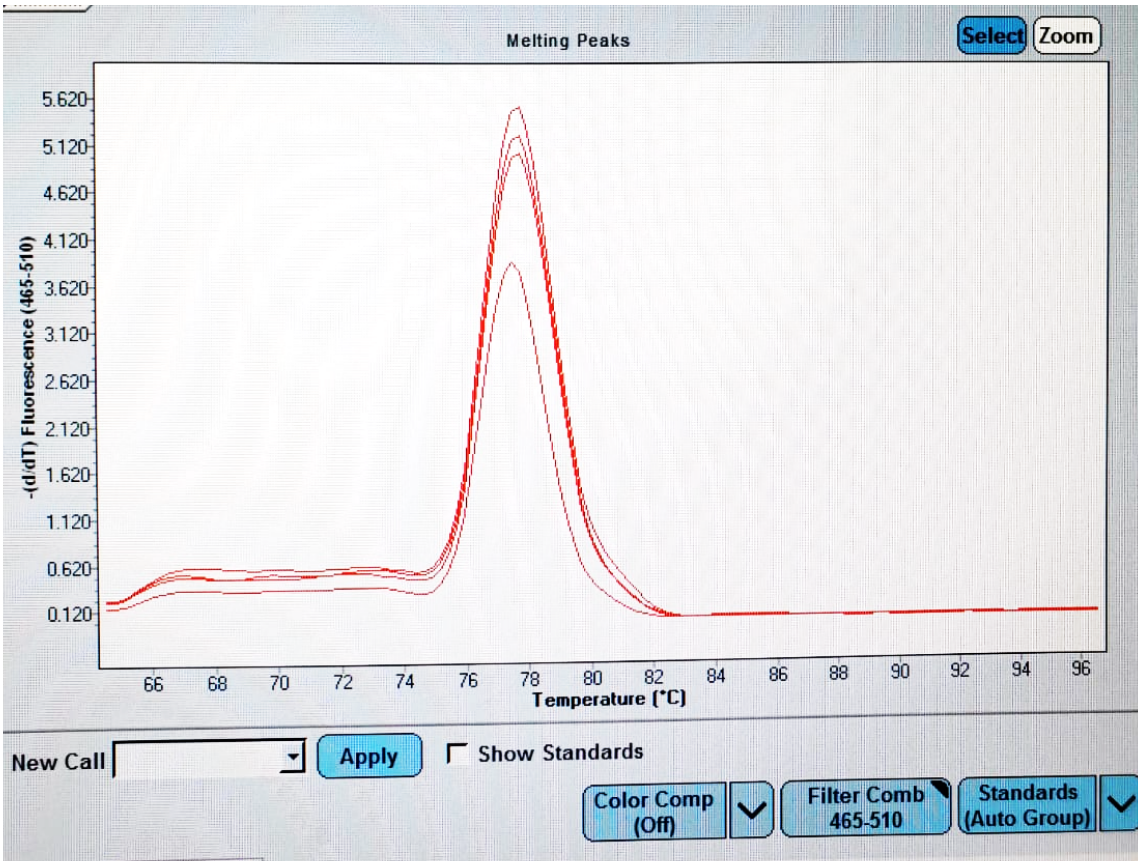

Figure 3. 5. Melting curve genotyping represented as melting peaks.

Primer-specific target amplification was verified by melt curve analysis and the appearance of the melting curve

.

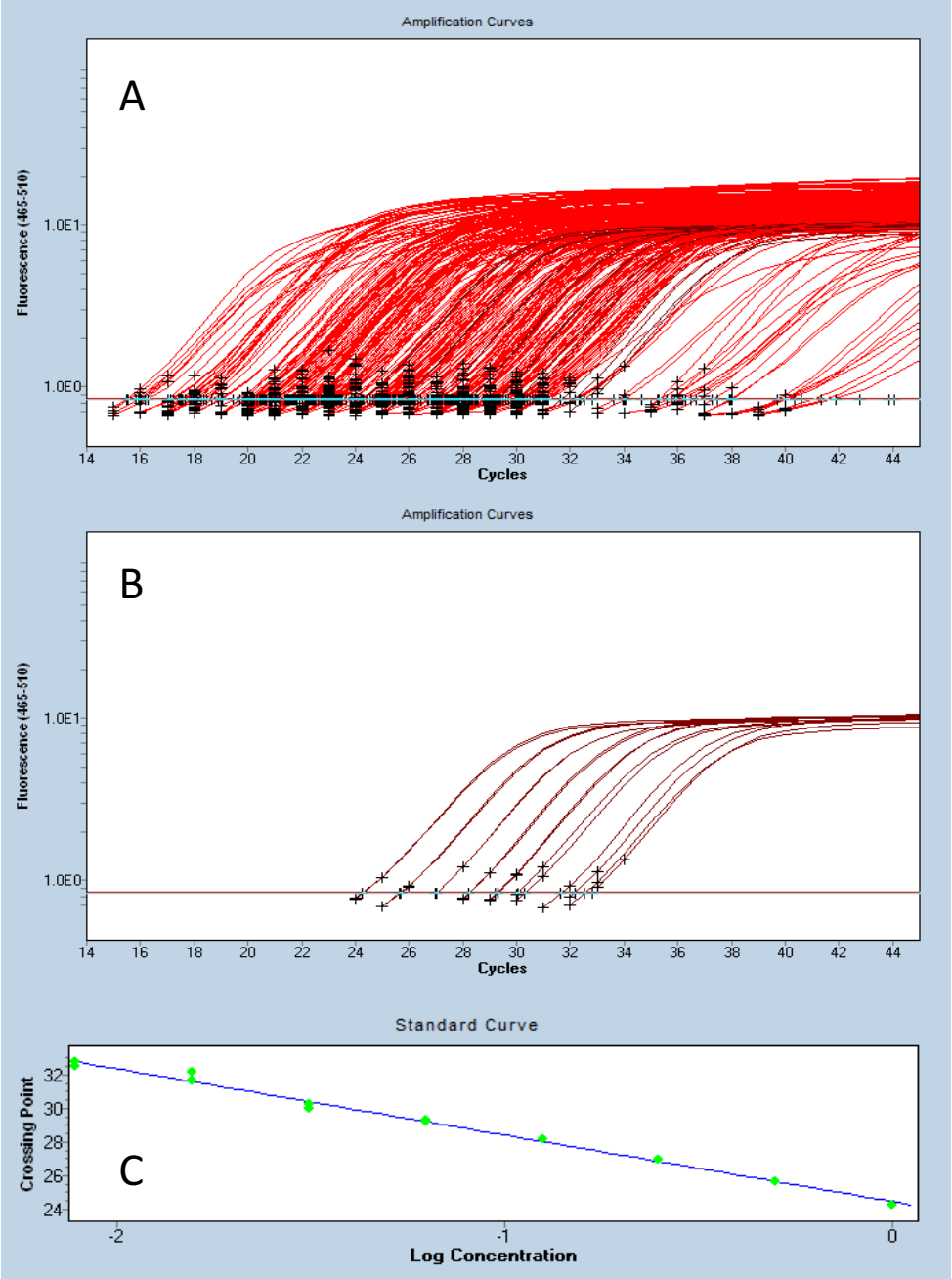

Figure 3. 6. Absolute Quantification – Fit Points method used to calculate Cycle threshold (C_T) values by the LightCycler® 480 II Software.

(A) Fluorescent detection and representation of amplification curves of the samples. **(B)** Fluorescent detection and representation of amplification curves of the standards with automatic threshold of 0.8339. **(C)** Efficiency of the amplification (*E*) reaction was calculated by using standard curve method: *E* = 1.783 and slope -3.983.

3.11 Statistical analysis

Statistical analysis was performed using GraphPad Prism 8 software. All experimental studies included three biological replicates as well as three technical replicates. It is a pilot study, therefore, all gathered data in this project will be used to establish a priori statistical power for further work. Technical replicates were averaged before performing statistical analysis and biological replicates expressed as mean ± SEM. If appropriate, outliers were removed using ROUT method with the Q=1% separately for each experimental group. The assumption of population distribution of the data was taken into consideration with 8 and more samples, otherwise population with less than 8 samples was assumed as not normally distributed. To evaluate the nature of the statistical test to be performed, distribution of 8 and more samples were plotted to:

1. calculate mean and median
2. determine the difference between mean and median
3. visually observe frequency distribution of the data by the histogram
4. test if the data is normally distributed (Gaussian) by D'Agostino-Pearson omnibus test and Shapiro-Wilk normality test
5. perform parametric test (normal distribution) or non-parametric (not normal distribution) test.

Statistical test performed for each experiment is stated individually in the figure legends. An Unpaired Student t or Mann-Whitney test was used to determine any statistically significant differences between the means of two independent groups with a significance threshold of 5% (or $P<0.05$). A One-Way Analysis of Variance (ANOVA) or Kruskal-Wallis test was used to determine any statistically significant differences between the means of three or more independent groups. When appropriate ($P<0.05$) this was followed by *post hoc* multiple comparisons test to assess differences between the groups. The statistical significance of two independent variables on multiple experimental groups was analysed using Two-Way ANOVA and when appropriate ($P<0.05$) this was followed by *post hoc* multiple comparisons test to assess differences between the groups. Multiple comparisons were made posteriori of the study, therefore a significance threshold of 5% ($P<0.05$) was applied to the entire family of comparisons

rather than to an individual comparison. P values reported in this study are multiplicity adjusted with the power of significance indicated by an asterisk (*). The nature of comparisons and sample size are stated in the figure legends separately.

Chapter 4

Inhibitory role of miR-122 in suppressing sFlt-1 in preeclampsia

4.1 Highlights

- MicroRNA-122 binds to 3'-UTR region of mature sFlt-1 mRNA and inhibits VEGF-E-induced sFlt-1 release in human endothelial cells
- MicroRNA-122 acts downstream of HO-1
- MicroRNA-122 expression in placenta inversely correlates with high plasma sFlt-1 levels found in human and mouse model of preeclampsia
- Poor pregnancy outcome in HO-1 compromised murine pregnancy is associated with low miR-122 placental expression and high serum sFlt-1 levels
- Adenovirus induced overexpression of miR-122 in placenta inhibits abnormal sFlt-1 levels, improves fetal weight and fetal:placental weight ratio in HO-1 compromised murine pregnancy while having no effect in normal pregnancy
- High expression of miR-122 positively affects fetal survival in both normal and HO-1 compromised pregnancy

4.2 Summary

Preeclampsia is the leading pregnancy related complication worldwide with no cure. HO-1 has been shown to negatively regulate sFlt-1 release. Low HO-1 and high sFlt-1 levels may be responsible for the development of the preeclampsia. However, the exact mechanism how HO-1 inhibits sFlt-1 is unknown. Here we show that preeclamptic patients with increased plasma sFlt-1 levels exhibit decreased miR-122 expression in the placenta. We identified that miR-122 has a sequence complementarity to sFlt-1 mRNA and inhibits sFlt-1 release in human endothelial cells. Adenovirus induced miR-122 expression in HO-1 compromised mouse placenta leads to effective inhibition of plasma sFlt-1 and improves fetal outcome. Increased miR-122 expression in wild-type placenta has no effect on normal sFlt-1 levels and fetal outcome highlighting pathology-specific miR-122 regulation. Evidence presented here shows a therapeutic miR-122 potential to prevent or treat preeclampsia.

4.3 Graphical Abstract

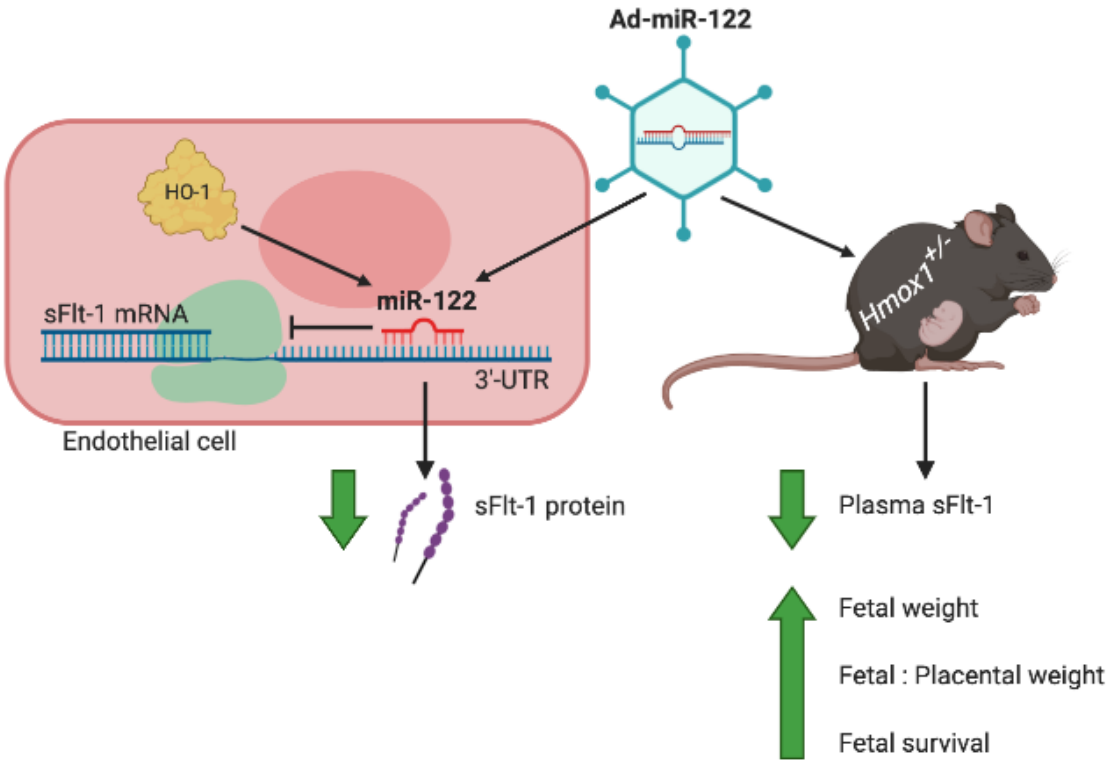

4.4 Introduction

Preeclampsia is a systemic *de novo* hypertensive disorder of pregnancy and a major contributor to neonatal and maternal morbidity and mortality (Huppertz, 2008, MacKay et al., 2001, World Health Organisation, 2005). The only effective method to relieve preeclamptic symptoms is the premature delivery of the baby and the removal of the placenta. If this intervention is not addressed on time, ongoing preeclamptic pregnancy will progress to a potentially life-threatening end-stage disorder of eclampsia.

It has been extremely challenging to find a treatment for preeclampsia. The aetiology of preeclampsia is unknown, and the condition is often referred to as a "disease of theories" because the understanding has been, in the most part, limited to observational studies after the event. Over two decades ago it was suggested that the loss of VEGF activity, possibly due to a rise in endogenous soluble form of VEGF receptor-1 (sFlt-1), may be a key event linked to the pathogenesis of preeclampsia (Ahmed, 1997). Now the culprit protein has been experimentally confirmed in both clinical prospective and in animal studies. Multiple studies showed that preeclamptic patients experience increased sFlt-1 levels in amniotic fluid (Vuorela et al., 2000), plasma or serum (Koga et al., 2003, Levine et al., 2004, Buhimschi et al., 2006, Crispi et al., 2006, Ramma et al., 2012), urine (Buhimschi et al., 2006) and placenta (Clark et al., 1998, Ahmad and Ahmed, 2001, Maynard et al., 2003), which dramatically drop within the 48 hours postpartum supporting the notion that the placenta is the major source of maternal sFlt-1 (Chaiworapongsa et al., 2004, McKeeman et al., 2004). In *vivo* studies showed that, anti-VEGF antibodies and recombinant sFlt-1 injected to healthy mice induced glomerular endothelial cell damage and hypertrophy leading to proteinuria (Sugimoto et al., 2003). Transduced blastocysts with lentiviral vector overexpressing sFlt-1 resulted in hypertensive pregnancy accompanied by the proteinuria and intrauterine growth restriction (Kumasawa et al., 2011). Administered adenovirus overexpressing sFlt-1 to pregnant rats and mice resulted in hypertension, proteinuria and glomerular endotheliosis (Maynard et al., 2003, Bergmann et al., 2010). On the other hand, removal of placental sFlt-1 by immunoprecipitation restored angiogenesis (Ahmad and Ahmed, 2004) and removal of circulating plasma sFlt-1 in human patients by apheresis with a

plasma-specific dextran sulfate reduced proteinuria, improved blood pressure and prolonged pregnancy (Thadhani et al., 2011, 2016). *In vivo,* VEGF treatment neutralised free circulating sFlt-1 below critical threshold and resolved sFlt-1 dependent damaging effects (Bergmann et al., 2010). Soluble Flt-1-targeting siRNAs injected to baboon preeclampsia model alleviated hypertension and proteinuria (Turanov et al., 2018). Therefore, excessive amount of sFlt-1 in preeclampsia as a stand-alone factor underlies the importance of the VEGF bioavailability, angiogenic balance and endothelial integrity.

HO-1 is critical for the successful outcome of the pregnancy (Bainbridge and Smith, 2005). Since pregnancy state is associated with oxidative stress and inflammation, it has been proposed by Ahmed et al. (2000) and other investigators that vascular protective factors such as HO-1 regulate oxidative stress and inflammation associated with healthy pregnancy and that the lack of such compensatory systems may lead to pregnancy complications including preeclampsia (Ahmed et al., 2000, Gozzelino et al., 2010, Otterbein et al., 2000a, Soares and Bach, 2009). A significant reduction in HO-1 protein (Ahmed et al., 2000, Lyall et al., 2000, Barber et al., 2001) was shown in the damaged infarcts of the placenta (Lash et al., 2003) and preeclamptic placenta in addition to decreased HO-1 mRNA found in the circulation (Nakamura et al., 2009). Importantly, HO-1 mRNA levels in preeclamptic placenta were found decreased as early as 11 weeks of gestation before the clinical onset of the disorder (Farina et al., 2008). Polymorphisms in microsatellite repeat located in the promoter region of *Hmox1* has been linked to higher risk of developing preeclampsia (Kaartokallio et al., 2014, Kaartokallio et al., 2018). Experiments looking at the restored HO-1 expression and activity showed that overexpression of HO-1 or treatment with carbon monoxide (CO), a HO-1 metabolite, attenuated sFlt-1 increase in human endothelial cells, whereas pharmacological inhibition of HO-1 promoted sFlt-1 release in not only endothelial cells but also normal and preeclamptic villous placental explants (Cudmore et al., 2007). Subsequent studies demonstrated that HO-1 induction and both CO and bilirubin can decrease hypoxia-induced sFlt-1 in rat placental explants, supporting a possible role for HO-1 in the suppression of sFlt-1 (George et al., 2012). Collectively, the evidence suggests that low HO-1 and high sFlt-1 may be responsible for the development of the preeclampsia (Ahmed and Ramma, 2015b) and the important role of negative HO-1-dependent regulation of sFlt-1. However, the exact mechanism how HO-1 inhibits sFlt-1 is unknown.

MicroRNA (miRNA) is approximately 20 nucleotides long, small non-coding RNA which binds to 3'-untranslated region (UTR) of the target mRNA with a partial complementarity leading to the translational repression (Cai et al., 2017a, Bartel, 2004). It has been shown that miRNAs are involved in the regulation of many developmental, physiological and pathological processes (Cai et al., 2017a, Bartel, 2004). Vast amount of evidence suggest that miRNA has a direct impact on physiological pathways involved in pregnancy and that the dysregulation at the molecular level may be associated with the pathological development of the preeclampsia (Pineles et al., 2007a, Zhu et al., 2009b, Hu et al., 2009). Since, sFlt-1 is a pivotal factor in the pathogenesis of preeclampsia (Ahmed et al., 1997, Maynard et al., 2003), few studies highlighted that the expression of sFlt-1 may be regulated by miRNAs (Eubank et al., 2011, Roybal et al., 2011). Based on the online prediction tool, miR-181a was suggested to target sFlt-1 mRNA. When peripheral blood monocytes were transfected with synthetic miR-181a mimic it reduced sFlt-1 protein production by 30% (Justiniano et al., 2013). In addition, miR-10 was shown to bind to 3'-UTR of sFlt-1 mRNA. Deficiency of miR-10 resulted in the increased sFlt-1 protein levels in HUVEC cells (Hassel et al., 2012). Interestingly, miR-210 was found upregulated in preeclampsia and a strong correlation between miR-210 and sFlt-1 was identified in preeclamptic placentas (Korkes et al., 2017). Since sFlt-1 mRNA structure differs from full-length Flt-1 in 3'-UTR region, it makes it a perfect candidate for miRNA-dependent regulation without affecting the full-length Flt-1.

Based on the evidence described, we hypothesise that HO-1 regulates sFlt-1 expression via miRNA-dependent gene silencing, which may provide a potential therapeutic strategy to treat abnormal sFlt-1 levels observed in preeclamptic setting. To test the hypothesis, human umbilical vein endothelial cells (HUVEC) were stimulated with well-known HO-1 inducer, hemin. Upregulated miRNAs were screened against mature sFlt-1 mRNA sequence to identify a suitable candidate. Synthetic double-stranded miRNA mimic was designed containing passenger strand and active guide strand, which allow for it to be loaded to the RISC complex and induce silencing of the target mRNAs by either translational repression or degradation (Lam et al., 2015). Selected miRNA was then tested *in vitro* to explore the link between HO-1-dependent miRNA regulation of sFlt-1. To identify a potential therapeutic effect of the selected miRNA to inhibit sFlt-1 expression, adenovirus encoding the miRNA sequence was injected to HO-1 heterozygous mice.

4.5 Results

4.5.1 Overexpression of miR-122 downregulates sFlt-1 in human endothelial cells

Up-regulation of HO-1 negatively regulates sFlt-1 release in endothelial cells (Cudmore et al., 2007) however, the mechanism is unknown. We hypothesised that HO-1 regulates sFlt-1 expression via miRNA-dependent gene silencing. To test this hypothesis, HUVECs were exposed to a well-known HO-1 inducer, hemin (Dulak et al., 2002). MicroRNA array analysis identified 24 upregulated and 26 downregulated miRNAs (Supplement A Figure 1 A and B), which were demonstrated in a heat map (Figure 4.1 A). By using a combination of online bioinformatic tools, miRNA target prediction websites (microRNA.org, miRWalk, miRTarBase) and online database libraries (GeneCards.org and miRbase.org), upregulated miRNAs were scanned against mature sFlt-1 (NM_001159920.2) mRNA sequence. We identified miR-122 as a potential candidate with a partial complementary to 3'-UTR of sFlt-1 mRNA (Figure 4.1 B). To confirm the theoretical prediction, a luciferase reporter assay was performed. Plasmids bearing luciferase promoter region and sFlt-1 3'UTR sequence or a mutant sFlt-1 3'-UTR sequence were designed and transfected into HUVEC cells with or without miR-122. Cells that received a combination of normal plasmid bearing sFlt-1 sequence and miR-122 had a significantly reduced luciferase activity, whereas no changes in luciferase activity was detected in cells co-transfected with mutant sFlt-1 plasmid (Figure 4.1 C). This suggests that miR-122 regulates sFlt-1 by directly targeting sFlt-1 3'UTR region.

To confirm the physical capability of miR-122 to downregulate sFlt-1, HUVEC cells were stimulated with VEGF-E followed by the transfection with miR-122 mimic. As a positive control, HUVECs were stimulated with VEGF-E in combination with hemin to inhibit sFlt-1 release (Supplement A Figure 3). Transfection efficiency and increased miR-122 expression was analysed by RT-qPCR (Figure 4.1 D), which confirmed miR-122 mimic as a reliable candidate for a transfection assay. VEGF-E induced sFlt-1 in dose-dependent manner (Supplement A Figure 2) and the lowest concentration of mimic (0.25 nmoles) significantly downregulated VEGF-E-induced sFlt-1 release from endothelial cells (Figure 4.1 E). The amount of 0.25 nmoles was therefore selected for subsequent experiments.

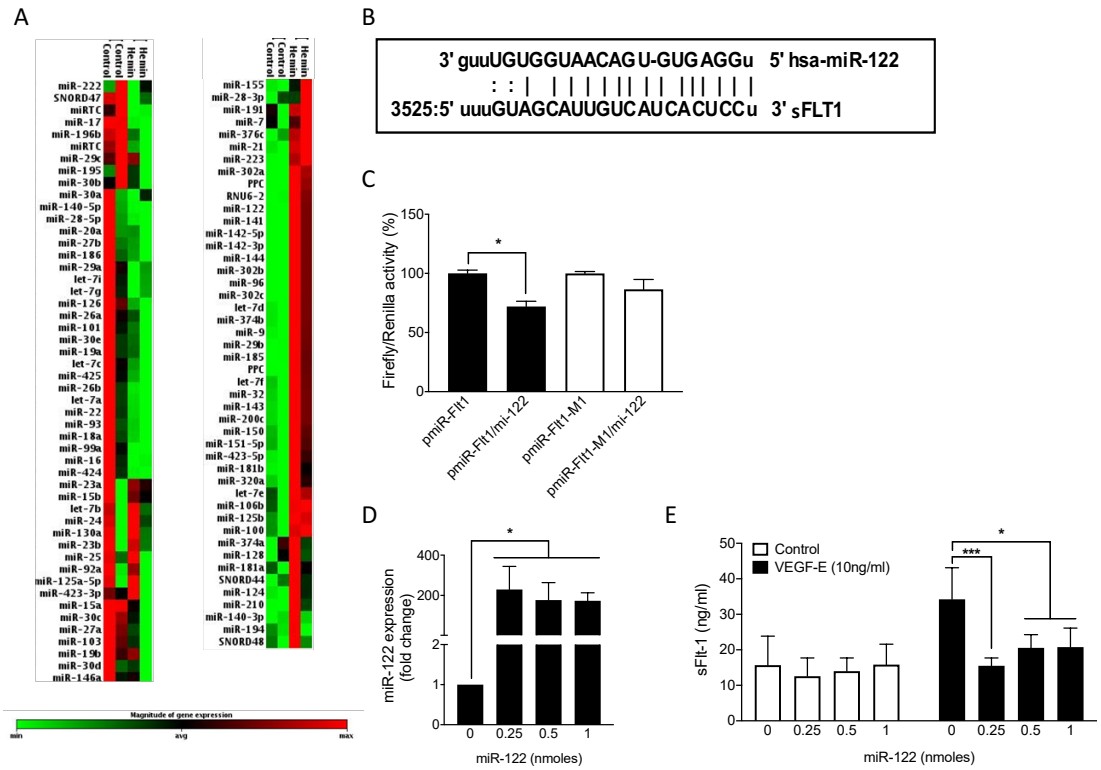

Figure 4. 1. Induced expression of miR-122 downregulates sFlt-1 in human endothelial cells.

(A) MicroRNA expression profiling was performed using qPCR-based miRNA array. HUVEC cells were treated with 10 µM hemin for 24h. Differentially expressed miRNAs were analysed and demonstrated as a heat map. **(B)** Selected miR-122 target alignment was predicted using online prediction programs. Region of 3'-UTR in sFlt-1 mRNA was identified as a targeting site for the complementary seed sequence of miR-122. **(C)** MicroRNA-122 target was confirmed by Luciferase promoter assay. HUVEC cells were transfected with the plasmid containing either normal or mutated 3'-UTR region of sFlt-1 in combination with or without miR-122 (n=4). Measured luciferase activity was normalised to renilla activity. Mann–Whitney test; **P<0.05*. Note: experiments A, B and C were performed by Dr Meng Cai. **(D)** HUVEC cells were transfected with the 0.25, 0.5 and 1 nmoles of the synthetic miR-122 mimic (n=4) followed by the stimulation of VEGF-E (10ng/ml; *P=0.001*). Two-Way ANOVA *post hoc* Dunnett's test with multiple comparisons to the control group; **P<0.05; ***P<0.0005.* **(E)** Transfection efficiency of miR-122 mimic was confirmed by the qPCR analysis of VEGF-E treated cells (n=4). Relative miRNA expression was normalised to RNU48 housekeeping gene. Kruskal-Wallis test *post hoc* Dunn's test with multiple comparisons to the control group; **P<0.05.*

4.5.2 HO-1-regulated miR-122 inhibits sFlt-1 release in human endothelial cells through direct targeting of sFlt-1 mRNA

Earlier experiments revealed that adenoviral overexpression of HO-1 inhibits VEGF-E-mediated release of sFlt-1, whereas knockdown of HO-1 promotes VEGF-E-mediated sFlt-1 secretion in human endothelial cells (Cudmore et al., 2007), describing HO-1 is a negative regulator of sFlt-1. To explore whether this regulation is miR-122-dependent, HUVEC cells were either infected with adenovirus encoding *Hmox1* gene or transfected with siRNA against HO-1. We found that HO-1 overexpression induced miR-122 relative expression (Figure 4.2 A), whereas siHO-1 reduced it (Figure 4.2 B). To confirm the link between HO-1 and sFlt-1 via miR-122, HUVECs were transfected with a combination of factors including siHO-1 alone, miR-122 alone and siHO-1 and miR-122 together. Endothelial cells were also treated with VEGF-E in order to induce significant sFlt-1 upregulation. As expected, compromised levels of HO-1 exacerbated the sFlt-1 increase, however when siHO-1 was combined with miR-122, sFlt-1 production was limited to the control level (Figure 4.2 C) suggesting that HO-1 negatively regulates sFlt-1 through up-regulation of miR-122.

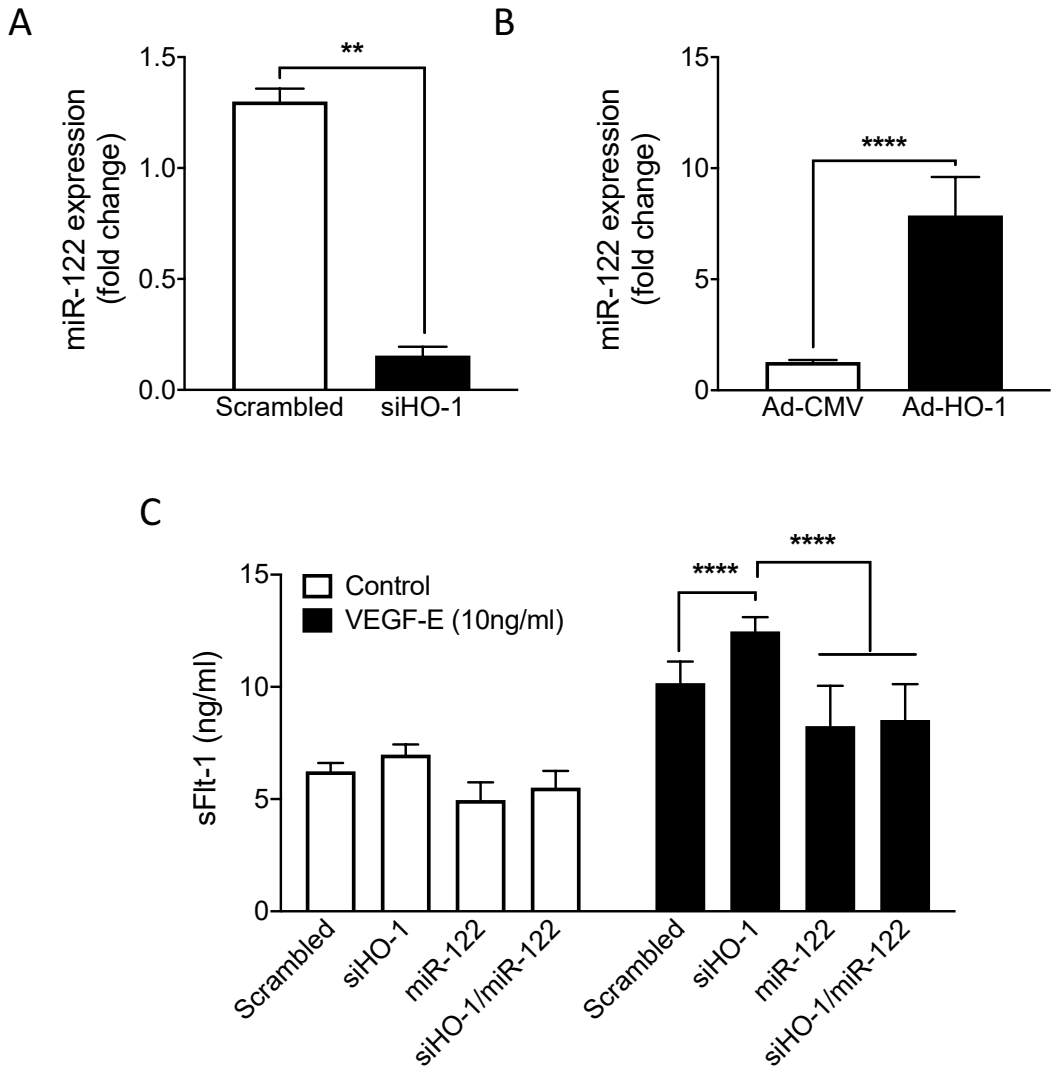

Figure 4. 2. HO-1 inhibits sFlt-1 production via miR-122 in human endothelial cells.

MicroRNA-122 expression was assessed in HUVEC cells infected with **(A)** adenovirus encoding HO-1 (Ad-CMV n=9; Ad-HO-1 n=9) or transfected with **(B)** HO-1 targeting siRNA (Scrambled n=6; siHO-1 n=6). Relative miRNA expression was normalised to RNU48 housekeeping gene. Mann-Whitney test; ***P<0.005; ****P<0.0001*. **(C)** HUVEC cells were transfected with siRNA against HO-1 in combination with miR-122 synthetic mimic followed by the VEGF-E (10ng/ml) stimulation for 24h (control group: scrambled n=20, siHO-1 n=12, miR-122 n=12, siHO-1/miR-122 n=6; VEGF-E treated group: scrambled n=18, siHO-1 n=8, miR-122 n=14, siHO-1/miR-122 n=6). Two-Way ANOVA *post hoc* Tukey's test with multiple comparisons to scrambled control; *****P<0.0001*.

4.5.3 Reduced expression of miR-122 is associated with sFlt-1 increase in preeclampsia

Plasma collected from the pregnant patients with preeclampsia had elevated levels of sFlt-1 (Figure 4.3 A). In accordance to increased sFlt-1, preeclamptic placenta was also tested for endogenous miR-122 expression. In these pathological placentas, miR-122 expression was significantly decreased when compared to healthy placentas (Figure 4.3 B). In addition, the expression levels of miR-122 and sFlt-1 were analysed in a well-established reduced uterine perfusion pressure preeclampsia mouse model (mRUPP). Mice were subjected to either sham or RUPP surgery on the day E11.5 to induce preeclampsia-like symptoms during murine pregnancy. On E17.5 plasma and placentas were collected and analysed for sFlt-1 and miR-122, respectively. As shown in Figure 4.3, mRUPP caused significant increase in circulating sFlt-1 levels (Figure 4.3 C) and decrease in placental miR-122 expression (Figure 4.3 D). Taken together, these results indicate that the mechanical relationship between miR-122 and sFlt-1 in murine preeclamptic model mirrors the relationship in human preeclampsia.

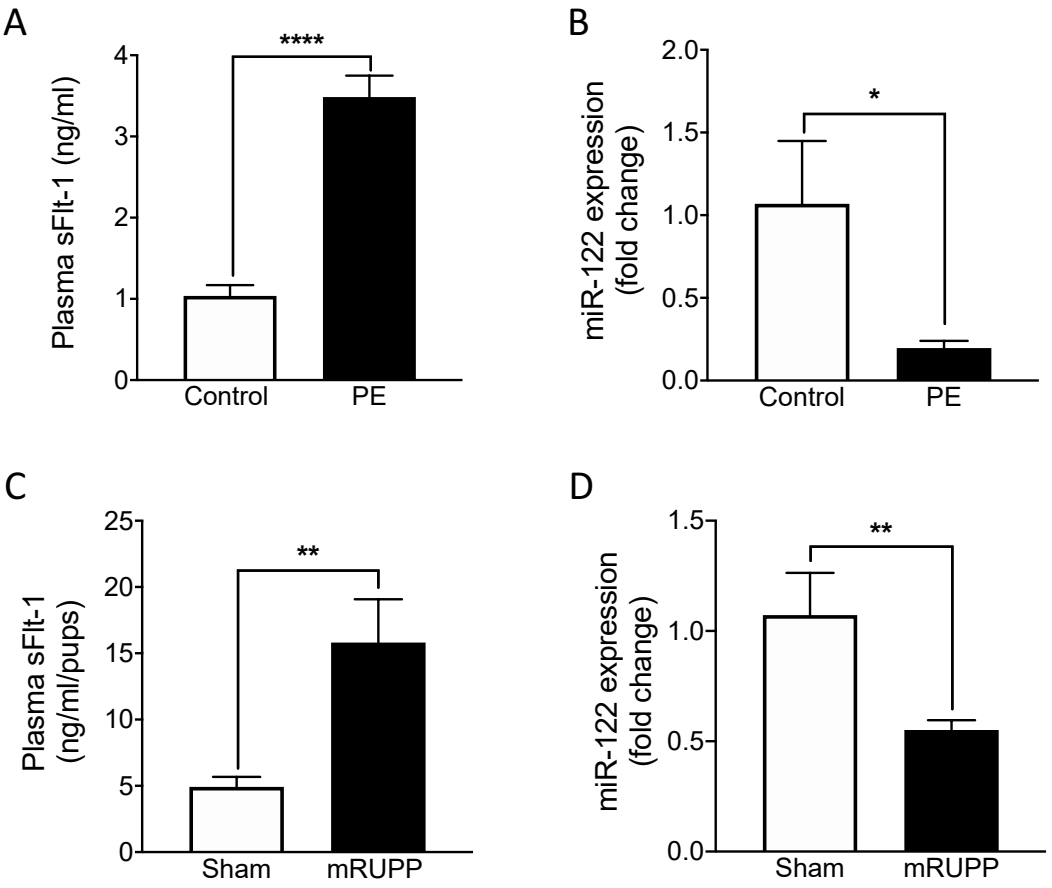

Figure 4. 3. Reduced expression of miR-122 leads to sFlt-1 increase in preeclampsia.

(A) Plasma collected from preeclamptic patients (PE) was tested for increased plasma sFlt-1 (control n=21; PE n=16). **(B)** Placentas collected from the PE patients were analysed for endogenous expression of miR-122 (control n=10; PE n=9). Unpaired Student t-test; **P<0.005; ****P<0.0001*. Mice were subjected to either sham or reduced uterine perfusion pressure (mRUPP) surgery on E11.5. On E17.5 plasma was collected to assess **(C)** sFlt-1 protein levels (Sham n=18; mRUPP n=15) followed by the placenta collection to assess **(D)** endogenous miR-122 expression (Sham n=6; mRUPP n=6) analysis. Relative miRNA expression was normalised to RNU48 housekeeping gene. Mann-Whitney test and unpaired Student t-test respectively; **P<0.05; **P<0.005*.

4.5.4 Reduced HO-1 expression increases plasma sFlt-1 and causes poor pregnancy outcome in murine pregnancy

Having discovered that HO-1 negatively regulates sFlt-1 via up-regulation of miR-122 in an *in vitro* setting (Figure 4.4 A), we then investigated the possible regulatory link between HO-1 and sFlt-1 via miR-122 in pregnant mice lacking HO-1. Generally, HO-1 knockout females are unable to sustain a healthy pregnancy (Zenclussen et al., 2011, Zenclussen et al., 2012) and because of the high embryo fatality rate (Poss and Tonegawa, 1997a, Zhao et al., 2009) we focused on HO-1 heterozygous pregnancy to explore miR-122-dependent sFlt-1 regulation.

HO-1 heterozygous females were crossed with HO-1 heterozygous males to produce heterozygous (HET) pregnancy, which was compared with a wild-type (WT) pregnancy produced by mating normal wild-type females with normal wild-type males. To assess the fetal outcome from both pregnancies, progeny form HET pregnancy was subdivided into *Hmox1*$^{+/+}$, *Hmox1*$^{+/-}$ and *Hmox1*$^{-/-}$ fetal and placental genotypes, whereas progeny produced by WT pregnancy had the same *Hmox1*^{wt} genotype. At the end of gestation (E17.5), both *Hmox1*$^{+/-}$ and *Hmox1*$^{-/-}$ placentas from HET pregnancies had decreased HO-1 mRNA expression. As expected, HO-1 mRNA expression in *Hmox1*$^{+/+}$ placenta was similar to *Hmox1*^{wt} placenta obtained from normal WT pregnancy (Figure 4.4 B). Placental miR-122 expression was decreased in *Hmox1*$^{-/-}$ placenta, whereas the expression of miR-122 in *Hmox1*$^{+/-}$ remained the same as in *Hmox1*$^{+/+}$ and *Hmox1*^{wt} placentas (Figure 4.4 C) supporting the *in vitro* data (Figure 4.4 A) showing that miR-122 acts downstream of HO-1. Lack of HO-1 expression in *Hmox1*$^{+/-}$ and *Hmox1*$^{-/-}$ placentas and low miR-122 expression in *Hmox1*$^{-/-}$ coincided with the increased circulating plasma sFlt-1 on day E15.5 of the pregnancy. By the end of the pregnancy at E17.5, sFlt-1 stabilised and reached the same level as in the normal wild-type pregnancy (Figure 4.4 D). Furthermore, the mRNA expression of sFlt-1 in placenta was the same between *Hmox1*^{wt}, *Hmox1*$^{+/+}$, *Hmox1*$^{+/-}$ and *Hmox1*$^{-/-}$ as all placentas were collected on E17.5 (Supplement A Figure 5A).

Fetal weight of *Hmox1*$^{+/+}$ and *Hmox1*$^{+/-}$ embryos was the same as healthy *Hmox1*^{wt} weights, however, fetal weight of *Hmox1*$^{-/-}$ embryos was significantly lower with an average weight of 0.77g $\pm$ 0.15 (Figure 4.5 A). The weight of *Hmox1*$^{+/+}$, *Hmox1*$^{+/-}$ and *Hmox1*$^{-/-}$ placentas was significantly lower when compared to *Hmox1*^{wt} placenta (Figure 4.5 B). The resorption rate was similar between WT and HET pregnancies (Figure 4.5 C), although the average count of live fetuses per pregnancy was significantly lower in HET pregnancy (Figure 4.5 D). Blood pressure in HET pregnancy remained the same as in WT pregnancy (Supplement A Figure 6A).

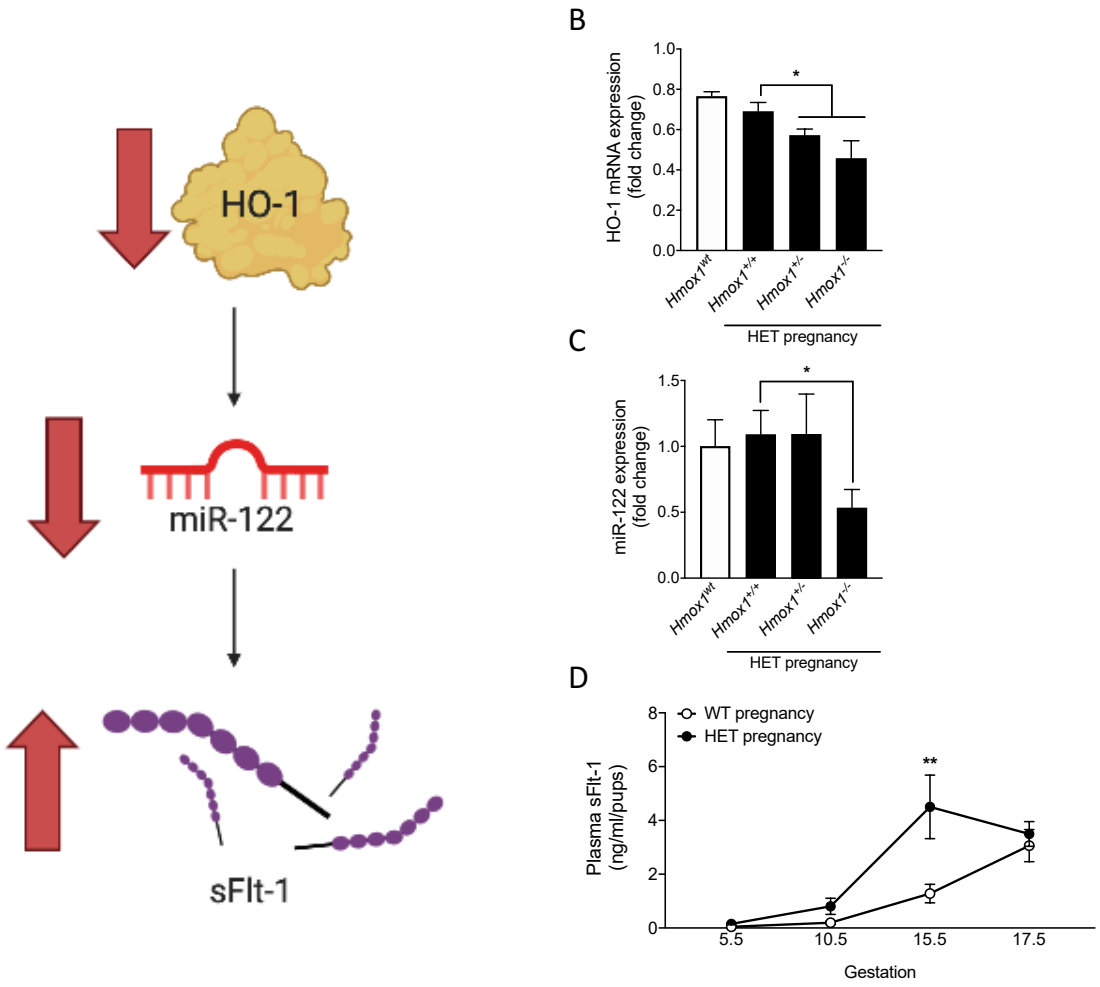

Figure 4. 4. During pregnancy reduced HO-1 mRNA expression leads to decreased miR-122 expression and increased plasma sFlt-1.

(A) During pregnancy low HO-1 expression results in diminished miR-122-dependent sFlt-1 suppression.

Total RNA was isolated from individual placentas obtained from normal WT and HET pregnancies to determine **(B)** HO-1 mRNA in placentas (*Hmox1*^{wt} n=17, *Hmox1*$^{+/+}$ n=15, *Hmox1*$^{+/-}$ n=19, *Hmox1*$^{-/-}$ n=5) and **(C)** miR-122 expression in placentas (*Hmox1*^{wt} n=17, *Hmox1*$^{+/+}$ n=15, *Hmox1*$^{+/-}$ n=19, *Hmox1*$^{-/-}$ n=5). Relative mRNA and miRNA expression was normalised to YWHAZ and RNU48, respectively. Kruskal-Wallis test *post hoc* Dunn's test with multiple comparisons to *Hmox1*$^{+/+}$ group; **P<0.05; **P<0.005; ***P<0.0005.* **(D)** Plasma was collected from WT and HET pregnant females to measure free circulating sFlt-1 at the gestational days E5.5 (WT n=8, HET n=12) , E10.5 (WT n=8, HET n=9), E15.5 (WT n=8, HET n=11) and E17.5 (WT n=9, HET n=19). Two-Way ANOVA test *post hoc* Sidak's test with multiple comparisons to WT pregnancy; ***P<0.005.*

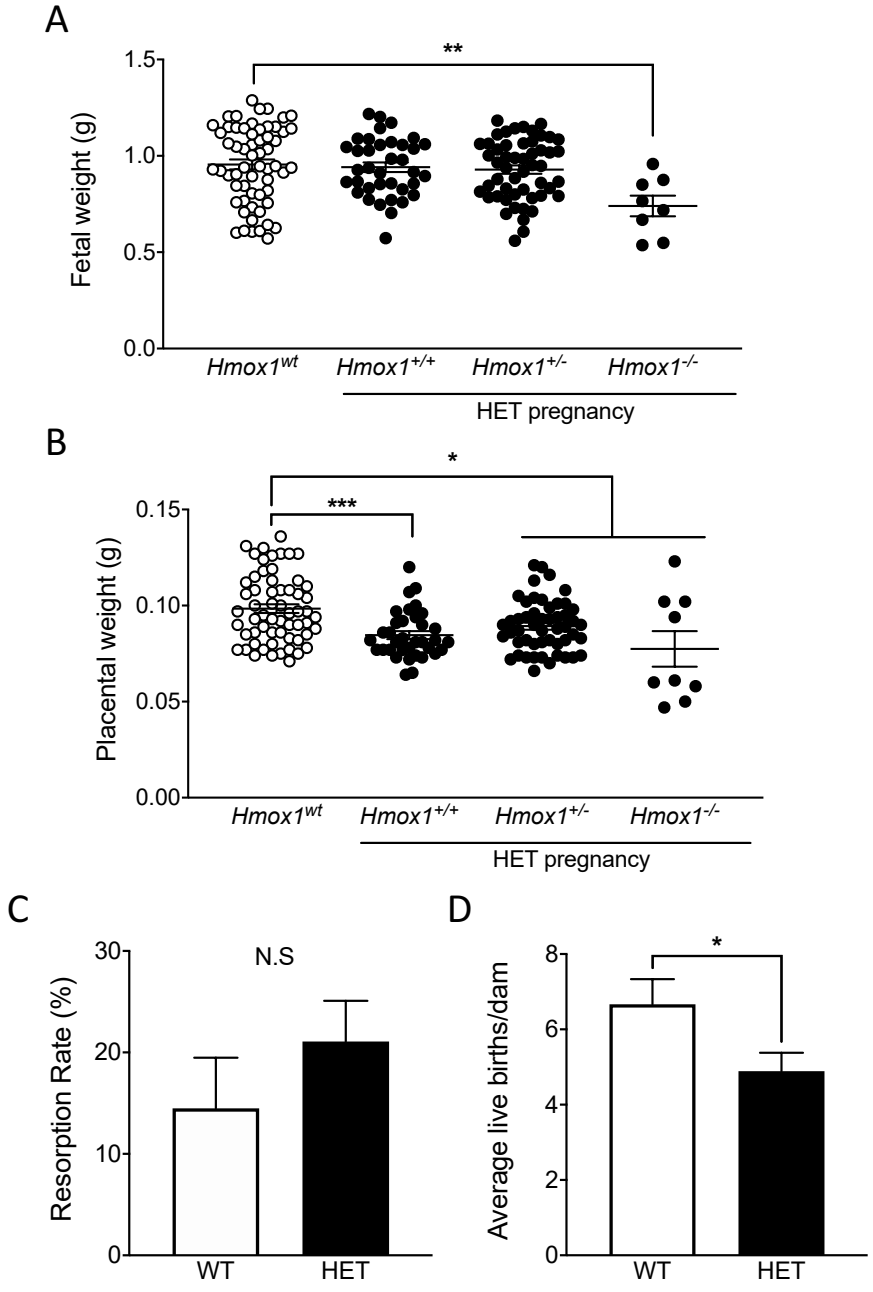

Figure 4. 5. Compromised HO-1 expression causes poor fetal outcome and low fetal count. Fetal outcome was assessed using combination of the parameters including weight of the fetal unit and count of live births at E17.5. Wet weight of the individual **(A)** fetuses (*Hmox1*^{wt} n=60, *Hmox1*$^{+/+}$ n=35, *Hmox1*$^{+/-}$ n=51, *Hmox1*$^{-/-}$ n=9) and **(B)** placentas (*Hmox1*^{wt} n=60, *Hmox1*$^{+/+}$ n=37, *Hmox1*$^{+/-}$ n=52, *Hmox1*$^{-/-}$ n=8) from WT and HET pregnancies. Kruskal-Wallis test; *post hoc* Dunn's test with multiple comparisons to *Hmox1*^{wt} *group; *P<0.05; **P<0.005; ***P<0.0005.* **(C)** Percentage of resorptions and **(D)** average count of live pups per WT and HET pregnancy (WT n=9; HET n=18). Unpaired Student t test; **P<0.05.*

4.5.5 MicroRNA-122 inhibits sFlt-1 production in murine pregnancy

Viral vectors encoding miRNAs are used to trigger RNAi and induce gene silencing (Couto and High, 2010, Kumar et al., 2008, Liu et al., 2010). We employed adenovirus (Ad-miR-122) as it is extremely efficient in transferring the RNA-encoding vectors into the nucleus of mammalian cells. It ensures high expression of RNA and target gene downregulation (Lanford et al., 2010, Lou et al., 2013) and efficiently infects both dividing and non-dividing cells without integrating into the host genome (Bessis et al., 2004, Cao et al., 2004). Ad-miR-122 has been explored in cancer (Ma et al., 2010) and fertility studies (Menon et al., 2017) leading to high expression levels of functional miR-122 and significant target downregulation.

To explore the potential therapeutic effect of miR-122 via down-regulation of sFlt-1, pregnant HET and WT females received either Ad-CMV or Ad-miR-122 intraperitoneal injection on day E10.5. The infectious capacity of the adenovirus was tested in the HUVEC cells prior to the *in vivo* experiments (Supplement A Figure 4). Plasma throughout the gestation starting from E5.5, E10.5. E15.5 and E17.5 was obtained to monitor sFlt-1 changes pre- and post-treatment. Ad-miR-122 treatment caused a significant drop in maternal circulating sFlt-1 at day E17.5 in HET pregnancy when compared to empty adenovirus treatment but not in WT pregnancy (Figure 4.6 A and B). Placental sFlt-1 mRNA expression at E17.5 remained unchanged (Supplement A Figure 5B). To confirm that adenoviral delivery of miR-122 led to overexpression of miR-122 in placenta, amniotic fluid (AF) was collected at the end of pregnancy and tested for miR-122 expression. Extracted particles from amniotic fluid from Ad-miR-122 treated HET pregnancy confirmed a 10-fold increase in miR-122 expression when compared to amniotic fluid from Ad-CMV treated females (Figure 4.6 C). Placental tissue was analysed for miR-122 expression; however, no changes were detected (Supplement A Figure 7A). HO-1 placental mRNA expression remained unaffected after Ad-miR-122 treatment (Supplement A Figure 7B).

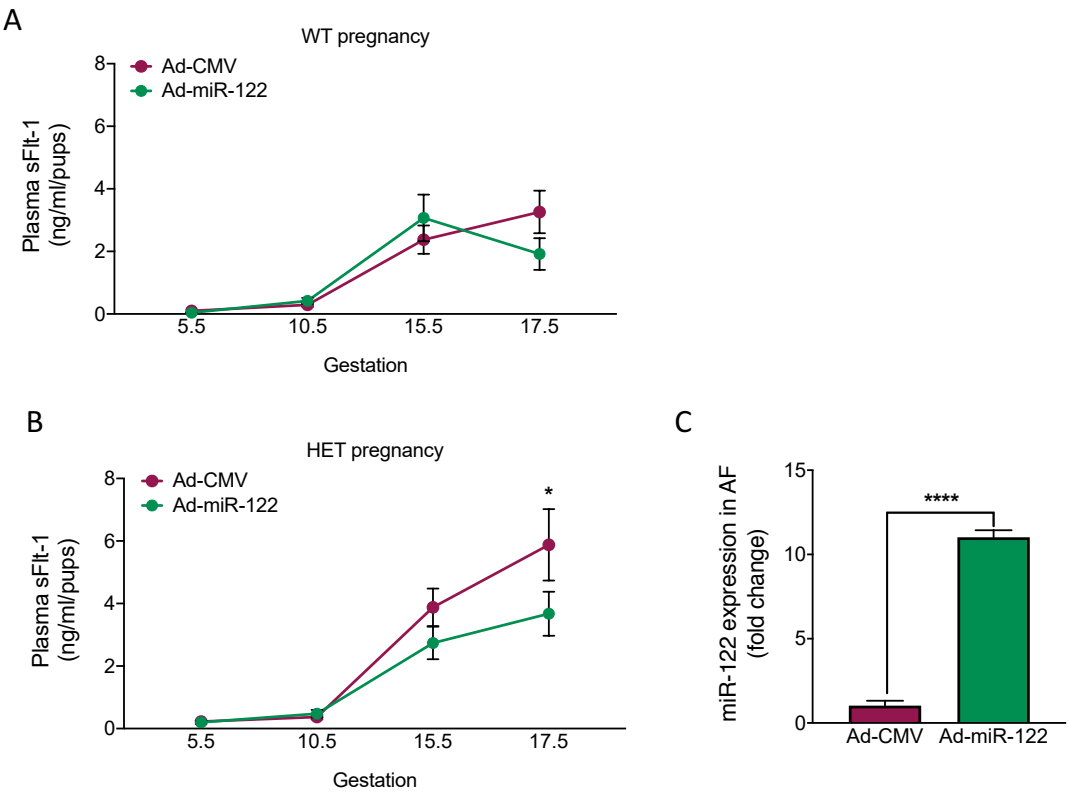

Figure 4. 6. MicroRNA-122 inhibits sFlt-1 production in HO-1 compromised pregnancy.

Pregnant **(A)** WT and **(B)** HET mice received either empty vector adenovirus (Ad-CMV) or adenovirus encoding miR-122 (Ad-miR-122) intraperitoneal injection on day E10.5. Circulating plasma levels of sFlt-1 were monitored throughout the gestation starting at E5.5 (Ad-CMV: WT n=5, HET n=8; Ad-miR-122: WT n=7, HET n=11), followed by E10.5 (Ad-CMV: WT n=8, HET n=11; Ad-miR-122: WT n=6, HET n=11), E15.5 (Ad-CMV: WT n=8, HET n=11; Ad-miR-122: WT n=7, HET n=11) and E17.5 (Ad-CMV: WT n=11, HET n=11; Ad-miR-122: WT n=11, HET n=10). Two-Way ANOVA test *post hoc* Sidak's test with multiple comparisons to Ad-CMV group; **P<0.05.* **(C)** Amniotic fluid (AF) from HET pregnancy was collected to confirm adenovirus induced placental miR-122 overexpression (Ad-CMV n=3, Ad-miR-122 n=3). Relative miRNA expression was normalised to commercially provided spike-in control. Unpaired Student t test; *****P<0.0001.*

4.5.6 Increased miR-122 expression improves fetal weight in HO-1 compromised murine pregnancy

To investigate the effect of miR-122 on pregnancy outcome, embryos from HET pregnancy were collected at E17.5 and compared to WT pregnancy. Ad-miR-122 treatment increased average fetal weight in HET pregnancy when compared with Ad-CMV treatment (Figure 4.7 A). Importantly, Ad-miR-122 treatment did not have any effect on fetal weight in WT pregnancy. Furthermore, when HET pregnancies were subdivided into genotypic groups of *Hmox1*$^{+/+}$, *Hmox1*$^{+/-}$ and *Hmox1*$^{-/-}$, we found that Ad-miR-122 increased fetal weight of *Hmox1*$^{+/+}$ and *Hmox1*$^{+/-}$ pups when compared to Ad-CMV treatment (Figure 4.7 B). The average weight of *Hmox1*$^{+/+}$ pups increased from 0.75g $\pm$ 0.13 to 0.9g $\pm$ 0.2 and the weight of *Hmox1*$^{+/-}$ pups increased from 0.78g $\pm$ 0.17 to 0.92g $\pm$ 0.19. Statistical analysis in *Hmox1*$^{-/-}$ group was not possible as there was only one pup that survived out of 10 pregnancies treated with Ad-CMV. This demonstrates that miR-122 increased the overall survival rate for *Hmox1*$^{-/-}$ pups treated with Ad-miR-122. Overall placental weights and those based-on-genotype remained the same (Figure 4.7 C and D), but Ad-miR-122 treatment increased overall fetal:placental weight ratio when compared to Ad-CMV treatment in HET pregnancy (Figure 4.8 A). Ad-miR-122 treatment also significantly improved fetal:placental ratio in all subdivided embryos from HET pregnancy when compared to Ad-miR-122 treated *Hmox1*^{wt} embryos (Figure 4.8 B). To eliminate the possibility that adenoviral treatment may influence selective survival based on the fetal genotype, the genotype of individual pups was plotted against the Ad-CMV and Ad-miR-122 treatments to identify any possible links. As expected, there was no relationship between the adenoviral treatment and the fetal survival of the particular genotype (Supplement A Figure 8).

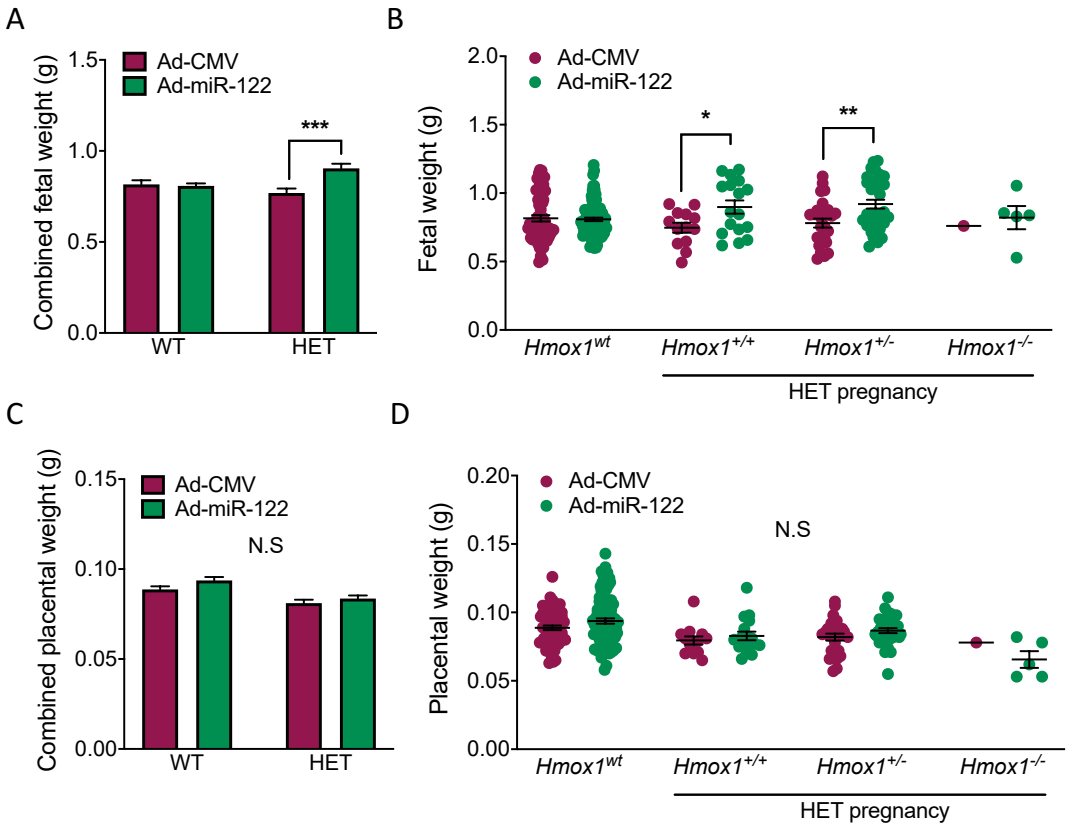

Figure 4. 7. Increased miR-122 expression improves fetal weight in HET pregnancy.

The effect of adenoviral treatment on fetal outcome was assessed on E17.5. Overall Ad-miR-122 effect on **(A)** combined (all genotypes together) fetal weight (WT: Ad-CMV n=60, Ad-miR-122 n=40; HET: Ad-CMV n=90, Ad-miR-122 n=56) and **(C)** combined placental weight (WT: Ad-CMV n=60, Ad-miR-122 n=90; HET: Ad-CMV n=40, Ad-miR-122 n=56) in HET pregnancy compared to WT. Two-Way ANOVA *post hoc* Sidak's test with multiple comparisons to Ad-CMV group; ****P<0.0005.*

Genotype specific Ad-miR-122 effect on **(B)** fetal weight (Ad-CMV: *Hmox1*^{wt} n=60, *Hmox1*$^{+/+}$ n=13, *Hmox1*$^{+/-}$ n=26, *Hmox1*$^{-/-}$ n=1; Ad-miR-122: *Hmox1*^{wt} n=90, *Hmox1*$^{+/+}$ n=17, *Hmox1*$^{+/-}$ n=34, *Hmox1*$^{-/-}$ n=5) and **(D)** placental weight (Ad-CMV: *Hmox1*^{wt} n=60, *Hmox1*$^{+/+}$ n=13, *Hmox1*$^{+/-}$ n=26, *Hmox1*$^{-/-}$ n=1; Ad-miR-122: *Hmox1*^{wt} n=90, *Hmox1*$^{+/+}$ n=17, *Hmox1*$^{+/-}$ n=34, *Hmox1*$^{-/-}$ n=5) in HET pregnancy compared to WT pregnancy. Two-Way ANOVA *post hoc* Sidak's test with multiple comparisons to Ad-CMV group; **P<0.05; **P<0.005.*

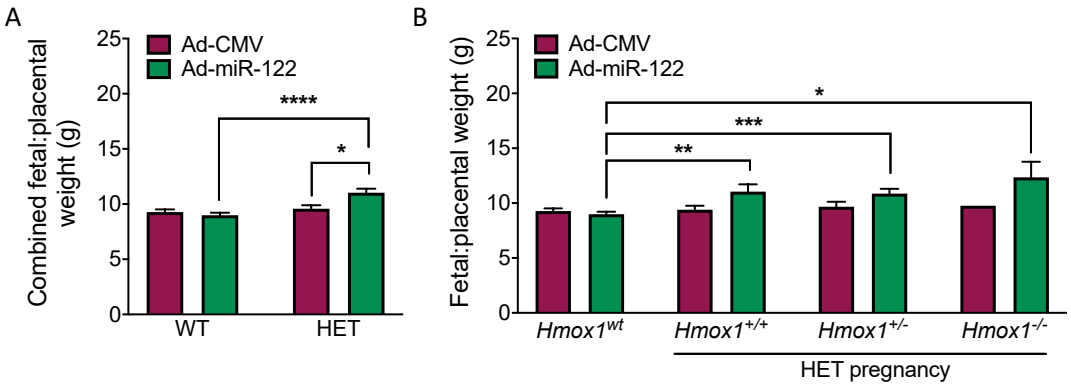

Figure 4. 8. Increased miR-122 expression improves fetal:placental weight ratio in HET mice. **(A)** Combined (all genotypes together) Ad-miR-122 effect on fetal:placental weight ratio (WT: Ad-CMV n=60, Ad-miR-122 n=90; HET: Ad-CMV n=40, Ad-miR-122 n=56). Two-Way ANOVA *post hoc* Sidak's test with multiple comparisons; **P<0.05; ***P<0.0001*. **(B)** Specific Ad-miR-122 effect on fetal:placental weight ratio based on the fetal genotype (Ad-CMV: *Hmox1*^{wt} n=60, *Hmox1*$^{+/+}$ n=13, *Hmox1*$^{+/-}$ n=26, *Hmox1*$^{-/-}$ n=1; Ad-miR-122: *Hmox1*^{wt} n=90, *Hmox1*$^{+/+}$ n=17, *Hmox1*$^{+/-}$ n=33, *Hmox1*$^{-/-}$ n=5). Two-Way ANOVA *post hoc* Sidak's test with multiple comparisons to *Hmox1*^{wt} group; **P<0.05; **P<0.005; ***P<0.0001*.

4.5.7 Increased miR-122 expression improves fetal survival

Ad-miR-122 treatment reduced resorption rate by 23% in both, WT and HET pregnancies (Figure 4.9 A). Even though the average number of live pups remained statistically the same across both treatment groups, a slight increasing trend in Ad-miR-122 treated WT and HET pregnancy was observed (Figure 4.9 B). Blood pressure after Ad-miR-122 treatment in HET and WT pregnancies remained unaffected (Supplement A Figure 6B).

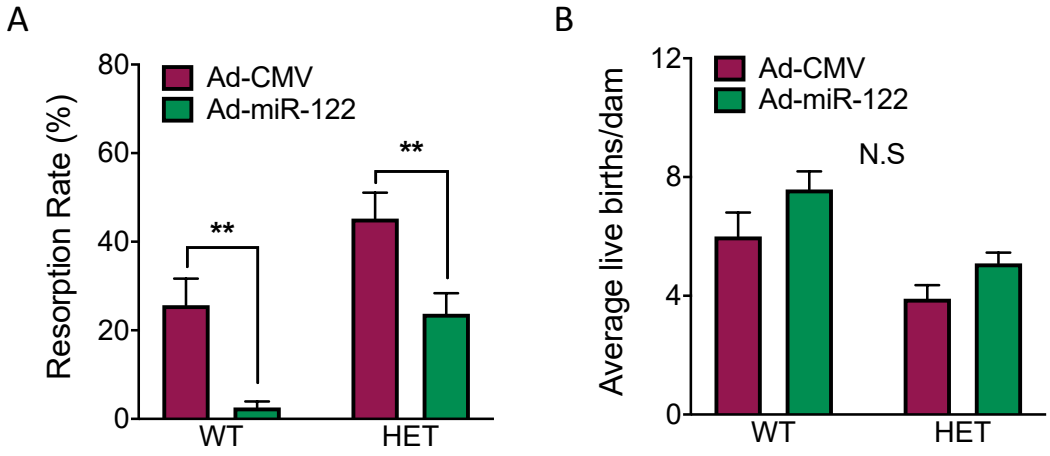

Figure 4. 9. Increased miR-122 expression improves fetal survival.
The effect of Ad-miR-122 treatment on **(A)** the resorption rate (WT: Ad-CMV n=10, Ad-miR-122 n=12; HET: Ad-CMV n=10, Ad-miR-122 n=11) and **(B)** live births count (WT: Ad-CMV n=10, Ad-miR-122 n=12; HET: Ad-CMV n=10, Ad-miR-122 n=11) from WT and HET pregnancies. Two-Way ANOVA *post hoc* Sidak's test with multiple comparisons to Ad-CMV treatment group; ***P<0.005.*

4.6 Discussion

Preeclampsia is one of the leading causes of the maternal and neonatal morbidity and mortality with devastating long-term consequences affecting 2% to 5% of pregnant women worldwide each year (Poon et al., 2019). There is no definitive treatment for this disorder and preventative measures are still elusive partly due to the lack of understanding of the pathogenesis of preeclampsia. Anti-angiogenic factor, sFlt-1, has been increasingly recognised as the major culprit of preeclampsia (Ramma and Ahmed, 2014, Ahmed and Cudmore, 2009). Removal of placental sFlt-1 released by preeclamptic placenta restores angiogenic balance (Ahmad and Ahmed, 2004). Neutralization of sFlt-1 below a critical threshold eliminates preeclampsia symptoms in mice (Bergmann et al., 2010) and women (Thadhani et al., 2011, 2016). The evidence suggest that therapeutics directed at decreasing circulating levels of sFlt-1 could be a possible treatment for preeclampsia. Previously, Cudmore and colleagues demonstrated that HO-1 negatively regulates sFlt-1 production in endothelial cells (Cudmore et al., 2007). However, the exact mechanism of how HO-1 regulates sFlt-1 is still unknow. Instead of exploring already reported common miRNAs in preeclampsia we utilised a different approach and performed miRNA array to identify miRNAs directly upregulated by HO-1, which may act as a downstream sFlt-1 down-regulator. Here we demonstrate for the first time that miR-122 has a partial complementarity to sFlt-1 mRNA and acts downstream of HO-1. Human endothelial cells transfected with miR-122 exhibited reduced VEGF-E-induced sFlt-1 release. Pregnant HO-1 compromised mice treated with adenoviral vector carrying miR-122 experienced reduced plasma sFlt-1 levels and improved fetal outcome when compared to healthy pregnancy. This data in concert with reduced miR-122 levels in preeclamptic placenta highlight a therapeutic potential of miR-122 replacement therapy.

4.6.1 MicroRNA-122 acts downstream of HO-1 and inhibits sFlt-1 in human endothelial cells

Our work showed that activation or overexpression of HO-1 in HUVECs was associated with miR-122 increase, whereas knockdown of HO-1 caused a decrease in miR-122. *In vitro* studies exploring HBV infectious capacity showed that HBV protein X binds to transcription factor peroxisome proliferator-activated receptor gamma (PPARγ) and inhibits miR-122 transcription (Song et al., 2013). Activation of PPARγ is known to directly induce *Hmox1* gene expression (Krönke et al., 2007, Li et al., 2010, Zhang et al., 2014). Our data in combination with these two studies strongly suggest that induction of HO-1 may regulate miR-122 expression. Since target mRNA selection revealed that the seed sequence of miR-122 binds to 3'UTR region of sFlt-1 mRNA, we found that HO-1 dependent downregulation of sFlt-1 (Cudmore et al., 2007) is directly regulated by miR-122-induced gene silencing. Furthermore, when HO-1 knockdown in endothelial cells was supplemented with miR-122, sFlt-1 release was halted to levels observed in cells with normal HO-1 levels indicating that miR-122 exerts its sFlt-1 suppressive effects downstream of HO-1.

The sequence of mature miR-122 is completely conserved between all species, which indicates that the entire sequence is important for the function (Burns et al., 2011). In humans, miR-122 is located on the positive strand of chromosome 18 at 18q21.31 (Gene ID: 406906; locus ID 406906). Intergenic miRNA-122 locus is in a non-coding RNA exon region and is not part of a cluster. Identification of the transcription start site and 3' end shows that pri-miR-122 gene is initially transcribed by RNA polymerase II into a 7.5 kb transcript, which is then spliced into 4.5 kb pri-miR-122 product containing 84 bp long pre-miR-122 hairpin structure. In the nucleus pri-miR-122 is cleaved by microprocessor complex (Dorsha and DGCR8) to yield 84 bp pre-miR-122 stem loop structure (Hinske et al., 2014, miriad-database.org) and exported to cytoplasm by Exportin 5 nuclear transport factor. Stem loop structure is cleaved by Dicer to yield double-stranded miR-122 containing miR-122-5p guide strand and miR-122-3p passenger strand (Figure 4.10). Mature miR-122-5p sequence is 23 nucleotides long (Jopling, 2012, miRbase.org, ID: MI0000442) remains loaded to miRISC complex, which allows complementary "seed" sequence-driven initiation of translational suppression of

target mRNA. CpG islands present within the upstream of the promoter region or within the promoter region of miR-122 coding gene identifies potential sites for alternative epigenetic regulation (Li et al., 2018, Cheng et al., 2018). It has been shown that DNA hypermethylation of the CpG islands is linked with oxidative stress (Bai et al., 2019) and downregulates miR-122 expression during induced liver injury (Li et al., 2018). DNA hypomethylation on the other hand, dramatically increased miR-122 expression level in the hepatocellular carcinoma cells, suggesting that miR-122 can be epigenetically suppressed via DNA methylation and contribute to hepatocellular tumorigenesis (Cheng et al., 2018).

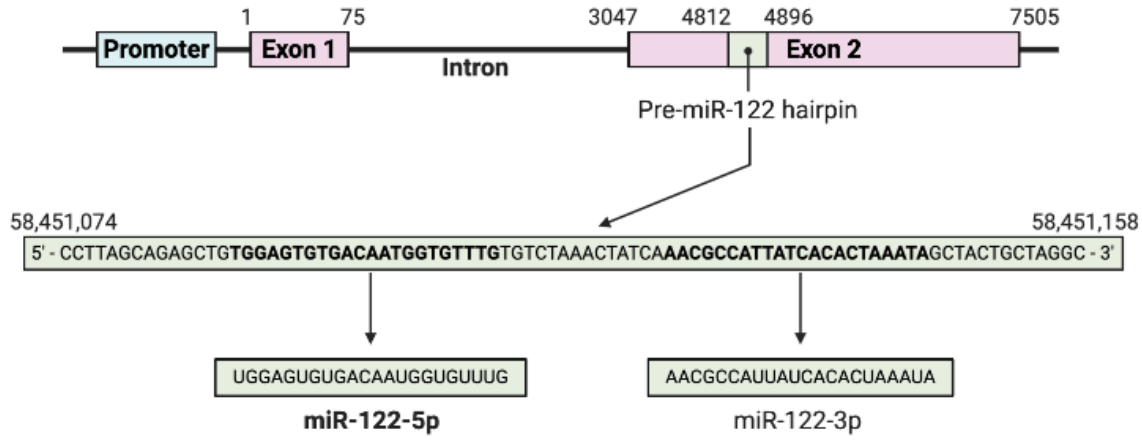

Figure 4. 10. Genomic location and structure of the human miR-122 gene.
Pri-miR-122 gene is transcribed into a 7.5 kb transcript followed by the splicing into 4.5 kb pri-miR-122 product, which contains 84 bp long pre-miR-122 hairpin structure. Pre-miR-122 hairpin structure is cleaved to yield mature 23 nucleotides long miR-122-5p sequence.

Generally, this miRNA is expressed across different species and is highly liver-specific (Denzler et al., 2014). It can also be detected in the nervous and respiratory systems, in cells of hematopoietic lineage (Landgraf et al., 2007) and placenta (Lasabová et al., 2015). MicroRNA-122 has a crucial role in liver physiology including stress response (Bhattacharyya et al., 2006), lipid metabolism (Esau et al., 2006), hepatic differentiation and maturation (Deng et al., 2014b, Jung et al., 2011, Laudadio et al., 2012, Kyrmizi et al., 2006, Xu et al., 2010). Loss of miR-122 expression was identified in hepatocellular carcinoma (HCC) (Möröy et al., 1989, Bai et al., 2009b, Coulouarn et al., 2009, Jung et al., 2011), hepatitis B virus (HBV), (Wang et al., 2012b), gastrointestinal cancer (Wang et al., 2009, Kunte et al., 2012), ductal pancreatic adenocarcinoma (Papaconstantinou et al., 2013), iron deficiency (Castoldi and Muckenthaler, 2012), Non-

Alcoholic Fatty Liver Disease (NAFLD), Non-Alcoholic Steatohepatitis (NASH) (Cheung et al., 2008) and sepsis (Wang et al., 2012a). In the literature miR-122 is often labelled as a tumour-suppressor miRNA and has been extensively explored in cells, human and rodent models of cancer (Kutay et al., 2006, Hsu et al., 2012).

4.6.2 MicroRNA-122 expression is downregulated in preeclampsia

MicroRNAs compose nearly 1 - 5% of animal genomes (Lim et al., 2005, Lewis et al., 2005). Since, a substantial amount of miRNA is expressed in the human placenta (Pineles et al., 2007b) and is implicated in a number of pathologies, we looked at miR-122 expression in preeclamptic placenta. Low HO-1 levels has been reported previously in animal model of preeclampsia (Gilbert et al., 2009) and human preeclampsia (Ahmed et al., 2000, Lyall et al., 2000, Barber et al., 2001, Farina et al., 2008, Lash et al., 2003). Consistent with the data of upregulated maternal serum levels of sFlt-1 in preeclampsia (Koga et al., 2003, Levine et al., 2004, Buhimschi et al., 2006, Crispi et al., 2006, Ramma et al., 2012), we found that both human preeclamptic and mouse RUPP placentas expressed significantly lower miR-122 expression. Earlier study reported reduced plasma miR-122 levels in women with premature acute coronary syndrome who had a history of preeclampsia (Dayan et al., 2018). Furthermore, downregulation of placental miR-122 was associated with intrauterine growth restricted human pregnancy (IUGR) (Hromadnikova et al., 2015). IUGR has been previously shown to have increased serum sFlt-1 (Birdir et al., 2018, Herraiz et al., 2014) and reduced HO-1 expression in rodent IUGR-like placenta (Kreiser et al., 2002, Zenclussen et al., 2014). However, unlike preeclampsia, which has low HO-1 expression, IUGR placenta is not associated with reduced HO-1 expression during human pregnancy (Ahmed et al 2000). Therefore, data supports our finding of miR-122 dependent sFlt-1 regulation and therapeutic potential for treating or preventing preeclampsia.

In contrast, a study by Lasabová and colleagues showed that the relative gene expression of miR-122 was significantly higher in placenta from patients with preeclampsia (Lasabová et al., 2015). Discrepancies between their study and ours can

be attributed to several factors. Extraction kits used for miRNA isolation were not the same in these two studies. Although methods were similar, Brown et al. (2018b) highlighted a number of differences. One of these was a higher yield of RNA and high-throughput design to isolate total content of RNA used in our study (Brown et al., 2018b). More importantly, our study used gestationally age-matched samples whereas Lasabová et al. (2015) used age-unmatched samples. Gestational age-matching allows better comparison between the control and disease, eliminating sensitive variables potentially affecting outcome of the study. This may explain the wide spread observed in the Lasabová et al. (2015) study compared to conserved control samples. Also, high variation in the sample population could be due to the placental sampling position. It has been shown previously that sampling of the chorionic or basal plate of the preeclamptic placenta leads to evident variations in miRNAs expression profile as several miRNAs were found differently expressed in trophoblast cells compared to endothelial cells (Xu et al., 2014). Therefore, we excluded outliers to eliminate such variation and provided a relatively conserved population of samples. Different outcomes in the results and multiple variables involved the study could be the reason why miR-122 role in normal pregnancy or preeclampsia is relatively underexplored.

4.6.3 Partial loss of HO-1 causes elevated sFlt-1 levels and poor fetal outcome in murine pregnancy

HO-1 deficiency is associated with severe and persistent endothelial damage in humans (Yachie et al., 1999b) and mice (Poss and Tonegawa, 1997a). It has been shown that *Hmox1* null mice produce significantly higher levels of sFlt-1 from highly vascularised tissue such as lung when compared with wild-type littermates (Cudmore et al., 2007). Also, rodent models of pregnancy showed that HO-1 is crucial in maintaining healthy pregnancy as partial (*Hmox1*$^{+/-}$) (Zhao et al., 2011a) and complete (*Hmox1*$^{-/-}$) (Zhao et al., 2009, Zenclussen et al., 2011) HO-1 knockout models are known to have poor pregnancy prognosis, due to prolonged blastocyst attachment (Zenclussen et al., 2011). In fact, *Hmox1*$^{-/-}$ females are unable to sustain a healthy pregnancy (Zenclussen et al., 2012, Zenclussen et al., 2011). They exhibit macromolecular oxidative damage,

tissue injury, chronic inflammation and anaemia in addition to accumulation of hepatic and renal iron (Poss and Tonegawa, 1997a) leading to a very low fetal survival rate of 2.4 - 5% (Poss and Tonegawa, 1997a, Zhao et al., 2009).

Consistent with previous findings (Zhao et al., 2009, Zhao et al., 2011a) we have reported a steady increase in sFlt-1 levels in maternal serum from WT and HET pregnancies. This rise in sFlt-1 could be a physiological requirement in normal pregnancy to regulate VEGF and PlGF function as was proposed for the advancing placental development (Clark et al., 1998, He et al., 1999). In our study, there was a significant spike in plasma sFlt-1 levels by day E15.5 in HET pregnancy. To protect the pregnancy by limiting rapid increase of sFlt-1 (Cudmore et al., 2007), HO-1 expression increases more than 3-fold by day E10.5 after which it remains elevated (Zhao et al., 2009, Zhao et al., 2011a). As HO-1 expression in HET pregnancy is reduced, the sudden increase in maternal sFlt-1 levels can be attributed to insufficient HO-1 protection. This may explain the resulting low miR-122 expression found in *Hmox1*$^{-/-}$ placenta.

Maternal sFlt-1 levels in HET pregnancy after E15.5 normalises to the levels observed in WT pregnancy. Approximately, 1 in 10 pups in HET pregnancy exhibited *Hmox1*$^{-/-}$ genotype. In contrast, pups with *Hmox1*$^{+/-}$ genotype were similar in numbers to those with *Hmox1*$^{+/+}$ genotype. Therefore, we suggest that the compensatory mechanism of miR-122 found in *Hmox1*$^{+/-}$ and *Hmox1*$^{+/+}$ placentas normalises maternal plasma sFlt-1 levels to maintain the pregnancy until the end. Despite this compensatory mechanism, the fetal outcome in HET pregnancies was affected and is consistent with previous observations as outlined above (Zhao et al., 2011a).

All placental weights from HET pregnancies were significantly affected when compared to WT pregnancy and can be attributed to increased sFlt-1 levels (Kumasawa et al., 2011) and poor placental development caused by insufficient spiral artery remodelling (Zhao et al., 2011a, Zenclussen et al., 2011). Fetal weights on the other hand, were only affected in *Hmox1*$^{-/-}$ pups (Zenclussen et al., 2011). It shows that partial HO-1 expression is sufficient to maintain normal fetal outcome whereas, HO-1 null phenotype severely impacts fetal and placental development, which may contribute to lower birth rate observed in HET pregnancy. Therefore, our data further supports crucial HO-1 role in the pregnancy development, maintenance and fetal outcome (Zhao et al., 2011a, Zhao et al., 2009, Zenclussen et al., 2011, Zenclussen et al., 2012) and that the

poor fetal prognosis observed in HO-1 compromised mice might be in part caused by low miR-122 expression induced sFlt-1 levels.

4.6.4 MicroRNA-122 overexpression reduces sFlt-1 levels and improves fetal outcome in HO-1 compromised pregnancy

Having established that HO-1 exerts its sFlt-1 inhibitory effects via miR-122 *in vitro*, we have utilised viral vector encoding miR-122 delivery strategy (Ma et al., 2010, Menon et al., 2017) to explore its potential therapeutic ability to reduce pathological sFlt-1 release in HO-1 compromised pregnancy. Consistent with the findings observed in human endothelial cells, miR-122 overexpression therapy significantly reduced plasma sFlt-1 levels in HO-1 compromised pregnancy without affecting normal sFlt-1 levels in WT pregnancy. This is important as it highlights the attractive and finely tuned regulatory nature of miRNA (Bartel, 2009, Bartel, 2004). As a consequence of lowered maternal sFlt-1, miR-122 treatment increased fetal weight and fetal:placental ratio in HET pregnancies. In fact, all pups benefited equally from miR-122 therapy regardless of their genotype. Surprisingly, miR-122 therapy selectively improved fetal:placental ratio of *Hmox1*$^{+/+}$, *Hmox1*$^{+/-}$ and *Hmox1*$^{-/-}$ pups when compared to miR-122 treated *Hmox1*^{wt}, pups, which further proves that increased placental miR-122 expression rescues pathological HO-1-compromised effects on fetal outcome. It has been shown previously that inhibition of HO-1 leads to complete resorption (Alexandreanu and Lawson, 2002), whereas adenoviral overexpression of HO-1 improves pregnancy outcome in a murine model of abortion (Zenclussen et al., 2006). In our study, miR-122 therapy halted resorption rate by almost one in four in HO-1 compromised animals, without affecting the total number of live births. Overall, data provides a direct proof that miR-122 is a promising therapeutic candidate with the ability to treat abnormal sFlt-1 levels in pregnancy and improve fetal outcome in preeclampsia.

4.6.5 MicroRNA-122 could serve as a potential therapeutic in limiting abnormal sFlt-1 levels and improving fetal outcome observed in preeclampsia

Preeclampsia is one of the leading causes of maternal and neonatal morbidity and mortality worldwide (Poon et al., 2019). There is no definitive treatment for this disorder and preventative measures are still elusive partly due to the lack of understanding of the pathogenesis of this disorder. Anti-angiogenic factor, sFlt-1, has been increasingly recognised as the major culprit of preeclampsia (Ahmad and Ahmed, 2004, Ahmed and Cudmore, 2009, Ramma and Ahmed, 2014, Maynard et al., 2003, Levine et al., 2004, Levine and Karumanchi, 2005, Levine et al., 2006), while protective HO-1 has been suggested to have a therapeutic potential in preventing pregnancy complications (Cudmore et al., 2007, George et al., 2011c, George et al., 2012, Ahmed et al., 2000). Although our laboratory had established a strong inverse relationship between these two proteins (Ahmed and Ramma, 2015b, Cudmore et al., 2007), the exact mechanism how HO-1 suppresses sFlt-1 had remained unknown.

Previous studies showed that HO-1 has the ability to regulate multiple miRNAs (Skrzypek et al., 2013, Kozakowska et al., 2012, Kozakowska et al., 2014). In addition, miR-210 and miR-10 were found associated with sFlt-1 decrease (Hassel et al., 2012, Korkes et al., 2017) and miR-181a have been shown to successfully inhibit sFlt-1 mRNA expression (Justiniano et al., 2013). MicroRNA has an important role in many physiological and pathological processes including preeclampsia (Jairajpuri et al., 2017, Lykoudi et al., 2018). Here we show that HO-1 regulates sFlt-1 via specific miR-122-dependent gene silencing and presents a clear evidence for its therapeutic potential to prevent or treat preeclampsia.

Several recent studies showed that HO-1 is able to exert its protective effects by stimulating different downstream targets independent of sFlt-1 (Venditti et al., 2014, Costantine et al., 2010, George et al., 2011a, Li et al., 2007, Mateus et al., 2011). When pregnant rats were continuously infused by mini osmotic pumps with recombinant sFlt-1 for 5 days, which caused circulating sFlt-1 increase similar to rats with RUPP, the induction of HO-1 with CoPP did not alter the maternal sFlt1 levels but increased

unbound circulating VEGF levels and improved endothelial function (George et al., 2011a). Same treatment also had no effect on fetal and placenta weight but improved placental ischaemia-induced hypertension, oxidative stress and angiogenic balance (George et al., 2011c). Low-dose CO treatment for 7 days prevented Ad-sFlt-1-induced late-gestation hypertension, proteinuria and histological kidney damage in mice but had no effect on litter size, fetal resorption and fetal or placental weights (Venditti et al., 2014). PPARy agonist that was injected into RUPP rats to induce plasma HO-1 levels, reduced hypertension, ameliorated endothelial dysfunction, improved proteinuria and abolished platelet aggregation but had no impact on sFlt-1 levels in addition to unchanged fetal number, fetal and placental weight (McCarthy et al., 2011). Therefore, these studies provide supporting evidence that increased HO-1 has multiple targets and functions, which not necessarily include the inhibition of sFlt-1. Since high sFlt-1 levels are heavily associated with poor fetal outcome (Kumasawa et al., 2011), we propose that the use of miR-122 replacement therapy, will improve fetal outcome in preeclampsia. Taken all of the observations together with, our group recently patented miRNA-122 (Meng Cai, 2020) in light that miR-122 replacement therapy alone or together with other therapeutics could serve as a therapeutic strategy to benefit patients with preeclampsia.

4.7 Study limitations and future perspectives

This study contains few limitations. Murine HET females treated with control and miR-122 adenovirus experienced low *Hmox1*$^{-/-}$ birth rate, which had an impact on the statistical analysis. Due to low number of the pups, we were unable to establish whether miR-122 would improve fetal and placental outcome of *Hmox1*$^{-/-}$ fetuses. Other groups using HO-1 compromised pregnancy model, even on different genetic backgrounds, C57Bl/6 (Zhao et al., 2009) and BALB/c (Zenclussen et al., 2011), experienced similar difficulties. Severe phenotype of HO-1 null pups was predominantly linked to increased chance of resorption.

Multiple studies observed that HO-1 deficiency in rodents is associated with severe placental insufficiency (Zhao et al., 2009, Zenclussen et al., 2011, Linzke et al., 2014), hypertension (Zhao et al., 2009, Linzke et al., 2014, George et al., 2013, George et al., 2011b, Zenclussen et al., 2011) and proteinuria (Venditti et al., 2014, Kaartokallio et al., 2014). Our study was focused on determining whether miR-122 was able to limit sFlt-1 release *in vitro* and *in vivo*, which is a primary culprit in preeclampsia (Ahmed et al., 1997, Maynard et al., 2003). A detail analysis of the pathological features associated with preeclampsia could reveal additional therapeutic benefits of miR-122. It is worth noting that we recorded no changes in systolic or diastolic blood pressure in HET pregnancy compared to WT pregnancy with or without miR-122 treatment. In contrast, high blood pressure was observed in HET pregnancy compared to WT pregnancy (Linzke et al., 2014, Zhao et al., 2011a). This may be due to genetic background differences in FVB/NJ (Zhao et al., 2011a) and BALB/c (Linzke et al., 2014) mice which are more susceptible to transgenic procedures or inflammation, respectively. Even though we have observed decreased HO-1 placental mRNA expression, measuring HO-1 activity could potentially explain unaffected blood pressure. Alternatively, in order to explore miR-122 effect on high blood pressure, either a better blood pressure monitoring technique should be employed such as telemetry or selection of an alternative preeclamptic *in vivo* model.

A study conducted by Qiu et al. (2010) reported that miR-122 regulates HO-1 expression. Overexpression of miR-122 *in vitro* caused downregulation of HO-1, which in turn increased production of HBV in transfected cells. Therefore, miR-122 plays a

negative role in the HO-1 - mediated inhibition of viral expression (Qiu et al., 2010). This indicates a new perspective of miR-122 therapy, which may be involved in a regulatory HO-1 feedback loop. Analysis of HO-1 expression and activity in miR-122 treated human endothelial cells and HO-1 compromised pregnancy could provide new insights for further studies.

Ad-CMV virus treatment increased resorptions rate in WT and HET pregnancies when compared to untreated animals. In the WT pregnancy resorption rate increased from 15% to 26% and in the HET pregnancy from 21% to 45%. The titre of the virus used for *in vivo* injections was relatively high, which most likely initiated innate immune response. Paired with reduced HO-1 protection against inflammation (Alcaraz et al., 2003) in HET pregnancy in addition to stress caused by the manual restrain for repetitive injections, may have further exacerbated inflammatory response explaining the increase in the resorption rate. Ad-miR-122 treatment reduced resorption rate in HET pregnancy similar to levels observed in the untreated HET pregnancy. This highlights miR-122 ability to overcome negative effects initiated by the virus. Further experiments are needed to explore adenovirus associated immune response and miR-122 anti-inflammatory effect.

MicroRNA is known to target multiple mRNA transcripts (Lam et al., 2015). By targeting more than one mRNA, miRNA is able to regulate components of the complex pathways leading to change in the overall phenotype. Some of them include cationic amino acid transporter-1 (CAT-1), serum response factor (SRF), hemochromatosis (Hfe) and hemojuvelin (Hjv), which regulate systemic iron homeostasis, glucose-6-phosphate-dehydrogenase (G6PD), which is often activated in human malignancies (Bhattacharyya et al., 2006, Bai et al., 2009a, Castoldi et al., 2011, Barajas et al., 2018) and many others identified using miRNA target prediction websites (microRNA.org, miRWalk, miRTarBase) and online database libraries (GeneCards.org and miRbase.org). Several targets including a distintegrin and metalloprotease family 10 (ADAM10), insulin-like growth factor 1 receptor (IGF1R) (Bai et al., 2009a) and ADAM17 (Tsai et al., 2009) that play a role in metastasis are also known to be involved in the pathogenesis of preeclampsia (Hu et al., 2015, Díaz et al., 2005, Loichinger et al., 2016). Protein expression and qPCR analysis of these targets in placenta and maternal organs could provide more information about miR-122 overexpression induced side effects and potential therapeutic targets relevant to miR-122 dependent treatment.

Finally, intraperitoneal injection of the adenovirus may infect other cells and overexpress miR-122 in organs other than placenta. Real-time quantitative PCR analysis of miR-122 and sFlt-1 in the maternal liver, kidney, spleen, lung and heart would provide an understanding of a potential side effects. Additionally, analysis of miR-122 in fetal tissues would identify placental transfer of miR-122.

Chapter 5

Placenta-targeted liposomal delivery of miR-122 to suppress sFlt-1 in a refined surgically induced preeclampsia model in mice

5.1 Highlights

- Our designed CGKRK surface modified neutral PC liposomes provide a suitable carrier complex to encapsulate miR-122 (CGKRK-PC-miR-122)
- CGKRK-PC-miR-122 formulation is well tolerated by human endothelial cells
- Cell-penetrating CGKRK targeting peptide facilitates cellular internalisation
- MicroRNA-122 delivered to human endothelial cells using our designed CGKRK-PC liposomes inhibits VEGF-E-induced sFlt-1 release *in vitro*
- CGKRK targeting peptide facilitates liposomal payload delivery to the mouse placenta with minimal off-target organ accumulation
- MicroRNA-122 delivered to mouse placenta in the surgically induced utero-placental insufficiency model of preeclampsia using our designed CGKRK-PC liposomes inhibits ischaemia-induced placental sFlt-1 release and improves fetal survival

5.2 Summary

In Chapter 4 we demonstrated that miR-122 overexpression using adenoviral vector inhibits sFlt-1 release and improves fetal outcome in HO-1 compromised murine pregnancy. This highlights therapeutic potential of miR-122 in preeclampsia. However, viral vectors exhibit multiple side effects associated with immune response and lack of target specificity. To provide a stable placenta-specific delivery vehicle for miR-122, we designed neutral PC liposomes, conjugated with CGKRK placenta-homing peptide. MicroRNA-122 delivered using our designed liposomes to human endothelial cells caused a significant inhibition of VEGF-E-induced sFlt-1 release. CGKRK decorated PC liposomes injected to pregnant mice accumulated within the placental tissue with minimal off-target organ accumulation confirming CGKRK placenta-targeting properties. Next, *in vivo* therapeutic potential of miR-122 was studied in the refined reduced uterine perfusion pressure murine model (mRUPP) of preeclampsia. Pregnant mice treated with CGKRK decorated PC liposomes loaded with miR-122 inhibited placental ischaemia-induced sFlt-1 release and improved fetal survival rate. These results offer a promising placenta-targeted miR-122 therapeutic strategy to treat preeclampsia.

5.3 Graphical abstract

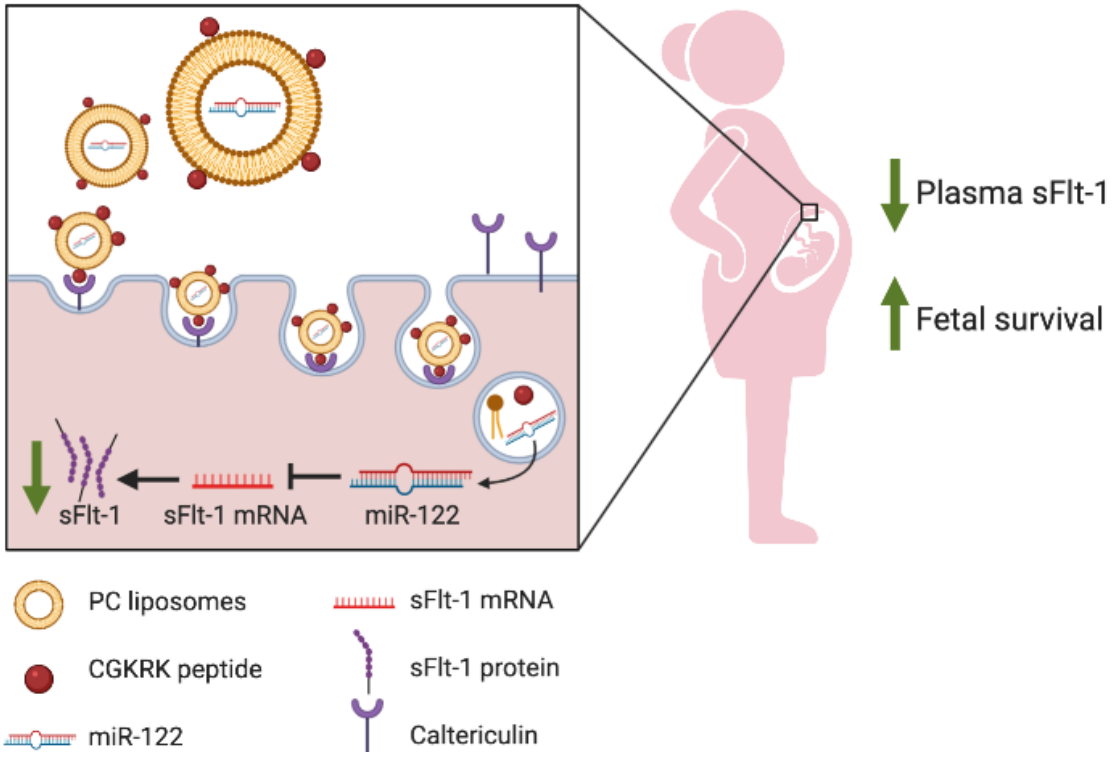

5.4 Introduction

A new class of therapeutic agents, miRNAs, offer a promise to treat various human diseases including cancers, viral infections, ocular conditions, genetic disorders, and cardiovascular diseases (Lam et al., 2015). We have discovered that Ad-miR-122 replacement therapy reduces sFlt-1, improves fetal weight and reduces fetal death rate in HO-1 compromised murine pregnancy. Even though adenovirus miR-122 vector is stripped of all viral proteins and made "gutless" (Amalfitano, 1999) to reduce toxicity and prolong transgene expression (Crettaz et al., 2009, Maione et al., 2001), it still possess the risk of innate and adaptive immune response (Marshall, 1999). Therefore, adenovirus is not an ideal vehicle to deliver miR-122 *in vivo*. To consider miR-122 as a potential therapeutic agent to treat preeclampsia, an alternative, safer option is required.

Liposomal complexes successfully encapsulate nucleic acids and provide stable protection against degradation and facilitate cellular uptake (Fu et al., 2019). Thus, liposomes are a good carrier system for therapeutically active agents owing to their unique characteristics including biodegradability, biocompatibility and lack of immune system activation (Deshpande et al., 2013). Liposomes loaded with miR-10b inhibitor in addition to paclitaxel provided an effective treatment against breast cancer metastasis (Zhang et al., 2015), whereas liposomal bubbles encapsulating miR-126 promoted angiogenesis in hindlimb ischemia mouse model (Endo-Takahashi et al., 2014). Therefore, miRNA delivered using liposomes not only provide stability and protection but also preserve biological function of the miRNA (Lam et al., 2015).

Therapeutic effectiveness of many pharmaceutical compounds, including liposomes, for the treatment of a range of diseases is low due to the lack of target specificity. This leads to the significant amounts of administered drug being delivered to both diseased and normal tissues (Ferrari, 2010). To increase the degree of site-specific localisation, studies have focused on modifying nanoparticle surface to facilitate cellular uptake, reduce dosage and minimise side effects (King et al., 2016, Liang et al., 2016). Circulating ligands, such as peptides, have been shown to bind to the tumour-specific receptors and promote the attachment of a therapeutic payload (Allen and Cullis, 2004, Ruoslahti, 2002). This results in localised and specialised accumulation within the

tumour tissue, improved therapeutic efficacy and reduced off-target exposure to normal tissues (Arap et al., 1998, Ruoslahti et al., 2010).

Recently, pentapeptide CGKRK (Cys-Gly-Lys-Arg-Lys) was identified as a tumour-homing peptide and successfully used to bind to receptors expressed by the epidermal cancer (Hoffman et al., 2003), glioblastoma (Agemy et al., 2011), breast cancer (Agemy et al., 2013) and even placenta (King et al., 2016, Beards et al., 2017). CGKRK peptide has been shown to mainly bind to the cell surface receptor p32 (Agemy et al., 2013, Fogal et al., 2008) and Ca^{2+}-binding molecular chaperone, calreticulin, localised in the endoplasmic reticulum (Michalak et al., 2009). Both of these receptors are highly expressed in the placenta (Matos et al., 2014, Højrup et al., 2001). King and colleagues reported high affinity of CGKRK to calreticulin in mouse and human placenta (King et al., 2016). They showed the ability of CGKRK peptide to localise in placenta within the labyrinth zone and decidual spiral arteries (King et al., 2016). The same group went on to show that miRNA inhibitor-CGKRK peptide PNA conjugates could be used to facilitate placenta-specific delivery of miRNA inhibitors to mouse placenta *in vivo* and human placenta *ex vivo*. This led to effective miR-145 and miR-675 downregulation (Beards et al., 2017). These studies provided the proof-of-concept needed to deliver active substance to the mouse and human placenta by attaching CGKRK peptide to the surface of delivery vehicle.

The role of CGKRK target, calreticulin, in pregnancy is relatively unknown. However, few studies explored its regulatory role in the invasion of extravillous trophoblasts (Yamamoto et al., 2017), migration of microvascular endothelial cells (Crawford et al., 2012) and apoptosis of trophoblast cells (Shi et al., 2012). In addition, calreticulin expression was found to be increased in preeclamptic placenta (Shi et al., 2012) and maternal plasma (Gu et al., 2008) suggesting a potential role in the pathogenesis of pregnancy disorders. Having discovered that miR-122 had the potential to treat poor pregnancy outcome associated with high sFlt-1 levels, we hypothesise that CGKRK targeted liposomal delivery of miR-122 will provide a placenta-specific therapy to suppress sFlt-1 and improve fetal outcome in preeclampsia.

In order to test the hypothesis, liposomal formulation was designed, loaded with miR-122 and validated using human umbilical vein endothelial cells. To facilitate placenta-specific delivery, the outer bilayer of the liposomes was decorated with

fluorescently labelled CGKRK peptides. Targeted liposomes were loaded with fluorescent dye and injected to normal pregnant C57Bl/6 mice to confirm placental uptake and analyse off-target localisation. Once the placenta-specific uptake was confirmed, normal pregnant C57Bl/6 mice were subjected to reduced uterine perfusion (mRUPP) surgery to mimic preeclampsia. CGKRK decorated liposomes loaded with miR-122 were intravenously injected at three different time points in gestation. At the end of pregnancy, sFlt-1 levels were measured in addition to evaluation of fetal outcome to assess a potential therapeutic effect of placenta-specific miR-122 liposomal treatment.

5.5 Results

5.5.1 Characterisation and stability of the liposomes

Initially, neutral PC liposomes were designed to provide an efficient delivery system of miR-122. Anchor lipid PC was formulated together with cholesterol to stabilise the formulation. DSPE-PEG-Maleimide was used to facilitate peptide conjugation via a Michael-type addition reaction (King et al., 2016) and DSPE-PEG to impart stealth properties and increase circulation half-life (Gjetting et al., 2010, Meyer et al., 1998, Immordino et al., 2006). Four different PC liposome formulations were designed to evaluate the effect of CGKRK conjugation and miR-122 encapsulation:

1. Undecorated empty PC liposomes – PC-empty
2. CGKRK-decorated empty PC liposomes – CGKRK-PC-empty
3. Undecorated miR-122-loaded PC liposomes – PC-miR-122
4. CGKRK-decorated miR-122-loaded PC liposomes – CGKRK-PC-miR-122

Electrostatic interaction is an important force affecting the structure, stability and function of the liposomes (Sou, 2011). We have used zeta potential (ζ) reading to measure the overall electrostatic charge of the particles in a medium. This gives information about the difference in potential between the static layer and bulk media layer around a particle and how it is affected by changes in the environment. Addition of CGKRK peptide had a significant impact towards the relative surface charge. The overall ζ potential of the nanoparticle dropped from -15.72 to -42.23 (Table 5.1). MicroRNA-122 encapsulation to CGKRK-PC liposomes decreased relative surface charge to -32.12. Addition of miR-122 to the formulation stabilised ζ potential, resulting in a non-significant difference between PC-empty and CGKRK-PC-miR-122 liposomes (Figure 5.1 A). PC is considered a charge neutral liposome, however negative ζ potential observed may be due to the other liposomal components and presence of counter ions.

Zeta potential was also used to determine the type of interaction between the miR-122 and the liposome carrier. No differences were observed between PC-empty and PC-miR-122 (Table 5.1) suggesting that miR-122 was entrapped within the liposome and not adsorbed on the outside (Laouini et al., 2012). Furthermore, based on the data

spread, addition of miR-122 to liposomes stabilised the formulation, forming more conserved population of the samples (Figure 5.1 A).

Table 5. 1. Zeta potential of PC liposomal formulations.

Liposomes	Zeta Potential (mV)	±SEM	Sample Size	Adjusted P[1]
PC-empty	-15.72	8.620	15	-
PC-miR-122	-36.84	2.189	27	0.0572
CGKRK-PC-empty	-42.23	1.346	18	0.0010
CGKRK-PC-miR-122	-32.12	2.235	19	>0.9999

[1]Kruskal-Wallis test *post hoc* Dunn's test with multiple comparisons to PC-empty group; ***P<0.005.*

Stability of the liposomes was determined by the size and polydispersity measured every 7 days for 21 days in total. Average size of all nanoparticle formulations remained unchanged, with the average size of CGKRK-PC-miR-122 liposomes being 126.7nm (Figure 5.1 B). This according to liposomes applied in a clinical setting fit within the 50 - 450 nm range (Etheridge et al., 2013). Homogeneity of the liposomal dispersion was determined by the polydispersity index (PI). Liposomal formulation with the PI below <0.3 was considered uniform. All four liposomal formulations remained within the suitable range. CGKRK-PC-miR-122 liposomes dispersion increased from PI = 0.15 on day one to PI = 0.21 on day 21 (Figure 5.1 C). The increase remained within the range and was statistically insignificant.

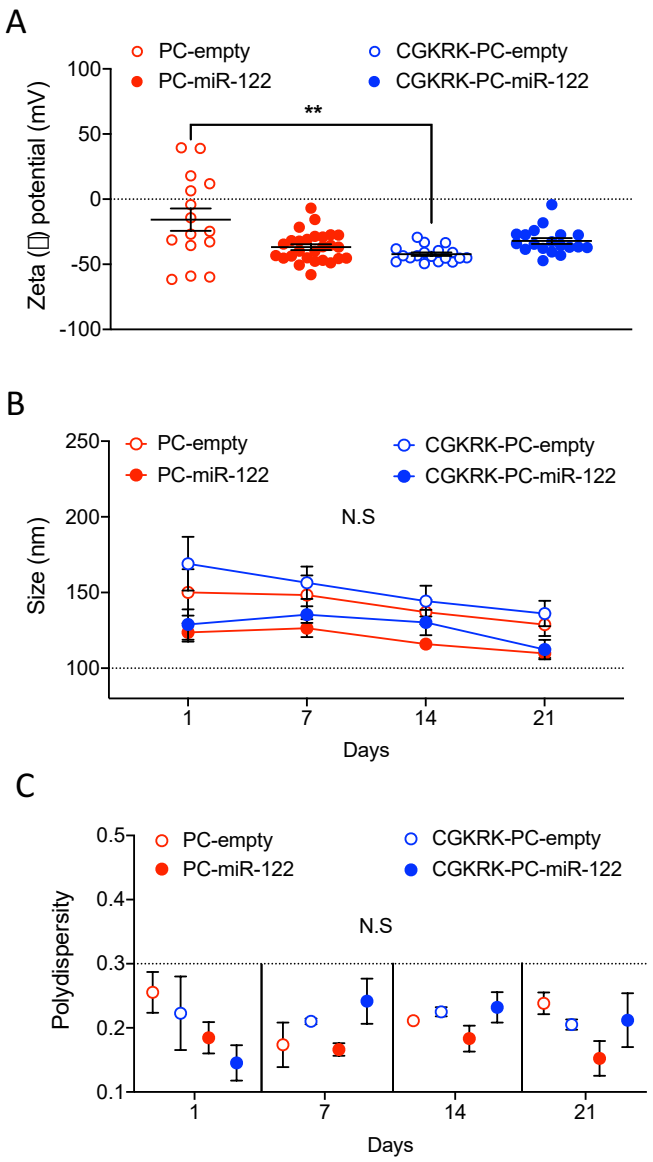

Figure 5. 1. Characterisation and stability of the CGKRK decorated and miR-122 loaded PC liposomal formulations.

PC liposomal formulations include four groups: (1) undecorated PC liposomes without any internal cargo (PC-empty), (2) undecorated PC liposomes encapsulating miR-122 sequence (PC-miR-122), (3) PC liposomes decorated with CGKRK peptide but without any internal cargo (CGKRK-PC-empty) and (4) PC liposomes decorated with CGKRK peptide and encapsulating miR-122 sequence (CGKRK-PC-miR-122). The stability of four groups were characterised using a combination of different parameters including size, zeta potential and polydispersity (PI). **(A)** Zeta potential of the nanoparticles in colloidal solution was determined on the day 1 (PC-empty n=15, PC-miR-122 n=28, CGKRK-PC-empty n=18, CGKRK-PC-miR-122 n=21). Kruskal-Wallis test *post hoc* Dunn's test with multiple comparisons to PC-empty group; ***P<0.005.* **(B)** To determine the stability of nanoparticles, the size of all liposomal formulations was recorded over the period of 21 days (PC-empty n=6, PC-miR-122 n=7, CGKRK-PC-empty n=6, CGKRK-PC-miR-122 n=4). Repeated measures Two-Way ANOVA; *P>0.05.* **(C)** Heterogeneity of the nanoparticles dispersion was determined as uniform when the range of polydispersity was within the PI < 0.3 limit (PC-empty n=6, PC-miR-122 n=7, CGKRK-PC-empty n=6, CGKRK-PC-miR-122 n=4). Repeated measures Two-Way ANOVA; *P>0.05.*

5.5.2 Peptide conjugation, miR-122 entrapment and release from the liposomes

PC liposomal formulations were incubated with the fluorescently tagged TAMRA-CGKRK peptides to assess the efficiency of peptide conjugation. To see whether miR-122 loading has impact on peptide conjugation and whether peptide conjugation has impact on miR-122 loading, miR-122 was added to the formulation. In empty and miR-122 loaded PC liposomes, 60% of added peptides were incorporated. Addition of miR-122 to the liposomes did not affect the peptide conjugation (Figure 5.2 A). Undecorated and CGKRK-decorated PC liposomes were loaded with fluorescently labelled miR-122 to evaluate the efficiency of encapsulation and release. Both formulations entrapped 65-70% of the total added miR-122 showing that CGKRK peptide conjugation has no negative effect on miR-122 loading (Figure 5.2 B).

Liposomal retention of miR-122 was measured over 21 days. On day one, undecorated PC and CGKRK-PC liposomes were prepared and loaded with miR-122. After 21 days, undecorated PC liposomes incurred a significant loss (10%) of the miR-122 content, whereas miR-122 loss from CGKRK-PC liposomes was statistically insignificant (Figure 5.2 C). Release of the fluorescent miR-122 was measured over 24 hours; after 4 hours, 50% and after 6 hours, 75% of the miR-122 was released. Complete release (100%) occurred at 24 hours (Figure 5.2 D).

Characterisation data confirmed that conjugation of CGKRK peptides and miR-122 encapsulation have no effect on the PC liposomal formulation stability, as well as the miR-122 entrapment and release.

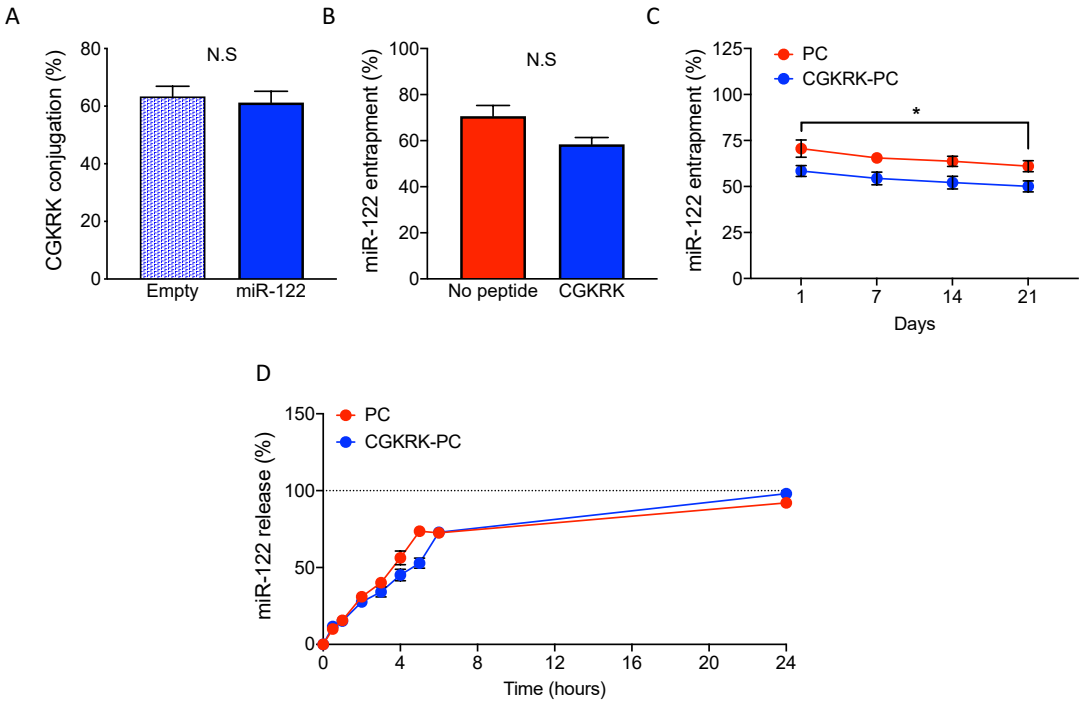

Figure 5. 2. CGKRK peptide conjugation, entrapment and release of the miR-122 from PC liposomes.

(A) PC liposomes were decorated with CGKRK peptide and the conjugation was measured by the TAMRA fluorescence intensity. Liposomal formulation loaded with fluorescent miR-122-6FAM was used to assess the loading influence upon the peptide conjugation (Empty n=3, miR-122 n=4). Mann-Whitney test*; P>0.05.* **(B)** Undecorated PC liposomes or PC liposomes decorated with CGKRK were used to entrap miR-122 sequence and assess the entrapment efficiency by the 6FAM fluorescence intensity (No peptide n=3, CGKRK n=3). Mann-Whitney test; *P>0.05.* **(C)** CGKRK decorated liposomes were mixed with fluorescent miR-122 followed by the 6FAM fluorescent reading on day 1, 7, 14 and 21 to analyse miR-122 retention within the liposomes (n=3). Repeated measures Two-Way ANOVA *post hoc* Sidak's test with multiple comparisons to day 1; **P<0.05.* **(D)** The percentage of miR-122 release over the period of 24 hours was measured using 6FAM fluorescence intensity (n=9). Repeated measures Two-Way ANOVA; *P>0.05.*

5.5.3 MicroRNA-122 containing liposomes are well-tolerated by human endothelial cells

Uptake of neutral PC liposomes using human umbilical vein endothelial (HUVEC) cells was reported previously as safe and well-tolerated (Papadimitriou and Antimisiaris, 2000). To confirm that our designed formulation is safe to use in cell culture and *in vivo*, HUVEC cells were treated either with empty, scrambled or miR-122 loaded CGKRK-PC liposomes at different dilutions. Total amount 1 nmole of fluorescent miR-122 was encapsulated per 100 µl of the liposomal formulation. Liposomes diluted at 1:100 and 1:10, liposomes to media ratio, showed no toxicological effects. Dilution at 1:5 reduced cell viability by 25%. Dilution at 1:2 reduced cell viability by 75%, which caused a significant cellular death compared to the PBS treated group (Figure 5.3). Entrapment of scrambled or miR-122 sequence within the liposomes in all dilution groups had no effect on the overall interaction between the liposomal formulation and the cells.

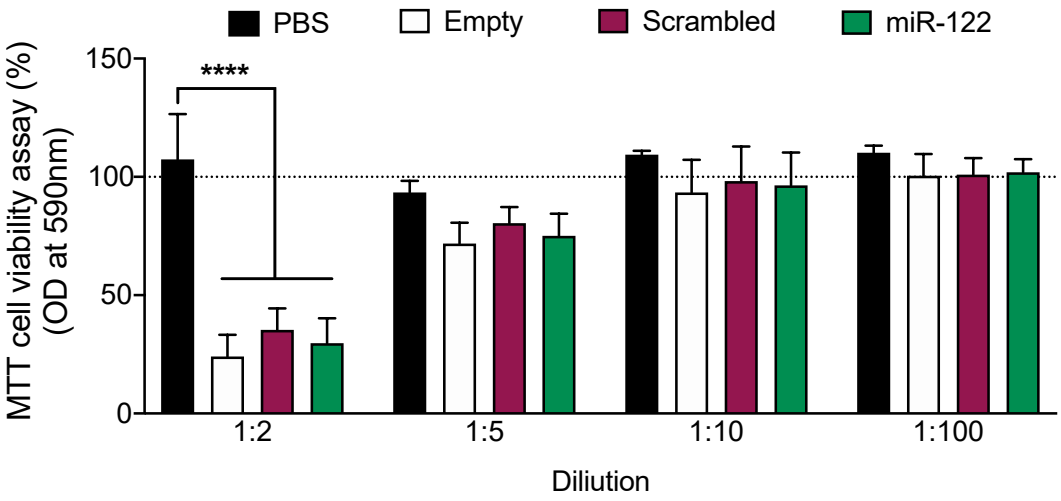

Figure 5. 3. MicroRNA-122 containing PC liposomes do not exhibit toxicity towards human endothelial cells when applied at 1:10 dilution.

PC liposomes were decorated with CGKRK peptide and loaded with fluorescent scrambled or miR-122 sequence. To assess the toxicity of the formulation and select a most optimal dose for cell culture experiments, HUVEC cells were treated with either empty, scrambled or miR-122 containing PC liposomes at 1:2, 1:5 1:10 and 1:100 dilutions for 6h (n=3). Percentage of live cells were normalised individually to the PBS treated group. Two-Way ANOVA *post hoc* Sidak's test with multiple comparisons to PBS; ***P<0.005.*

5.5.4 PC liposomes are internalised by human endothelial cells

Certain lipids within the liposome's bilayer promote cellular membrane attachment rather than active internalisation (Daraee et al., 2016). This challenges the efficiency of the internal liposomal cargo delivery. To confirm that our designed liposomes are internalised, we used fluorescence trypan blue quenching technique (Patiño et al., 2015). PC liposomes were loaded with 6FAM fluorescent dye to analyse the efficiency of the cellular uptake and localisation of the internalised liposomes. Four different PC liposomal formulations were prepared:

1. Undecorated empty PC liposomes – PC-empty
2. CGKRK-decorated empty PC liposomes – CGKRK-PC-empty
3. Undecorated 6FAM-loaded PC liposomes – PC-6FAM
4. CGKRK-decorated 6FAM-loaded PC liposomes – CGKRK-PC-6FAM

Liposomal suspension in media at 1:10 ratio was added to HUVEC cells. After 6 hours outer fluorescence was quenched with trypan blue allowing internalised fluorescence to be picked up by the flow cytometry. PC-6FAM liposomes coated either with or without CGKRK were able to deliver more than 80% of 6FAM to HUVEC cells (Figure 5.4). Cellular internalisation and release of the liposomes content in HUVEC cells ranges between 5-10 min (Papadimitriou and Antimisiaris, 2000) indicating that period of 6 hours does not affect fluorescent sensitivity and it allows sufficient time for miR-122 to be released.

HUVECs internalise whole liposomes most likely via receptor-mediated endocytosis (Papadimitriou and Antimisiaris, 2000). Internalisation of 6FAM cargo from the PC-6FAM and CGKRK-PC-6FAM liposomes was localised using fluorescent imaging. 6FAM was localised in the cell cytoplasm after 6 hours post-treatment and higher 6FAM fluorescence intensity was observed in CGKRK decorated liposome group (Figure 5.5). No autofluorescence exhibited by the human cells or liposomal formulation was detected in PC-empty treatment group when compared to untreated group (Supplement B Figure 1).

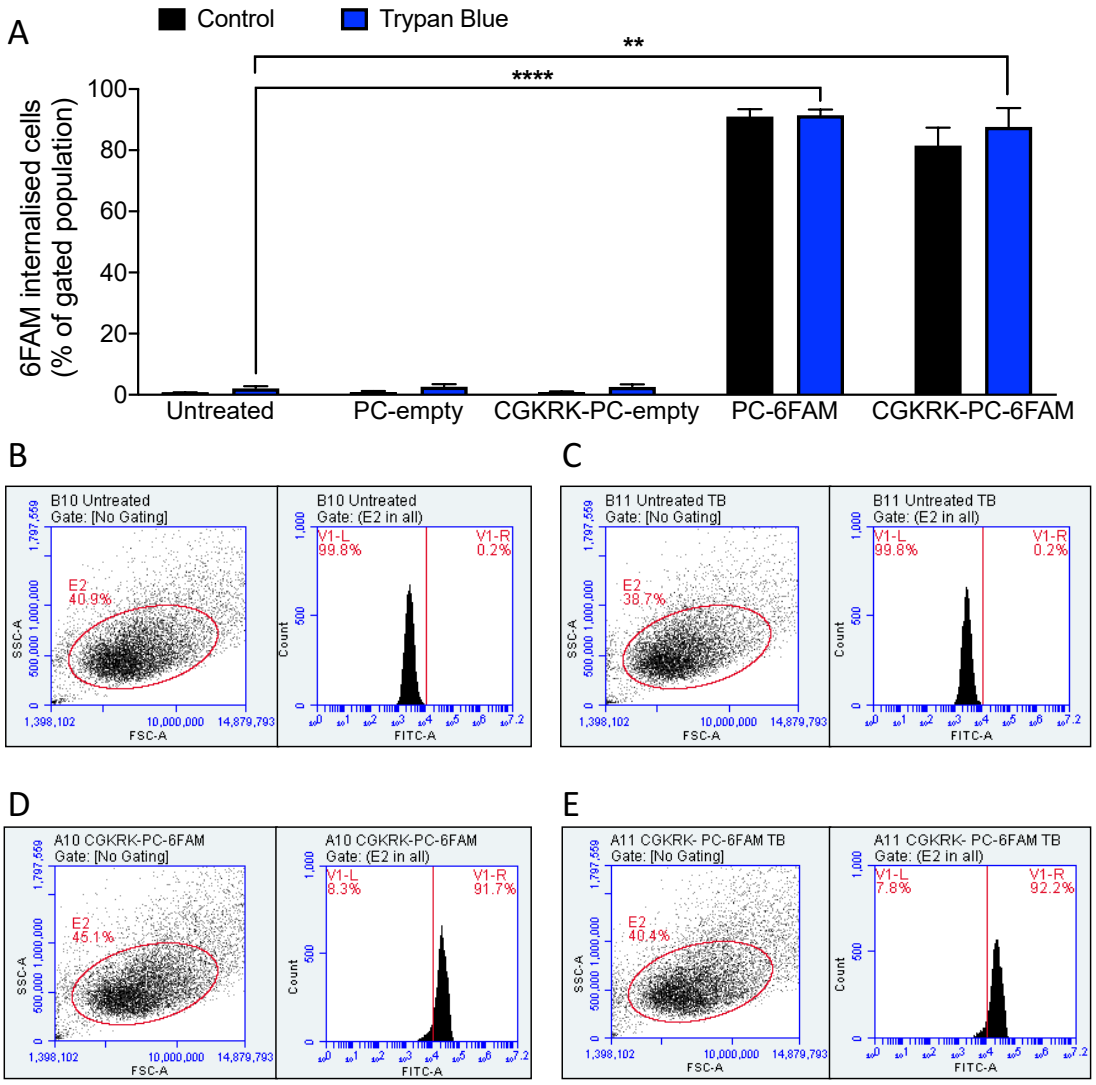

Figure 5. 4. Liposomes internalisation by human endothelial cells.

PC liposomes were decorated with CGKRK peptide and loaded with 6FAM fluorescent dye to analyse liposomal cargo cellular internalisation. (**A)** HUVEC cells treated with four PC liposomal formulations: PC-empty, CGKRK-PC-empty, PC-6FAM and CGKRK-PC-6FAM for 6h (n=3) followed by flow cytometry fluorescence detection. Cellular fluorescent quenching was performed using 2mg/ml Trypan Blue solution (TB). Baseline of the FITC fluorescence was set using untreated HUVECs control group before and after the addition of TB. Two-Way ANOVA *post hoc* Sidak's test with multiple comparisons to Untreated group; ***P<0.005; ****P<0.0001*. The panel below includes representative flow cytometry graphs of untreated and CGKRK-PC-6FAM treated groups. Baseline of the FITC fluorescence was set using untreated HUVECs control group before **(B)** and after **(C)** the addition of TB. CGKRK-PC-6FAM cellular uptake was confirmed before **(D)** and after **(E)** the addition of TB.

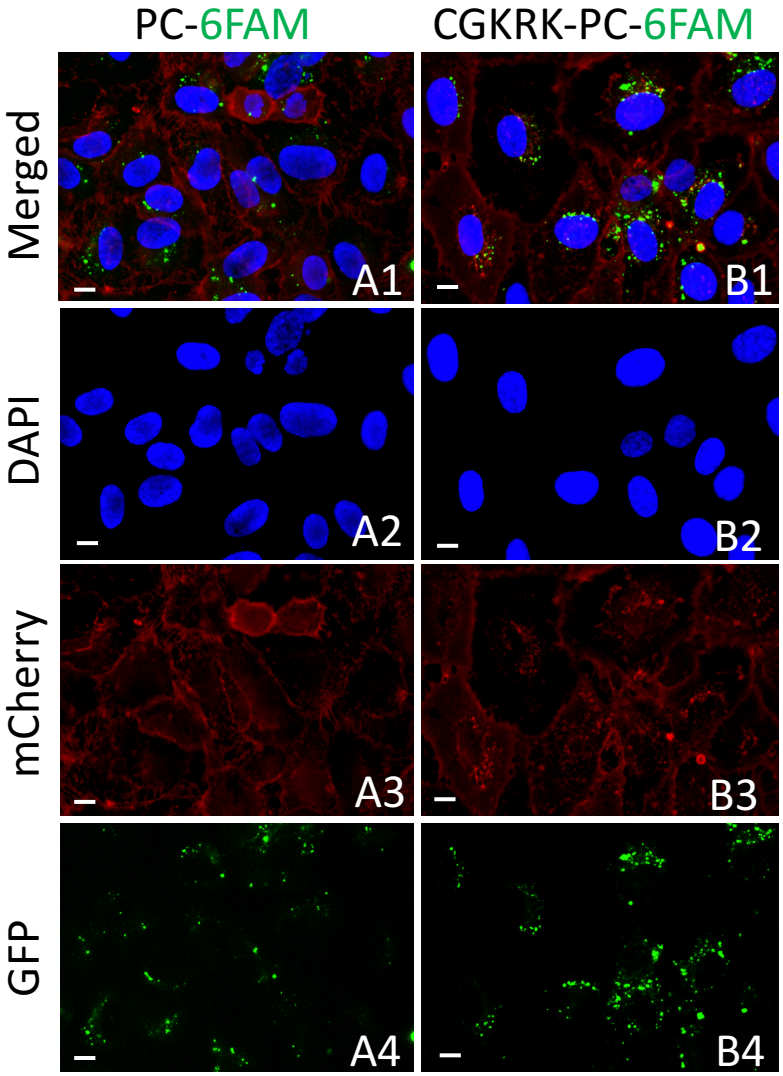

Figure 5. 5 Liposomal payload localises in the cytoplasm of human endothelial cells.

Representative images of HUVEC cells treated with undecorated PC-6FAM (A1-A4) and CGKRK-PC-6FAM (A1-A4) liposomes for 6h. Cells were fixed and stained with WGA (red, mCherry) to define cellular membrane and with DAPI (blue, DAPI) to stain the nuclei. Localisation of 6FAM (green, GFP) fluorescence was observed under the microscope. Scale bar 10µm. Images randomly sampled from 3 independent experiments (n=3).

5.5.5 Liposomal delivery of miR-122 inhibits sFlt-1 in human endothelial cells

Our results established that CGKRK-PC-miR-122 liposomal formulation is well tolerated and rapidly internalised by human endothelial cells. We next looked to see whether miR-122 delivered using liposomes inhibits sFlt-1 *in vitro*. To establish optimal miR-122 loading to liposomes, fluorescent miR-122 was loaded to CGKRK-PC liposomes at different concentrations and applied to the HUVEC cells at 1:10 dilution (100 µl of liposomes) for 6 hours. Fluorescent analysis revealed that 1 nmole of miR-122 was the most optimal loading amount with the highest cellular uptake (Table 5.2).

We have shown in Chapter 4 that 0.25 nmoles of naked miR-122 is sufficient to inhibit VEGF-E-induced sFlt-1 release in HUVEC cells. Based on these studies, we chose 1 nmole of non-fluorescent miR-122 as fluorescent label impairs miR-122 gene suppressive ability (Supplement B Figure 2) (Lu et al., 2016). HUVEC cells were treated with empty, scrambled or miR-122 loaded CGKRK-PC liposomes at a 1:10 dilution (100 µl liposomes) for 24 hours. Successful intracellular delivery of miR-122 was confirmed by real-time qPCR (Figure 5.6 B). CGKRK-PC-miR-122 treatment caused a significant inhibition of VEGF-E-induced sFlt-1 release when compared to liposomes loaded with scrambled control treatment (Figure 5.6 A). Thus, a dose of 1 nmole of miR-122 per 100 µl of liposomes (0.01nmole/µl) was well tolerated by endothelial cells, showed the highest intracellular delivery and effectively inhibited in VEGF-E-induced sFlt-1 release *in vitro.* This dosage was therefore selected for *in vivo* experiments.

Table 5. 2. Cellular uptake of miR-122 loaded at different concentrations to PC liposomes.

Starting Amount (nmole) Pre-entrapment	Treatment Amount (nmole) Post-entrapment	Internalised Amount (nmole)	Cellular Uptake
0.5	0.3	0.1	33.3%
1	0.6	0.25	42%
5	3	1.13	37.7%
10	6	1	16.6%
25	15	1.22	8.1%

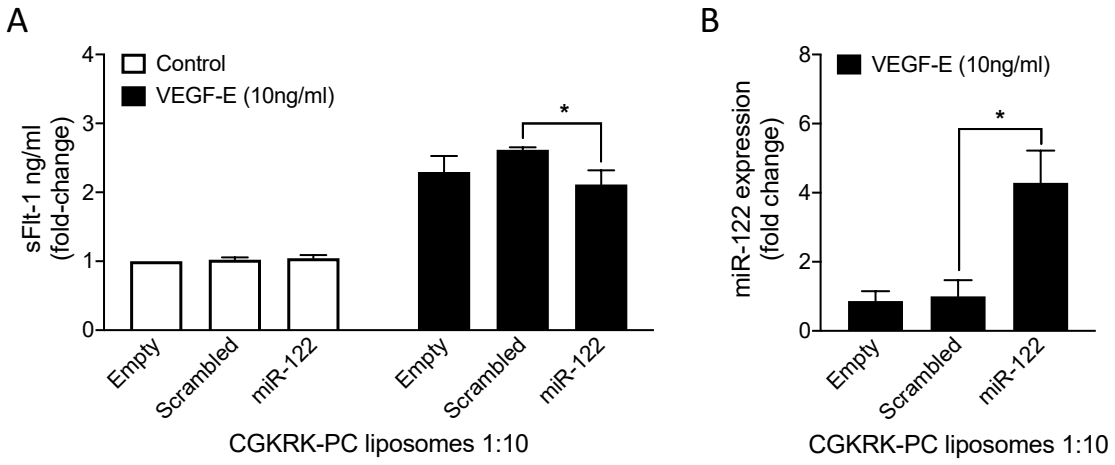

Figure 5. 6. MicroRNA-122 delivered by CGKRK decorated PC liposomes inhibits VEGF-E-induced sFlt-1 release in human endothelial cells.

(A) HUVECs were treated with either empty, scrambled or miR-122 encapsulating PC liposomes at the dilution 1:10 for 24h (1nmol/100µl per treatment) and stimulated with VEGF-E (10ng/ml). Conditioned media was collected to determine sFlt-1 protein concentration (Control n=5; VEGF-E n=4). Two-Way ANOVA *post hoc* Dunnett's test with multiple comparisons to Scrambled group; *$P<0.05$. **(B)** Cells from VEGF-E stimulated group were analysed with real-time qPCR to determine relative miR-122 expression (n=4). Relative miRNA expression was normalised to RNU48 housekeeping gene. Kruskal-Wallis test *post hoc* Dunn's test with multiple comparisons to Scrambled group; *$P<0.05$.

5.5.6 CGKRK peptide guides PC liposomes to the mouse placenta with minimal unspecific off-target organ delivery

CGKRK surface modified liposomal formulations were designed and loaded with 6FAM fluorescent dye to analyse placenta-specific guiding of the nanoparticles. Pregnant C57Bl/6 mice were administered 100 µl of the liposomes via tail vein injection and placental tissues were harvested for fluorescent analysis 6 hours post-injection. Placental-specific targeting of CGKRK modified liposomes was confirmed with red (TAMRA) fluorescence (Figure 5.7 B3). Liposomal delivery of the internal payload to placenta was confirmed with green (6FAM) fluorescence (Figure 5.7 B4). Higher fluorescence intensity of 6FAM was observed in the placenta from CGKRK-PC-6FAM treated mice when compared to PC-6FAM treated mice (Figure 5.7 A4 and B4). No autofluorescence of the tissues or liposomal formulation was detected in PC-empty treatment group when compared to untreated group (Supplement B Figure 3).

Maternal organs were collected to assess the off-target liposomal payload delivery. High accumulation of PC-6FAM and CGKRK-PC-6FAM was observed in maternal spleen (Figure 5.8 A3 and B3). Minimal CGKRK-PC-6FAM fluorescent accumulation was observed in maternal liver (Figure 5.8 B1) and kidney (Figure 5.8 B2) and negligible fluorescence in lung (Figure 5.8 B4). PC-6FAM caused high off-target organ accumulation in maternal kidney (Figure 5.8 A2) and lung (Figure 5.8 A4) and low accumulation in liver (Figure 5.8 A1). No accumulation of liposomes was observed in the maternal heart (Figure 5.8 A5 and B5) as well as no autofluorescence of the tissues or liposomal formulation in the maternal organs (Supplement B Figure 4).

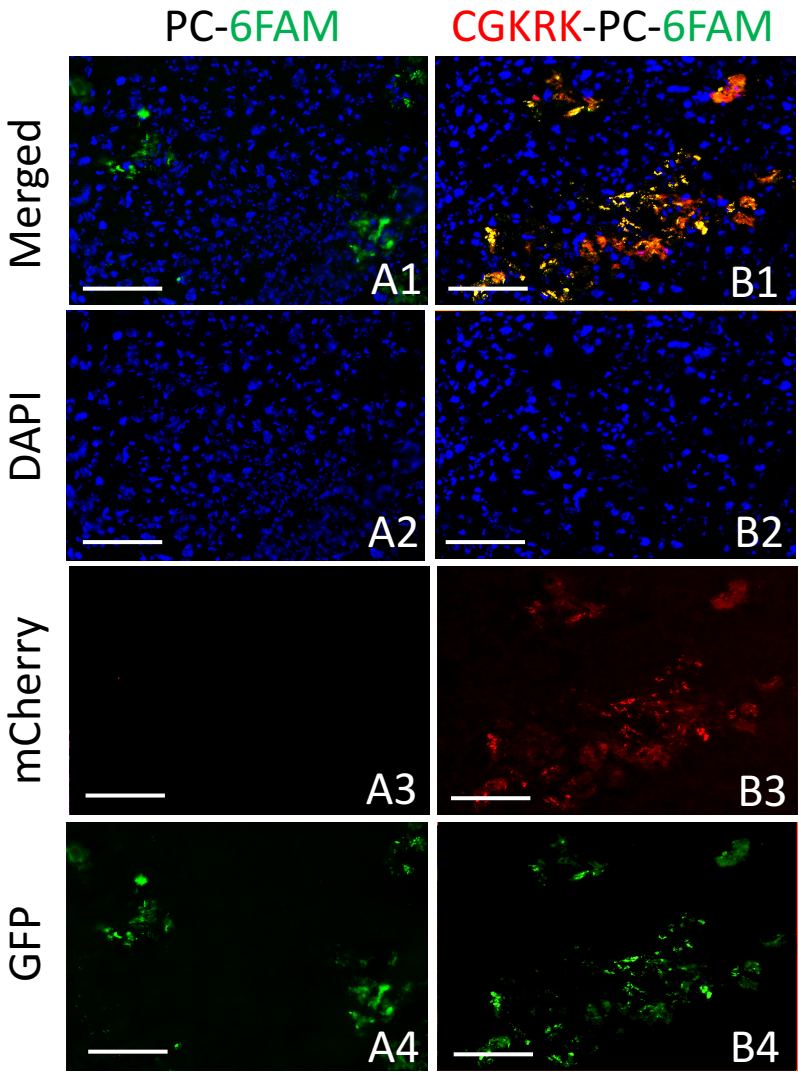

Figure 5. 7. CGKRK peptide guides liposomal payload to the mouse placenta.

WT mice received intravenous (IV) injection of CGKRK decorated (red, mCherry) liposomes loaded with 6FAM (green, GFP) on E17.5. After 6 hours placental tissues were collected, fixed and imaged. Treatment groups included: PC-6FAM (A1-A4) and CGKRK-PC-6FAM (B1-B4). Nuclei was stained with DAPI (blue, DAPI). Scale bar 100µm. Images randomly sampled from 3 pregnant mice (n=3).

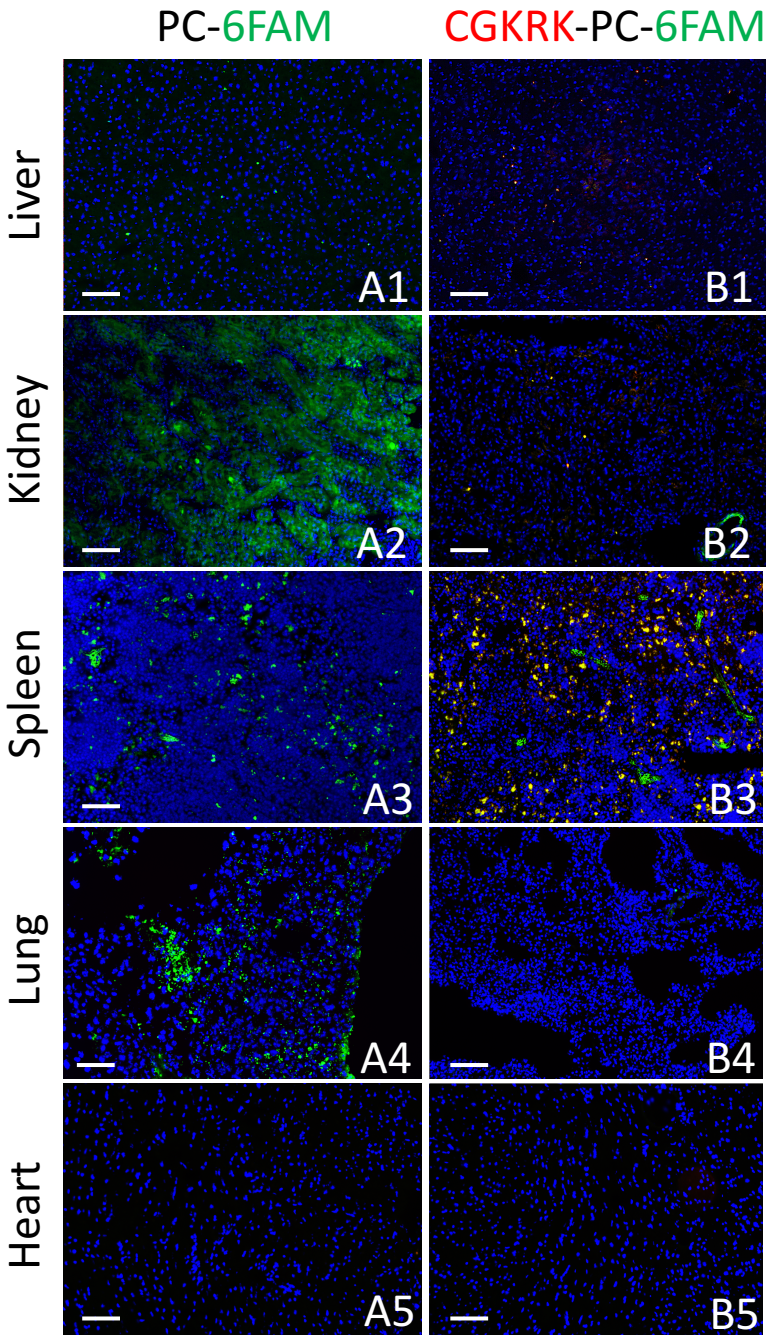

Figure 5. 8. CGKRK peptide reduces off-target liposomal payload delivery to the maternal organs.

WT mice received intravenous (IV) injection of CGKRK decorated (red, mCherry) liposomes loaded with 6FAM (green, GFP) on E17.5. After 6 hours liver, kidney, spleen, lung and heart tissues were collected, fixed and imaged. Treatment groups included: PC-6FAM (A1-A5) and CGKRK-PC-6FAM (B1-B5). Nuclei was stained with DAPI (blue, DAPI). Scale bar 100µm. Images randomly sampled from 3 pregnant mice (n=3).

5.5.7 Placenta-targeted miR-122 liposomal treatment reduces RUPP-induced sFlt-1 levels in vivo

Reduced uterine perfusion pressure (RUPP) preeclamptic animal model has been explored in multiple studies (Morton et al., 2019, Fushima et al., 2016). This refined mouse model was selected to test a therapeutic effect of placenta-targeted miR-122. Pregnant mice received either Sham or double ovarian RUPP surgery on day E11.5. Mice that undergone RUPP surgical procedure (mRUPP) received three intravenous injections of CGKRK-PC-Scrambled or CGKRK-PC-miR-122 liposomes at E12.5, E14.5 and E16.5 followed by the tissue collection on E17.5.

At the end of the pregnancy, sFlt-1 levels increased 3-fold in maternal plasma and 2-fold in amniotic fluid in mRUPP (Figure 5.9 A and B). Successful placenta-targeted liposomal miR-122 delivery was confirmed using RT-qPCR, which showed 4-fold increase in placental miR-122 expression (Figure 5.9 D). Placenta-targeted miR-122 delivery significantly reduced placental ischaemia-induced maternal plasma sFlt-1 levels similar to levels observed in the Sham group (Figure 5.9 A). Placenta-targeted miR-122 also reduced sFlt-1 levels in amniotic fluid and placental sFlt-1 mRNA expression was also reduced but only when compared to the untreated mRUPP (Figure 5.9 B and C).

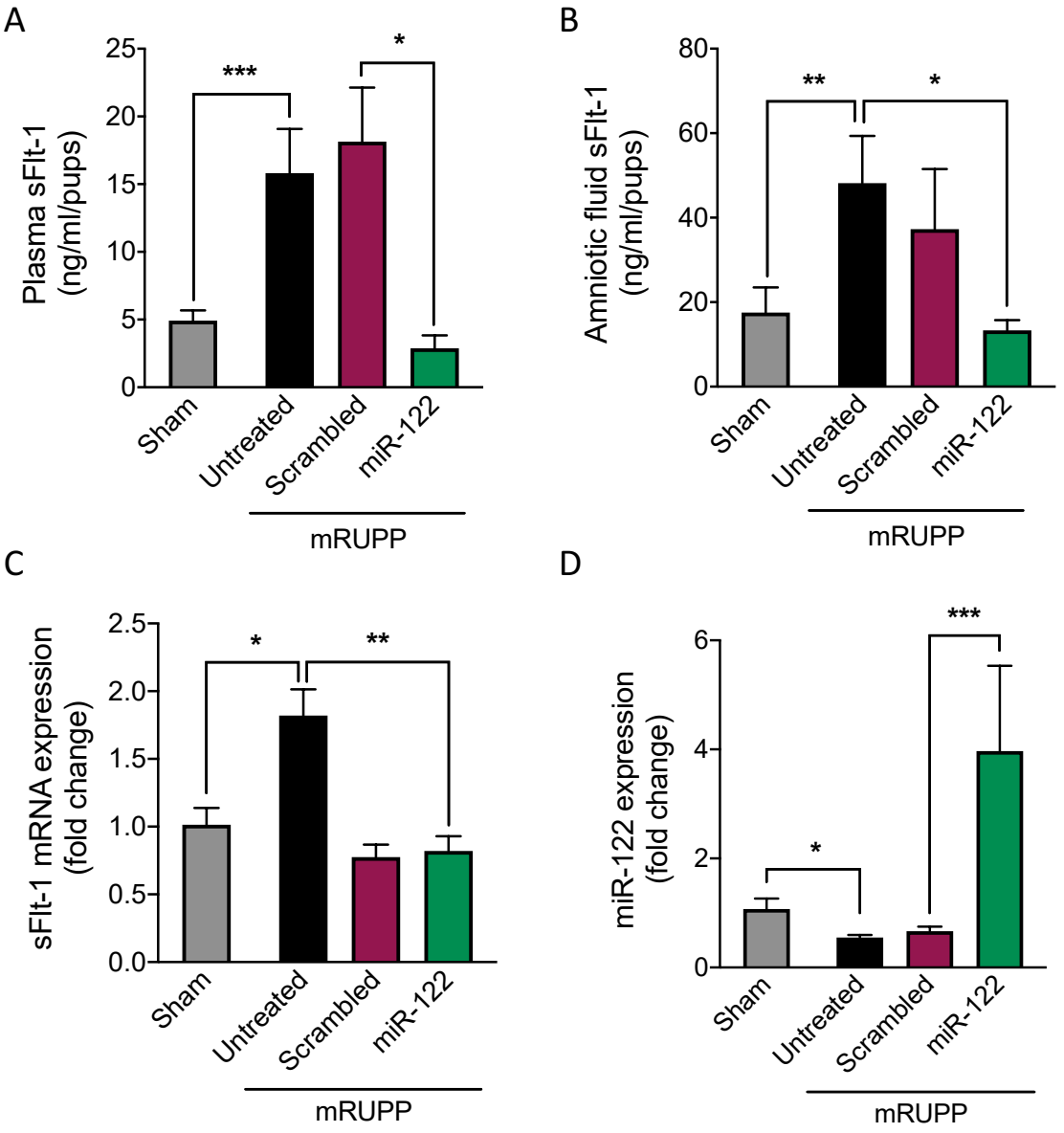

Figure 5. 9. Placental directed liposomal treatment with miR-122 reduces RUPP-induced sFlt-1 release.

Placenta, amniotic fluid and plasma were collected from mice on E17.5 that were subjected to mRUPP surgery on E11.5. **(A)** Plasma (Sham n=18; mRUPP: Untreated n=15, Scrambled n=4, miR-122 n=3) and **(B)** amniotic fluid (Sham n=11; mRUPP: Untreated n=10, Scrambled n=4, miR-122 n=3) were analysed to determine sFlt-1 protein concentration. Endogenous placental **(C)** sFlt-1 and **(D)** miR-122 expression (Sham n=8; mRUPP: Untreated n=8, Scrambled n=10, miR-122 n=9) were analysed with RT-qPCR. Relative mRNA and miRNA expression was normalised to YWHAZ and RNU48 housekeeping genes, respectively. Kruskal-Wallis test *post hoc* uncorrected Dunn's test with independent comparisons; **P<0.05; **P<0.005; ***P<0.0005.*

5.5.8 Placenta-targeted miR-122 liposomal treatment improves fetal survival in RUPP mice

In addition to elevated sFlt-1 levels, mice that underwent RUPP surgery also experienced low fetal weight, high fetal death and elevated mean arterial blood pressure (Figure 5.10 A, C and D). Fetal and placental weights after placenta-targeted miR-122 liposomal treatment remained unchanged when compared to the scrambled treatment. However, when compared to untreated RUPP control both, fetal and placental weights were decreased (Figure 5.10 A and B). Placenta-targeted miR-122 treatment significantly improved resorption rate by approximately 30% when compared to RUPP procedure alone, but no statistical significance was observed between miR-122 and scrambled treatment (Figure 5.10 C). Mean arterial blood pressure after miR-122 treatment remained elevated (Figure 5.10 D).

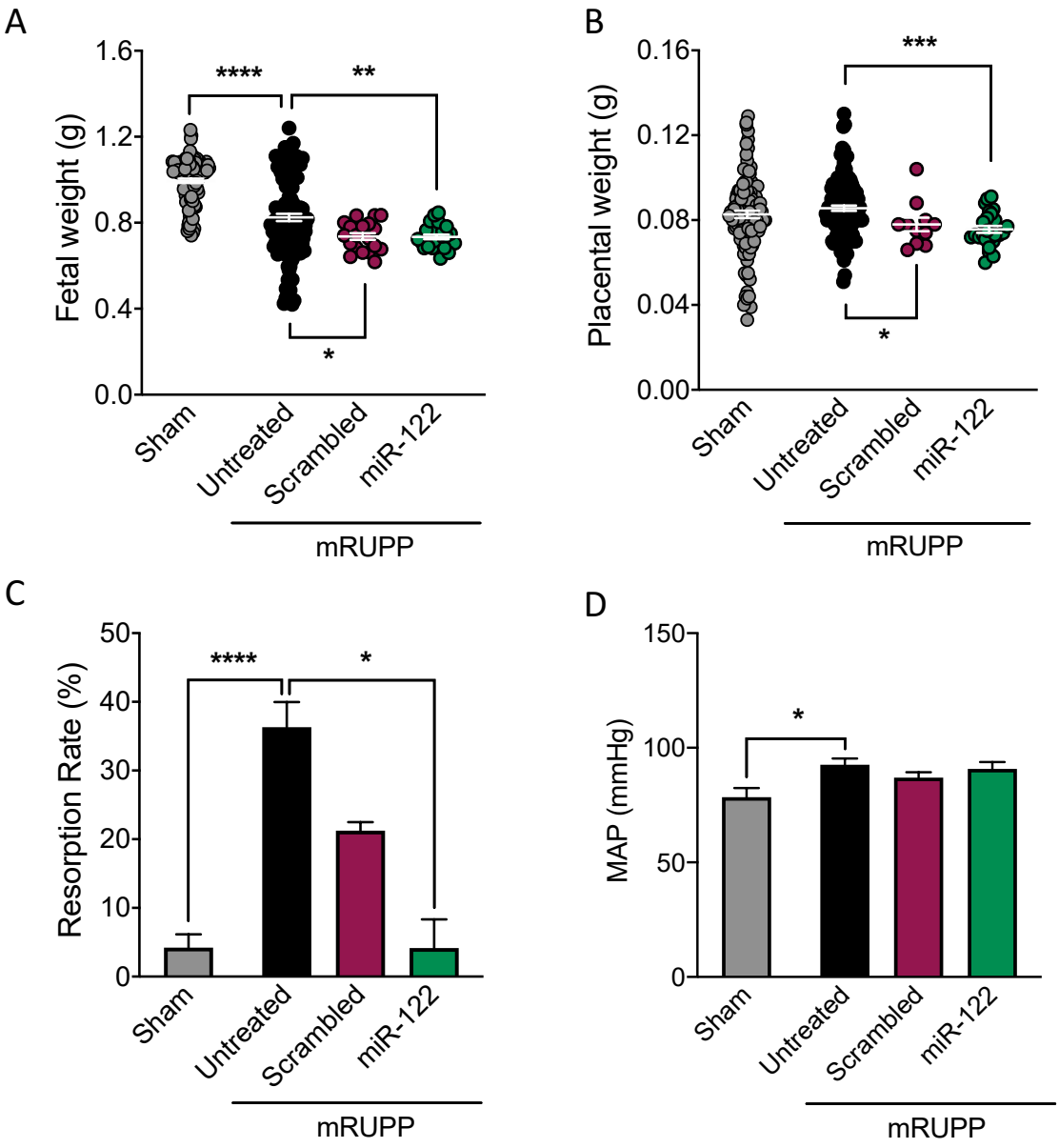

Figure 5. 10. Placenta targeted liposomal treatment with miR-122 reduces RUPP-induced resorption.

Pregnant mice undergone either Sham or RUPP surgery on E11.5. Individual **(A)** embryos (Sham: dams n=14, pups n=109; mRUPP: Untreated dams n=19, pups n=119; Scrambled dams n=3, pups n=19; miR-122 dams n=3, pups n=25) and **(B)** placentas (Sham: dams n=14, pups n=111; mRUPP: Untreated dams n=19, pups n=120; Scrambled dams n=3, pups n=19; miR-122 dams n=3, pups n=25) were collected on E17.5 and their wet weights recorded. **(C)** All resorptions were recorded on the same day (Sham: dams n=15; mRUPP: Untreated dams n=11, Scrambled dams n=4, miR-122 dams n=3. **(D)** On E17.5 the mean blood pressure (MAP) was recorded using carotid artery isolation method (Sham: dams n=10; mRUPP: Untreated dams n=10, Scrambled dams n=3, miR-122 dams n=3). Kruskal-Wallis test *post hoc* uncorrected Dunn's test with independent comparisons; **P<0.05; **P<0.005; ***P<0.0005; ****P<0.0001.*

5.6 Discussion

Liposomal complexes are generally stable enough to protect nucleic acids from degradation (Scherer et al., 2002). Liposomes encapsulating miRNA have been shown to provide a suitable delivery vehicle to induce successful gene regulation observed in cancer studies (Zhang et al., 2015) and *in vivo* model of angiogenesis (Endo-Takahashi et al., 2014). However, nanoparticles lacking targeting moiety might deliver liposomal cargo to other tissues inducing off-target side effects. Recent studies with peptide surface modification of the nanoparticles showed successful organ-specific payload delivery (Zhou et al., 2016). Here we demonstrate that our designed CGKRK placenta-targeted PC liposomes can be used to deliver payload to the mouse placenta with negligible off-target organ effects. In addition, miR-122 delivered to mouse placenta using this formulation inhibited placental ischaemia-induced sFlt-1 release and improved fetal survival in murine pregnancy.

5.6.1 CGKRK decorated neutral PC liposomes offer suitable vehicle to encapsulate miR-122

Depending on the payload of interest and destination target, liposomal complexes can be designed to have a neutral, positive or negative overall charge (Fu et al., 2019). Charge neutral liposomes avoid immune response, have a reduced toxicity profile (Rupaimoole and Slack, 2017, Scherer et al., 2002) and have been successfully used to deliver siRNA (Landen et al., 2005, Halder et al., 2006) and miRNA (Endo-Takahashi et al., 2014) *in vivo*. Although cationic liposomes offer better condensation and protection of miRNA (Felgner et al., 1987, Bozzuto and Molinari, 2015), it often results in reduced payload release (Marwah et al., 2020 manuscript in preparation). Due to spontaneous electrostatic interaction between positively charged lipids and negatively charged miRNA, cationic liposomes are commonly associated with cell toxicity including cell membrane integrity disruption (Zhao and Huang, 2014, Lee et al., 2019), cytoplasm vacuolization and decrease in cell activity (Lv et al., 2006, Zhang et al., 2013, Lee et al., 2019). It also increases clearance rates and interaction with negatively charged serum proteins leading to formation of aggregates (Piao et al., 2012, Wu et al., 2011). As a result cationic liposomes exhibit markedly reduced circulation half-life (Immordino et al., 2006).

To establish an efficient placenta-targeted delivery of miR-122, we designed charge-neutral liposomes with a PC anchor lipid and conjugated with CGKRK placenta-targeting peptide. PC is a safe and flexible, natural occurring lipid used for number of approved and clinically used liposomal formulations to treat fungal infections and multiple cancers (Bulbake et al., 2017, Li et al., 2015a). In our study surface modification with CGKRK and miR-122 encapsulation had no effect to the stability, overall charge and homogeneity of the formulation. Liposomes are known for lower miRNA encapsulation efficiency (Lee et al., 2019). CGKRK decorated PC liposomes showed only 60% miR-122 entrapment. This apparent loss in miR-122 during encapsulation step can be attributed to the hydrophilic nature of the miRNA molecule and high affinity to water (Cun et al., 2011). Nevertheless, neutral charge of the liposomes had no negative effect on miR-122 release as a full miR-122 payload was released within 24 hours. Characteristic data of

the liposomes suggest that CGKRK modified neutral PC liposomes provide a suitable vehicle to entrap miR-122.

5.6.2 PC liposomes decorated with CGKRK and loaded with miR-122 effectively inhibit sFlt-1 release in human endothelial cells

Ingredients within the liposomal composition may affect the cellular internalisation of the liposomes. Liposomes have been shown to attach to the extracellular membrane instead of being internalised (Patiño et al., 2015, Illien et al., 2016). Uptake of neutral PC liposomes using human endothelial cells was reported by Papadimitriou and Antimisiaris (2000), who observed the capability of human endothelial cells to internalise whole PC liposomes via endocytosis (Scherer et al., 2002). Consistently, we showed that almost the entire cell population we analysed, internalised our designed liposomes with no toxicity attributed to the cellular viability. In fact, CGKRK peptide induced higher accumulation of the liposomal payload within the cytoplasm confirming previously described cell-penetrating properties of the CGKRK peptide (King et al., 2016). Our designed liposomal formulation proved to be well tolerated and fully internalised by the human endothelial cells suggesting *in vitro* and *in vivo* compatible use.

To establish whether encapsulated miR-122 preserves and exerts its inhibitory effect *in vitro*, we stimulated human endothelial cells with VEGF-E to induce sFlt-1 release followed by the treatment with PC liposomes encapsulating non-fluorescent miR-122. Previous studies showed that hydrophilic fluorescent dyes such as 6FAM exhibit weak non-specific binding resulting in reduced miRNA function (Lu et al., 2016). It is worth noting that we observed a lack of fluorescent miR-122-6FAM-dependent sFlt-1 inhibition. Hence, non-fluorescent miR-122 was used for functional assays. CGKRK decorated liposomes successfully delivered miR-122 to the cells which led to effective VEGF-E-induced sFlt-1 inhibition. Data suggest that neutral PC liposomal formulation

loaded with non-fluorescent miR-122 provides an efficient treatment against high sFlt-1 levels *in vitro*.

5.6.3 Conjugation with CGKRK peptide guides PC liposomes to mouse placenta with minimal off-target organ effect

High calreticulin expression is found in the labyrinth, junctional zone, and spiral arteries of the mouse placenta (King et al., 2016). Study conducted by King and colleagues identified that CGKRK peptides bind to calreticulin and accumulate within mouse and human placenta (King et al., 2016). Fluorescent peptides intravenously administered to pregnant mice were shown to accumulate within the endovascular trophoblast lining, endothelial and trophoblast cells within the labyrinth and endothelium of decidual spiral arteries. There was no fluorescence detected in the junctional zone (King et al., 2016). Additionally, intravenous administration of fluorescent CGKRK peptides to pregnant mice showed no negative effects on placental morphology or fetal outcome, rendering these peptides safe for *in vivo* use (King et al., 2016). CGKRK peptide conjugated to miR-675 inhibitor showed efficient miRNA knockdown in mouse placenta, which subsequently increased fetal and placental weight, whereas CGKRK peptide conjugated to miR-145 inhibitor induced significant cytotrophoblast proliferation in the first trimester human placenta (Beards et al., 2017). The ability of the CGKRK to guide nanoparticles to placenta was confirmed by using nanoworms and neutral DSPC liposomes (King et al., 2016). When pregnant mice were intravenously administered with CGKRK decorated liposomes loaded with fluorescent dye, high accumulation was observed within the labyrinth zone of mouse placenta and negligible off-target accumulation within maternal and fetal organs (King et al., 2016). This highlights CGKRK as having exclusive placenta-targeting properties and that CGKRK decorated liposomes present an innovative strategy for placenta-specialised delivery.

To explore the effectiveness of our PC liposomal formulation to deliver cargo to the placenta, we have injected normal pregnant mice with the PC liposomes decorated with CGRKR and loaded with 6FAM fluorescent dye. CGKRK decorated PC liposomes

successfully delivered fluorescent cargo to the mouse placenta. As with human endothelial cells, CGKRK decorated liposomes offered higher delivery rate when compared to undecorated PC liposomes further confirming CGKRK cell-penetrating properties *in vivo*.

Off-target organ effect analysis revealed that undecorated PC liposomes accumulate within the maternal lung and kidney, whereas CGKRK decorated liposomes showed negligible accumulation in these organs. High accumulation of untargeted liposomes in kidney is most likely caused by the excretion of the unbound liposomes (King et al., 2016), which can be prevented by using CGKRK targeted liposomes. Also, placenta targeting CGKRK peptide prevents liposomal accumulation within highly vascularised lung tissue. This prevents critical off-target side effect as high miR-122 accumulation has been linked with pulmonary inflammation and lung dysfunction (Wang et al., 2019, Liang et al., 2017). Similar to King et al. (2016) study, we have observed accumulation of both liposomes in the maternal spleen and liver as both of these organs are known for their non-selective uptake of the nanoparticles (Agemy et al., 2010, Agemy et al., 2011, King et al., 2016). Internalisation of neutral liposomes by Kupffer cells and hepatocytes has already been reported (Senior, 1987). Collectively, our data suggest that our designed liposomal formulation provides effective cargo delivery to the mouse placenta with minimal off-target organ effects.

5.6.4 CGKRK decorated PC liposomes offer an effective strategy to deliver miR-122 to mouse placenta and inhibit RUPP-induced sFlt-1 release

Having demonstrated that HO-1 inhibits sFlt-1 release via direct miR-122-dependent gene silencing, we aimed to determine the therapeutic potential of miR-122 using an established rodent model of preeclampsia. Numerous studies show that RUPP is a suitable model to study preeclampsia as it mimics many of the key characteristics observed in human preeclampsia. Studies in rats showed that RUPP (rRUPP) induces hypertension (Gilbert et al., 2007, Faulkner et al., 2016, Bauer Ashley et al., 2013, Gilbert

et al., 2012, Banek et al., 2013, Morton et al., 2019, Ushida et al., 2016), elevated sFlt-1 levels in the placenta (Gilbert et al., 2007) and maternal circulation (Gilbert et al., 2007, Faulkner et al., 2016, Bauer Ashley et al., 2013, Banek et al., 2013, Ushida et al., 2016) contributing to poor pregnancy outcome. In mice, similar results were observed. Murine RUPP (mRUPP)-induced placental ischaemia caused elevated blood pressure (Fushima et al., 2016, Intapad et al., 2014), proteinuria (Fushima et al., 2016), increased placental sFlt-1 mRNA (Fushima et al., 2016) and plasma sFlt-1 levels (Intapad et al., 2014) resulting in impaired maintenance of the pregnancy and retarded embryonic growth. Placenta from rRUPP exhibits low HO-1 expression (Gilbert et al., 2009), which may be in part responsible for several preeclamptic-like symptoms observed in these animals. Therefore, it has been suggested that restored HO-1 activity may improve rRUPP-induced symptoms. Pharmacological induction of HO-1 in rRUPP normalised blood pressure and reduced sFlt-1:VEGF ratio favouring angiogenesis (George et al., 2011c). Rat placental explants that were isolated from rRUPP showed reduced HO-1 expression and elevated sFlt-1 under hypoxic conditions, which were later improved by HO-1 activation (George et al., 2012).

Consistent with previous findings (Fushima et al., 2016, Intapad et al., 2014), we observed decreased fetal weight, hypertension and increased serum and placental mRNA sFlt-1 levels in mRUPP complicated pregnancy. As expected, significantly upregulated placental and maternal levels of sFlt-1 were associated with low miR-122 placental expression. To explore the benefits of placenta-specific miR-122 treatment, we treated mRUPP with CGKRK decorated liposomes loaded with miR-122. CGKRK decorated PC liposomes successfully delivered miR-122 to the placenta, resulting in 4-fold increase in miR-122 expression. Increased miR-122 expression led to effective inhibition of sFlt-1 transcription resulting in reduced plasma and amniotic fluid sFlt-1 protein levels. However, it is worth noting that the miR-122-dependent significant downregulation of sFlt-1 mRNA in placenta and sFlt-1 protein release inhibition in amniotic fluid, was only observed when compared to untreated mRUPP. This observation indicates dysfunctional scrambled sequence, which possibly had a negative impact upon the sFlt-1 synthesis machinery. Although commercially available scrambled sequence has been reported to have no effects, a study using scrambled control for miRNA inhibition studies reported negatively affected fetal weight distribution (Beards et al., 2017). This may explain irregular side-effects observed in animals treated with

scrambled sequence encapsulating liposomes. Nevertheless, therapeutic effect of miR-122 to inhibit sFlt-1 *in vivo* provided extremely potent inhibitory effect.

It has been previously reported that induction of HO-1 in rRUPP has no demonstrable increase in fetal or placenta weight (George et al., 2011c). Consistently, we have reported no change in fetal or placental weight after miR-122 liposomal treatment. The treatment also had no effect on placental ischaemia-induced hypertension. Evidence suggests that mechanistic irreversible obstruction of blood flow to placenta during RUPP surgery is too severe to be improved by the induction of HO-1 (George et al., 2011c, McCarthy et al., 2011) or placenta-targeted miR-122 treatment. Animals in scrambled and miR-122 treatment groups had lower mean fetal and placental weight when compared to untreated mRUPP. The effect behind this is unknow, but we suggest that the combination of RUPP procedure and stress caused by the manual restrain for three intravenous injections post-surgery had a severe impact on the recovery rate when compared to untreated RUPP animals. Regardless, CGKRK placenta-homing miR-122 liposomal treatment was sufficient enough to reduce resorption rate from 40% to 5% when compared to untreated mRUPP, which is similar to the untreated sham group. It is worth noting, that in this case liposomes loaded with scrambled sequence also had an effect on the resorption rate, which further supports scrambled sequence-induced negative impact. Further experiments are required to assess negative side-effects associated with scrambled sequence. Based on our evidence, CGKRK decorated neutral PC liposomes offer an efficient placenta targeted delivery of miR-122, which exerts a potential therapeutic ability to reduce sFlt-1 release and improve fetal survival in preeclamptic animal model.

5.6.5 CGKRK decorated PC liposomes loaded with miR-122 may be considered as a therapeutic strategy for preeclamptic patients

Following the placenta-targeted liposomal accumulation within mouse placenta (King et al., 2016), we formulated CGKRK decorated PC liposomes and loaded them with miR-122. The formulation proved to be stable and reliable in delivering miR-122 to

human umbilical vein endothelial cells where it efficiently inhibited VEGF-E-mediated sFlt-1 release. Experiments in pregnant animals further confirmed placenta targeting properties of the CGKRK peptide and effective delivery of liposomal cargo without major off-target organ accumulation. MicroRNA-122, encapsulated to our designed liposomes, was successfully delivered to mouse placenta leading to placenta ischaemia-induced sFlt-1 inhibition and reduction in fetal death rate.

Placenta-homing peptide CGKRK exerts its targeting properties through binding to calreticulin (King et al., 2016). Although calreticulin is predominantly an intracellular endoplasmic reticulum receptor, it has also been detected on the cell surface (Bedard et al., 2005, Gold et al., 2010, Goicoechea et al., 2000) of apoptotic cells and human cancer cells (Chao et al., 2010, Obeid et al., 2007b, Obeid et al., 2007a). Translocation of the calreticulin from the endoplasmic reticulum to the surface of the cell (Johnson et al., 2001, Højrup et al., 2001) has been described as a consequence initiated by the endoplasmic reticulum stress (Pekáriková et al., 2010, Peters and Raghavan, 2011, Tufi et al., 2008). In fact, high levels of endoplasmic reticulum stress showed significant association between oxidative stress, apoptosis, impaired cell proliferation, inflammation and maternal endothelial cell activation (Burton and Yung, 2011) linked with preeclampsia (Lian et al., 2011, Fu et al., 2015, Du et al., 2017). Calreticulin is highly abundant in the syncytium of human first-trimester and term placenta (King et al., 2016). More importantly, calreticulin expression is significantly increased in preeclamptic placenta (Shi et al., 2012). Based on the evidence, CGKRK decorated liposomes can be used to deliver miR-122 directly to human placenta to treat abnormal sFlt-1 levels associated with preeclampsia. Further optimisation of the liposomal formulation, dosage and treatment frequency to relevant animal models of preeclampsia are required to develop a clinically suitable treatment.

5.7 Study limitations and future perspectives

Placenta homing liposomes containing an active pharmaceutical ingredient offer an exciting opportunity for preeclamptic drug development. Although our study provides foundation for a possible therapy, we acknowledge few drawbacks that must be addressed in future to generate a valid and compelling therapeutic strategy.

We have used CGKRK decorated liposomes to deliver 6FAM fluorescent dye to mouse placenta. To determine the efficiency of the delivery and highlight any possible off-target effects, we compared CGKRK targeted to untargeted delivery of 6FAM. Although CGKRK provided higher accumulation of the liposomes, it may not be CGKRK specific. Non-targeting peptide such as ARA (King et al., 2016) would provide more insight whether CGKRK-induced placental accumulation is CGKRK-specific. Previously, the accumulation of ARA peptide was detected in the decidua and in the labyrinth of the placenta, but also in maternal lung and clearance organs and high levels in fetal tissues (King et al., 2016). Therefore, ARA peptide exhibits similar response to untargeted liposomes, which suggest that CGKRK provides unique placental targeting.

To explore miR-122 therapeutic effect *in vivo*, we injected mRUPP with CGKRK decorated liposomes loaded either with scrambled control or miR-122. Although miR-122 treatment reduced sFlt-1 and improved fetal survival in mRUPP, effect of miR-122 liposomal treatment in healthy pregnancy is unknown. Our data demonstrated that miR-122 treatment using adenoviral vector had no negative effects on normal wild-type pregnancy providing evidence that miR-122 targets abnormal sFlt-1 levels observed in HO-1 compromised pregnancy. Inclusion of Sham group treated with CGKRK decorated liposomes loaded with either scrambled control or miR-122 would provide a better insight to possible effects of placenta-targeted miR-122 delivery during normal pregnancy.

Fluorescently labelled miR-122 proved to have impaired inhibitory effect when compared to non-fluorescently labelled miRNA. It was shown that fluorescently labelled cell penetrating peptides may alter the mode and degree of membrane interaction (Hedegaard et al., 2018). Fluorescent analysis of TAMRA-CGKRK modified liposomes loaded with 6FAM dye confirmed cellular internalisation by the cells *in vitro* and accumulation within organ tissues *in vivo.* Although, we have not observed any negative

effects associated with the fluorescent peptides use, a non-fluorescently labelled CGKRK peptide might provide more insight whether TAMRA fluorescence has an impact upon cellular penetration.

Scrambled sequence as a control allows a direct comparison between the control and miR-122 treatment groups. Unfortunately, either the selection of scrambled control from Qiagen for our study or liposomal formulation appeared to have a non-specific side effect *in vivo*. Even though scrambled sequence is advertised as being thoroughly tested with no homology to any known mammalian gene, it still possesses a risk of being incorporated into RISK complex. Negative effects observed in a group treated with scrambled sequence may be attributed to either scrambled sequence (Beards et al., 2017), the formulation (King et al., 2016) or both. Inclusion of empty loaded CGKRK decorated liposomes treatment would determine the nature of side effects.

It has been shown previously that undecorated liposomes loaded with 6FAM fluorescent dye were observed in the fetus from 24 to 72 hours (King et al., 2016). To the contrary, a study performed in 1998 used a dually perfused human term placental cotyledon to show that irrespective of the liposome size (70 – 300 nm), charge (neutral, positive or negative) or choice of anchor lipid (PC or DSPC), intact liposomes do not cross the placenta (Bajoria and Sooranna, 1998). Anatomical differences between mouse and human placenta may explain accumulation in the mouse fetus. Also, it has been recognised that human placenta acts as a sequestration organ and retains nanoparticles (Myllynen et al., 2008) allowing passage of lipophilic and amphiphilic drugs, which are less than 500 Da in size (Ward, 1993, Evseenko et al., 2006). Carboxyfluorescein (6FAM) is approximately 376 Da and can easily cross the fetoplacental barrier whereas transfer of miRNA (14 kDa) is practically impossible unless specific receptors exist (Malek et al., 1998). This and anatomical differences between human and mouse placenta may explain the accumulation of 6FAM within the fetal tissues (King et al., 2016). As significantly lower fetal and placental weights were observed in mice treated with CGKRK decorated PC liposomes loaded with scrambled or miR-122 sequence, we suggest that the formulation itself may have a negative impact on the fetal outcome. We have not observed any negative effects of adenovirus-induced overexpression of miR-122 to fetal, placental weights and fetal survival, which further supports that negative effects associated with poor fetal outcome are most likely associated with

liposomal formulation or scrambled sequence. Further experiments are required to explore placental transfer, distribution of our designed liposomes and miR-122 within the fetal tissues.

It has been shown that the expression of CGKRK target, calreticulin, was found increased in preeclamptic placenta (Shi et al., 2012). However, Gu et al. (2008) showed increased plasma calreticulin levels whereas mRNA and protein levels in preeclamptic placenta remained unchanged (Gu et al., 2008, Crawford et al., 2013). Another study showed that neither plasma nor placental expression of calreticulin was affected by fetal growth restriction in both the human and rat pregnancies (Crawford et al., 2013). Since calreticulin expression in placenta and other organs potentially poses a risk for off-target delivery, evaluation of calreticulin expression in placenta, maternal and fetal organs in health and disease would help to identify the likelihood of the off-target sites.

Finally, CGKRK initially was designed to target receptors present on malignant tumours (Hoffman et al., 2003, Agemy et al., 2011, Agemy et al., 2013). Therefore, undiagnosed malignancies may compromise the effective delivery of the therapeutics to the placenta (King et al., 2016). Additional screening would potentially be needed to assess whether the use of this particular treatment offers the benefit to patients with existing malignancies. Therefore, formulating an adequate liposomal system to deliver pharmaceutic compounds to placenta remains a considerable challenge for nano-pharmaceutical science (Salata, 2004), requiring careful and extensive evaluation at multiple levels.

Chapter 6

General discussion and conclusion

Preeclampsia is a systemic disorder that effects 1 in 12 pregnancies worldwide and is responsible for over 76,000 maternal deaths and over 500,000 infant deaths each year (Ahmed and Ramma, 2015b, preeclampsia.org). There is no cure for preeclampsia and preventative measures are still elusive due to the lack of understanding of the disease pathogenesis. The only effective method to relieve preeclamptic symptoms is the premature delivery of the baby and the removal of the placenta. If preeclampsia is not addressed on time, it progresses to eclampsia, which is a life threatening to both the mother and the unborn child.

Over two decades ago, sFlt-1 was proposed as a possible protein involved in the pathogenesis of preeclampsia due to its ability to antagonise VEGF activity (Ahmed, 1997). It was shown that preeclamptic women experience elevated sFlt-1 levels in amniotic fluid (Vuorela et al., 2000), placenta (Clark et al., 1998, Ahmad and Ahmed, 2001, Maynard et al., 2003) and plasma (Koga et al., 2003, Levine et al., 2004, Buhimschi et al., 2006, Crispi et al., 2006, Ramma et al., 2012). Maternal levels of sFlt-1 drop to non-pregnant levels postpartum highlighting placenta as the major source of sFlt-1 (Chaiworapongsa et al., 2004, McKeeman et al., 2004). Experiments *in vivo* revealed that excessive amount of sFlt-1 as a stand-alone factor is sufficient to induce key preeclamptic characteristics in rodents (Maynard et al., 2003, Bergmann et al., 2010). Removal, neutralisation or inhibition of sFlt-1 on the other hand, restores angiogenesis *in vitro* (Ahmad and Ahmed, 2004), improves kidney damage (Bergmann et al., 2010), hypertension (Turanov et al., 2018), proteinuria (Bergmann et al., 2010, Turanov et al., 2018) *in vivo*, reduces hypertension, proteinuria and increases duration of the pregnancy in human preeclamptic patients (Thadhani et al., 2011, 2016). Evidence suggests that placenta-derived sFlt-1 is a culprit linked to the pathogenesis of the preeclampsia.

A significant reduction in antioxidant HO-1 protein was demonstrated in preeclamptic placenta (Ahmed et al., 2000, Lyall et al., 2000, Barber et al., 2001). HO-1 is critical for the maintenance of healthy pregnancy (Acevedo and Ahmed, 1998, Bainbridge and Smith, 2005). When activation of the placental HO was shown to prevent cytokine-induced cellular placental damage (Ahmed et al., 2000), it was proposed that partial loss of HO-1 activity plays a key role in the pathogenesis of preeclampsia (Ahmed et al., 2000, Gozzelino et al., 2010, Otterbein et al., 2000a, Soares and Bach, 2009).

Inhibition of HO-1 has been directly linked with increased sFlt-1 release in endothelial cells and normal and preeclamptic villous placental explants (Cudmore et al., 2007), whereas restored HO-1 expression attenuated sFlt-1 increase *in vitro* (Cudmore et al., 2007) and rat placental explants (George et al., 2012). Collectively, the evidence shows that HO-1 has the ability to inhibit sFlt-1 release and that dysregulation of this enzyme in combination with high sFlt-1 are crucial for the development of preeclampsia. It was proposed that therapeutics directed at decreasing circulating levels of sFlt-1 could present a possible treatment for preeclampsia (Ahmed and Ramma, 2015b). However, HO-1-dependent sFlt-1 regulation as potential prevention strategy requires a greater understanding of the exact mechanism of how HO-1 inhibits sFlt-1.

Nearly 50% of human RNAs are regulated by more that 2000 endogenous miRNAs (Krol et al., 2010). By binding to 3'-UTR of the target mRNA, miRNA provides an important fine-tuned gene regulation (Cai et al., 2017a). It plays crucial part in wide range of processes including cellular development, apoptosis, fat metabolism, neuronal gene expression, brain morphogenesis, muscle differentiation, stem cell division (Mattick and Makunin, 2006, Kim and Nam, 2006), angiogenesis and vascular inflammation (Urbich et al., 2008). Dysregulation of miRNA expression has been linked with many human diseases (Christopher et al., 2016) including cardiovascular disease, liver disease, immune dysfunction, metabolic disorders, cancer (Zhang, 2008, Chai et al., 2013) and most importantly preeclampsia (Pineles et al., 2007b, Zhu et al., 2009b, Enquobahrie et al., 2011, Jairajpuri et al., 2017, Lykoudi et al., 2018).

Following Cudmore et al. (2007) study we hypothesised that HO-1 inhibits sFlt-1 levels via miRNA-dependent gene silencing. Indeed, several studies showed that HO-1 has the ability to regulate miR-378 in non-small lung carcinoma (Skrzypek et al., 2013) and bundle of miR-1, miR-133a, miR-133b, and miR-206 in stem cell differentiation (Skrzypek et al., 2013, Kozakowska et al., 2012, Kozakowska et al., 2014). Additionally, miR-210 and miR-10 were demonstrated to inversely corelate with sFlt-1 decrease (Hassel et al., 2012, Korkes et al., 2017) and miR-181a to inhibit sFlt-1 mRNA expression (Justiniano et al., 2013). Following gene array analysis of endothelial cells exposed to HO inducer, a number of differentially regulated miRNAs were determined in the laboratory. We have identified miR-122 with a "seed sequence" complementary to sFlt-1 mRNA 3'-UTR sequence. Experiments in human endothelial cells revealed that miR-

122 acts downstream of HO-1 and inhibits VEGF-E-induced sFlt-1 release. MicroRNA-122 expression was found decreased in mouse placenta isolated from mRUPP, a well-established preeclamptic model *in vivo,* and human preeclamptic placenta. Our data suggest that low levels of miR-122 found in placenta lead to excessive sFlt-1 production, a culprit event in preeclampsia pathogenesis.

Increased endogenous placental expression of miR-122 by using miR-122 replacement therapy highlights a potential therapy to treat or prevent preeclampsia. However, systemic administration of naked miRNA exhibits inefficient delivery due to negative charge, limited stability, short half-life, and innate immune response activation (Fabbri et al., 2013, Krutzfeldt, 2016, Deng et al., 2014c, Chen et al., 2015b). Viral delivery of miRNAs is known to provide overexpression of target miRNA (Couto and High, 2010, Kumar et al., 2008, Liu et al., 2010). The virus is usually stripped of all viral proteins (Amalfitano, 1999) to reduce toxicity and prolong transgene expression (Crettaz et al., 2009, Maione et al., 2001). We have employed adenoviral vector overexpressing miR-122 and intraperitoneally injected to pregnant HO-1 compromised mice. The treatment led to significantly reduced maternal sFlt-1 levels and improved fetal outcome when compared to normal pregnancy. In fact, adenovirus miR-122 treatment had no effect in normal pregnancy highlighting fine-tuned regulatory nature of miR-122 to target abnormal sFlt-1 production. A detailed analysis of other pathological features associated with preeclampsia is required to identify any other beneficial characteristics of miR-122 treatment. However, adenovirus carrier is known to initiate innate and adaptive immune response (Marshall, 1999). Further experiments are needed to explore adenovirus associated immune response in addition to off-target effects. Alternatively, a safer placenta-specific delivery system is required for miR-122 delivery to be considered as a therapeutic tool with a clinical significance.

In clinic, nanoparticles-based treatments are used to treat various cancers, fungal infections, chronic pain, rheumatoid arthritis, atopic dermatitis, hepatitis and many others (Hafner et al., 2014, Choi and Han, 2018). In particular, liposomes encapsulating miRNA have been proposed for colon cancer (Akao et al., 2010), Non-small-cell lung cancer (Wu et al., 2013), hepatic carcinoma (Xu et al., 2017), glioblastoma (Costa et al., 2015), breast cancer (Zhang et al., 2015) and several other (Lee et al., 2019). Liposomes offer flexibility, protection against degradation, increased stability in blood

circulation, prolonged circulation half-life, minimal immune response and can be easily customised based on the size, charge and payload preferences. Liposomes exhibit negligible fetal transfer and are safe to use in pregnancy as long as the benefits outweigh potential maternal and fetal risks (Barzago et al., 1996, Menezes et al., 2011). Neutral PC liposomal formulation AmBisome® approved for clinical use to treat fungal infections is considered relatively safe and not contraindicated for use during pregnancy (Stone et al., 2016).

Untargeted liposomes, same as adenoviral vector carriers, are known to bind and deliver internal payload to multiple tissues in the organism. To minimise off target effects, short-chain peptides were shown to guide nanoparticles loaded with miRNA to the site of interest (Zhou et al., 2016). Recently, tumour-homing peptide CGKRK was determined to have placenta-homing properties and guide liposomes to the human and mouse placenta with negligible off-target organ accumulation (King et al., 2016). Based on this evidence, we designed neutral PC liposomes decorated with CGKRK peptides and loaded with miR-122. Liposomal formulation proved to be suitable carrier to encapsulate miR-122 and deliver it to human endothelial cells. MicroRNA-122 delivered to cells, retained its function and inhibited VEGF-E-induced sFlt-1 release. To confirm CGKRK placenta guiding properties, we intravenously injected normal pregnant mice with undecorated and CGKRK decorated liposomes. Surface functionalisation of the liposomes with CGKRK peptides led to higher placental uptake and prevented liposomal accumulation within the maternal kidney and lung. Having established an adequate placenta-targeted carrier for miR-122, we utilised murine preeclampsia model to determine the therapeutic effect of placenta-specialised miR-122 delivery *in vivo*. Treatment increased placental expression of miR-122 by 4-fold, which subsequently led to effective inhibition of maternal sFlt-1 levels *in vivo*. In addition, placenta-specialised miR-122 treatment reduced resorption rate by approximately 35% when compared to mRUPP surgery alone.

Collectively, our evidence suggests that miR-122 can be considered as a therapeutic to limit sFlt-1 release and benefit preeclamptic patients. Adenovirus and placenta-targeted liposomes delivery studies confirmed both methods are suitable to deliver miR-122 to the placenta and induce effective sFlt-1 inhibition. However, CGKRK decorated liposomes strategy was associated with few side effects, including reduced

fetal and placental weight. It requires further investigation to determine the cause of these negative effects and whether the formulation could be improved further to provide a suitable therapeutic strategy. Adenoviral miR-122 treatment on the other hand, had no negative effects on normal or HO-1 compromised pregnancy.

Use of adenovirus in clinical setting is viewed sceptically due to risks associated with immune response (Shaw and Suzuki, 2019). However, improved technologies and advanced modification of adenoviruses pushed cancer-targeted adenovirus-based therapies to preclinical and clinical studies. There are more than fifty active clinical trials for oncolytic gene therapy vectors and therapeutic vaccines for the treatment of multiple cancers (Shaw and Suzuki, 2019). In fact, nine viral-based vectors were approved for clinical use, including three using adeno-associated viral vectors (EU-approved until 2017 Glybera®, FDA-approved Zolgensma® and FDA/EU-approved Luxturna®) and one using adenoviral vector for the patients with tumours carrying a mutated p53 gene (Gendicine™) licenced in China since 2003 and awaiting FDA approval (Goswami et al., 2019, Daley, 2019). Therefore, adenoviral miR-122 treatment could potentially be considered as a clinical therapeutic candidate. However, off-target effects associated with non-specific viral infection have to be addressed.

Untargeted adenoviral vectors infect multiple cells in the organism leading to a potential miR-122 overexpression in other organs than placenta. To address this issue adenovirus vector can be modified using adapter-based strategy to create a molecular bridge and retarget the adenovirus carrier from its native primary receptor to a cell surface receptor of interest (Beatty and Curiel, 2012). Pseudotyping and genetic manipulation of the viral capsid incorporates targeting ligands such as peptides to specialise viral deliver (Wickham et al., 1997, Dmitriev et al., 1998, Hemminki et al., 2001). Adenoviruses targeted with peptide sequence have been shown to facilitate delivery of the genetic material to many types of cancer including head and neck squamous cell carcinoma (Li et al., 2008), medullary thyroid carcinoma (Schmidt et al., 2011), glioma (Piao et al., 2009) and renal cell carcinoma (Diaconu et al., 2009). Short-chain RGD peptide modified adenoviruses proved to be successful in targeting ovarian (Dmitriev et al., 1998, Hemminki et al., 2001, Murugesan et al., 2007), cervical (Rein et al., 2004), colon (Lavilla-Alonso et al., 2010) and melanoma (Okada et al., 2005) cancers. Based on the success rate, several RGD modified adenoviruses reached clinical trials

(Kimball et al., 2010, Page et al., 2007, Nokisalmi et al., 2010, Matthews et al., 2009). Our peptide of interest, CGKRK, linked with adenovirus carrier showed specialised endocytosis-driven delivery strategy to liver tumour cells leaving healthy tissues unaffected (Yao et al., 2012). CGKRK modified adenovirus carrying herpes simplex virus thymidine kinase (HSVtk) gene proved to be a safe and efficient for cancer gene therapy in mouse model of metastasis (Yao et al., 2009, Yao et al., 2011). Modifying miR-122 carrying adenovirus with CGKRK peptide might facilitate placenta-specific delivery and reduce side effects associated with non-targeted adenovirus use. However, miRNA is known to target multiple mRNAs, therefore additional expression analysis of potential miR-122 targets in fetal and maternal tissues is required to identify local side effects associated with miR-122-dependent gene downregulation.

Current therapeutics market for pregnancy complications, including preeclampsia is severely deprived (Fisk and Atun, 2008) putting NHS under heavy financial burden (Fisk and Atun, 2008, Goldenberg and Jobe, 2001). To address this therapeutic shortfall, we have identified miR-122, a potential therapeutic candidate to treat high sFlt-1 levels and improve fetal outcome observed in preeclampsia. Targeting CGKRK peptide proved to be a crucial ingredient in formulating placenta-specialised delivery of miR-122. Expression of the calreticulin, a CGKRK receptor, in mouse and human placenta (King et al., 2016) together with data gathered from *in vivo* studies suggest that CGKRK-targeted delivery can be translated into clinic and used for human studies. Increased calreticulin expression in preeclamptic placenta (Shi et al., 2012) suggests potentially higher affinity of the CGKRK modified delivery system and increased efficacy of the treatment. We have used two different miR-122 delivery strategies, including adenovirus vector and CGKRK decorated PC liposomes. Although, adenoviral vector caused less side effects compared to the liposomal treatment, further optimisation of the liposomal formulation or modification of adenoviral vector are required to ensure the safety of the delivery vehicle and develop a clinically suitable treatment for preeclampsia.

Appendix

Appendix – A

Chapter 4

Supplement

A

Hemin vs. Control Group			
Position	**Mature ID**	**Fold Regulation**	**RT2 Catalog**
A01	miR-142-5p	284.296	MPH00043A
A03	miR-142-3p	284.296	MPH01176A
A04	miR-21	6.3258	MPH00106A
A06	miR-29b	10.03	MPH01245A
A09	miR-143	13.5128	MPH01177A
A12	let-7f	7.9241	MPH00006A
B01	miR-9	12.0943	MPH00456A
B07	miR-124	10.0648	MPH01157A
B08	miR-144	284.296	MPH01178A
B12	miR-122	131.7126	MPH00020A
C02	miR-32	11.5614	MPH00156A
C06	miR-141	283.3124	MPH01175A
D04	miR-200c	12.0107	MPH01218A
E09	miR-302a	154.4772	MPH01247A
F01	let-7d	5.0674	MPH00004A
F03	miR-181b	12.9623	MPH00065A
F04	miR-223	57.3313	MPH01231A
F09	miR-374b	6.0681	MPH00190A
G02	miR-96	195.5305	MPH00479A
G03	miR-302b	284.296	MPH01248A
G06	miR-423-5p	18.3951	MPH00210A
G12	miR-302c	250.9489	MPH01249A
H02	miR-185	9.9953	MPH00071A
H04	miR-210	13.0978	MPH00107A

B

Hemin vs. Control Group			
Position	**Mature ID**	**Fold Regulation**	**RT2 Catalog**
A02	miR-16	-2.7967	MPH00062A
A05	miR-15a	-2.1867	MPH00060A
A07	let-7a	-3.0711	MPH00001A
A08	miR-126	-2.0262	MPH01161A
A11	miR-27a	-2.1791	MPH01239A
B04	miR-30e	-2.4859	MPH00154A
B06	miR-29a	-3.6903	MPH01244A
B11	miR-22	-1.9983	MPH01228A
C04	miR-140-5p	-2.3194	MPH00041A
C08	miR-424	-5.3286	MPH00211A
C10	miR-17	-2.5558	MPH00063A
C12	miR-20a	-2.0544	MPH00104A
D01	miR-27b	-2.1491	MPH01240A
D02	miR-26b	-9.3746	MPH00131A
D03	miR-146a	-2.7203	MPH00047A
D05	miR-99a	-4.2686	MPH00481A
D06	miR-19a	-2.6367	MPH01214A
D09	let-7i	-2.4012	MPH00008A
D10	miR-93	-2.3274	MPH00465A
E01	miR-101	-2.8065	MPH00011A
E02	let-7g	-3.0711	MPH00007A
E03	miR-425	-4.7199	MPH00212A
E06	miR-18a	-2.2404	MPH00075A
F02	miR-30c	-2.2796	MPH00152A
F10	miR-196b	-2.5646	MPH00086A
H03	miR-30b	-2.1049	MPH00151A

Supplement A Figure 1. MicroRNA expression profile after hemin treatment.

HUVEC cells were treated with hemin for 24h. MicroRNA expression profiles were obtain using a qPCR-based array system. The panel includes a profile of **(A)** 24 upregulated and **(B)** 26 downregulated miRNAs expression.

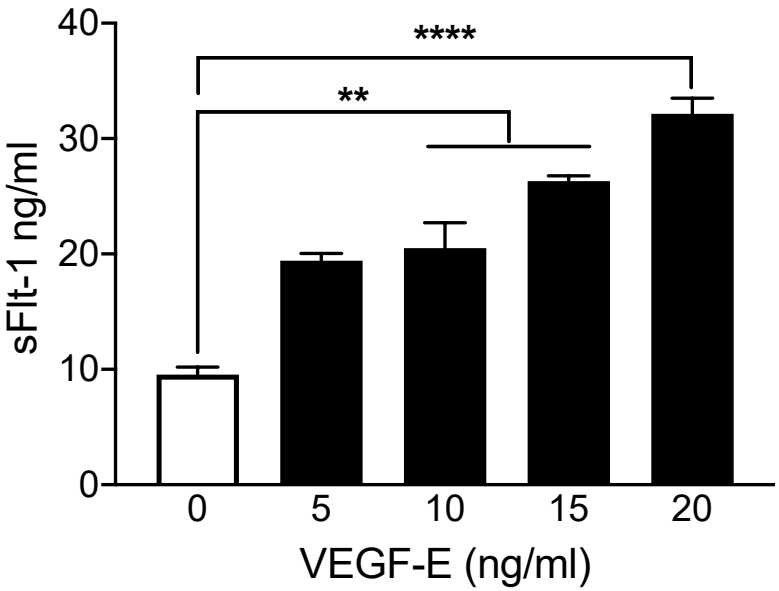

Supplement A Figure 2. VEGF-E-dependent sFlt-1 regulation in human endothelial cells.

HUVEC cells were tested for the ability to upregulate sFlt-1 levels when stimulated with appropriate stimuli. HUVEC cells were treated with VEGF-E at different concentrations including 5, 10, 15 and 20 ng/ml for 24h. Conditioned media was collected and sFlt-1 was measured (0ng/ml n=15, 5ng/ml n=3, 10ng/ml n=10, 15ng/ml n=3, 20ng/ml n=4). Kruskal-Wallis test *post hoc* Dunn's test with multiple comparisons to 0ng/ml treated group; ***P<0.005; ****P<0.0001.*

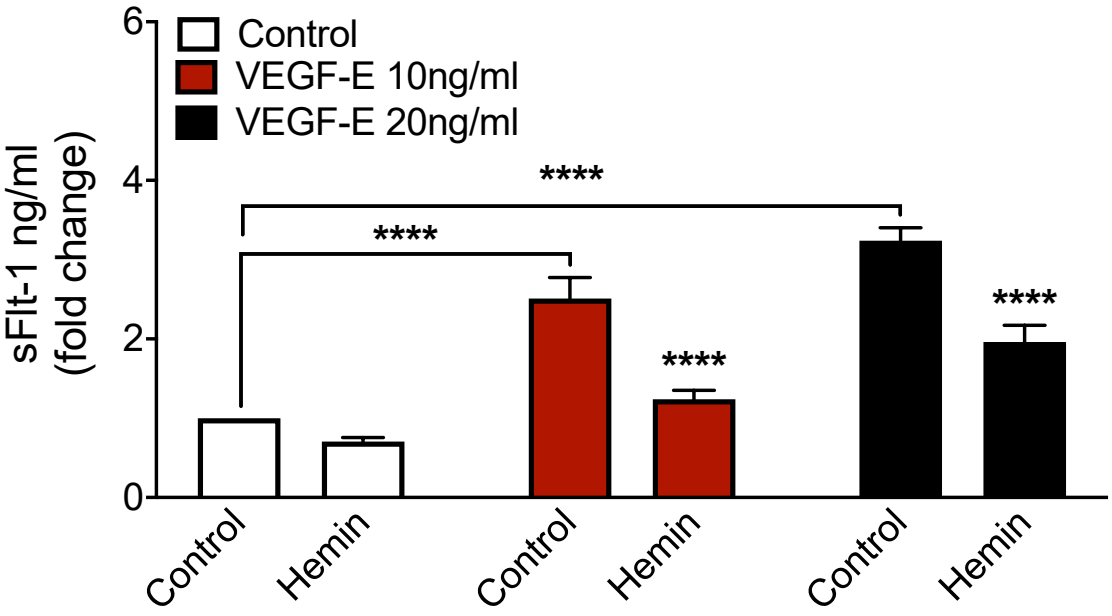

Supplement A Figure 3. Hemin-dependent sFlt-1 inhibition in human endothelial cells.

The ability of HUVEC cells to reduce sFlt-1 was tested. HUVECs were stimulated with VEGF-E at two different concentrations 10 ng/ml and 20ng/ml for 24h to upregulate sFlt-1 production (n=12). Kruskal-Wallis test post hoc Dunn's test with multiple comparisons to control group; ****P<0.0001. Additionally, to VEGF-E stimulation, HUVEC cells were treated with Hemin (20 µM) for 24h to limit VEGF-E-dependent sFlt-1 increase. Conditioned media was collected and sFlt-1 was measured. Two-Way ANOVA post hoc Sidak's test with multiple comparisons to control group; ****P<0.0001.

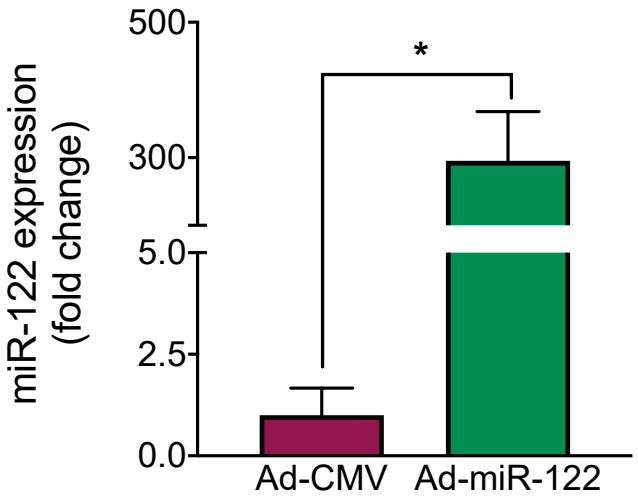

Supplement A Figure 4. Confirmation of Ad-miR-122 infectious capacity in human endothelial cells.

HUVEC cells were infected either with empty vector virus Ad-CMV or Ad-miR-122 adenovirus at MOI 50 followed by incubation for 24h. Post treatment cells were lysed for miRNA isolation and RT-qPCR analysis. Relative miRNA expression was normalised to RNU48 housekeeping gene. Unpaired Student t test; **P<0.05.*

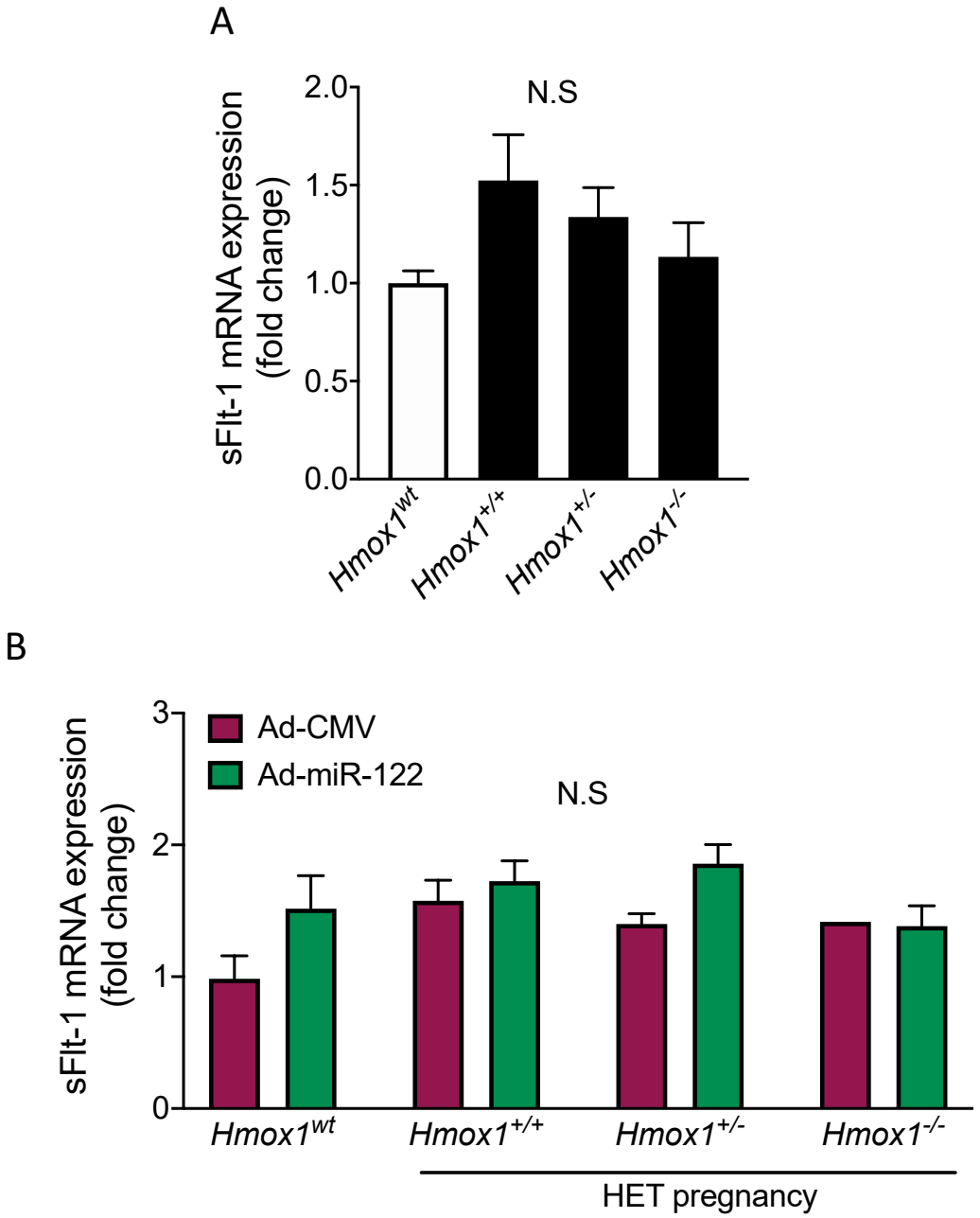

Supplement A Figure 5. The sFlt-1 mRNA expression at E17.5 remained unchanged in untreated and adenovirus treated WT and Hmox1 HET pregnancies.

Placenta from untreated and Ad-miR-122 treated mice was collected for real-time qPCR analysis. **(A)** Total RNA was isolated from individual placentas obtained from wild-type *Hmox1*^{wt} (WT) and Hmox1$^{+/-}$ heterozygous (HET) pregnancies to determine sFlt-1 mRNA expression (*Hmox1*^{wt} n=17, *Hmox1*$^{+/+}$ n=15, *Hmox1*$^{+/-}$ n=19, *Hmox1*$^{-/-}$ n=5). Kruskal-Wallis test; *P>0.05*. **(B)** Total RNA was isolated from individual placentas obtained from wild-type *Hmox1*^{wt} and heterozygous *Hmox1*$^{+/-}$ mice treated with either Ad-CMV or Ad-miR-122 adenovirus to analyse sFlt-1 mRNA expression (Ad-CMV: *Hmox1*^{wt} n=10, *Hmox1*$^{+/+}$ n=6, *Hmox1*$^{+/-}$ n=9, *Hmox1*$^{-/-}$ n=1; Ad-miR-122: *Hmox1*^{wt} n=12, *Hmox1*$^{+/+}$ n=11, *Hmox1*$^{+/-}$ n=11, *Hmox1*$^{-/-}$ n=5). Relative mRNA relative expression normalised to YWHAZ housekeeping gene. Two-Way ANOVA; *P>0.05*.

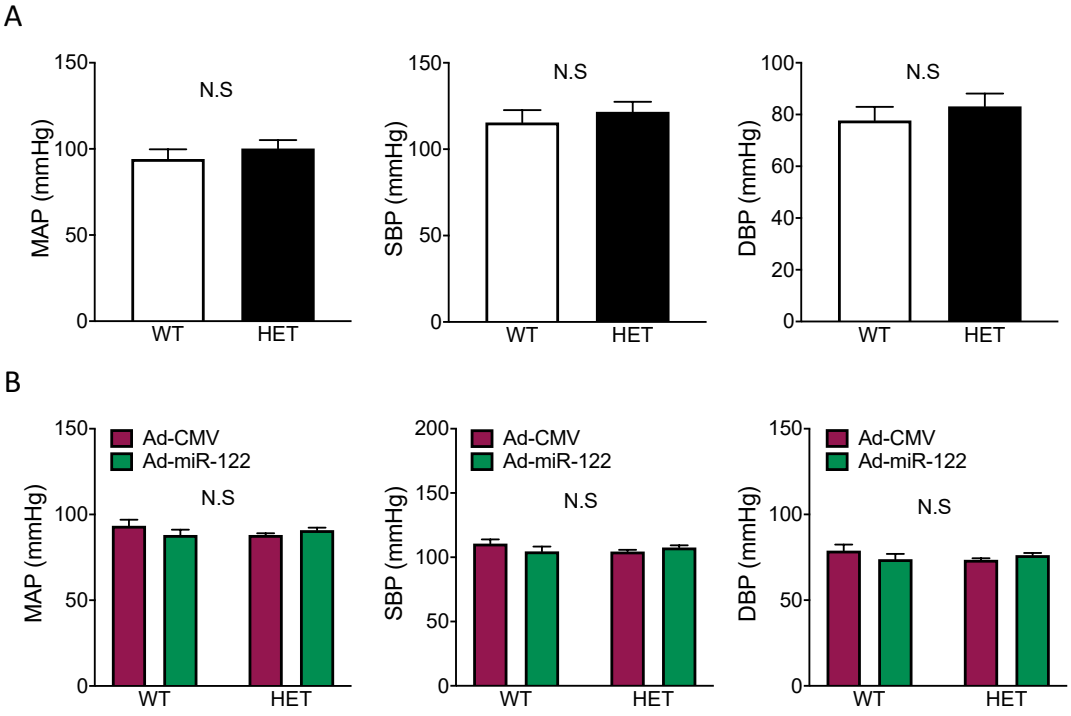

Supplement A Figure 6. Increased miR-122 expression does not affect blood pressure during pregnancy.

(A) Blood pressure parameters including mean blood pressure (MAP), systolic blood pressure (SBP) and diastolic blood pressure (DBP) were recorded on day E17.5 in wild-type *Hmox1*^{wt} (WT, n=3) and heterozygous *Hmox1*$^{+/-}$ (HET, n=7) pregnant mice. Mann-Whitney test; *P>0.05*. **(B)** MAP, SBP and DBP was also measured in pregnant WT and HET mice that received either empty vector adenovirus (Ad-CMV: WT n=7; HET n=10) or adenovirus encoding miR-122 (Ad-miR-122: WT n=6; HET n=11) intraperitoneal injection on day E10.5. Two-Way ANOVA, *P>0.05*.

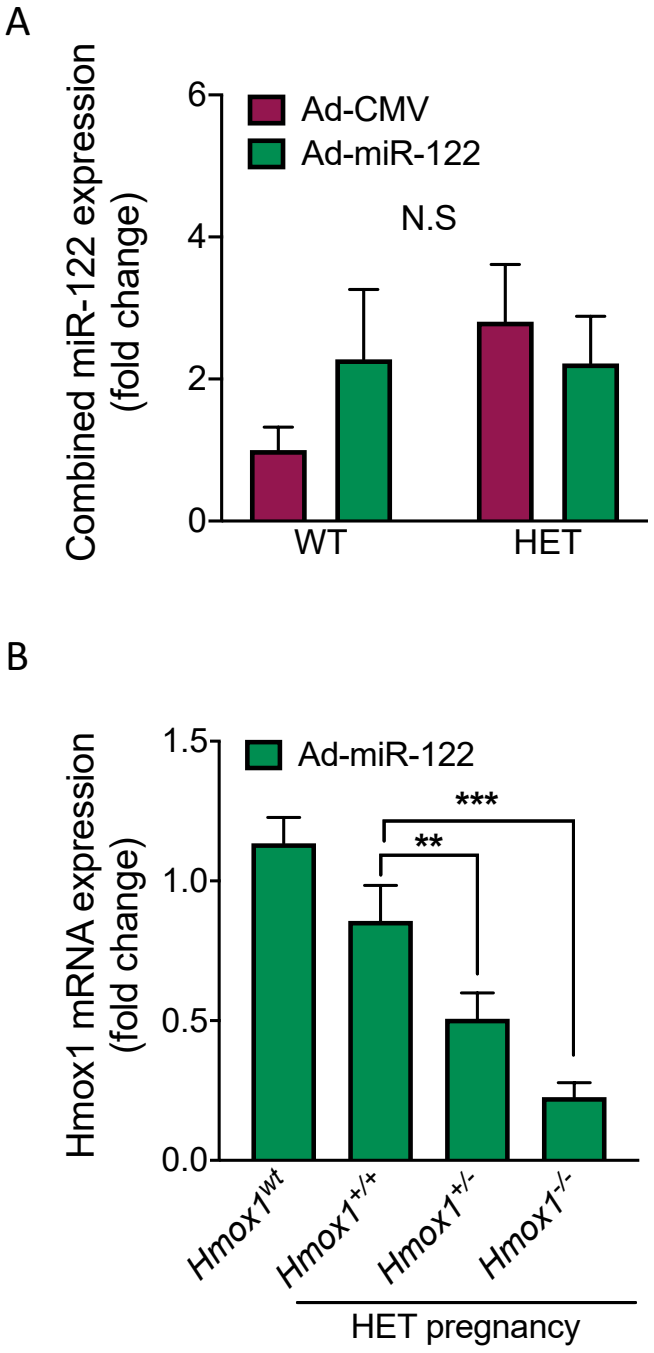

Supplement A Figure 7. Ad-miR-122 did not affect placental miR-122 and HO-1 mRNA expression in murine pregnancy.

Placenta from Ad-miR-122 treated mice was collected for real-time qPCR analysis. Overall Ad-miR-122 effect on **(A)** combined miR-122 expression regardless of the fetal genotype (WT: Ad-CMV n=7, Ad-miR-122 n=7; HET: Ad-CMV n=16, Ad-miR-122 n=27). MicroRNA expression was normalised to RNU48 housekeeping gene. Two-Way ANOVA; *P>0.05.* Ad-miR-122 treatment effect on **(B)** HO-1 placental mRNA expression based on fetal genotype (Ad-CMV: *Hmox1*^{wt} n=10, *Hmox1*$^{+/+}$ n=6, *Hmox1*$^{+/-}$ n=9, *Hmox1*$^{-/-}$ n=1; Ad-miR-122: *Hmox1*^{wt} n=12, *Hmox1*$^{+/+}$ n=11, *Hmox1*$^{+/-}$ n=11, *Hmox1*$^{-/-}$ n=4). Relative mRNA and miRNA expression was normalised to YWHAZ and RNU48 housekeeping genes, respectively. Two-Way ANOVA *post hoc* Sidak's test with multiple comparisons to *Hmox1*^{wt}; **P<0.05; **P<0.005; ***P<0.0005.*

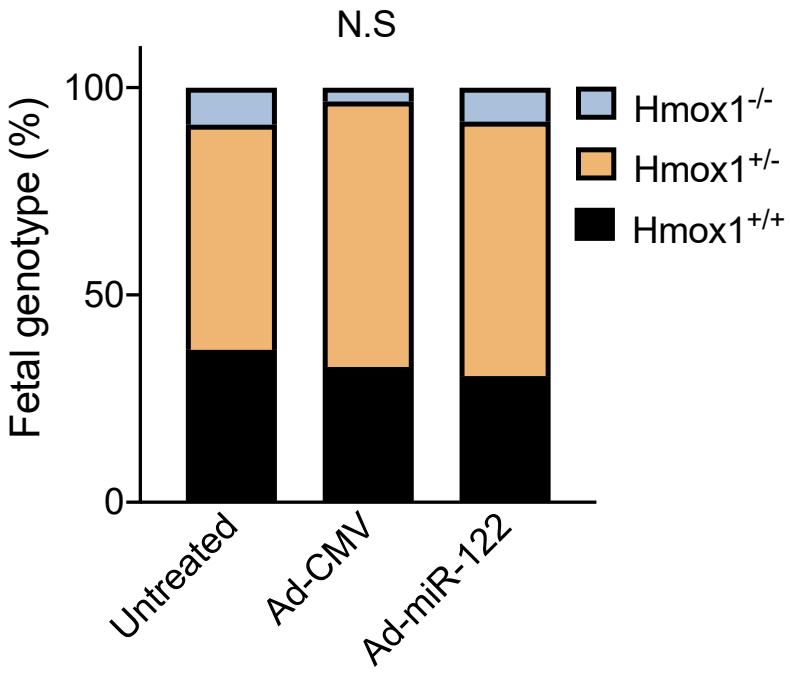

Supplement A Figure 8. Ad-miR-122 treatment has no influence on genotypic outcome in HET pregnancy.

Pregnant heterozygous *Hmox1*$^{+/-}$ mice received either empty vector adenovirus (Ad-CMV) or adenovirus encoding miR-122 (Ad-miR-122) intraperitoneal injection on day E10.5. On day E17.5 individual pups were genotyped and the relationship between genotype and the adenoviral treatment plotted as percentage (untreated: *Hmox1*$^{+/+}$ n=38, *Hmox1*$^{+/-}$ n=51, *Hmox1*$^{-/-}$ n=8; Ad-CMV: *Hmox1*$^{+/+}$ n=13, *Hmox1*$^{+/-}$ n=26, *Hmox1*$^{-/-}$ n=1; Ad-miR-122: *Hmox1*$^{+/+}$ n=17, *Hmox1*$^{+/-}$ n=35, *Hmox1*$^{-/-}$ n=5). Two-Way ANOVA; *P>0.05*.

Appendix – B

Chapter 5

Supplement

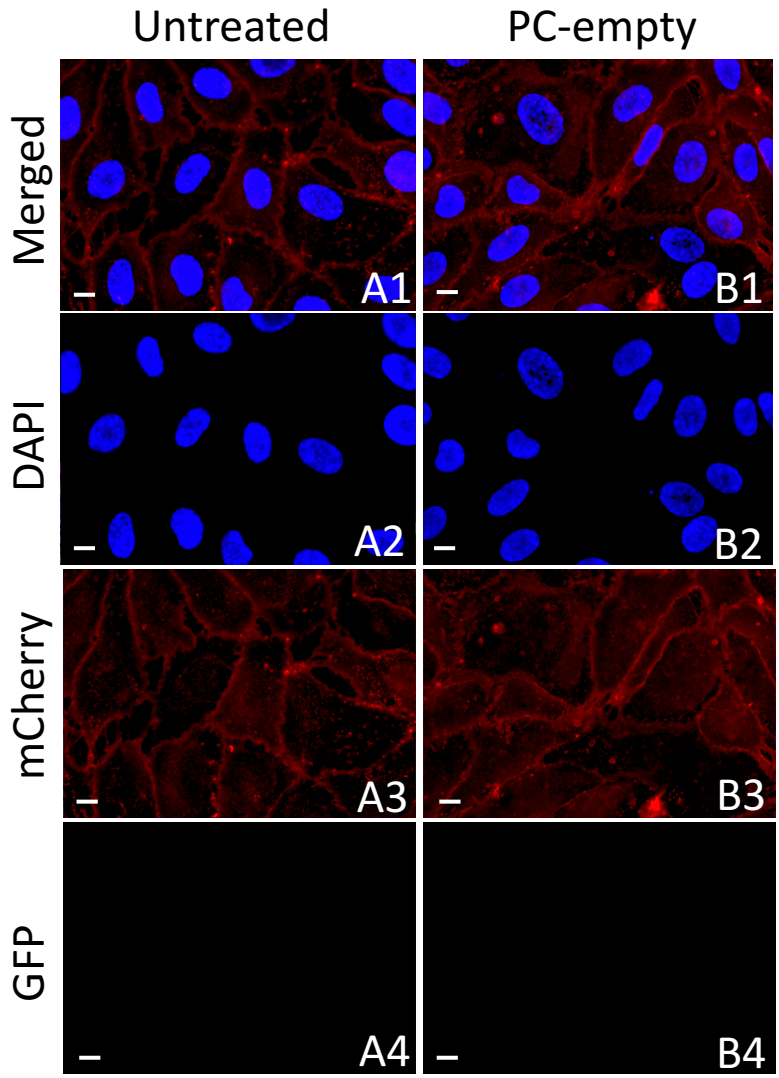

Supplement B Figure 1. No autofluorescence is detected in the cells treated with empty liposomes.

Representative images of HUVEC cells treated with empty undecorated PC-6FAM (B1-B4) liposomes for 6h. Cells were fixed and stained with WGA (red, mCherry) to define cellular membrane and with DAPI (blue, DAPI) to stain the nuclei. Localisation of green (GFP) fluorescence signal was observed under the microscope to identify any autofluorescence signal exhibited by the cells or liposomal formulation and compared to untreated group. Scale bar 10µm. Images randomly sampled from 3 independent experiments (n=3).

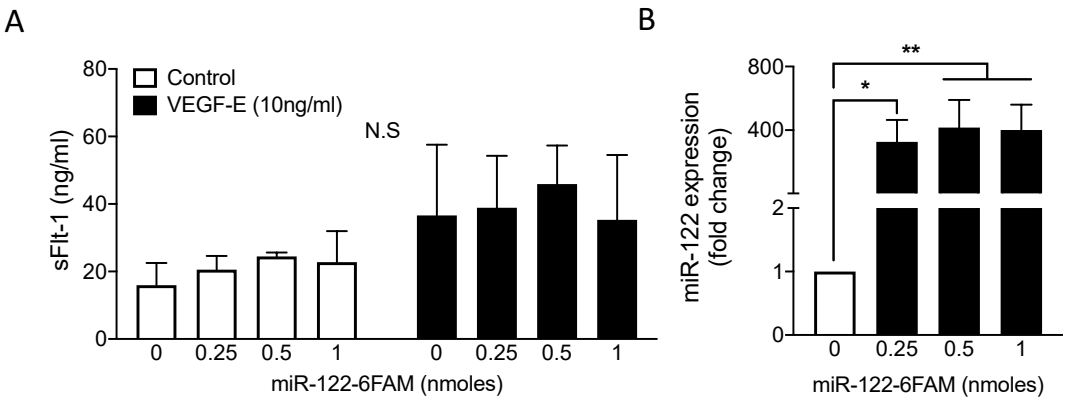

Supplement B Figure 2. Fluorescent label on miR-122 inhibits miR-122-dependent sFlt-1 supressing activity.

HUVEC cells were transfected with fluorescently labelled miR-122 (miR-122-6FAM) and stimulated with VEGF-E (10ng/ml) for 24h. **(A)** Conditioned media was collected to determine sFlt-1 protein concentration (n=3). Two-Way ANOVA; *P>0.05*. **(B)** Cells from VEGF-E stimulated group were lysed and analysed with real-time qPCR to determine relative miR-122 expression (n=4). Relative miRNA expression was normalised to RNU48 housekeeping gene. Kruskal-Wallis test *post hoc* Dunn's test with multiple comparisons to 0 nmoles group; **P<0.05; **P<0.005.*

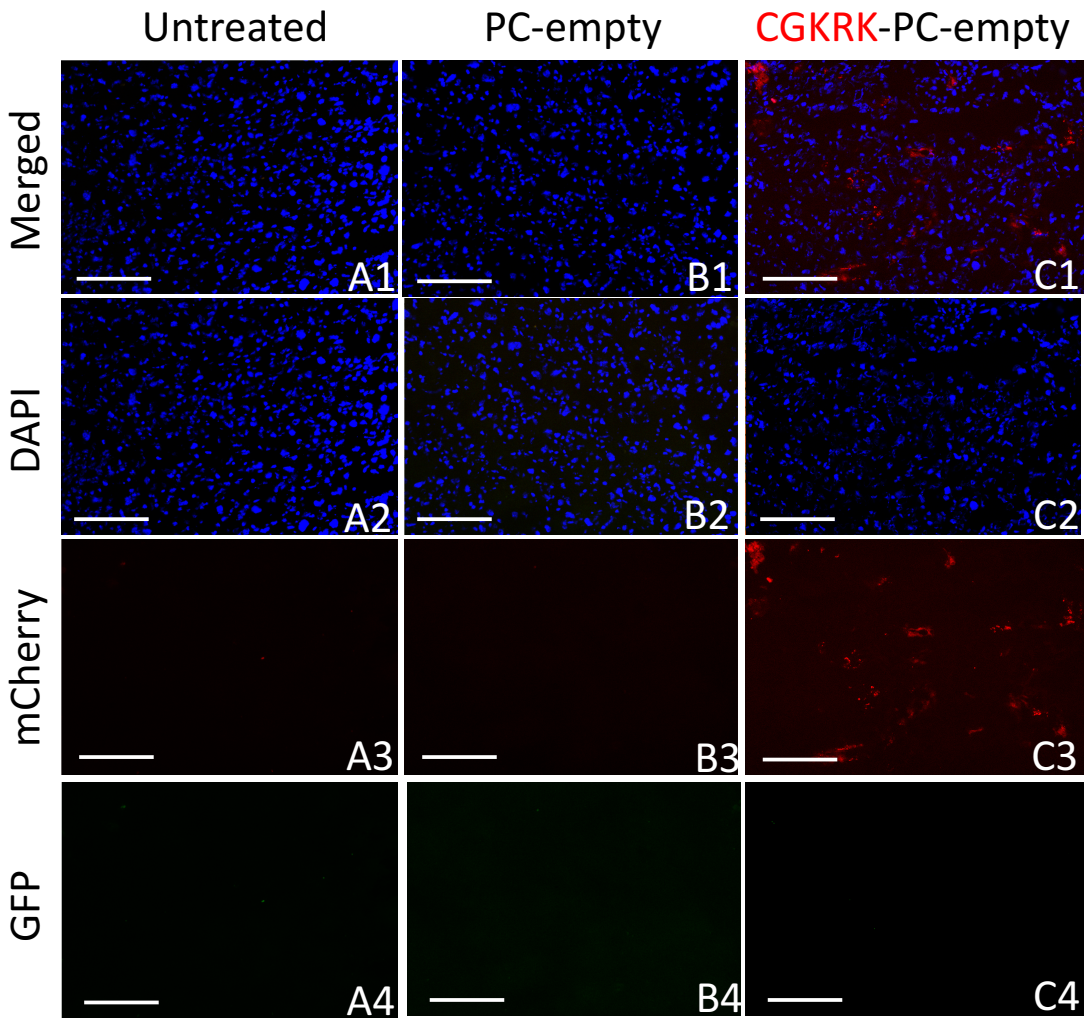

Supplement B Figure 3. No autofluorescence is detected in the mouse placenta from mice treated with empty liposomes.

WT mice received intravenous (IV) injection of undecorated empty (PC-empty; B1-B4) and CGKRK decorated (red, mCherry) empty liposomes (CGKRK-PC-empty; C1-C4) on E17.5. After 6 hours placental tissues were collected, fixed and imaged. Nuclei was stained with DAPI (blue, DAPI). Localisation of green (GFP) signal was observed under the microscope to identify any autofluorescence signal exhibited by the placental tissue or liposomal formulation and compared to untreated group. Scale bar 10µm. Images randomly sampled from 3 independent experiments (n=3).

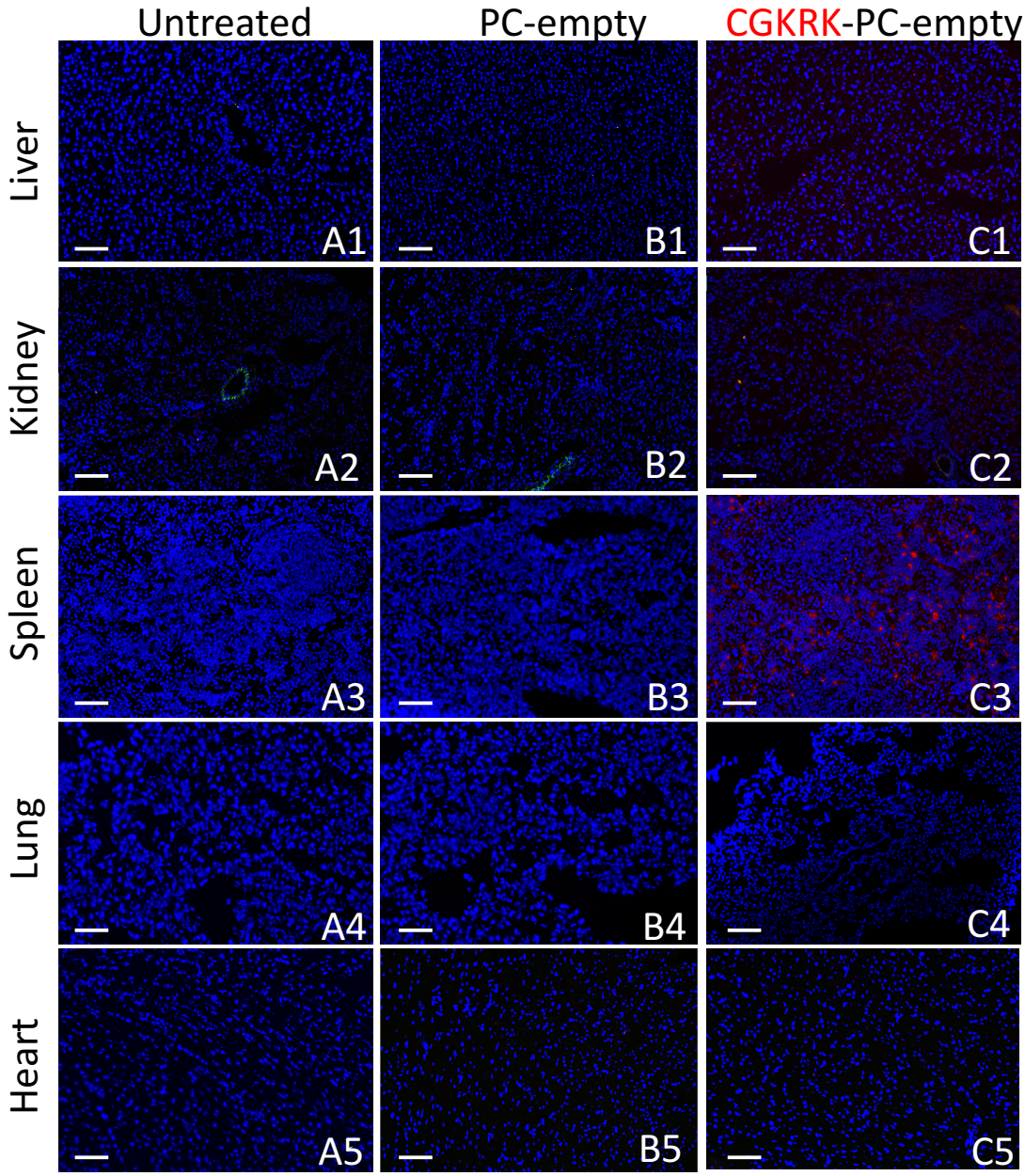

Supplement B Figure 4. No autofluorescence is detected in the maternal organs from mice treated with empty liposomes.

WT mice received intravenous (IV) injection of undecorated empty (PC-empty; B1-B4) and CGKRK decorated (red, mCherry) empty liposomes (CGKRK-PC-empty; C1-C4) on E17.5. After 6 hours liver, kidney, spleen, lung and heart tissues were collected, fixed and imaged. Nuclei was stained with DAPI (blue, DAPI). Localisation of green (GFP) signal was observed under the microscope to identify any autofluorescence signal exhibited by the maternal tissues or liposomal formulation and compared to untreated group. Scale bar 10µm. Images randomly sampled from 3 independent experiments (n=3).

References

Illustrations used in the thesis were created using BioRender.com platform.

ACEVEDO, C. H. & AHMED, A. 1998. Hemeoxygenase-1 inhibits human myometrial contractility via carbon monoxide and is upregulated by progesterone during pregnancy. *Journal of Clinical Investigation,* 101**,** 949-955.

AGEMY, L., FRIEDMANN-MORVINSKI, D., KOTAMRAJU, V. R., ROTH, L., SUGAHARA, K. N., GIRARD, O. M., MATTREY, R. F., VERMA, I. M. & RUOSLAHTI, E. 2011. Targeted nanoparticle enhanced proapoptotic peptide as potential therapy for glioblastoma. *Proc Natl Acad Sci U S A,* 108**,** 17450-5.

AGEMY, L., KOTAMRAJU, V. R., FRIEDMANN-MORVINSKI, D., SHARMA, S., SUGAHARA, K. N. & RUOSLAHTI, E. 2013. Proapoptotic peptide-mediated cancer therapy targeted to cell surface p32. *Mol Ther,* 21**,** 2195-204.

AGEMY, L., SUGAHARA, K. N., KOTAMRAJU, V. R., GUJRATY, K., GIRARD, O. M., KONO, Y., MATTREY, R. F., PARK, J. H., SAILOR, M. J., JIMENEZ, A. I., CATIVIELA, C., ZANUY, D., SAYAGO, F. J., ALEMAN, C., NUSSINOV, R. & RUOSLAHTI, E. 2010. Nanoparticle-induced vascular blockade in human prostate cancer. *Blood,* 116**,** 2847-56.

AHMAD, S. & AHMED, A. 2001. Regulation of soluble VEGFR-1 by VEGF and oxygen and its elevation in pre-eclampsia and fetal growth restriction. *Placenta***,** 8-9.

AHMAD, S. & AHMED, A. 2004. Elevated placental soluble vascular endothelial growth factor receptor-1 inhibits angiogenesis in preeclampsia. *Circulation Research,* 95**,** 884-891.

AHMAD, S., HEWETT, P. W., AL-ANI, B., SISSAOUI, S., FUJISAWA, T., CUDMORE, M. J. & AHMED, A. 2011. Autocrine activity of soluble Flt-1 controls endothelial cell function and angiogenesis. *Vascular Cell,* 3**,** 15-15.

AHMED, A. 1997. Heparin-binding angiogenic growth factors in pregnancy. *Placenta,* 18**,** 215-258.

AHMED, A. & CUDMORE, M. J. 2009. Can the biology of VEGF and haem oxygenases help solve pre-eclampsia? *Biochem Soc Trans,* 37**,** 1237-42.

AHMED, A., DUNK, C., KNISS, D. & WILKES, M. 1997. Role of VEGF receptor-1 (Flt-1) in mediating calcium-dependent nitric oxide release and limiting DNA synthesis in human trophoblast cells. *Lab Invest,* 76**,** 779-91.

AHMED, A., RAHMAN, M., ZHANG, X., ACEVEDO, C. H., NIJJAR, S., RUSHTON, I., BUSSOLATI, B. & ST JOHN, J. 2000. Induction of placental heme oxygenase-1 is protective against TNF alpha-induced cytotoxicity and promotes vessel relaxation. *Molecular Medicine,* 6**,** 391-409.

AHMED, A. & RAMMA, W. 2015a. Unravelling the theories of pre-eclampsia: are the protective pathways the new paradigm? *Br J Pharmacol,* 172**,** 1574-86.

AHMED, A. & RAMMA, W. 2015b. Unravelling the theories of pre-eclampsia: are the protective pathways the new paradigm? *British Journal of Pharmacology,* 172**,** 1574-1586.

AHMED, A., REZAI, H. & BROADWAY-STRINGER, S. 2016. Evidence-Based Revised View of the Pathophysiology of Preeclampsia. Boston, MA: Springer US.

AHMED, A., WILLIAMS, D. J., CHEED, V., MIDDLETON, L. J., AHMAD, S., WANG, K., VINCE, A. T., HEWETT, P., SPENCER, K., KHAN, K. S. & DANIELS, J. P. 2020. Pravastatin for early-onset pre-eclampsia: a randomised, blinded, placebo-controlled trial. *Bjog,* 127**,** 478-488.

AKAO, Y., NAKAGAWA, Y., HIRATA, I., IIO, A., ITOH, T., KOJIMA, K., NAKASHIMA, R., KITADE, Y. & NAOE, T. 2010. Role of anti-oncomirs miR-143 and -145 in human colorectal tumors. *Cancer Gene Therapy,* 17**,** 398-408.

ALCARAZ, M. J., FERNÁNDEZ, P. & GUILLÉN, M. I. 2003. Anti-inflammatory actions of the heme oxygenase-1 pathway. *Curr Pharm Des,* 9**,** 2541-51.

ALEXANDREANU, I. C. & LAWSON, D. M. 2002. Effects of chronic administration of a heme oxygenase substrate or inhibitor on progression of the estrous cycle, pregnancy and lactation of Sprague-Dawley rats. *Life Sciences,* 72**,** 153-162.

ALLEN, T. M. & CULLIS, P. R. 2004. Drug delivery systems: entering the mainstream. *Science,* 303**,** 1818-22.

AMALFITANO, A. 1999. Next-generation adenoviral vectors: new and improved. *Gene Ther,* 6**,** 1643-5.

ANDRÉ, M. & FELLEY-BOSCO, E. 2003. Heme oxygenase-1 induction by endogenous nitric oxide: influence of intracellular glutathione. *FEBS Letters,* 546**,** 223-227.

ARAP, W., PASQUALINI, R. & RUOSLAHTI, E. 1998. Cancer treatment by targeted drug delivery to tumor vasculature in a mouse model. *Science,* 279**,** 377-80.

ASHAR-PATEL, A., KAYMAZ, Y., RAJAKUMAR, A., BAILEY, J. A., KARUMANCHI, S. A. & MOORE, M. J. 2017. FLT1 and transcriptome-wide polyadenylation site (PAS) analysis in preeclampsia. *Scientific reports,* 7**,** 12139-12139.

BABU, A., TEMPLETON, A. K., MUNSHI, A. & RAMESH, R. 2014. Nanodrug Delivery Systems: A Promising Technology for Detection, Diagnosis, and Treatment of Cancer. *Aaps Pharmscitech,* 15**,** 709-721.

BAI, J., YU, J., WANG, J., XUE, B., HE, N., TIAN, Y., YANG, L., WANG, Y., WANG, Y. & TANG, Q. 2019. DNA Methylation of miR-122 Aggravates Oxidative Stress in Colitis Targeting SELENBP1 Partially by p65NFκB Signaling. *Oxidative Medicine and Cellular Longevity,* 2019**,** 5294105.

BAI, S., NASSER, M. W., WANG, B., HSU, S.-H., DATTA, J., KUTAY, H., YADAV, A., NUOVO, G., KUMAR, P. & GHOSHAL, K. 2009a. MicroRNA-122 inhibits tumorigenic properties of hepatocellular carcinoma cells and sensitizes these cells to sorafenib. *The Journal of biological chemistry,* 284**,** 32015-32027.

BAI, S., NASSER, M. W., WANG, B., HSU, S. H., DATTA, J., KUTAY, H., YADAV, A., NUOVO, G., KUMAR, P. & GHOSHAL, K. 2009b. MicroRNA-122 inhibits tumorigenic properties of hepatocellular carcinoma cells and sensitizes these cells to sorafenib. *J Biol Chem,* 284**,** 32015-27.

BAI, Y., ZHANG, X., YANG, X. & LI, F. 2017. Relevance of microRNA-122 to pathogenesis of preeclampsia in rats. *International Journal of Clinical and Experimental Medicine,* 10**,** 10103-10112.

BAINBRIDGE, S. A. & SMITH, G. N. 2005. HO in pregnancy. *Free Radical Biology and Medicine,* 38**,** 979-988.

BAJORIA, R. & SOORANNA, S. R. 1998. Liposome as a drug carrier system: Prospects for safer prescribing during pregnancy: A review. *Placenta,* 19**,** 265-287.

BALLA, G., JACOB, H. S., BALLA, J., ROSENBERG, M., NATH, K., APPLE, F., EATON, J. W. & VERCELLOTTI, G. M. 1992. Ferritin: a cytoprotective antioxidant strategem of endothelium. *J Biol Chem,* 267**,** 18148-53.

BANEK, C. T., BAUER, A. J., NEEDHAM, K. M., DREYER, H. C. & GILBERT, J. S. 2013. AICAR administration ameliorates hypertension and angiogenic imbalance in a model of preeclampsia in the rat. *American journal of physiology. Heart and circulatory physiology,* 304**,** H1159-H1165.

BARAJAS, J. M., REYES, R., GUERRERO, M. J., JACOB, S. T., MOTIWALA, T. & GHOSHAL, K. 2018. The role of miR-122 in the dysregulation of glucose-6-phosphate dehydrogenase (G6PD) expression in hepatocellular cancer. *Scientific Reports,* 8**,** 9105.

BARBER, A., ROBSON, S. C., MYATT, L., BULMER, J. N. & LYALL, F. 2001. Heme oxygenase expression in human placenta and placental bed: reduced expression of placenta endothelial HO-2 in preeclampsia and fetal growth restriction. *The FASEB Journal,* 15**,** 1158-1168.

BARLEON, B., REUSCH, P., TOTZKE, F., HERZOG, C., KECK, C., MARTINY-BARON, G. & MARME, D. 2001. Soluble VEGFR-1 secreted by endothelial cells and monocytes is present in human serum and plasma from healthy donors. *Angiogenesis,* 4**,** 143-54.

BARLEON, B., SOZZANI, S., ZHOU, D., WEICH, H. A., MANTOVANI, A. & MARME, D. 1996. Migration of human monocytes in response to vascular endothelial growth factor (VEGF) is mediated via the VEGF receptor flt-1. *Blood,* 87**,** 3336-43.

BARTEL, D. P. 2004. MicroRNAs: genomics, biogenesis, mechanism, and function. *Cell,* 116**,** 281-97.

BARTEL, D. P. 2009. MicroRNAs: target recognition and regulatory functions. *Cell,* 136**,** 215-33.

BARZAGO, M. M., BORTOLOTTI, A., STELLARI, F. F., DIOMEDE, L., ALGERI, M., EFRATI, S., SALMONA, M. & BONATI, M. 1996. Placental transfer of valproic acid after liposome encapsulation during in vitro human placenta perfusion. *Journal of Pharmacology and Experimental Therapeutics,* 277**,** 79.

BATZRI, S. & KORN, E. D. 1973. Single bilayer liposomes prepared without sonication. *Biochim Biophys Acta,* 298**,** 1015-9.

BAUER ASHLEY, J., BANEK CHRISTOPHER, T., NEEDHAM, K., GILLHAM, H., CAPOCCIA, S., REGAL JEAN, F. & GILBERT JEFFREY, S. 2013. Pravastatin Attenuates Hypertension, Oxidative Stress, and Angiogenic Imbalance in Rat Model of Placental Ischemia-Induced Hypertension. *Hypertension,* 61**,** 1103-1110.

BAUM, M., SCHIFF, E., KREISER, D., DENNERY, P. A., STEVENSON, D. K., ROSENTHAL, T. & SEIDMAN, D. S. 2000. End-tidal carbon monoxide measurements in women with pregnancy-induced hypertension and preeclampsia. *American Journal of Obstetrics and Gynecology,* 183**,** 900-903.

BAUMANN, V. & WINKLER, J. 2014. miRNA-based therapies: strategies and delivery platforms for oligonucleotide and non-oligonucleotide agents. *Future Medicinal Chemistry,* 6**,** 1967-1984.

BEARDS, F., JONES, L. E., CHARNOCK, J., FORBES, K. & HARRIS, L. K. 2017. Placental Homing Peptide-microRNA Inhibitor Conjugates for Targeted Enhancement of Intrinsic Placental Growth Signaling. *Theranostics,* 7**,** 2940-2955.

BEATTY, M. S. & CURIEL, D. T. 2012. Chapter two--Adenovirus strategies for tissue-specific targeting. *Advances in cancer research,* 115**,** 39-67.

BEDARD, K., SZABO, E., MICHALAK, M. & OPAS, M. 2005. Cellular functions of endoplasmic reticulum chaperones calreticulin, calnexin, and ERp57. *Int Rev Cytol,* 245**,** 91-121.

BEJERANO, T., ETZION, S., ELYAGON, S., ETZION, Y. & COHEN, S. 2018. Nanoparticle Delivery of miRNA-21 Mimic to Cardiac Macrophages Improves Myocardial Remodeling after Myocardial Infarction. *Nano Letters,* 18**,** 5885-5891.

BELGORE, F. M., LIP, G. Y. & BLANN, A. D. 2000. Vascular endothelial growth factor and its receptor, Flt-1, in smokers and non-smokers. *Br J Biomed Sci,* 57**,** 207-13.

BELLAMY, L., CASAS, J.-P., HINGORANI, A. D. & WILLIAMS, D. J. 2007. Pre-eclampsia and risk of cardiovascular disease and cancer in later life: systematic review and meta-analysis. *BMJ,* 335**,** 974.

BERBERAT, P. O., KATORI, M., KACZMAREK, E., ANSELMO, D., LASSMAN, C., KE, B., SHEN, X., BUSUTTIL, R. W., YAMASHITA, K., CSIZMADIA, E., TYAGI, S., OTTERBEIN, L. E., BROUARD, S., TOBIASCH, E., BACH, F. H., KUPIEC-WEGLINSKI, J. W. & SOARES, M. P. 2003. Heavy chain ferritin acts as an anti-apoptotic gene that protects livers from ischemia-reperfusion injury. *The FASEB Journal,* 17**,** 1724-1726.

BERGMANN, A., AHMAD, S., CUDMORE, M., GRUBER, A. D., WITTSCHEN, P., LINDENMAIER, W., CHRISTOFORI, G., GROSS, V., GONZALVES, A., GRONE, H. J., AHMED, A. & WEICH, H. A. 2010. Reduction of circulating soluble Flt-1 alleviates preeclampsia-like symptoms in a mouse model. *J Cell Mol Med,* 14**,** 1857-67.

BERNSTEIN, E., CAUDY, A. A., HAMMOND, S. M. & HANNON, G. J. 2001. Role for a bidentate ribonuclease in the initiation step of RNA interference. *Nature,* 409**,** 363-6.

BESSIS, N., GARCIACOZAR, F. J. & BOISSIER, M. C. 2004. Immune responses to gene therapy vectors: influence on vector function and effector mechanisms. *Gene Therapy,* 11**,** S10-S17.

BHATTACHARYYA, S. N., HABERMACHER, R., MARTINE, U., CLOSS, E. I. & FILIPOWICZ, W. 2006. Relief of microRNA-mediated translational repression in human cells subjected to stress. *Cell,* 125**,** 1111-24.

BILBAN, M., HASLINGER, P., PRAST, J., KLINGLMÜLLER, F., WOELFEL, T., HAIDER, S., SACHS, A., OTTERBEIN, L. E., DESOYE, G., HIDEN, U., WAGNER, O. & KNÖFLER, M. 2009. Identification of novel trophoblast invasion-related genes: heme oxygenase-1 controls motility via peroxisome proliferator-activated receptor gamma. *Endocrinology,* 150**,** 1000-1013.

BIRDIR, C., DROSTE, L., FOX, L., FRANK, M., FRYZE, J., ENEKWE, A., KÖNINGER, A., KIMMIG, R., SCHMIDT, B. & GELLHAUS, A. 2018. Predictive value of sFlt-1, PlGF, sFlt-1/PlGF ratio and PAPP-A for late-onset preeclampsia and IUGR between 32 and 37 weeks of pregnancy. *Pregnancy Hypertens,* 12**,** 124-128.

BIRÓ, O., NAGY, B. & RIGÓ, J., JR. 2017. Identifying miRNA regulatory mechanisms in preeclampsia by systems biology approaches. *Hypertens Pregnancy,* 36**,** 90-99.

BLACK, R. A. & HILL, D. A. 2003. Over-the-counter medications in pregnancy. *Am Fam Physician,* 67**,** 2517-24.

BLEEKER, E. A. J., DE JONG, W. H., GEERTSMA, R. E., GROENEWOLD, M., HEUGENS, E. H. W., KOERS-JACQUEMIJNS, M., VAN DE MEENT, D., POPMA, J. R., RIETVELD, A. G., WIJNHOVEN, S. W. P., CASSEE, F. R. & OOMEN, A. G. 2013. Considerations on the EU definition of a nanomaterial: Science to support policy making. *Regulatory Toxicology and Pharmacology,* 65**,** 119-125.

BOZZUTO, G. & MOLINARI, A. 2015. Liposomes as nanomedical devices. *International journal of nanomedicine,* 10**,** 975-999.

BRAMHAM, K., PARNELL, B., NELSON-PIERCY, C., SEED, P. T., POSTON, L. & CHAPPELL, L. C. 2014. Chronic hypertension and pregnancy outcomes: systematic review and meta-analysis. *The BMJ,* 348**,** g2301.

BRAMSEN, J. B. & KJEMS, J. 2013. Engineering small interfering RNAs by strategic chemical modification. *Methods Mol Biol,* 942**,** 87-109.

BROUARD, S., OTTERBEIN, L. E., ANRATHER, J., TOBIASCH, E., BACH, F. H., CHOI, A. M. K. & SOARES, M. P. 2000. Carbon Monoxide Generated by Heme Oxygenase 1 Suppresses Endothelial Cell Apoptosis. *Journal of Experimental Medicine,* 192**,** 1015-1026.

BROWN, M. A., LINDHEIMER, M. D., DE SWIET, M., VAN ASSCHE, A. & MOUTQUIN, J. M. 2001. The classification and diagnosis of the hypertensive disorders of pregnancy: statement from the International Society for the Study of Hypertension in Pregnancy (ISSHP). *Hypertens Pregnancy,* 20**,** Ix-xiv.

BROWN, M. A., MAGEE, L. A., KENNY, L. C., KARUMANCHI, S. A., MCCARTHY, F. P., SAITO, S., HALL, D. R., WARREN, C. E., ADOYI, G. & ISHAKU, S. 2018a. Hypertensive Disorders of Pregnancy: ISSHP Classification, Diagnosis, and Management Recommendations for International Practice. *Hypertension,* 72**,** 24-43.

BROWN, R. A. M., EPIS, M. R., HORSHAM, J. L., KABIR, T. D., RICHARDSON, K. L. & LEEDMAN, P. J. 2018b. Total RNA extraction from tissues for microRNA and target gene expression analysis: not all kits are created equal. *BMC Biotechnology,* 18**,** 16.

BROWNFOOT, F. C., TONG, S., HANNAN, N. J., BINDER, N. K., WALKER, S. P., CANNON, P., HASTIE, R., ONDA, K. & KAITU'U-LINO, T. J. 2015. Effects of Pravastatin on Human Placenta, Endothelium, and Women With Severe Preeclampsia. *Hypertension,* 66**,** 687-97; discussion 445.

BROWNFOOT, F. C., TONG, S., HANNAN, N. J., HASTIE, R., CANNON, P. & KAITU'U-LINO, T. U. J. 2016. Effects of simvastatin, rosuvastatin and pravastatin on soluble fms-like tyrosine kinase 1 (sFlt-1) and soluble endoglin (sENG) secretion from human

umbilical vein endothelial cells, primary trophoblast cells and placenta. *BMC pregnancy and childbirth,* 16**,** 117-117.

BUHIMSCHI, C. S., MAGLOIRE, L., FUNAI, E., NORWITZ, E. R., KUCZYNSKI, E., MARTIN, R., RICHMAN, S., GULLER, S., LOCKWOOD, C. J. & BUHIMSCHI, I. A. 2006. Fractional excretion of angiogenic factors in women with severe preeclampsia. *Obstet Gynecol,* 107**,** 1103-13.

BULBAKE, U., DOPPALAPUDI, S., KOMMINENI, N. & KHAN, W. 2017. Liposomal Formulations in Clinical Use: An Updated Review. *Pharmaceutics,* 9**,** 12.

BURNS, D. M., D'AMBROGIO, A., NOTTROTT, S. & RICHTER, J. D. 2011. CPEB and two poly(A) polymerases control miR-122 stability and p53 mRNA translation. *Nature,* 473**,** 105-108.

BURTON, G. J. & YUNG, H.-W. 2011. Endoplasmic reticulum stress in the pathogenesis of early-onset pre-eclampsia. *Pregnancy Hypertension,* 1**,** 72-78.

BUSSOLATI, B., DUNK, C., GROHMAN, M., KONTOS, C. D., MASON, J. & AHMED, A. 2001. Vascular endothelial growth factor receptor-1 modulates vascular endothelial growth factor-mediated angiogenesis via nitric oxide. *Am J Pathol,* 159**,** 993-1008.

BUURMA, A. J., TURNER, R. J., DRIESSEN, J. H., MOOYAART, A. L., SCHOONES, J. W., BRUIJN, J. A., BLOEMENKAMP, K. W., DEKKERS, O. M. & BAELDE, H. J. 2013. Genetic variants in pre-eclampsia: a meta-analysis. *Hum Reprod Update,* 19**,** 289-303.

CAI, M., KOLLURU, G. K. & AHMED, A. 2017a. Small Molecule, Big Prospects: MicroRNA in Pregnancy and Its Complications. *J Pregnancy,* 2017**,** 6972732.

CAI, M., WANG, K., MURDOCH, C. E., GU, Y. & AHMED, A. 2017b. Heterodimerisation between VEGFR-1 and VEGFR-2 and not the homodimers of VEGFR-1 inhibit VEGFR-2 activity. *Vascular Pharmacology,* 88**,** 11-20.

CAI, X., HAGEDORN, C. H. & CULLEN, B. R. 2004. Human microRNAs are processed from capped, polyadenylated transcripts that can also function as mRNAs. *RNA (New York, N.Y.),* 10**,** 1957-1966.

CAO, H., KOEHLER, D. R. & HU, J. 2004. Adenoviral vectors for gene replacement therapy. *Viral Immunol,* 17**,** 327-33.

CASTOLDI, M. & MUCKENTHALER, M. U. 2012. Regulation of iron homeostasis by microRNAs. *Cell Mol Life Sci,* 69**,** 3945-52.

CASTOLDI, M., VUJIC SPASIC, M., ALTAMURA, S., ELMÉN, J., LINDOW, M., KISS, J., STOLTE, J., SPARLA, R., D'ALESSANDRO, L. A., KLINGMÜLLER, U., FLEMING, R. E., LONGERICH, T., GRÖNE, H. J., BENES, V., KAUPPINEN, S., HENTZE, M. W. & MUCKENTHALER, M. U. 2011. The liver-specific microRNA miR-122 controls systemic iron homeostasis in mice. *The Journal of clinical investigation,* 121**,** 1386-1396.

CHAI, Z.-T., KONG, J., ZHU, X.-D., ZHANG, Y.-Y., LU, L., ZHOU, J.-M., WANG, L.-R., ZHANG, K.-Z., ZHANG, Q.-B., AO, J.-Y., WANG, M., WU, W.-Z., WANG, L., TANG, Z.-Y. & SUN, H.-C. 2013. MicroRNA-26a inhibits angiogenesis by down-regulating VEGFA

through the PIK3C2α/Akt/HIF-1α pathway in hepatocellular carcinoma. *PloS one,* 8**,** e77957-e77957.

CHAIWORAPONGSA, T., ROMERO, R., ESPINOZA, J., BUJOLD, E., MEE KIM, Y., GONÇALVES, L. F., GOMEZ, R. & EDWIN, S. 2004. Evidence supporting a role for blockade of the vascular endothelial growth factor system in the pathophysiology of preeclampsia. Young Investigator Award. *Am J Obstet Gynecol,* 190**,** 1541-7; discussion 1547-50.

CHAO, M. P., JAISWAL, S., WEISSMAN-TSUKAMOTO, R., ALIZADEH, A. A., GENTLES, A. J., VOLKMER, J., WEISKOPF, K., WILLINGHAM, S. B., RAVEH, T., PARK, C. Y., MAJETI, R. & WEISSMAN, I. L. 2010. Calreticulin is the dominant pro-phagocytic signal on multiple human cancers and is counterbalanced by CD47. *Science translational medicine,* 2**,** 63ra94-63ra94.

CHARNOCK-JONES, D. S., SHARKEY, A. M., BOOCOCK, C. A., AHMED, A., PLEVIN, R., FERRARA, N. & SMITH, S. K. 1994. Vascular endothelial growth factor receptor localization and activation in human trophoblast and choriocarcinoma cells. *Biol Reprod,* 51**,** 524-30.

CHELOUFI, S., DOS SANTOS, C. O., CHONG, M. M. W. & HANNON, G. J. 2010. A dicer-independent miRNA biogenesis pathway that requires Ago catalysis. *Nature,* 465**,** 584-589.

CHEN, J. & KHALIL, R. A. 2017. Chapter Four - Matrix Metalloproteinases in Normal Pregnancy and Preeclampsia. *In:* KHALIL, R. A. (ed.) *Progress in Molecular Biology and Translational Science.* Academic Press.

CHEN, X., GU, S., CHEN, B.-F., SHEN, W.-L., YIN, Z., XU, G.-W., HU, J.-J., ZHU, T., LI, G., WAN, C., OUYANG, H.-W., LEE, T.-L. & CHAN, W.-Y. 2015a. Nanoparticle delivery of stable miR-199a-5p agomir improves the osteogenesis of human mesenchymal stem cells via the HIF1a pathway. *Biomaterials,* 53**,** 239-250.

CHEN, Y., ZHU, X., ZHANG, X., LIU, B. & HUANG, L. 2010a. Nanoparticles Modified With Tumor-targeting scFv Deliver siRNA and miRNA for Cancer Therapy. *Molecular Therapy,* 18**,** 1650-1656.

CHEN, Y. C., GAO, D. Y. & HUANG, L. 2015b. In vivo delivery of miRNAs for cancer therapy: Challenges and strategies. *Advanced Drug Delivery Reviews,* 81**,** 128-141.

CHEN, Z., LI, Y., ZHANG, H., HUANG, P. & LUTHRA, R. 2010b. Hypoxia-regulated microRNA-210 modulates mitochondrial function and decreases ISCU and COX10 expression. *Oncogene,* 29**,** 4362-8.

CHENG, D., DENG, J., ZHANG, B., HE, X., MENG, Z., LI, G., YE, H., ZHENG, S., WEI, L., DENG, X., CHEN, R. & ZHOU, J. 2018. LncRNA HOTAIR epigenetically suppresses miR-122 expression in hepatocellular carcinoma via DNA methylation. *EBioMedicine,* 36**,** 159-170.

CHENG, W., LIU, T., JIANG, F., LIU, C., ZHAO, X., GAO, Y., WANG, H. & LIU, Z. 2011. microRNA-155 regulates angiotensin II type 1 receptor expression in umbilical vein endothelial cells from severely pre-eclamptic pregnant women. *Int J Mol Med,* 27**,** 393-9.

CHEUNG, O., PURI, P., EICKEN, C., CONTOS, M. J., MIRSHAHI, F., MAHER, J. W., KELLUM, J. M., MIN, H., LUKETIC, V. A. & SANYAL, A. J. 2008. Nonalcoholic steatohepatitis is associated with altered hepatic MicroRNA expression. *Hepatology,* 48**,** 1810-20.

CHIOU, G.-Y., CHERNG, J.-Y., HSU, H.-S., WANG, M.-L., TSAI, C.-M., LU, K.-H., CHIEN, Y., HUNG, S.-C., CHEN, Y.-W., WONG, C.-I., TSENG, L.-M., HUANG, P.-I., YU, C.-C., HSU, W.-H. & CHIOU, S.-H. 2012. Cationic polyurethanes-short branch PEI-mediated delivery of Mir145 inhibited epithelial–mesenchymal transdifferentiation and cancer stem-like properties and in lung adenocarcinoma. *Journal of Controlled Release,* 159**,** 240-250.

CHOI, S., PARK, M., KIM, J., PARK, W., KIM, S., LEE, D. K., HWANG, J. Y., CHOE, J., WON, M. H., RYOO, S., HA, K. S., KWON, Y. G. & KIM, Y. M. 2018. TNF-α elicits phenotypic and functional alterations of vascular smooth muscle cells by miR-155-5p-dependent down-regulation of cGMP-dependent kinase 1. *J Biol Chem,* 293**,** 14812-14822.

CHOI, S. Y., YUN, J., LEE, O. J., HAN, H. S., YEO, M. K., LEE, M. A. & SUH, K. S. 2013. MicroRNA expression profiles in placenta with severe preeclampsia using a PNA-based microarray. *Placenta,* 34**,** 799-804.

CHOI, Y. H. & HAN, H.-K. 2018. Nanomedicines: current status and future perspectives in aspect of drug delivery and pharmacokinetics. *Journal of Pharmaceutical Investigation,* 48**,** 43-60.

CHRISTOPHER, A. F., KAUR, R. P., KAUR, G., KAUR, A., GUPTA, V. & BANSAL, P. 2016. MicroRNA therapeutics: Discovering novel targets and developing specific therapy. *Perspectives in Clinical Research,* 7**,** 68-74.

CLARK, D. E., SMITH, S. K., HE, Y., DAY, K. A., LICENCE, D. R., CORPS, A. N., LAMMOGLIA, R. & CHARNOCK-JONES, D. S. 1998. A vascular endothelial growth factor antagonist is produced by the human placenta and released into the maternal circulation. *Biol Reprod,* 59**,** 1540-8.

CLAUSS, M., WEICH, H., BREIER, G., KNIES, U., ROCKL, W., WALTENBERGER, J. & RISAU, W. 1996. The vascular endothelial growth factor receptor Flt-1 mediates biological activities. Implications for a functional role of placenta growth factor in monocyte activation and chemotaxis. *J Biol Chem,* 271**,** 17629-34.

CLEAL, J. K., DAY, P., HANSON, M. A. & LEWIS, R. M. 2009. Measurement of Housekeeping Genes in Human Placenta. *Placenta,* 30**,** 1002-1003.

CONDE-AGUDELO, A., ALTHABE, F., BELIZÁN, J. M. & KAFURY-GOETA, A. C. 1999. Cigarette smoking during pregnancy and risk of preeclampsia: a systematic review. *Am J Obstet Gynecol,* 181**,** 1026-35.

COSTA, P. M., CARDOSO, A. L., CUSTÓDIA, C., CUNHA, P., PEREIRA DE ALMEIDA, L. & PEDROSO DE LIMA, M. C. 2015. MiRNA-21 silencing mediated by tumor-targeted nanoparticles combined with sunitinib: A new multimodal gene therapy approach for glioblastoma. *Journal of Controlled Release,* 207**,** 31-39.

COSTANTINE, M. M., CLEARY, K., HEBERT, M. F., AHMED, M. S., BROWN, L. M., REN, Z., EASTERLING, T. R., HAAS, D. M., HANELINE, L. S., CARITIS, S. N.,

VENKATARAMANAN, R., WEST, H., D'ALTON, M., HANKINS, G., EUNICE KENNEDY SHRIVER NATIONAL INSTITUTE OF CHILD, H. & HUMAN DEVELOPMENT OBSTETRIC-FETAL PHARMACOLOGY RESEARCH UNITS, N. 2016. Safety and pharmacokinetics of pravastatin used for the prevention of preeclampsia in high-risk pregnant women: a pilot randomized controlled trial. *American journal of obstetrics and gynecology,* 214**,** 720.e1-720.e17.

COSTANTINE, M. M., TAMAYO, E., LU, F., BYTAUTIENE, E., LONGO, M., HANKINS, G. D. & SAADE, G. R. 2010. Using pravastatin to improve the vascular reactivity in a mouse model of soluble fms-like tyrosine kinase-1-induced preeclampsia. *Obstet Gynecol,* 116**,** 114-20.

COULOUARN, C., FACTOR, V. M., ANDERSEN, J. B., DURKIN, M. E. & THORGEIRSSON, S. S. 2009. Loss of miR-122 expression in liver cancer correlates with suppression of the hepatic phenotype and gain of metastatic properties. *Oncogene,* 28**,** 3526-36.

COUTO, L. B. & HIGH, K. A. 2010. Viral vector-mediated RNA interference. *Curr Opin Pharmacol,* 10**,** 534-42.

CRAWFORD, K. E., KALIONIS, B., STEVENSON, J. L., BRENNECKE, S. P. & GUDE, N. M. 2012. Calreticulin has opposing effects on the migration of human trophoblast and myometrial endothelial cells. *Placenta,* 33**,** 416-23.

CRAWFORD, K. E., STEVENSON, J. L., WLODEK, M. E. & GUDE, N. M. 2013. No change in calreticulin with fetal growth restriction in human and rat pregnancies. *Placenta,* 34**,** 1066-71.

CRETTAZ, J., OTANO, I., OCHOA-CALLEJERO, L., BENITO, A., PANEDA, A., AURREKOETXEA, I., BERRAONDO, P., RODRÍGUEZ-MADOZ, J. R., ASTUDILLO, A., KREPPEL, F., KOCHANEK, S., RUIZ, J., MENNE, S., PRIETO, J. & GONZALEZ-ASEGUINOLAZA, G. 2009. Treatment of chronic viral hepatitis in woodchucks by prolonged intrahepatic expression of interleukin-12. *J Virol,* 83**,** 2663-74.

CRISPI, F., DOMÍNGUEZ, C., LLURBA, E., MARTÍN-GALLÁN, P., CABERO, L. & GRATACÓS, E. 2006. Placental angiogenic growth factors and uterine artery Doppler findings for characterization of different subsets in preeclampsia and in isolated intrauterine growth restriction. *Am J Obstet Gynecol,* 195**,** 201-7.

CUDMORE, M., AHMAD, S., AL-ANI, B., FUJISAWA, T., COXALL, H., CHUDASAMA, K., DEVEY, L. R., WIGMORE, S. J., ABBAS, A., HEWETT, P. W. & AHMED, A. 2007. Negative regulation of soluble Flt-1 and soluble endoglin release by heme oxygenase-1. *Circulation,* 115**,** 1789-1797.

CUDMORE, M. J., HEWETT, P. W., AHMAD, S., WANG, K. Q., CAI, M., AL-ANI, B., FUJISAWA, T., MA, B., SISSAOUI, S., RAMMA, W., MILLER, M. R., NEWBY, D. E., GU, Y., BARLEON, B., WEICH, H. & AHMED, A. 2012. The role of heterodimerization between VEGFR-1 and VEGFR-2 in the regulation of endothelial cell homeostasis. *Nat Commun,* 3**,** 972.

CUN, D., JENSEN, D. K., MALTESEN, M. J., BUNKER, M., WHITESIDE, P., SCURR, D., FOGED, C. & NIELSEN, H. M. 2011. High loading efficiency and sustained release of siRNA encapsulated in PLGA nanoparticles: quality by design optimization and

characterization. *European journal of pharmaceutics and biopharmaceutics,* 77**,** 26-35.

CURETON, N., KOROTKOVA, I., BAKER, B., GREENWOOD, S., WAREING, M., KOTAMRAJU, V. R., TEESALU, T., CELLESI, F., TIRELLI, N., RUOSLAHTI, E., APLIN, J. D. & HARRIS, L. K. 2017. Selective Targeting of a Novel Vasodilator to the Uterine Vasculature to Treat Impaired Uteroplacental Perfusion in Pregnancy. *Theranostics,* 7**,** 3715-3731.

DAI, Y., QIU, Z., DIAO, Z., SHEN, L., XUE, P., SUN, H. & HU, Y. 2012. MicroRNA-155 inhibits proliferation and migration of human extravillous trophoblast derived HTR-8/SVneo cells via down-regulating cyclin D1. *Placenta,* 33**,** 824-9.

DALEY, J. 2019. Gene Therapy Arrives. *Nature,* 576**,** S12-S13.

DARAEE, H., ETEMADI, A., KOUHI, M., ALIMIRZALU, S. & AKBARZADEH, A. 2016. Application of liposomes in medicine and drug delivery. *Artificial Cells, Nanomedicine, and Biotechnology,* 44**,** 381-391.

DAYAN, N., SCHLOSSER, K., STEWART, D. J., DELLES, C., KAUR, A. & PILOTE, L. 2018. Circulating MicroRNAs Implicate Multiple Atherogenic Abnormalities in the Long-Term Cardiovascular Sequelae of Preeclampsia. *American journal of hypertension,* 31**,** 1093-1097.

DENG, X., CAO, M., ZHANG, J., HU, K., YIN, Z., ZHOU, Z., XIAO, X., YANG, Y., SHENG, W., WU, Y. & ZENG, Y. 2014a. Hyaluronic acid-chitosan nanoparticles for co-delivery of MiR-34a and doxorubicin in therapy against triple negative breast cancer. *Biomaterials,* 35**,** 4333-4344.

DENG, X. G., QIU, R. L., WU, Y. H., LI, Z. X., XIE, P., ZHANG, J., ZHOU, J. J., ZENG, L. X., TANG, J., MAHARJAN, A. & DENG, J. M. 2014b. Overexpression of miR-122 promotes the hepatic differentiation and maturation of mouse ESCs through a miR-122/FoxA1/HNF4a-positive feedback loop. *Liver Int,* 34**,** 281-95.

DENG, Y., WANG, C. C., CHOY, K. W., DU, Q., CHEN, J., WANG, Q., LI, L., CHUNG, T. K. & TANG, T. 2014c. Therapeutic potentials of gene silencing by RNA interference: principles, challenges, and new strategies. *Gene,* 538**,** 217-27.

DENNERY, P. A. 2014. Signaling function of heme oxygenase proteins. *Antioxidants & redox signaling,* 20**,** 1743-1753.

DENSCHLAG, D., MARCULESCU, R., UNFRIED, G., HEFLER, L. A., EXNER, M., HASHEMI, A., RIENER, E. K., KECK, C., TEMPFER, C. B. & WAGNER, O. 2004. The size of a microsatellite polymorphism of the haem oxygenase 1 gene is associated with idiopathic recurrent miscarriage. *Mol Hum Reprod,* 10**,** 211-4.

DENZLER, R., AGARWAL, V., STEFANO, J., BARTEL, D. P. & STOFFEL, M. 2014. Assessing the ceRNA hypothesis with quantitative measurements of miRNA and target abundance. *Mol Cell,* 54**,** 766-76.

DEWS, M., HOMAYOUNI, A., YU, D., MURPHY, D., SEVIGNANI, C., WENTZEL, E., FURTH, E. E., LEE, W. M., ENDERS, G. H., MENDELL, J. T. & THOMAS-TIKHONENKO, A. 2006. Augmentation of tumor angiogenesis by a Myc-activated microRNA cluster. *Nature genetics,* 38**,** 1060-1065.

DIACONU, I., DENBY, L., PESONEN, S., CERULLO, V., BAUERSCHMITZ, G. J., GUSE, K., RAJECKI, M., DIAS, J. D., TAARI, K., KANERVA, A., BAKER, A. H. & HEMMINKI, A. 2009. Serotype chimeric and fiber-mutated adenovirus Ad5/19p-HIT for targeting renal cancer and untargeting the liver. *Hum Gene Ther,* 20**,** 611-20.

DÍAZ, E., CÁRDENAS, M., ARIZA, A. C., LARREA, F. & HALHALI, A. 2005. Placental insulin and insulin-like growth factor I receptors in normal and preeclamptic pregnancies. *Clinical Biochemistry,* 38**,** 243-247.

DMITRIEV, I., KRASNYKH, V., MILLER, C. R., WANG, M., KASHENTSEVA, E., MIKHEEVA, G., BELOUSOVA, N. & CURIEL, D. T. 1998. An adenovirus vector with genetically modified fibers demonstrates expanded tropism via utilization of a coxsackievirus and adenovirus receptor-independent cell entry mechanism. *Journal of virology,* 72**,** 9706-9713.

DORIDOT, L., MIRALLES, F., BARBAUX, S. & VAIMAN, D. 2013. Trophoblasts, invasion, and microRNA. *Frontiers in genetics,* 4**,** 248-248.

DOUGLAS, K. A. & REDMAN, C. W. 1994. Eclampsia in the United Kingdom. *Bmj,* 309**,** 1395-400.

DREWLO, S., LEVYTSKA, K. & KINGDOM, J. 2012. Revisiting the housekeeping genes of human placental development and insufficiency syndromes. *Placenta,* 33**,** 952-954.

DU, L., HE, F., KUANG, L., TANG, W., LI, Y. & CHEN, D. 2017. eNOS/iNOS and endoplasmic reticulum stress-induced apoptosis in the placentas of patients with preeclampsia. *Journal of Human Hypertension,* 31**,** 49-55.

DUCKITT, K. & HARRINGTON, D. 2005. Risk factors for pre-eclampsia at antenatal booking: systematic review of controlled studies. *BMJ : British Medical Journal,* 330**,** 565-565.

DULAK, J., JÓZKOWICZ, A., FORESTI, R., KASZA, A., FRICK, M., HUK, I., GREEN, C. J., PACHINGER, O., WEIDINGER, F. & MOTTERLINI, R. 2002. Heme oxygenase activity modulates vascular endothelial growth factor synthesis in vascular smooth muscle cells. *Antioxid Redox Signal,* 4**,** 229-40.

DULEY, L. 1992. Maternal mortality associated with hypertensive disorders of pregnancy in Africa, Asia, Latin America and the Caribbean. *Br J Obstet Gynaecol,* 99**,** 547-53.

DULEY, L. 2009. The Global Impact of Pre-eclampsia and Eclampsia. *Seminars in Perinatology,* 33**,** 130-137.

DUNK, C. & AHMED, A. 2001. Vascular Endothelial Growth Factor Receptor-2-Mediated Mitogenesis Is Negatively Regulated by Vascular Endothelial Growth Factor Receptor-1 in Tumor Epithelial Cells. *The American Journal of Pathology,* 158**,** 265-273.

EDISON, R. J. & MUENKE, M. 2004. Mechanistic and epidemiologic considerations in the evaluation of adverse birth outcomes following gestational exposure to statins. *American Journal of Medical Genetics Part A,* 131A**,** 287-298.

ENDO-TAKAHASHI, Y., NEGISHI, Y., NAKAMURA, A., UKAI, S., OOAKU, K., ODA, Y., SUGIMOTO, K., MORIYASU, F., TAKAGI, N., SUZUKI, R., MARUYAMA, K. &

ARAMAKI, Y. 2014. Systemic delivery of miR-126 by miRNA-loaded Bubble liposomes for the treatment of hindlimb ischemia. *Scientific reports,* 4**,** 3883-3883.

ENGLAND, L. & ZHANG, J. 2007. Smoking and risk of preeclampsia: a systematic review. *Front Biosci,* 12**,** 2471-83.

ENQUOBAHRIE, D. A., ABETEW, D. F., SORENSEN, T. K., WILLOUGHBY, D., CHIDAMBARAM, K. & WILLIAMS, M. A. 2011. Placental microRNA expression in pregnancies complicated by preeclampsia. *American journal of obstetrics and gynecology,* 204**,** 178.e12-178.e21.

ESAU, C., DAVIS, S., MURRAY, S. F., YU, X. X., PANDEY, S. K., PEAR, M., WATTS, L., BOOTEN, S. L., GRAHAM, M., MCKAY, R., SUBRAMANIAM, A., PROPP, S., LOLLO, B. A., FREIER, S., BENNETT, C. F., BHANOT, S. & MONIA, B. P. 2006. miR-122 regulation of lipid metabolism revealed by in vivo antisense targeting. *Cell Metab,* 3**,** 87-98.

ESPLIN, M. S., FAUSETT, M. B., FRASER, A., KERBER, R., MINEAU, G., CARRILLO, J. & VARNER, M. W. 2001. Paternal and maternal components of the predisposition to preeclampsia. *N Engl J Med,* 344**,** 867-72.

EUBANK, T. D., RODA, J. M., LIU, H., O'NEIL, T. & MARSH, C. B. 2011. Opposing roles for HIF-1α and HIF-2α in the regulation of angiogenesis by mononuclear phagocytes. *Blood,* 117**,** 323-332.

EVSEENKO, D., PAXTON, J. W. & KEELAN, J. A. 2006. Active transport across the human placenta: impact on drug efficacy and toxicity. *Expert Opin Drug Metab Toxicol,* 2**,** 51-69.

FABBRI, M., PAONE, A., CALORE, F., GALLI, R. & CROCE, C. M. 2013. A new role for microRNAs, as ligands of Toll-like receptors. *RNA Biology,* 10**,** 169-174.

FARINA, A., SEKIZAWA, A., DE SANCTIS, P., PURWOSUNU, Y., OKAI, T., CHA, D. H., KANG, J. H., VICENZI, C., TEMPESTA, A., WIBOWO, N., VALVASSORI, L. & RIZZO, N. 2008. Gene expression in chorionic villous samples at 11 weeks' gestation from women destined to develop preeclampsia. *Prenat Diagn,* 28**,** 956-61.

FASANARO, P., D'ALESSANDRA, Y., DI STEFANO, V., MELCHIONNA, R., ROMANI, S., POMPILIO, G., CAPOGROSSI, M. C. & MARTELLI, F. 2008. MicroRNA-210 modulates endothelial cell response to hypoxia and inhibits the receptor tyrosine kinase ligand Ephrin-A3. *The Journal of biological chemistry,* 283**,** 15878-15883.

FAULKNER, J. L., CORNELIUS, D. C., AMARAL, L. M., HARMON, A. C., CUNNINGHAM, M. W., JR., DARBY, M. M., IBRAHIM, T., THOMAS, D. A. S., HERSE, F., WALLUKAT, G., DECHEND, R. & LAMARCA, B. 2016. Vitamin D supplementation improves pathophysiology in a rat model of preeclampsia. *American journal of physiology. Regulatory, integrative and comparative physiology,* 310**,** R346-R354.

FELGNER, P. L., GADEK, T. R., HOLM, M., ROMAN, R., CHAN, H. W., WENZ, M., NORTHROP, J. P., RINGOLD, G. M. & DANIELSEN, M. 1987. Lipofection: a highly efficient, lipid-mediated DNA-transfection procedure. *Proc Natl Acad Sci U S A,* 84**,** 7413-7.

FERRARA, N. 2004. Vascular Endothelial Growth Factor: Basic Science and Clinical Progress. *Endocrine Reviews,* 25**,** 581-611.

FERRARA, N., CARVER-MOORE, K., CHEN, H., DOWD, M., LU, L., O'SHEA, K. S., POWELL-BRAXTON, L., HILLAN, K. J. & MOORE, M. W. 1996. Heterozygous embryonic lethality induced by targeted inactivation of the VEGF gene. *Nature,* 380**,** 439-42.

FERRARA, N. & DAVIS-SMYTH, T. 1997. The Biology of Vascular Endothelial Growth Factor. *Endocrine Reviews,* 18**,** 4-25.

FERRARA, N., GERBER, H.-P. & LECOUTER, J. 2003. The biology of VEGF and its receptors. *Nature Medicine,* 9**,** 669-676.

FERRETTI, C., BRUNI, L., DANGLES-MARIE, V., PECKING, A. P. & BELLET, D. 2007. Molecular circuits shared by placental and cancer cells, and their implications in the proliferative, invasive and migratory capacities of trophoblasts. *Hum Reprod Update,* 13**,** 121-41.

FIGUEROA-ESPADA, C. G., MITCHELL, M. J. & RILEY, R. S. 2020. Exploiting the placenta for nanoparticle-mediated drug delivery during pregnancy. *Advanced Drug Delivery Reviews*.

FISH, J. E., SANTORO, M. M., MORTON, S. U., YU, S., YEH, R.-F., WYTHE, J. D., IVEY, K. N., BRUNEAU, B. G., STAINIER, D. Y. R. & SRIVASTAVA, D. 2008. miR-126 regulates angiogenic signaling and vascular integrity. *Developmental cell,* 15**,** 272-284.

FISK, N. M. & ATUN, R. 2008. Market failure and the poverty of new drugs in maternal health. *PLoS medicine,* 5**,** e22-e22.

FOGAL, V., ZHANG, L., KRAJEWSKI, S. & RUOSLAHTI, E. 2008. Mitochondrial/cell-surface protein p32/gC1qR as a molecular target in tumor cells and tumor stroma. *Cancer Res,* 68**,** 7210-8.

FORBES, K., FARROKHNIA, F., APLIN, J. D. & WESTWOOD, M. 2012. Dicer-dependent miRNAs provide an endogenous restraint on cytotrophoblast proliferation. *Placenta,* 33**,** 581-5.

FOSTER, D. J., BROWN, C. R., SHAIKH, S., TRAPP, C., SCHLEGEL, M. K., QIAN, K., SEHGAL, A., RAJEEV, K. G., JADHAV, V., MANOHARAN, M., KUCHIMANCHI, S., MAIER, M. A. & MILSTEIN, S. 2018. Advanced siRNA Designs Further Improve In Vivo Performance of GalNAc-siRNA Conjugates. *Molecular therapy : the journal of the American Society of Gene Therapy,* 26**,** 708-717.

FOX, K. A., LONGO, M., TAMAYO, E., KECHICHIAN, T., BYTAUTIENE, E., HANKINS, G. D., SAADE, G. R. & COSTANTINE, M. M. 2011. Effects of pravastatin on mediators of vascular function in a mouse model of soluble Fms-like tyrosine kinase-1-induced preeclampsia. *Am J Obstet Gynecol,* 205**,** 366.e1-5.

FRANCESCHINI, N., FOX, E., ZHANG, Z., EDWARDS, T. L., NALLS, M. A., SUNG, Y. J., TAYO, B. O., SUN, Y. V., GOTTESMAN, O., ADEYEMO, A., JOHNSON, A. D., YOUNG, J. H., RICE, K., DUAN, Q., CHEN, F., LI, Y., TANG, H., FORNAGE, M., KEENE, K. L., ANDREWS, J. S., SMITH, J. A., FAUL, J. D., GUANGFA, Z., GUO, W., LIU, Y., MURRAY, S. S., MUSANI, S. K., SRINIVASAN, S., VELEZ EDWARDS, D. R., WANG, H., BECKER, L. C., BOVET, P., BOCHUD, M., BROECKEL, U., BURNIER, M., CARTY, C., CHASMAN, D. I., EHRET, G., CHEN, W.-M., CHEN, G., CHEN, W., DING, J.,

DREISBACH, A. W., EVANS, M. K., GUO, X., GARCIA, M. E., JENSEN, R., KELLER, M. F., LETTRE, G., LOTAY, V., MARTIN, L. W., MOORE, J. H., MORRISON, A. C., MOSLEY, T. H., OGUNNIYI, A., PALMAS, W., PAPANICOLAOU, G., PENMAN, A., POLAK, J. F., RIDKER, P. M., SALAKO, B., SINGLETON, A. B., SHRINER, D., TAYLOR, K. D., VASAN, R., WIGGINS, K., WILLIAMS, S. M., YANEK, L. R., ZHAO, W., ZONDERMAN, A. B., BECKER, D. M., BERENSON, G., BOERWINKLE, E., BOTTINGER, E., CUSHMAN, M., EATON, C., NYBERG, F., HEISS, G., HIRSCHHRON, J. N., HOWARD, V. J., KARCZEWSK, K. J., LANKTREE, M. B., LIU, K., LIU, Y., LOOS, R., MARGOLIS, K., SNYDER, M., ASIAN GENETIC EPIDEMIOLOGY NETWORK, C., PSATY, B. M., SCHORK, N. J., WEIR, D. R., ROTIMI, C. N., SALE, M. M., HARRIS, T., KARDIA, S. L. R., HUNT, S. C., ARNETT, D., REDLINE, S., COOPER, R. S., RISCH, N. J., et al. 2013. Genome-wide association analysis of blood-pressure traits in African-ancestry individuals reveals common associated genes in African and non-African populations. *American journal of human genetics,* 93**,** 545-554.

FU, J., ZHAO, L., WANG, L. & ZHU, X. 2015. Expression of markers of endoplasmic reticulum stress-induced apoptosis in the placenta of women with early and late onset severe pre-eclampsia. *Taiwan J Obstet Gynecol,* 54**,** 19-23.

FU, Y., CHEN, J. & HUANG, Z. 2019. Recent progress in microRNA-based delivery systems for the treatment of human disease. *ExRNA,* 1**,** 24.

FUSHIMA, T., SEKIMOTO, A., MINATO, T., ITO, T., OE, Y., KISU, K., SATO, E., FUNAMOTO, K., HAYASE, T., KIMURA, Y., ITO, S., SATO, H. & TAKAHASHI, N. 2016. Reduced Uterine Perfusion Pressure (RUPP) Model of Preeclampsia in Mice. *PLOS ONE,* 11**,** e0155426.

GEORGE, E. M., ARANY, M., COCKRELL, K., STORM, M. V., STEC, D. E. & GRANGER, J. P. 2011a. Induction of heme oxygenase-1 attenuates sFlt-1-induced hypertension in pregnant rats. *Am J Physiol Regul Integr Comp Physiol,* 301**,** R1495-500.

GEORGE, E. M., ARANY, M., COCKRELL, K., STORM, M. V., STEC, D. E. & GRANGER, J. P. 2011b. Induction of heme oxygenase-1 attenuates sFlt-1-induced hypertension in pregnant rats. *American journal of physiology. Regulatory, integrative and comparative physiology,* 301**,** R1495-R1500.

GEORGE, E. M., COCKRELL, K., ARANAY, M., CSONGRADI, E., STEC, D. E. & GRANGER, J. P. 2011c. Induction of heme oxygenase 1 attenuates placental ischemia-induced hypertension. *Hypertension,* 57**,** 941-8.

GEORGE, E. M., COLSON, D., DIXON, J., PALEI, A. C. & GRANGER, J. P. 2012. Heme Oxygenase-1 Attenuates Hypoxia-Induced sFlt-1 and Oxidative Stress in Placental Villi through Its Metabolic Products CO and Bilirubin. *International journal of hypertension,* 2012**,** 486053-486053.

GEORGE, E. M., HOSICK, P. A., STEC, D. E. & GRANGER, J. P. 2013. Heme oxygenase inhibition increases blood pressure in pregnant rats. *Am J Hypertens,* 26**,** 924-30.

GILBERT, J. S., BABCOCK, S. A. & GRANGER, J. P. 2007. Hypertension Produced by Reduced Uterine Perfusion in Pregnant Rats Is Associated With Increased Soluble Fms-Like Tyrosine Kinase-1 Expression. *Hypertension,* 50**,** 1142.

GILBERT, J. S., BAUER, A. J., GINGERY, A., BANEK, C. T. & CHASSON, S. 2012. Circulating and utero-placental adaptations to chronic placental ischemia in the rat. *Placenta,* 33**,** 100-105.

GILBERT, J. S., GILBERT, S. A., ARANY, M. & GRANGER, J. P. 2009. Hypertension produced by placental ischemia in pregnant rats is associated with increased soluble endoglin expression. *Hypertension,* 53**,** 399-403.

GJETTING, T., ARILDSEN, N. S., CHRISTENSEN, C. L., POULSEN, T. T., ROTH, J. A., HANDLOS, V. N. & POULSEN, H. S. 2010. In vitro and in vivo effects of polyethylene glycol (PEG)-modified lipid in DOTAP/cholesterol-mediated gene transfection. *Int J Nanomedicine,* 5**,** 371-83.

GOICOECHEA, S., ORR, A. W., PALLERO, M. A., EGGLETON, P. & MURPHY-ULLRICH, J. E. 2000. Thrombospondin mediates focal adhesion disassembly through interactions with cell surface calreticulin. *J Biol Chem,* 275**,** 36358-68.

GOLD, L. I., EGGLETON, P., SWEETWYNE, M. T., VAN DUYN, L. B., GREIVES, M. R., NAYLOR, S.-M., MICHALAK, M. & MURPHY-ULLRICH, J. E. 2010. Calreticulin: non-endoplasmic reticulum functions in physiology and disease. *The FASEB Journal,* 24**,** 665-683.

GOLDENBERG, R. L. & JOBE, A. H. 2001. Prospects for research in reproductive health and birth outcomes. *Jama,* 285**,** 633-9.

GOSWAMI, R., SUBRAMANIAN, G., SILAYEVA, L., NEWKIRK, I., DOCTOR, D., CHAWLA, K., CHATTOPADHYAY, S., CHANDRA, D., CHILUKURI, N. & BETAPUDI, V. 2019. Gene Therapy Leaves a Vicious Cycle. *Frontiers in Oncology,* 9.

GOZZELINO, R., JENEY, V. & SOARES, M. P. 2010. Mechanisms of cell protection by heme oxygenase-1. *Annu Rev Pharmacol Toxicol,* 50**,** 323-54.

GRANGER, J. P., LAMARCA, B. B., COCKRELL, K., SEDEEK, M., BALZI, C., CHANDLER, D. & BENNETT, W. 2006. Reduced uterine perfusion pressure (RUPP) model for studying cardiovascular-renal dysfunction in response to placental ischemia. *Methods Mol Med,* 122**,** 383-92.

GRAY KATHRYN, J., KOVACHEVA VESELA, P., MIRZAKHANI, H., BJONNES ANDREW, C., ALMOGUERA, B., DEWAN ANDREW, T., TRICHE ELIZABETH, W., SAFTLAS AUDREY, F., HOH, J., BODIAN DALE, L., KLEIN, E., HUDDLESTON KATHI, C., INGLES SUE, A., LOCKWOOD CHARLES, J., HAKONARSON, H., MCELRATH THOMAS, F., MURRAY JEFFREY, C., WILSON MELISSA, L., NORWITZ ERROL, R., KARUMANCHI, S. A., BATEMAN BRIAN, T., KEATING BRENDAN, J. & SAXENA, R. 2018. Gene-Centric Analysis of Preeclampsia Identifies Maternal Association at PLEKHG1. *Hypertension,* 72**,** 408-416.

GROSSER, N., HEMMERLE, A., BERNDT, G., ERDMANN, K., HINKELMANN, U., SCHÜRGER, S., WIJAYANTI, N., IMMENSCHUH, S. & SCHRÖDER, H. 2004. The antioxidant defense protein heme oxygenase 1 is a novel target for statins in endothelial cells. *Free Radic Biol Med,* 37**,** 2064-71.

GU, V. Y., WONG, M. H., STEVENSON, J. L., CRAWFORD, K. E., BRENNECKE, S. P. & GUDE, N. M. 2008. Calreticulin in human pregnancy and pre-eclampsia. *MHR: Basic science of reproductive medicine,* 14**,** 309-315.

GULLA, S. K., KOTCHERLAKOTA, R., NIMUSHAKAVI, S., NIMMU, N. V., KHALID, S., PATRA, C. R. & CHAUDHURI, A. 2018. Au-CGKRK Nanoconjugates for Combating Cancer through T-Cell-Driven Therapeutic RNA Interference. *ACS Omega,* 3**,** 8663-8676.

HA, M. & KIM, V. N. 2014. Regulation of microRNA biogenesis. *Nat Rev Mol Cell Biol,* 15**,** 509-24.

HAFNER, A., LOVRIĆ, J., LAKOŠ, G. P. & PEPIĆ, I. 2014. Nanotherapeutics in the EU: an overview on current state and future directions. *International journal of nanomedicine,* 9**,** 1005-1023.

HAHN, S. 2015. Preeclampsia - will orphan drug status facilitate innovative biological therapies? *Frontiers in surgery,* 2**,** 7-7.

HALDER, J., KAMAT, A. A., LANDEN, C. N., HAN, L. Y., LUTGENDORF, S. K., LIN, Y. G., MERRITT, W. M., JENNINGS, N. B., CHAVEZ-REYES, A., COLEMAN, R. L., GERSHENSON, D. M., SCHMANDT, R., COLE, S. W., LOPEZ-BERESTEIN, G. & SOOD, A. K. 2006. Focal Adhesion Kinase Targeting Using In vivo Short Interfering RNA Delivery in Neutral Liposomes for Ovarian Carcinoma Therapy. *Clinical Cancer Research,* 12**,** 4916-4924.

HAMMOND, S. M. 2005. Dicing and slicing: the core machinery of the RNA interference pathway. *FEBS Lett,* 579**,** 5822-9.

HANNA, J., HOSSAIN, G. S. & KOCERHA, J. 2019. The Potential for microRNA Therapeutics and Clinical Research. *Frontiers in genetics,* 10**,** 478-478.

HANNAN, N. J., BROWNFOOT, F. C., CANNON, P., DEO, M., BEARD, S., NGUYEN, T. V., PALMER, K. R., TONG, S. & KAITU'U-LINO, T. J. 2017. Resveratrol inhibits release of soluble fms-like tyrosine kinase (sFlt-1) and soluble endoglin and improves vascular dysfunction - implications as a preeclampsia treatment. *Sci Rep,* 7**,** 1819.

HASSEL, D., CHENG, P., WHITE, M. P., IVEY, K. N., KROLL, J., AUGUSTIN, H. G., KATUS, H. A., STAINIER, D. Y. R. & SRIVASTAVA, D. 2012. miR-10 Regulates the Angiogenic Behavior of Zebrafish and Human Endothelial Cells by Promoting VEGF Signaling. *Circulation research,* 111**,** 1421-1433.

HE, Y., SMITH, S. K., DAY, K. A., CLARK, D. E., LICENCE, D. R. & CHARNOCK-JONES, D. S. 1999. Alternative splicing of vascular endothelial growth factor (VEGF)-R1 (FLT-1) pre-mRNA is important for the regulation of VEGF activity. *Mol Endocrinol,* 13**,** 537-45.

HEDEGAARD, S. F., DERBAS, M. S., LIND, T. K., KASIMOVA, M. R., CHRISTENSEN, M. V., MICHAELSEN, M. H., CAMPBELL, R. A., JORGENSEN, L., FRANZYK, H., CÁRDENAS, M. & NIELSEN, H. M. 2018. Fluorophore labeling of a cell-penetrating peptide significantly alters the mode and degree of biomembrane interaction. *Scientific Reports,* 8**,** 6327.

HEMMINKI, A., BELOUSOVA, N., ZINN, K. R., LIU, B., WANG, M., CHAUDHURI, T. R., ROGERS, B. E., BUCHSBAUM, D. J., SIEGAL, G. P., BARNES, M. N., GOMEZ-NAVARRO, J., CURIEL, D. T. & ALVAREZ, R. D. 2001. An adenovirus with enhanced infectivity mediates molecular chemotherapy of ovarian cancer cells and allows imaging of gene expression. *Mol Ther,* 4**,** 223-31.

HERRAIZ, I., DRÖGE, L. A., GÓMEZ-MONTES, E., HENRICH, W., GALINDO, A. & VERLOHREN, S. 2014. Characterization of the Soluble fms-Like Tyrosine Kinase-1 to Placental Growth Factor Ratio in Pregnancies Complicated by Fetal Growth Restriction. *Obstetrics & Gynecology,* 124.

HETTIARACHCHI, N., DALLAS, M., AL-OWAIS, M., GRIFFITHS, H., HOOPER, N., SCRAGG, J., BOYLE, J. & PEERS, C. 2014. Heme oxygenase-1 protects against Alzheimer's amyloid-β1-42-induced toxicity via carbon monoxide production. *Cell Death & Disease,* 5**,** e1569-e1569.

HEYDARIAN, M., MCCAFFREY, T., FLOREA, L., YANG, Z., ROSS, M. M., ZHOU, W. & MAYNARD, S. E. 2009. Novel splice variants of sFlt1 are upregulated in preeclampsia. *Placenta,* 30**,** 250-5.

HINSKE, L. C., FRANÇA, G. S., TORRES, H. A. M., OHARA, D. T., LOPES-RAMOS, C. M., HEYN, J., REIS, L. F. L., OHNO-MACHADO, L., KRETH, S. & GALANTE, P. A. F. 2014. miRIAD-integrating microRNA inter- and intragenic data. *Database : the journal of biological databases and curation,* 2014**,** bau099.

HOFFMAN, J. A., GIRAUDO, E., SINGH, M., ZHANG, L., INOUE, M., PORKKA, K., HANAHAN, D. & RUOSLAHTI, E. 2003. Progressive vascular changes in a transgenic mouse model of squamous cell carcinoma. *Cancer Cell,* 4**,** 383-91.

HØJRUP, P., ROEPSTORFF, P. & HOUEN, G. 2001. Human placental calreticulin characterization of domain structure and post-translational modifications. *Eur J Biochem,* 268**,** 2558-65.

HROMADNIKOVA, I., KOTLABOVA, K., HYMPANOVA, L. & KROFTA, L. 2015. Cardiovascular and Cerebrovascular Disease Associated microRNAs Are Dysregulated in Placental Tissues Affected with Gestational Hypertension, Preeclampsia and Intrauterine Growth Restriction. *PloS one,* 10**,** e0138383-e0138383.

HSU, S.-H., WANG, B., KOTA, J., YU, J., COSTINEAN, S., KUTAY, H., YU, L., BAI, S., LA PERLE, K., CHIVUKULA, R. R., MAO, H., WEI, M., CLARK, K. R., MENDELL, J. R., CALIGIURI, M. A., JACOB, S. T., MENDELL, J. T. & GHOSHAL, K. 2012. Essential metabolic, anti-inflammatory, and anti-tumorigenic functions of miR-122 in liver. *The Journal of clinical investigation,* 122**,** 2871-2883.

HSU, S.-H., YU, B., WANG, X., LU, Y., SCHMIDT, C. R., LEE, R. J., LEE, L. J., JACOB, S. T. & GHOSHAL, K. 2013. Cationic lipid nanoparticles for therapeutic delivery of siRNA and miRNA to murine liver tumor. *Nanomedicine: Nanotechnology, Biology and Medicine,* 9**,** 1169-1180.

HU, Q., GAO, X., KANG, T., FENG, X., JIANG, D., TU, Y., SONG, Q., YAO, L., JIANG, X., CHEN, H. & CHEN, J. 2013. CGKRK-modified nanoparticles for dual-targeting drug delivery to tumor cells and angiogenic blood vessels. *Biomaterials,* 34**,** 9496-508.

HU, T., WANG, G., ZHU, Z., HUANG, Y., GU, H. & NI, X. 2015. Increased ADAM10 expression in preeclamptic placentas is associated with decreased expression of hydrogen sulfide production enzymes. *Placenta,* 36**,** 947-50.

HU, Y., LI, P., HAO, S., LIU, L., ZHAO, J. & HOU, Y. 2009. Differential expression of microRNAs in the placentae of Chinese patients with severe pre-eclampsia. *Clin Chem Lab Med,* 47**,** 923-9.

HUCKLE, W. R. & ROCHE, R. I. 2004. Post-transcriptional control of expression of sFlt-1, an endogenous inhibitor of vascular endothelial growth factor. *J Cell Biochem,* 93**,** 120-32.

HUPPERTZ, B. 2008. Placental origins of preeclampsia: challenging the current hypothesis. *Hypertension,* 51**,** 970-5.

IBRAHIM, A. F., WEIRAUCH, U., THOMAS, M., GRÜNWELLER, A., HARTMANN, R. K. & AIGNER, A. 2011. MicroRNA Replacement Therapy for miR-145 and miR-33a Is Efficacious in a Model of Colon Carcinoma. *Cancer Research,* 71**,** 5214.

ILLIEN, F., RODRIGUEZ, N., AMOURA, M., JOLIOT, A., PALLERLA, M., CRIBIER, S., BURLINA, F. & SAGAN, S. 2016. Quantitative fluorescence spectroscopy and flow cytometry analyses of cell-penetrating peptides internalization pathways: optimization, pitfalls, comparison with mass spectrometry quantification. *Scientific reports,* 6**,** 36938-36938.

IMMORDINO, M. L., DOSIO, F. & CATTEL, L. 2006. Stealth liposomes: review of the basic science, rationale, and clinical applications, existing and potential. *Int J Nanomedicine,* 1**,** 297-315.

INTAPAD, S., WARRINGTON, J. P., SPRADLEY, F. T., PALEI, A. C., DRUMMOND, H. A., RYAN, M. J., GRANGER, J. P. & ALEXANDER, B. T. 2014. Reduced uterine perfusion pressure induces hypertension in the pregnant mouse. *American journal of physiology. Regulatory, integrative and comparative physiology,* 307**,** R1353-R1357.

ITO, K., IKEDA, S., SHIBATA, T., YANO, T. & HORIKAWA, S. 1997. Immunohistochemical analysis of heme oxygenase-I in rat liver after ischemia. *Biochemistry and Molecular Biology International,* 43**,** 551-556.

JAIRAJPURI, D. S., MALALLA, Z. H., MAHMOOD, N. & ALMAWI, W. Y. 2017. Circulating microRNA expression as predictor of preeclampsia and its severity. *Gene,* 627**,** 543-548.

JANAS, M. M., SCHLEGEL, M. K., HARBISON, C. E., YILMAZ, V. O., JIANG, Y., PARMAR, R., ZLATEV, I., CASTORENO, A., XU, H., SHULGA-MORSKAYA, S., RAJEEV, K. G., MANOHARAN, M., KEIRSTEAD, N. D., MAIER, M. A. & JADHAV, V. 2018. Selection of GalNAc-conjugated siRNAs with limited off-target-driven rat hepatotoxicity. *Nature Communications,* 9**,** 723.

JEBBINK, J., KEIJSER, R., VEENBOER, G., VAN DER POST, J., RIS-STALPERS, C. & AFINK, G. 2011. Expression of placental FLT1 transcript variants relates to both gestational hypertensive disease and fetal growth. *Hypertension,* 58**,** 70-6.

JEYABALAN, A., POWERS, R. W., DURICA, A. R., HARGER, G. F., ROBERTS, J. M. & NESS, R. B. 2008. Cigarette smoke exposure and angiogenic factors in pregnancy and preeclampsia. *American journal of hypertension,* 21**,** 943-947.

JOHNSON, M. P., BRENNECKE, S. P., EAST, C. E., GÖRING, H. H. H., KENT, J. W., JR., DYER, T. D., SAID, J. M., ROTEN, L. T., IVERSEN, A.-C., ABRAHAM, L. J., HEINONEN, S.,

KAJANTIE, E., KERE, J., KIVINEN, K., POUTA, A., LAIVUORI, H., GROUP, F. S., AUSTGULEN, R., BLANGERO, J. & MOSES, E. K. 2012. Genome-wide association scan identifies a risk locus for preeclampsia on 2q14, near the inhibin, beta B gene. *PloS one,* 7**,** e33666-e33666.

JOHNSON, S., MICHALAK, M., OPAS, M. & EGGLETON, P. 2001. The ins and outs of calreticulin: from the ER lumen to the extracellular space. *Trends Cell Biol,* 11**,** 122-9.

JOPLING, C. 2012. Liver-specific microRNA-122: Biogenesis and function. *RNA biology,* 9**,** 137-142.

JUNG, C. J., IYENGAR, S., BLAHNIK, K. R., AJUHA, T. P., JIANG, J. X., FARNHAM, P. J. & ZERN, M. 2011. Epigenetic modulation of miR-122 facilitates human embryonic stem cell self-renewal and hepatocellular carcinoma proliferation. *PLoS One,* 6**,** e27740.

JUNN, E. & MOURADIAN, M. M. 2012. MicroRNAs in neurodegenerative diseases and their therapeutic potential. *Pharmacol Ther,* 133**,** 142-50.

JUSTINIANO, S. E., ELAVAZHAGAN, S., FATEHCHAND, K., SHAH, P., MEHTA, P., RODA, J. M., MO, X., CHENEY, C., HERTLEIN, E., EUBANK, T. D., MARSH, C., MUTHUSAMY, N., BUTCHAR, J. P., BYRD, J. C. & TRIDANDAPANI, S. 2013. Fcγ receptor-induced soluble vascular endothelial growth factor receptor-1 (VEGFR-1) production inhibits angiogenesis and enhances efficacy of anti-tumor antibodies. *The Journal of biological chemistry,* 288**,** 26800-26809.

KAARTOKALLIO, T., KLEMETTI, M. M., TIMONEN, A., UOTILA, J., HEINONEN, S., KAJANTIE, E., KERE, J., KIVINEN, K., POUTA, A., LAKKISTO, P. & LAIVUORI, H. 2014. Microsatellite polymorphism in the heme oxygenase-1 promoter is associated with nonsevere and late-onset preeclampsia. *Hypertension,* 64**,** 172-7.

KAARTOKALLIO, T., UTGE, S., KLEMETTI, M. M., PAANANEN, J., PULKKI, K., ROMPPANEN, J., TIKKANEN, I., HEINONEN, S., KAJANTIE, E., KERE, J., KIVINEN, K., POUTA, A., LAKKISTO, P. & LAIVUORI, H. 2018. Fetal Microsatellite in the Heme Oxygenase 1 Promoter Is Associated With Severe and Early-Onset Preeclampsia. *Hypertension,* 71**,** 95-102.

KAITU'U-LINO, T. J., HASTIE, R., CANNON, P., LEE, S., STOCK, O., HANNAN, N. J., HISCOCK, R. & TONG, S. 2014. Stability of absolute copy number of housekeeping genes in preeclamptic and normal placentas, as measured by digital PCR. *Placenta,* 35**,** 1106-1109.

KAITU'U-LINO, T. J., PATTISON, S., YE, L., TUOHEY, L., SLUKA, P., MACDIARMID, J., BRAHMBHATT, H., JOHNS, T., HORNE, A. W., BROWN, J. & TONG, S. 2013. Targeted Nanoparticle Delivery of Doxorubicin Into Placental Tissues to Treat Ectopic Pregnancies. *Endocrinology,* 154**,** 911-919.

KARKKAINEN, M. J. & PETROVA, T. V. 2000. Vascular endothelial growth factor receptors in the regulation of angiogenesis and lymphangiogenesis. *Oncogene,* 19**,** 5598-5605.

KATORI, M., ANSELMO, D. M., BUSUTTIL, R. W. & KUPIEC-WEGLINSKI, J. W. 2002. A novel strategy against ischemia and reperfusion injury: cytoprotection with heme oxygenase system. *Transpl Immunol,* 9**,** 227-33.

KAZMIN, A., GARCIA-BOURNISSEN, F. & KOREN, G. 2007. Risks of statin use during pregnancy: a systematic review. *J Obstet Gynaecol Can,* 29**,** 906-908.

KENDALL, R. L. & THOMAS, K. A. 1993. Inhibition of vascular endothelial cell growth factor activity by an endogenously encoded soluble receptor. *Proc Natl Acad Sci U S A,* 90**,** 10705-9.

KENDALL, R. L., WANG, G. & THOMAS, K. A. 1996. Identification of a natural soluble form of the vascular endothelial growth factor receptor, FLT-1, and its heterodimerization with KDR. *Biochem Biophys Res Commun,* 226**,** 324-8.

KENIRY, A., OXLEY, D., MONNIER, P., KYBA, M., DANDOLO, L., SMITS, G. & REIK, W. 2012. The H19 lincRNA is a developmental reservoir of miR-675 that suppresses growth and Igf1r. *Nature Cell Biology,* 14**,** 659-665.

KEYSE, S. M. & TYRRELL, R. M. 1989. Heme oxygenase is the major 32-kDa stress protein induced in human skin fibroblasts by UVA radiation, hydrogen peroxide, and sodium arsenite. *Proc Natl Acad Sci U S A,* 86**,** 99-103.

KHAN, K. S., WOJDYLA, D., SAY, L., GÜLMEZOGLU, A. M. & VAN LOOK, P. F. A. 2006. WHO analysis of causes of maternal death: a systematic review. *The Lancet,* 367**,** 1066-1074.

KIM, D. H. & ROSSI, J. J. 2007. Strategies for silencing human disease using RNA interference. *Nat Rev Genet,* 8**,** 173-84.

KIM, V. N. & NAM, J. W. 2006. Genomics of microRNA. *Trends Genet,* 22**,** 165-73.

KIM, Y.-M., PAE, H.-O., PARK, J. E., LEE, Y. C., WOO, J. M., KIM, N.-H., CHOI, Y. K., LEE, B.-S., KIM, S. R. & CHUNG, H.-T. 2011. Heme oxygenase in the regulation of vascular biology: from molecular mechanisms to therapeutic opportunities. *Antioxidants & redox signaling,* 14**,** 137-167.

KIMBALL, K. J., PREUSS, M. A., BARNES, M. N., WANG, M., SIEGAL, G. P., WAN, W., KUO, H., SADDEKNI, S., STOCKARD, C. R., GRIZZLE, W. E., HARRIS, R. D., AURIGEMMA, R., CURIEL, D. T. & ALVAREZ, R. D. 2010. A phase I study of a tropism-modified conditionally replicative adenovirus for recurrent malignant gynecologic diseases. *Clinical cancer research : an official journal of the American Association for Cancer Research,* 16**,** 5277-5287.

KING, A., NDIFON, C., LUI, S., WIDDOWS, K., KOTAMRAJU, V. R., AGEMY, L., TEESALU, T., GLAZIER, J. D., CELLESI, F., TIRELLI, N., APLIN, J. D., RUOSLAHTI, E. & HARRIS, L. K. 2016. Tumor-homing peptides as tools for targeted delivery of payloads to the placenta. *Science Advances,* 2**,** e1600349.

KLEINROUWELER, C. E., VAN UITERT, M., MOERLAND, P. D., RIS-STALPERS, C., VAN DER POST, J. A. M. & AFINK, G. B. 2013. Differentially Expressed Genes in the Pre-Eclamptic Placenta: A Systematic Review and Meta-Analysis. *Plos One,* 8.

KOGA, K., OSUGA, Y., TAJIMA, T., HIROTA, Y., IGARASHI, T., FUJII, T., YANO, T. & TAKETANI, Y. 2010. Elevated serum soluble fms-like tyrosine kinase 1 (sFlt1) level in women with hydatidiform mole. *Fertility and Sterility,* 94**,** 305-308.

KOGA, K., OSUGA, Y., YOSHINO, O., HIROTA, Y., RUIMENG, X., HIRATA, T., TAKEDA, S., YANO, T., TSUTSUMI, O. & TAKETANI, Y. 2003. Elevated Serum Soluble Vascular Endothelial Growth Factor Receptor 1 (sVEGFR-1) Levels in Women with Preeclampsia. *The Journal of Clinical Endocrinology & Metabolism,* 88**,** 2348-2351.

KOO, K. H. & KWON, H. 2018. MicroRNA miR-4779 suppresses tumor growth by inducing apoptosis and cell cycle arrest through direct targeting of PAK2 and CCND3. *Cell death & disease,* 9**,** 77-77.

KOPRIVA, S. E., CHIASSON, V. L., MITCHELL, B. M. & CHATTERJEE, P. 2013. TLR3-induced placental miR-210 down-regulates the STAT6/interleukin-4 pathway. *PLoS One,* 8**,** e67760.

KORKES, H. A., DE OLIVEIRA, L., SASS, N., SALAHUDDIN, S., KARUMANCHI, S. A. & RAJAKUMAR, A. 2017. Relationship between hypoxia and downstream pathogenic pathways in preeclampsia. *Hypertens Pregnancy,* 36**,** 145-150.

KOURI, F. M., HURLEY, L. A., DANIEL, W. L., DAY, E. S., HUA, Y., HAO, L., PENG, C. Y., MERKEL, T. J., QUEISSER, M. A., RITNER, C., ZHANG, H., JAMES, C. D., SZNAJDER, J. I., CHIN, L., GILJOHANN, D. A., KESSLER, J. A., PETER, M. E., MIRKIN, C. A. & STEGH, A. H. 2015. miR-182 integrates apoptosis, growth, and differentiation programs in glioblastoma. *Genes Dev,* 29**,** 732-45.

KOZAKOWSKA, M., CIESLA, M., STEFANSKA, A., SKRZYPEK, K., WAS, H., JAZWA, A., GROCHOT-PRZECZEK, A., KOTLINOWSKI, J., SZYMULA, A., BARTELIK, A., MAZAN, M., YAGENSKY, O., FLORCZYK, U., LEMKE, K., ZEBZDA, A., DYDUCH, G., NOWAK, W., SZADE, K., STEPNIEWSKI, J., MAJKA, M., DERLACZ, R., LOBODA, A., DULAK, J. & JOZKOWICZ, A. 2012. Heme oxygenase-1 inhibits myoblast differentiation by targeting myomirs. *Antioxidants & redox signaling,* 16**,** 113-127.

KOZAKOWSKA, M., SZADE, K., DULAK, J. & JOZKOWICZ, A. 2014. Role of heme oxygenase-1 in postnatal differentiation of stem cells: a possible cross-talk with microRNAs. *Antioxidants & redox signaling,* 20**,** 1827-1850.

KREISER, D., BAUM, M., SEIDMAN, D. S., FANAROFF, A., SHAH, D., HENDLER, I., STEVENSON, D. K., SCHIFF, E. & DRUZIN, M. L. 2004. End tidal carbon monoxide levels are lower in women with gestational hypertension and pre-eclampsia. *J Perinatol,* 24**,** 213-7.

KREISER, D., NGUYEN, X., WONG, R., SEIDMAN, D., STEVENSON, D., QUAN, S., ABRAHAM, N. & DENNERY, P. A. 2002. Heme Oxygenase-1 Modulates Fetal Growth in the Rat. *Laboratory Investigation,* 82**,** 687-692.

KROL, J., LOEDIGE, I. & FILIPOWICZ, W. 2010. The widespread regulation of microRNA biogenesis, function and decay. *Nat Rev Genet,* 11**,** 597-610.

KRÖNKE, G., KADL, A., IKONOMU, E., BLÜML, S., FÜRNKRANZ, A., SAREMBOCK IAN, J., BOCHKOV VALERY, N., EXNER, M., BINDER BERND, R. & LEITINGER, N. 2007. Expression of Heme Oxygenase-1 in Human Vascular Cells Is Regulated by Peroxisome Proliferator-Activated Receptors. *Arteriosclerosis, Thrombosis, and Vascular Biology,* 27**,** 1276-1282.

KRUTZFELDT, J. 2016. Strategies to use microRNAs as therapeutic targets. *Best Practice & Research Clinical Endocrinology & Metabolism,* 30**,** 551-561.

KUHNERT, F., MANCUSO, M. R., HAMPTON, J., STANKUNAS, K., ASANO, T., CHEN, C. Z. & KUO, C. J. 2008. Attribution of vascular phenotypes of the murine Egfl7 locus to the microRNA miR-126. *Development,* 135**,** 3989-93.

KULLBERG, G., LINDEBERG, S. & HANSON, U. 2002. Eclampsia in Sweden. *Hypertens Pregnancy,* 21**,** 13-21.

KULSHRESHTHA, R., FERRACIN, M., WOJCIK, S. E., GARZON, R., ALDER, H., AGOSTO-PEREZ, F. J., DAVULURI, R., LIU, C.-G., CROCE, C. M., NEGRINI, M., CALIN, G. A. & IVAN, M. 2007. A microRNA signature of hypoxia. *Molecular and cellular biology,* 27**,** 1859-1867.

KUMAR, M. S., ERKELAND, S. J., PESTER, R. E., CHEN, C. Y., EBERT, M. S., SHARP, P. A. & JACKS, T. 2008. Suppression of non-small cell lung tumor development by the let-7 microRNA family. *Proc Natl Acad Sci U S A,* 105**,** 3903-8.

KUMAR, P., LUO, Y., TUDELA, C., ALEXANDER, J. M. & MENDELSON, C. R. 2013. The c-Myc-regulated microRNA-17~92 (miR-17~92) and miR-106a~363 clusters target hCYP19A1 and hGCM1 to inhibit human trophoblast differentiation. *Mol Cell Biol,* 33**,** 1782-96.

KUMASAWA, K., IKAWA, M., KIDOYA, H., HASUWA, H., SAITO-FUJITA, T., MORIOKA, Y., TAKAKURA, N., KIMURA, T. & OKABE, M. 2011. Pravastatin induces placental growth factor (PGF) and ameliorates preeclampsia in a mouse model. *Proc Natl Acad Sci U S A,* 108**,** 1451-5.

KUNTE, D. P., DELACRUZ, M., WALI, R. K., MENON, A., DU, H., STYPULA, Y., PATEL, A., BACKMAN, V. & ROY, H. K. 2012. Dysregulation of microRNAs in colonic field carcinogenesis: implications for screening. *PLoS One,* 7**,** e45591.

KUPFERMINC, M. J., DANIEL, Y., ENGLENDER, T., BARAM, A., MANY, A., JAFFA, A. J., GULL, I. & LESSING, J. B. 1997. Vascular endothelial growth factor is increased in patients with preeclampsia. *Am J Reprod Immunol,* 38**,** 302-6.

KUTAY, H., BAI, S., DATTA, J., MOTIWALA, T., POGRIBNY, I., FRANKEL, W., JACOB, S. T. & GHOSHAL, K. 2006. Downregulation of miR-122 in the rodent and human hepatocellular carcinomas. *Journal of cellular biochemistry,* 99**,** 671-678.

KYRMIZI, I., HATZIS, P., KATRAKILI, N., TRONCHE, F., GONZALEZ, F. J. & TALIANIDIS, I. 2006. Plasticity and expanding complexity of the hepatic transcription factor network during liver development. *Genes Dev,* 20**,** 2293-305.

LAM, J. K. W., CHOW, M. Y. T., ZHANG, Y. & LEUNG, S. W. S. 2015. siRNA Versus miRNA as Therapeutics for Gene Silencing. *Molecular therapy. Nucleic acids,* 4**,** e252-e252.

LANDEN, C. N., CHAVEZ-REYES, A., BUCANA, C., SCHMANDT, R., DEAVERS, M. T., LOPEZ-BERESTEIN, G. & SOOD, A. K. 2005. Therapeutic EphA2 Gene Targeting In vivo Using Neutral Liposomal Small Interfering RNA Delivery. *Cancer Research,* 65**,** 6910-6918.

LANDGRAF, P., RUSU, M., SHERIDAN, R., SEWER, A., IOVINO, N., ARAVIN, A., PFEFFER, S., RICE, A., KAMPHORST, A. O., LANDTHALER, M., LIN, C., SOCCI, N. D., HERMIDA,

L., FULCI, V., CHIARETTI, S., FOÀ, R., SCHLIWKA, J., FUCHS, U., NOVOSEL, A., MÜLLER, R. U., SCHERMER, B., BISSELS, U., INMAN, J., PHAN, Q., CHIEN, M., WEIR, D. B., CHOKSI, R., DE VITA, G., FREZZETTI, D., TROMPETER, H. I., HORNUNG, V., TENG, G., HARTMANN, G., PALKOVITS, M., DI LAURO, R., WERNET, P., MACINO, G., ROGLER, C. E., NAGLE, J. W., JU, J., PAPAVASILIOU, F. N., BENZING, T., LICHTER, P., TAM, W., BROWNSTEIN, M. J., BOSIO, A., BORKHARDT, A., RUSSO, J. J., SANDER, C., ZAVOLAN, M. & TUSCHL, T. 2007. A mammalian microRNA expression atlas based on small RNA library sequencing. *Cell,* 129**,** 1401-14.

LANFORD, R. E., HILDEBRANDT-ERIKSEN, E. S., PETRI, A., PERSSON, R., LINDOW, M., MUNK, M. E., KAUPPINEN, S. & ØRUM, H. 2010. Therapeutic silencing of microRNA-122 in primates with chronic hepatitis C virus infection. *Science,* 327**,** 198-201.

LAOUINI, A., JAAFAR-MAALEJ, C., LIMAYEM-BLOUZA, I., SFAR, S., CHARCOSSET, C. & FESSI, H. 2012. Preparation, characterization and applications of liposomes: state of the art. *Journal of colloid Science and Biotechnology,* 1**,** 147-168.

LASABOVÁ, Z., VAZAN, M., ZIBOLENOVA, J. & SVECOVA, I. 2015. Overexpression of miR-21 and miR-122 in preeclamptic placentas. *Neuro Endocrinol Lett,* 36**,** 695-9.

LASH, G. E., MCLAUGHLIN, B. E., MACDONALD-GOODFELLOW, S. K., SMITH, G. N., BRIEN, J. F., MARKS, G. S., NAKATSU, K. & GRAHAM, C. H. 2003. Relationship between tissue damage and heme oxygenase expression in chorionic villi of term human placenta. *Am J Physiol Heart Circ Physiol,* 284**,** H160-7.

LAUDADIO, I., MANFROID, I., ACHOURI, Y., SCHMIDT, D., WILSON, M. D., CORDI, S., THORREZ, L., KNOOPS, L., JACQUEMIN, P., SCHUIT, F., PIERREUX, C. E., ODOM, D. T., PEERS, B. & LEMAIGRE, F. P. 2012. A feedback loop between the liver-enriched transcription factor network and miR-122 controls hepatocyte differentiation. *Gastroenterology,* 142**,** 119-29.

LAVILLA-ALONSO, S., BAUERSCHMITZ, G., ABO-RAMADAN, U., HALAVAARA, J., ESCUTENAIRE, S., DIACONU, I., TATLISUMAK, T., KANERVA, A., HEMMINKI, A. & PESONEN, S. 2010. Adenoviruses with an αvβ integrin targeting moiety in the fiber shaft or the HI-loop increase tumor specificity without compromising antitumor efficacy in magnetic resonance imaging of colorectal cancer metastases. *Journal of translational medicine,* 8**,** 80-80.

LAYZER, J. M., MCCAFFREY, A. P., TANNER, A. K., HUANG, Z., KAY, M. A. & SULLENGER, B. A. 2004. In vivo activity of nuclease-resistant siRNAs. *RNA (New York, N.Y.),* 10**,** 766-771.

LEE, D. C., ROMERO, R., KIM, J. S., TARCA, A. L., MONTENEGRO, D., PINELES, B. L., KIM, E., LEE, J., KIM, S. Y., DRAGHICI, S., MITTAL, P., KUSANOVIC, J. P., CHAIWORAPONGSA, T., HASSAN, S. S. & KIM, C. J. 2011. miR-210 targets iron-sulfur cluster scaffold homologue in human trophoblast cell lines: siderosis of interstitial trophoblasts as a novel pathology of preterm preeclampsia and small-for-gestational-age pregnancies. *Am J Pathol,* 179**,** 590-602.

LEE, S. W. L., PAOLETTI, C., CAMPISI, M., OSAKI, T., ADRIANI, G., KAMM, R. D., MATTU, C. & CHIONO, V. 2019. MicroRNA delivery through nanoparticles. *Journal of Controlled Release,* 313**,** 80-95.

LEE, T. S., CHANG, C. C., ZHU, Y. & SHYY, J. Y. 2004a. Simvastatin induces heme oxygenase-1: a novel mechanism of vessel protection. *Circulation,* 110**,** 1296-302.

LEE, Y., AHN, C., HAN, J., CHOI, H., KIM, J., YIM, J., LEE, J., PROVOST, P., RÅDMARK, O., KIM, S. & KIM, V. N. 2003. The nuclear RNase III Drosha initiates microRNA processing. *Nature,* 425**,** 415-419.

LEE, Y., KIM, M., HAN, J., YEOM, K.-H., LEE, S., BAEK, S. H. & KIM, V. N. 2004b. MicroRNA genes are transcribed by RNA polymerase II. *The EMBO journal,* 23**,** 4051-4060.

LEFKOU, E., MAMOPOULOS, A., DAGKLIS, T., VOSNAKIS, C., ROUSSO, D. & GIRARDI, G. 2016. Pravastatin improves pregnancy outcomes in obstetric antiphospholipid syndrome refractory to antithrombotic therapy. *The Journal of clinical investigation,* 126**,** 2933-2940.

LEVINE, R. J. & KARUMANCHI, S. A. 2005. Circulating angiogenic factors in preeclampsia. *Clin Obstet Gynecol,* 48**,** 372-86.

LEVINE, R. J., LAM, C., QIAN, C., YU, K. F., MAYNARD, S. E., SACHS, B. P., SIBAI, B. M., EPSTEIN, F. H., ROMERO, R., THADHANI, R. & KARUMANCHI, S. A. 2006. Soluble endoglin and other circulating antiangiogenic factors in preeclampsia. *N Engl J Med,* 355**,** 992-1005.

LEVINE , R. J., MAYNARD , S. E., QIAN , C., LIM , K.-H., ENGLAND , L. J., YU , K. F., SCHISTERMAN , E. F., THADHANI , R., SACHS , B. P., EPSTEIN , F. H., SIBAI , B. M., SUKHATME , V. P. & KARUMANCHI , S. A. 2004. Circulating Angiogenic Factors and the Risk of Preeclampsia. *New England Journal of Medicine,* 350**,** 672-683.

LEWIS, B. P., BURGE, C. B. & BARTEL, D. P. 2005. Conserved Seed Pairing, Often Flanked by Adenosines, Indicates that Thousands of Human Genes are MicroRNA Targets. *Cell,* 120**,** 15-20.

LI, D., GUANG, W., ABUZEID, W. M., ROY, S., GAO, G. P., SAUK, J. J. & O'MALLEY, B. W., JR. 2008. Novel adenoviral gene delivery system targeted against head and neck cancer. *Laryngoscope,* 118**,** 650-8.

LI, H., GE, Q., GUO, L. & LU, Z. 2013. Maternal plasma miRNAs expression in preeclamptic pregnancies. *Biomed Res Int,* 2013**,** 970265.

LI, J., WANG, X., ZHANG, T., WANG, C., HUANG, Z., LUO, X. & DENG, Y. 2015a. A review on phospholipids and their main applications in drug delivery systems. *Asian Journal of Pharmaceutical Sciences,* 10**,** 81-98.

LI, L., YANG, H., CHEN, P., XIN, T., ZHOU, Q., WEI, D., ZHANG, Y. & WANG, S. 2020. Trophoblast-Targeted Nanomedicine Modulates Placental sFLT1 for Preeclampsia Treatment. *Frontiers in bioengineering and biotechnology,* 8**,** 64-64.

LI, M., LI, Z., SUN, X., YANG, L., FANG, P., LIU, Y., LI, W., XU, J., LU, J., XIE, M. & ZHANG, D. 2010. Heme oxygenase-1/p21WAF1 mediates peroxisome proliferator-

activated receptor-gamma signaling inhibition of proliferation of rat pulmonary artery smooth muscle cells. *Febs j,* 277**,** 1543-50.

LI, Q., LONG, A., JIANG, L., CAI, L., XIE, L. I., GU, J. A., CHEN, X. & TAN, L. 2015b. Quantification of preeclampsia-related microRNAs in maternal serum. *Biomedical reports,* 3**,** 792-796.

LI, T., WU, M., ZHU, Y. Y., CHEN, J. & CHEN, L. 2014a. Development of RNA interference-based therapeutics and application of multi-target small interfering RNAs. *Nucleic Acid Ther,* 24**,** 302-12.

LI, X., LI, C., DONG, X. & GOU, W. 2014b. MicroRNA-155 inhibits migration of trophoblast cells and contributes to the pathogenesis of severe preeclampsia by regulating endothelial nitric oxide synthase. *Mol Med Rep,* 10**,** 550-4.

LI, Y., REN, Q., ZHU, L., LI, Y., LI, J., ZHANG, Y., ZHENG, G., HAN, T., SUN, S. & FENG, F. 2018. Involvement of methylation of MicroRNA-122, -125b and -106b in regulation of Cyclin G1, CAT-1 and STAT3 target genes in isoniazid-induced liver injury. *BMC pharmacology & toxicology,* 19**,** 11-11.

LI, Z., ZHANG, Y., YING MA, J., KAPOUN, A. M., SHAO, Q., KERR, I., LAM, A., O'YOUNG, G., SANNAJUST, F., STATHIS, P., SCHREINER, G., KARUMANCHI, S. A., PROTTER, A. A. & POLLITT, N. S. 2007. Recombinant vascular endothelial growth factor 121 attenuates hypertension and improves kidney damage in a rat model of preeclampsia. *Hypertension,* 50**,** 686-92.

LIAN, I. A., LØSET, M., MUNDAL, S. B., FENSTAD, M. H., JOHNSON, M. P., EIDE, I. P., BJØRGE, L., FREED, K. A., MOSES, E. K. & AUSTGULEN, R. 2011. Increased endoplasmic reticulum stress in decidual tissue from pregnancies complicated by fetal growth restriction with and without pre-eclampsia. *Placenta,* 32**,** 823-829.

LIANG, G., ZHU, Y., JING, A., WANG, J., HU, F., FENG, W., XIAO, Z. & CHEN, B. 2016. Cationic microRNA-delivering nanocarriers for efficient treatment of colon carcinoma in xenograft model. *Gene therapy,* 23**,** 829-838.

LIANG, H., LIU, Y. & ZEN, K. 2017. The miR-122 released by hepatocytes during liver disease binds to TLR7 to promote lung dysfunction. *The Journal of Immunology,* 198**,** 55.29.

LIM, L. P., LAU, N. C., GARRETT-ENGELE, P., GRIMSON, A., SCHELTER, J. M., CASTLE, J., BARTEL, D. P., LINSLEY, P. S. & JOHNSON, J. M. 2005. Microarray analysis shows that some microRNAs downregulate large numbers of target mRNAs. *Nature,* 433**,** 769-73.

LINZKE, N., SCHUMACHER, A., WOIDACKI, K., CROY, B. A. & ZENCLUSSEN, A. C. 2014. Carbon monoxide promotes proliferation of uterine natural killer cells and remodeling of spiral arteries in pregnant hypertensive heme oxygenase-1 mutant mice. *Hypertension,* 63**,** 580-8.

LIU, X., LI, G., SU, Z., JIANG, Z., CHEN, L., WANG, J., YU, S. & LIU, Z. 2013. Poly(amido amine) is an ideal carrier of miR-7 for enhancing gene silencing effects on the EGFR pathway in U251 glioma cells. *Oncol Rep,* 29**,** 1387-1394.

LIU, Y. P., VINK, M. A., WESTERINK, J. T., RAMIREZ DE ARELLANO, E., KONSTANTINOVA, P., TER BRAKE, O. & BERKHOUT, B. 2010. Titers of lentiviral vectors encoding shRNAs and miRNAs are reduced by different mechanisms that require distinct repair strategies. *Rna,* 16**,** 1328-39.

LOICHINGER, M. H., TOWNER, D., THOMPSON, K. S., AHN, H. J. & BRYANT-GREENWOOD, G. D. 2016. Systemic and placental α-klotho: Effects of preeclampsia in the last trimester of gestation. *Placenta,* 41**,** 53-61.

LOU, W., CHEN, Q., MA, L., LIU, J., YANG, Z., SHEN, J., CUI, Y., BIAN, X. W. & QIAN, C. 2013. Oncolytic adenovirus co-expressing miRNA-34a and IL-24 induces superior antitumor activity in experimental tumor model. *J Mol Med (Berl),* 91**,** 715-25.

LU, T., LIN, Z., REN, J., YAO, P., WANG, X., WANG, Z. & ZHANG, Q. 2016. The Non-Specific Binding of Fluorescent-Labeled MiRNAs on Cell Surface by Hydrophobic Interaction. *PloS one,* 11**,** e0149751-e0149751.

LUND, E., GUTTINGER, S., CALADO, A., DAHLBERG, J. E. & KUTAY, U. 2004. Nuclear export of microRNA precursors. *Science,* 303**,** 95-8.

LV, H., ZHANG, S., WANG, B., CUI, S. & YAN, J. 2006. Toxicity of cationic lipids and cationic polymers in gene delivery. *Journal of controlled release,* 114**,** 100-109.

LYALL, F., BARBER, A., MYATT, L., BULMER, J. N. & ROBSON, S. C. 2000. Hemeoxygenase expression in human placenta and placental bed implies a role in regulation of trophoblast invasion and placental function. *Faseb j,* 14**,** 208-19.

LYALL, F., ROBSON, S. C. & BULMER, J. N. 2013. Spiral artery remodeling and trophoblast invasion in preeclampsia and fetal growth restriction: relationship to clinical outcome. *Hypertension,* 62**,** 1046-54.

LYKKE-ANDERSEN, K., GILCHRIST, M. J., GRABAREK, J. B., DAS, P., MISKA, E. & ZERNICKA-GOETZ, M. 2008. Maternal Argonaute 2 is essential for early mouse development at the maternal-zygotic transition. *Molecular biology of the cell,* 19**,** 4383-4392.

LYKOUDI, A., KOLIALEXI, A., LAMBROU, G. I., BRAOUDAKI, M., SIRISTATIDIS, C., PAPAIOANOU, G. K., TZETIS, M., MAVROU, A. & PAPANTONIOU, N. 2018. Dysregulated placental microRNAs in Early and Late onset Preeclampsia. *Placenta,* 61**,** 24-32.

MA, L., LIU, J., SHEN, J., LIU, L., WU, J., LI, W., LUO, J., CHEN, Q. & QIAN, C. 2010. Expression of miR-122 mediated by adenoviral vector induces apoptosis and cell cycle arrest of cancer cells. *Cancer Biol Ther,* 9**,** 554-61.

MACK, G. S. 2007. MicroRNA gets down to business. *Nat Biotechnol,* 25**,** 631-8.

MACKAY, A. P., BERG, C. J. & ATRASH, H. K. 2001. Pregnancy-related mortality from preeclampsia and eclampsia. *Obstet Gynecol,* 97**,** 533-8.

MAINES, M. D., MAYER, R. D., EWING, J. F. & MCCOUBREY, W. K. 1993. Induction of kidney heme oxygenase-1 (HSP32) mRNA and protein by ischemia/reperfusion: possible role of heme as both promotor of tissue damage and regulator of HSP32. *Journal of Pharmacology and Experimental Therapeutics,* 264**,** 457.

MAIONE, D., DELLA ROCCA, C., GIANNETTI, P., D'ARRIGO, R., LIBERATOSCIOLI, L., FRANLIN, L. L., SANDIG, V., CILIBERTO, G., LA MONICA, N. & SAVINO, R. 2001. An improved helper-dependent adenoviral vector allows persistent gene expression

after intramuscular delivery and overcomes preexisting immunity to adenovirus. *Proceedings of the National Academy of Sciences of the United States of America,* 98**,** 5986-5991.

MALEK, A., SAGER, R. & SCHNEIDER, H. 1998. Transport of Proteins Across the Human Placenta. *American Journal of Reproductive Immunology,* 40**,** 347-351.

MAMIYA, T., KATSUOKA, F., HIRAYAMA, A., NAKAJIMA, O., KOBAYASHI, A., MAHER, J. M., MATSUI, H., HYODO, I., YAMAMOTO, M. & HOSOYA, T. 2008. Hepatocyte-specific deletion of heme oxygenase-1 disrupts redox homeostasis in basal and oxidative environments. *Tohoku J Exp Med,* 216**,** 331-9.

MANSFIELD, J. H., HARFE, B. D., NISSEN, R., OBENAUER, J., SRINEEL, J., CHAUDHURI, A., FARZAN-KASHANI, R., ZUKER, M., PASQUINELLI, A. E., RUVKUN, G., SHARP, P. A., TABIN, C. J. & MCMANUS, M. T. 2004. MicroRNA-responsive 'sensor' transgenes uncover Hox-like and other developmentally regulated patterns of vertebrate microRNA expression. *Nat Genet,* 36**,** 1079-83.

MARSHALL, E. 1999. Gene therapy death prompts review of adenovirus vector. *Science,* 286**,** 2244-5.

MATEUS, J., BYTAUTIENE, E., LU, F., TAMAYO, E. H., BETANCOURT, A., HANKINS, G. D., LONGO, M. & SAADE, G. R. 2011. Endothelial growth factor therapy improves preeclampsia-like manifestations in a murine model induced by overexpression of sVEGFR-1. *Am J Physiol Heart Circ Physiol,* 301**,** H1781-7.

MATOS, P., HORN, J. A., BEARDS, F., LUI, S., DESFORGES, M. & HARRIS, L. K. 2014. A role for the mitochondrial-associated protein p32 in regulation of trophoblast proliferation. *Mol Hum Reprod,* 20**,** 745-55.

MATTHEWS, K., NOKER, P. E., TIAN, B., GRIMES, S. D., FULTON, R., SCHWEIKART, K., HARRIS, R., AURIGEMMA, R., WANG, M., BARNES, M. N., SIEGAL, G. P., HEMMINKI, A., ZINN, K., CURIEL, D. T. & ALVAREZ, R. D. 2009. Identifying the safety profile of Ad5.SSTR/TK.RGD, a novel infectivity-enhanced bicistronic adenovirus, in anticipation of a phase I clinical trial in patients with recurrent ovarian cancer. *Clin Cancer Res,* 15**,** 4131-7.

MATTICK, J. S. & MAKUNIN, I. V. 2006. Non-coding RNA. *Human Molecular Genetics,* 15**,** R17-R29.

MAURER, N., WONG, K. F., STARK, H., LOUIE, L., MCINTOSH, D., WONG, T., SCHERRER, P., SEMPLE, S. C. & CULLIS, P. R. 2001. Spontaneous Entrapment of Polynucleotides upon Electrostatic Interaction with Ethanol-Destabilized Cationic Liposomes. *Biophysical Journal,* 80**,** 2310-2326.

MAYNARD, S. E., MIN, J.-Y., MERCHAN, J., LIM, K.-H., LI, J., MONDAL, S., LIBERMANN, T. A., MORGAN, J. P., SELLKE, F. W., STILLMAN, I. E., EPSTEIN, F. H., SUKHATME, V. P. & KARUMANCHI, S. A. 2003. Excess placental soluble fms-like tyrosine kinase 1 (sFlt1) may contribute to endothelial dysfunction, hypertension, and proteinuria in preeclampsia. *Journal of Clinical Investigation,* 111**,** 649-658.

MAYOR-LYNN, K., TOLOUBEYDOKHTI, T., CRUZ, A. C. & CHEGINI, N. 2011. Expression profile of microRNAs and mRNAs in human placentas from pregnancies complicated by preeclampsia and preterm labor. *Reprod Sci,* 18**,** 46-56.

MCCARTHY, F. P., DREWLO, S., KINGDOM, J., JOHNS, E. J., WALSH, S. K. & KENNY, L. C. 2011. Peroxisome Proliferator-Activated Receptor-{gamma} as a Potential Therapeutic Target in the Treatment of Preeclampsia. *Hypertension,* 58**,** 280-6.

MCCOUBREY, W. K., JR., HUANG, T. J. & MAINES, M. D. 1997. Isolation and characterization of a cDNA from the rat brain that encodes hemoprotein heme oxygenase-3. *Eur J Biochem,* 247**,** 725-32.

MCDONALD, S. D., MALINOWSKI, A., ZHOU, Q., YUSUF, S. & DEVEREAUX, P. J. 2008. Cardiovascular sequelae of preeclampsia/eclampsia: A systematic review and meta-analyses. *American Heart Journal,* 156**,** 918-930.

MCGEARY, R. P., SZYCZEW, A. J. & TOTH, I. 2003. Biological properties and therapeutic potential of bilirubin. *Mini Rev Med Chem,* 3**,** 253-6.

MCGINNIS, R., STEINTHORSDOTTIR, V., WILLIAMS, N. O., THORLEIFSSON, G., SHOOTER, S., HJARTARDOTTIR, S., BUMPSTEAD, S., STEFANSDOTTIR, L., HILDYARD, L., SIGURDSSON, J. K., KEMP, J. P., SILVA, G. B., THOMSEN, L. C. V., JÄÄSKELÄINEN, T., KAJANTIE, E., CHAPPELL, S., KALSHEKER, N., MOFFETT, A., HIBY, S., LEE, W. K., PADMANABHAN, S., SIMPSON, N. A. B., DOLBY, V. A., STAINES-URIAS, E., ENGEL, S. M., HAUGAN, A., TROGSTAD, L., SVYATOVA, G., ZAKHIDOVA, N., NAJMUTDINOVA, D., LAIVUORI, H., HEINONEN, S., KAJANTIE, E., KERE, J., KIVINEN, K., POUTA, A., MORGAN, L., PIPKIN, F. B., KALSHEKER, N., WALKER, J. J., MACPHAIL, S., KILBY, M., HABIBA, M., WILLIAMSON, C., O'SHAUGHNESSY, K., O'BRIEN, S., CAMERON, A., POSTON, L., MIEDZYBRODZKA, Z., REDMAN, C. W. G., FARRALL, M., CAULFIELD, M., DOMINICZAK, A. F., DOMINICZAK, A. F., GJESSING, H. K., CASAS, J. P., DUDBRIDGE, F., WALKER, J. J., PIPKIN, F. B., THORSTEINSDOTTIR, U., GEIRSSON, R. T., LAWLOR, D. A., IVERSEN, A.-C., MAGNUS, P., LAIVUORI, H., STEFANSSON, K., MORGAN, L., THE, F. C. & THE, G. C. 2017. Variants in the fetal genome near FLT1 are associated with risk of preeclampsia. *Nature Genetics,* 49**,** 1255-1260.

MCKEEMAN, G. C., ARDILL, J. E., CALDWELL, C. M., HUNTER, A. J. & MCCLURE, N. 2004. Soluble vascular endothelial growth factor receptor-1 (sFlt-1) is increased throughout gestation in patients who have preeclampsia develop. *Am J Obstet Gynecol,* 191**,** 1240-6.

MEHENDALE, R., HIBBARD, J., FAZLEABAS, A. & LEACH, R. 2007. Placental angiogenesis markers sFlt-1 and PlGF: response to cigarette smoke. *American Journal of Obstetrics & Gynecology,* 197**,** 363.e1-363.e5.

MEISSNER, J. M., TOPORKIEWICZ, M., CZOGALLA, A., MATUSEWICZ, L., KULICZKOWSKI, K. & SIKORSKI, A. F. 2015. Novel antisense therapeutics delivery systems: In vitro and in vivo studies of liposomes targeted with anti-CD20 antibody. *Journal of Controlled Release,* 220**,** 515-528.

MELLER, M., VADACHKORIA, S., LUTHY, D. A. & WILLIAMS, M. A. 2004. Evaluation of housekeeping genes in placental comparative gene expression studies. *Placenta,* 25**,** A21-A21.

MENEZES, V., MALEK, A. & KEELAN, J. A. 2011. Nanoparticulate drug delivery in pregnancy: placental passage and fetal exposure. *Curr Pharm Biotechnol,* 12**,** 731-42.

MENG CAI, K. W., ASIF AHMED. 2020. *United States Patent US20180050060A1*. United States patent application 15/559815.

MENON, B., GULAPPA, T. & MENON, K. M. 2017. Molecular regulation of LHCGR expression by miR-122 during follicle growth in the rat ovary. *Mol Cell Endocrinol,* 442**,** 81-89.

MEYER, O., KIRPOTIN, D., HONG, K., STERNBERG, B., PARK, J. W., WOODLE, M. C. & PAPAHADJOPOULOS, D. 1998. Cationic liposomes coated with polyethylene glycol as carriers for oligonucleotides. *Journal of Biological Chemistry,* 273**,** 15621-15627.

MICHALAK, M., GROENENDYK, J., SZABO, E., GOLD, L. I. & OPAS, M. 2009. Calreticulin, a multi-process calcium-buffering chaperone of the endoplasmic reticulum. *Biochem J,* 417**,** 651-66.

MILLER, M. T. 1991. Thalidomide embryopathy: a model for the study of congenital incomitant horizontal strabismus. *Transactions of the American Ophthalmological Society,* 89**,** 623-674.

MINAMINO, T., CHRISTOU, H., HSIEH, C.-M., LIU, Y., DHAWAN, V., ABRAHAM, N. G., PERRELLA, M. A., MITSIALIS, S. A. & KOUREMBANAS, S. 2001. Targeted expression of heme oxygenase-1 prevents the pulmonary inflammatory and vascular responses to hypoxia. *Proceedings of the National Academy of Sciences of the United States of America,* 98**,** 8798-8803.

MISHRA, S., YADAV, T. & RANI, V. 2016. Exploring miRNA based approaches in cancer diagnostics and therapeutics. *Critical Reviews in Oncology Hematology,* 98**,** 12-23.

MÖRÖY, T., ETIEMBLE, J., BOUGUELERET, L., HADCHOUEL, M., TIOLLAIS, P. & BUENDIA, M. A. 1989. Structure and expression of hcr, a locus rearranged with c-myc in a woodchuck hepatocellular carcinoma. *Oncogene,* 4**,** 59-65.

MORTON, J. S., LEVASSEUR, J., GANGULY, E., QUON, A., KIRSCHENMAN, R., DYCK, J. R. B., FRASER, G. M. & DAVIDGE, S. T. 2019. Characterisation of the Selective Reduced Uteroplacental Perfusion (sRUPP) Model of Preeclampsia. *Scientific Reports,* 9**,** 9565.

MOUILLET, J.-F., CHU, T. & SADOVSKY, Y. 2011. Expression patterns of placental microRNAs. *Birth defects research. Part A, Clinical and molecular teratology,* 91**,** 737-743.

MUCHOVA, L., WONG, R. J., HSU, M., MORIOKA, I., VITEK, L., ZELENKA, J., SCHRÖDER, H. & STEVENSON, D. K. 2007. Statin treatment increases formation of carbon monoxide and bilirubin in mice: a novel mechanism of in vivo antioxidant protection. *Can J Physiol Pharmacol,* 85**,** 800-10.

MÜLLER-DEILE, J., SCHRÖDER, P., BEVERLY-STAGGS, L., HISS, R., FIEDLER, J., NYSTRÖM, J., THUM, T., HALLER, H. & SCHIFFER, M. 2018. Overexpression of preeclampsia

induced microRNA-26a-5p leads to proteinuria in zebrafish. *Scientific Reports,* 8**,** 3621.

MUNAUT, C., TEBACHE, L., BLACHER, S., NOËL, A., NISOLLE, M. & CHANTRAINE, F. 2016. Dysregulated circulating miRNAs in preeclampsia. *Biomedical reports,* 5**,** 686-692.

MUÑOZ-SÁNCHEZ, J. & CHÁNEZ-CÁRDENAS, M. E. 2014. A Review on Hemeoxygenase-2: Focus on Cellular Protection and Oxygen Response. *Oxidative Medicine and Cellular Longevity,* 2014**,** 604981.

MURALIMANOHARAN, S., MALOYAN, A., MELE, J., GUO, C., MYATT, L. G. & MYATT, L. 2012. MIR-210 modulates mitochondrial respiration in placenta with preeclampsia. *Placenta,* 33**,** 816-823.

MURUGESAN, S. R., AKIYAMA, M., EINFELD, D. A., WICKHAM, T. J. & KING, C. R. 2007. Experimental treatment of ovarian cancers by adenovirus vectors combining receptor targeting and selective expression of tumor necrosis factor. *Int J Oncol,* 31**,** 813-22.

MYLLYNEN, P. K., LOUGHRAN, M. J., HOWARD, C. V., SORMUNEN, R., WALSH, A. A. & VÄHÄKANGAS, K. H. 2008. Kinetics of gold nanoparticles in the human placenta. *Reprod Toxicol,* 26**,** 130-7.

NAIR, J. K., ATTARWALA, H., SEHGAL, A., WANG, Q., ALURI, K., ZHANG, X., GAO, M., LIU, J., INDRAKANTI, R., SCHOFIELD, S., KRETSCHMER, P., BROWN, C. R., GUPTA, S., WILLOUGHBY, J. L. S., BOSHAR, J. A., JADHAV, V., CHARISSE, K., ZIMMERMANN, T., FITZGERALD, K., MANOHARAN, M., RAJEEV, K. G., AKINC, A., HUTABARAT, R. & MAIER, M. A. 2017. Impact of enhanced metabolic stability on pharmacokinetics and pharmacodynamics of GalNAc-siRNA conjugates. *Nucleic Acids Res,* 45**,** 10969-10977.

NAKAMURA, M., SEKIZAWA, A., PURWOSUNU, Y., OKAZAKI, S., FARINA, A., WIBOWO, N., SHIMIZU, H. & OKAI, T. 2009. Cellular mRNA expressions of anti-oxidant factors in the blood of preeclamptic women. *Prenat Diagn,* 29**,** 691-6.

NATIONAL COLLABORATING CENTRE FOR, W. S. & CHILDREN'S, H. 2010. National Institute for Health and Clinical Excellence: Guidance. *Hypertension in Pregnancy: The Management of Hypertensive Disorders During Pregnancy.* London: RCOG Press

Copyright © 2011, Royal College of Obstetricians and Gynaecologists.

NATIONAL GUIDELINE, A. 2019. National Institute for Health and Care Excellence: Clinical Guidelines. *Hypertension in pregnancy: diagnosis and management.* London: National Institute for Health and Care Excellence (UK)

Copyright © NICE 2019.

NAU, H., ZIERER, R., SPIELMANN, H., NEUBERT, D. & GANSAU, C. 1981. A new model for embryotoxicity testing: teratogenicity and pharmacokinetics of valproic acid following constant-rate administration in the mouse using human therapeutic drug and metabolite concentrations. *Life Sci,* 29**,** 2803-14.

NOACK, F., RIBBAT-IDEL, J., THORNS, C., CHIRIAC, A., AXT-FLIEDNER, R., DIEDRICH, K. & FELLER, A. C. 2011. miRNA expression profiling in formalin-fixed and paraffin-embedded placental tissue samples from pregnancies with severe preeclampsia. *J Perinat Med,* 39**,** 267-71.

NOKISALMI, P., PESONEN, S., ESCUTENAIRE, S., SÄRKIOJA, M., RAKI, M., CERULLO, V., LAASONEN, L., ALEMANY, R., ROJAS, J., CASCALLO, M., GUSE, K., RAJECKI, M., KANGASNIEMI, L., HAAVISTO, E., KARIOJA-KALLIO, A., HANNUKSELA, P., OKSANEN, M., KANERVA, A., JOENSUU, T., AHTIAINEN, L. & HEMMINKI, A. 2010. Oncolytic adenovirus ICOVIR-7 in patients with advanced and refractory solid tumors. *Clin Cancer Res,* 16**,** 3035-43.

OBEID, M., PANARETAKIS, T., TESNIERE, A., JOZA, N., TUFI, R., APETOH, L., GHIRINGHELLI, F., ZITVOGEL, L. & KROEMER, G. 2007a. Leveraging the immune system during chemotherapy: moving calreticulin to the cell surface converts apoptotic death from "silent" to immunogenic. *Cancer Res,* 67**,** 7941-4.

OBEID, M., TESNIERE, A., GHIRINGHELLI, F., FIMIA, G. M., APETOH, L., PERFETTINI, J. L., CASTEDO, M., MIGNOT, G., PANARETAKIS, T., CASARES, N., MÉTIVIER, D., LAROCHETTE, N., VAN ENDERT, P., CICCOSANTI, F., PIACENTINI, M., ZITVOGEL, L. & KROEMER, G. 2007b. Calreticulin exposure dictates the immunogenicity of cancer cell death. *Nat Med,* 13**,** 54-61.

OFORI, B., REY, E. & BÉRARD, A. 2007. Risk of congenital anomalies in pregnant users of statin drugs. *British Journal of Clinical Pharmacology,* 64**,** 496-509.

OGAWA, S., OKU, A., SAWANO, A., YAMAGUCHI, S., YAZAKI, Y. & SHIBUYA, M. 1998. A novel type of vascular endothelial growth factor, VEGF-E (NZ-7 VEGF), preferentially utilizes KDR/Flk-1 receptor and carries a potent mitotic activity without heparin-binding domain. *J Biol Chem,* 273**,** 31273-82.

OKADA, Y., OKADA, N., MIZUGUCHI, H., HAYAKAWA, T., NAKAGAWA, S. & MAYUMI, T. 2005. Transcriptional targeting of RGD fiber-mutant adenovirus vectors can improve the safety of suicide gene therapy for murine melanoma. *Cancer Gene Ther,* 12**,** 608-16.

OTTERBEIN, L. E., BACH, F. H., ALAM, J., SOARES, M., TAO LU, H., WYSK, M., DAVIS, R. J., FLAVELL, R. A. & CHOI, A. M. 2000a. Carbon monoxide has anti-inflammatory effects involving the mitogen-activated protein kinase pathway. *Nat Med,* 6**,** 422-8.

OTTERBEIN, L. E., BACH, F. H., ALAM, J., SOARES, M., TAO LU, H., WYSK, M., DAVIS, R. J., FLAVELL, R. A. & CHOI, A. M. K. 2000b. Carbon monoxide has anti-inflammatory effects involving the mitogen-activated protein kinase pathway. *Nature Medicine,* 6**,** 422-428.

PAGE, J. G., TIAN, B., SCHWEIKART, K., TOMASZEWSKI, J., HARRIS, R., BROADT, T., POLLEY-NELSON, J., NOKER, P. E., WANG, M., MAKHIJA, S., AURIGEMMA, R., CURIEL, D. T. & ALVAREZ, R. D. 2007. Identifying the safety profile of a novel infectivity-enhanced conditionally replicative adenovirus, Ad5-delta24-RGD, in anticipation of a phase I trial for recurrent ovarian cancer. *Am J Obstet Gynecol,* 196**,** 389.e1-9; discussion 389.e9-10.

PALMER, K. R., KAITU'U-LINO, T. U. J., HASTIE, R., HANNAN, N. J., YE, L., BINDER, N., CANNON, P., TUOHEY, L., JOHNS, T. G., SHUB, A. & TONG, S. 2015. Placental-Specific sFLT-1 e15a Protein Is Increased in Preeclampsia, Antagonizes Vascular Endothelial Growth Factor Signaling, and Has Antiangiogenic Activity. *Hypertension,* 66**,** 1251.

PALMER, K. R., TONG, S., TUOHEY, L., CANNON, P., YE, L., HANNAN, N. J., BROWNFOOT, F. C., ILLANES, S. E. & KAITU'U-LINO, T. U. J. 2016. Jumonji Domain Containing Protein 6 Is Decreased in Human Preeclamptic Placentas and Regulates sFLT-1 Splice Variant Production1. *Biology of Reproduction,* 94**,** 59, 1-9-59, 1-9.

PAPACONSTANTINOU, I. G., MANTA, A., GAZOULI, M., LYBEROPOULOU, A., LYKOUDIS, P. M., POLYMENEAS, G. & VOROS, D. 2013. Expression of microRNAs in patients with pancreatic cancer and its prognostic significance. *Pancreas,* 42**,** 67-71.

PAPADIMITRIOU, E. & ANTIMISIARIS, S. 2000. Interactions of PC/Chol and PS/Chol Liposomes with Human Cells in Vitro. *Journal of Drug Targeting,* 8**,** 335-351.

PATEL, P., BOYD, C. A. R., JOHNSTON, D. G. & WILLIAMSON, C. 2002. Analysis of GAPDH as a standard for gene expression quantification in human placenta. *Placenta,* 23**,** 697-698.

PATIÑO, T., SORIANO, J., BARRIOS, L., IBÁÑEZ, E. & NOGUÉS, C. 2015. Surface modification of microparticles causes differential uptake responses in normal and tumoral human breast epithelial cells. *Scientific reports,* 5**,** 11371-11371.

PEKÁRIKOVÁ, A., SÁNCHEZ, D., PALOVÁ-JELÍNKOVÁ, L., SIMSOVÁ, M., BENES, Z., HOFFMANOVÁ, I., DRASTICH, P., JANATKOVÁ, I., MOTHES, T., TLASKALOVÁ-HOGENOVÁ, H. & TUCKOVÁ, L. 2010. Calreticulin is a B cell molecular target in some gastrointestinal malignancies. *Clinical and experimental immunology,* 160**,** 215-222.

PETERS, L. R. & RAGHAVAN, M. 2011. Endoplasmic reticulum calcium depletion impacts chaperone secretion, innate immunity, and phagocytic uptake of cells. *Journal of immunology (Baltimore, Md. : 1950),* 187**,** 919-931.

PETRAGLIA, F., LUISI, S., BENEDETTO, C., ZONCA, M., FLORIO, P., CASAROSA, E., VOLPE, A., BERNASCONI, S. & GENAZZANI, A. R. 1997. Changes of dimeric inhibin B levels in maternal serum throughout healthy gestation and in women with gestational diseases. *J Clin Endocrinol Metab,* 82**,** 2991-5.

PHIPPS, E. A., THADHANI, R., BENZING, T. & KARUMANCHI, S. A. 2019. Pre-eclampsia: pathogenesis, novel diagnostics and therapies. *Nature reviews. Nephrology,* 15**,** 275-289.

PIAO, L., ZHANG, M., DATTA, J., XIE, X., SU, T., LI, H., TEKNOS, T. N. & PAN, Q. 2012. Lipid-based nanoparticle delivery of Pre-miR-107 inhibits the tumorigenicity of head and neck squamous cell carcinoma. *Mol Ther,* 20**,** 1261-9.

PIAO, Y., JIANG, H., ALEMANY, R., KRASNYKH, V., MARINI, F. C., XU, J., ALONSO, M. M., CONRAD, C. A., ALDAPE, K. D., GOMEZ-MANZANO, C. & FUEYO, J. 2009. Oncolytic adenovirus retargeted to Delta-EGFR induces selective antiglioma activity. *Cancer gene therapy,* 16**,** 256-265.

PIERING, W. F., GARANCIS, J. G., BECKER, C. G., BERES, J. A. & LEMANN, J., JR. 1993. Preeclampsia related to a functioning extrauterine placenta: report of a case and 25-year follow-up. *Am J Kidney Dis,* 21**,** 310-3.

PIJNENBORG, R., VERCRUYSSE, L. & HANSSENS, M. 2006. The uterine spiral arteries in human pregnancy: facts and controversies. *Placenta,* 27**,** 939-58.

PINELES, B. L., ROMERO, R., MONTENEGRO, D., TARCA, A. L., HAN, Y. M., KIM, Y. M., DRAGHICI, S., ESPINOZA, J., KUSANOVIC, J. P., MITTAL, P., HASSAN, S. S. & KIM, C. J. 2007a. Distinct subsets of microRNAs are expressed differentially in the human placentas of patients with preeclampsia. *Am J Obstet Gynecol,* 196**,** 261 e1-6.

PINELES, B. L., ROMERO, R., MONTENEGRO, D., TARCA, A. L., HAN, Y. M., KIM, Y. M., DRAGHICI, S., ESPINOZA, J., KUSANOVIC, J. P., MITTAL, P., HASSAN, S. S. & KIM, C. J. 2007b. Distinct subsets of microRNAs are expressed differentially in the human placentas of patients with preeclampsia. *American Journal of Obstetrics and Gynecology,* 196**,** 261.e1-261.e6.

POLISENO, L., TUCCOLI, A., MARIANI, L., EVANGELISTA, M., CITTI, L., WOODS, K., MERCATANTI, A., HAMMOND, S. & RAINALDI, G. 2006. MicroRNAs modulate the angiogenic properties of HUVECs. *Blood,* 108**,** 3068-71.

POON, L. C., SHENNAN, A., HYETT, J. A., KAPUR, A., HADAR, E., DIVAKAR, H., MCAULIFFE, F., DA SILVA COSTA, F., VON DADELSZEN, P., MCINTYRE, H. D., KIHARA, A. B., DI RENZO, G. C., ROMERO, R., D'ALTON, M., BERGHELLA, V., NICOLAIDES, K. H. & HOD, M. 2019. The International Federation of Gynecology and Obstetrics (FIGO) initiative on pre-eclampsia: A pragmatic guide for first-trimester screening and prevention. *International Journal of Gynecology & Obstetrics,* 145**,** 1-33.

POSS, K. D. & TONEGAWA, S. 1997a. Heme oxygenase 1 is required for mammalian iron reutilization. *Proceedings of the National Academy of Sciences of the United States of America,* 94**,** 10919-10924.

POSS, K. D. & TONEGAWA, S. 1997b. Reduced stress defense in heme oxygenase 1-deficient cells. *Proceedings of the National Academy of Sciences of the United States of America,* 94**,** 10925-10930.

POWE, C. E., LEVINE, R. J. & KARUMANCHI, S. A. 2011. Preeclampsia, a Disease of the Maternal Endothelium: the role of antiangiogenic factors and implications for later cardiovascular disease. *Circulation,* 123**,** 2856.

PULKKINEN, K., MALM, T., TURUNEN, M., KOISTINAHO, J. & YLÄ-HERTTUALA, S. 2008. Hypoxia induces microRNA miR-210 in vitro and in vivo ephrin-A3 and neuronal pentraxin 1 are potentially regulated by miR-210. *FEBS Lett,* 582**,** 2397-401.

QIU, L., FAN, H., JIN, W., ZHAO, B., WANG, Y., JU, Y., CHEN, L., CHEN, Y., DUAN, Z. & MENG, S. 2010. miR-122-induced down-regulation of HO-1 negatively affects miR-122-mediated suppression of HBV. *Biochemical and Biophysical Research Communications,* 398**,** 771-777.

RADHAKRISHNAN, N., YADAV, S. P., SACHDEVA, A., WADA, T. & YACHIE, A. 2009. Human Heme Oxygenase-1 Deficiency Presenting with Hemolysis, Bleeding, Nephritis, Asplenia and Inflammation. *Blood,* 114**,** 3013-3013.

RAJU, V. S. & MAINES, M. D. 1996. Renal ischemia/reperfusion up-regulates heme oxygenase-1 (HSP32) expression and increases cGMP in rat heart. *Journal of Pharmacology and Experimental Therapeutics,* 277**,** 1814.

RAMMA, W. & AHMED, A. 2011. Is inflammation the cause of pre-eclampsia? *Biochemical Society Transactions,* 39**,** 1619-1627.

RAMMA, W. & AHMED, A. 2014. Therapeutic potential of statins and the induction of heme oxygenase-1 in preeclampsia. *Journal of Reproductive Immunology,* 101–102**,** 153-160.

RAMMA, W., BUHIMSCHI, I. A., ZHAO, G., DULAY, A. T., NAYERI, U. A., BUHIMSCHI, C. S. & AHMED, A. 2012. The elevation in circulating anti-angiogenic factors is independent of markers of neutrophil activation in preeclampsia. *Angiogenesis*.

REDECHA, P., VAN ROOIJEN, N., TORRY, D. & GIRARDI, G. 2009. Pravastatin prevents miscarriages in mice: role of tissue factor in placental and fetal injury. *Blood,* 113**,** 4101-4109.

REDMAN, C. W. 1991. Current topic: pre-eclampsia and the placenta. *Placenta,* 12**,** 301-8.

REIN, D. T., BREIDENBACH, M., WU, H., HAN, T., HAVIV, Y. S., WANG, M., KIRBY, T. O., KAWAKAMI, Y., DALL, P., ALVAREZ, R. D. & CURIEL, D. T. 2004. Gene transfer to cervical cancer with fiber-modified adenoviruses. *Int J Cancer,* 111**,** 698-704.

RESENDE, M., NIELSEN, M. A., DAHLBÄCK, M., DITLEV, S. B., ANDERSEN, P., SANDER, A. F., NDAM, N. T., THEANDER, T. G. & SALANTI, A. 2008. Identification of glycosaminoglycan binding regions in the Plasmodium falciparum encoded placental sequestration ligand, VAR2CSA. *Malar J,* 7**,** 104.

RIEHEMANN, K., SCHNEIDER, S. W., LUGER, T. A., GODIN, B., FERRARI, M. & FUCHS, H. 2009. Nanomedicine—Challenge and Perspectives. *Angewandte Chemie International Edition,* 48**,** 872-897.

ROBERTS, J. M. & COOPER, D. W. 2001. Pathogenesis and genetics of pre-eclampsia. *The Lancet,* 357**,** 53-56.

ROBILLARD, P. Y., HULSEY, T. C., PERIANIN, J., JANKY, E., MIRI, E. H. & PAPIERNIK, E. 1994. Association of pregnancy-induced hypertension with duration of sexual cohabitation before conception. *Lancet,* 344**,** 973-5.

ROBSON, A., HARRIS, L. K., INNES, B. A., LASH, G. E., ALJUNAIDY, M. M., APLIN, J. D., BAKER, P. N., ROBSON, S. C. & BULMER, J. N. 2012. Uterine natural killer cells initiate spiral artery remodeling in human pregnancy. *Faseb j,* 26**,** 4876-85.

ROSSI, M., THIERRY, A., DELBAUVE, S., PREYAT, N., SOARES, M. P., ROUMEGUÈRE, T., LEO, O., FLAMAND, V., LE MOINE, A. & HOUGARDY, J.-M. 2017. Specific expression of heme oxygenase-1 by myeloid cells modulates renal ischemia-reperfusion injury. *Scientific Reports,* 7**,** 197.

ROYBAL, J. D., ZANG, Y., AHN, Y.-H., YANG, Y., GIBBONS, D. L., BAIRD, B. N., ALVAREZ, C., THILAGANATHAN, N., LIU, D. D., SAINTIGNY, P., HEYMACH, J. V., CREIGHTON, C. J. & KURIE, J. M. 2011. miR-200 Inhibits lung adenocarcinoma cell invasion and metastasis by targeting Flt1/VEGFR1. *Molecular cancer research : MCR,* 9**,** 25-35.

RUOSLAHTI, E. 2002. Specialization of tumour vasculature. *Nat Rev Cancer,* 2**,** 83-90.

RUOSLAHTI, E., BHATIA, S. N. & SAILOR, M. J. 2010. Targeting of drugs and nanoparticles to tumors. *J Cell Biol,* 188**,** 759-68.

RUPAIMOOLE, R. & SLACK, F. J. 2017. MicroRNA therapeutics: towards a new era for the management of cancer and other diseases. *Nat Rev Drug Discov,* 16**,** 203-222.

SAAD, A. F., KECHICHIAN, T., YIN, H., SBRANA, E., LONGO, M., WEN, M., TAMAYO, E., HANKINS, G. D. V., SAADE, G. R. & COSTANTINE, M. M. 2014. Effects of Pravastatin on Angiogenic and Placental Hypoxic Imbalance in a Mouse Model of Preeclampsia. *Reproductive Sciences,* 21**,** 138-145.

SABATEL, C., MALVAUX, L., BOVY, N., DEROANNE, C., LAMBERT, V., GONZALEZ, M.-L. A., COLIGE, A., RAKIC, J.-M., NOËL, A., MARTIAL, J. A. & STRUMAN, I. 2011. MicroRNA-21 exhibits antiangiogenic function by targeting RhoB expression in endothelial cells. *PloS one,* 6**,** e16979-e16979.

SALANTI, A., DAHLBÄCK, M., TURNER, L., NIELSEN, M. A., BARFOD, L., MAGISTRADO, P., JENSEN, A. T. R., LAVSTSEN, T., OFORI, M. F., MARSH, K., HVIID, L. & THEANDER, T. G. 2004. Evidence for the involvement of VAR2CSA in pregnancy-associated malaria. *The Journal of experimental medicine,* 200**,** 1197-1203.

SALANTI, A., STAALSOE, T., LAVSTSEN, T., JENSEN, A. T., SOWA, M. P., ARNOT, D. E., HVIID, L. & THEANDER, T. G. 2003. Selective upregulation of a single distinctly structured var gene in chondroitin sulphate A-adhering Plasmodium falciparum involved in pregnancy-associated malaria. *Mol Microbiol,* 49**,** 179-91.

SALATA, O. V. 2004. Applications of nanoparticles in biology and medicine. *Journal of Nanobiotechnology,* 2**,** 3.

SANDRIM, V. C., LUIZON, M. R., PALEI, A. C., TANUS-SANTOS, J. E. & CAVALLI, R. C. 2016. Circulating microRNA expression profiles in pre-eclampsia: evidence of increased miR-885-5p levels. *Bjog,* 123**,** 2120-2128.

SAWANO, A., IWAI, S., SAKURAI, Y., ITO, M., SHITARA, K., NAKAHATA, T. & SHIBUYA, M. 2001. Flt-1, vascular endothelial growth factor receptor 1, is a novel cell surface marker for the lineage of monocyte-macrophages in humans. *Blood,* 97**,** 785-91.

SCHERER, F., ANTON, M., SCHILLINGER, U., HENKE, J., BERGEMANN, C., KRUGER, A., GANSBACHER, B. & PLANK, C. 2002. Magnetofection: enhancing and targeting gene delivery by magnetic force in vitro and in vivo. *Gene Ther,* 9**,** 102-9.

SCHMIDT, A., EIPEL, C., FÜRST, K., SOMMER, N., PAHNKE, J. & PÜTZER, B. M. 2011. Evaluation of systemic targeting of RET oncogene-based MTC with tumor-selective peptide-tagged Ad vectors in clinical mouse models. *Gene Ther,* 18**,** 418-23.

SCHUMACHER, A., WAFULA, P. O., TELES, A., EL-MOUSLEH, T., LINZKE, N., ZENCLUSSEN, M. L., LANGWISCH, S., HEINZE, K., WOLLENBERG, I., CASALIS, P. A., VOLK, H.-D., FEST, S. & ZENCLUSSEN, A. C. 2012. Blockage of heme oxygenase-1 abrogates the protective effect of regulatory T cells on murine pregnancy and promotes the maturation of dendritic cells. *PloS one,* 7**,** e42301-e42301.

SCHWARZ, D. S., HUTVAGNER, G., DU, T., XU, Z., ARONIN, N. & ZAMORE, P. D. 2003. Asymmetry in the assembly of the RNAi enzyme complex. *Cell,* 115**,** 199-208.

SELA, S., ITIN, A., NATANSON-YARON, S., GREENFIELD, C., GOLDMAN-WOHL, D., YAGEL, S. & KESHET, E. 2008. A novel human-specific soluble vascular endothelial growth factor receptor 1: cell-type-specific splicing and implications to vascular endothelial growth factor homeostasis and preeclampsia. *Circ Res,* 102**,** 1566-74.

SENIOR, J. 1987. Fate and behavior of liposomes in vivo: a review of controlling factors. *Critical reviews in therapeutic drug carrier systems,* 3**,** 123-193.

SHAN, H., BAI, X. & CHEN, X. 2008. Angiotensin II induces endothelial cell senescence via the activation of mitogen-activated protein kinases. *Cell Biochemistry and Function,* 26**,** 459-466.

SHARKEY, A. M., CHARNOCKJONES, D. S., BOOCOCK, C. A., BROWN, K. D. & SMITH, S. K. 1993. Expression of Messenger-Rna for Vascular Endothelial Growth-Factor in Human Placenta. *Journal of Reproduction and Fertility,* 99**,** 609-615.

SHARKEY, A. M., COOPER, J. C., BALMFORTH, J. R., MCLAREN, J., CLARK, D. E., CHARNOCK-JONES, D. S., MORRIS, N. H. & SMITH, S. K. 1996. Maternal plasma levels of vascular endothelial growth factor in normotensive pregnancies and in pregnancies complicated by pre-eclampsia. *Eur J Clin Invest,* 26**,** 1182-5.

SHAW, A. R. & SUZUKI, M. 2019. Immunology of Adenoviral Vectors in Cancer Therapy. *Molecular Therapy - Methods & Clinical Development,* 15**,** 418-429.

SHEN, L., LI, Y., LI, R., DIAO, Z., YANY, M., WU, M., SUN, H., YAN, G. & HU, Y. 2018. Placenta-associated serum exosomal miR-155 derived from patients with preeclampsia inhibits eNOS expression in human umbilical vein endothelial cells. *Int J Mol Med,* 41**,** 1731-1739.

SHI, S., HAN, L., DENG, L., ZHANG, Y., SHEN, H., GONG, T., ZHANG, Z. & SUN, X. 2014. Dual drugs (microRNA-34a and paclitaxel)-loaded functional solid lipid nanoparticles for synergistic cancer cell suppression. *Journal of Controlled Release,* 194**,** 228-237.

SHI, S., HAN, L., GONG, T., ZHANG, Z. & SUN, X. 2013. Systemic delivery of microRNA-34a for cancer stem cell therapy. *Angew Chem Int Ed Engl,* 52**,** 3901-5.

SHI, Z., HOU, W., HUA, X., ZHANG, X., LIU, X., WANG, X. & WANG, X. 2012. Overexpression of calreticulin in pre-eclamptic placentas: effect on apoptosis, cell invasion and severity of pre-eclampsia. *Cell Biochem Biophys,* 63**,** 183-9.

SIDLE, E. H., CASSELMAN, R. & SMITH, G. N. 2007. Effect of cigarette smoke on placental antioxidant enzyme expression. *Am J Physiol Regul Integr Comp Physiol,* 293**,** R754-8.

SKRZYPEK, K., TERTIL, M., GOLDA, S., CIESLA, M., WEGLARCZYK, K., COLLET, G., GUICHARD, A., KOZAKOWSKA, M., BOCZKOWSKI, J., WAS, H., GIL, T., KUZDZAL, J., MUCHOVA, L., VITEK, L., LOBODA, A., JOZKOWICZ, A., KIEDA, C. & DULAK, J. 2013. Interplay Between Heme Oxygenase-1 and miR-378 Affects Non-Small Cell Lung Carcinoma Growth, Vascularization, and Metastasis. *Antioxidants & Redox Signaling,* 19**,** 644-660.

SOARES, M. P. & BACH, F. H. 2009. Heme oxygenase-1: from biology to therapeutic potential. *Trends Mol Med,* 15**,** 50-8.

SOARES, S., SOUSA, J., PAIS, A. & VITORINO, C. 2018. Nanomedicine: Principles, Properties, and Regulatory Issues. *Frontiers in chemistry,* 6**,** 360-360.

SOLLWEDEL, A., BERTOJA, A. Z., ZENCLUSSEN, M. L., GERLOF, K., LISEWSKI, U., WAFULA, P., SAWITZKI, B., WOICIECHOWSKY, C., VOLK, H. D. & ZENCLUSSEN, A. C. 2005. Protection from abortion by heme oxygenase-1 up-regulation is associated with increased levels of Bag-1 and neuropilin-1 at the fetal-maternal interface. *J Immunol,* 175**,** 4875-85.

SONG, K., HAN, C., ZHANG, J., LU, D., DASH, S., FEITELSON, M., LIM, K. & WU, T. 2013. Epigenetic regulation of MicroRNA-122 by peroxisome proliferator activated receptor-gamma and hepatitis b virus X protein in hepatocellular carcinoma cells. *Hepatology,* 58**,** 1681-92.

SONG, Y. K. & KIM, C. K. 2006. Topical delivery of low-molecular-weight heparin with surface-charged flexible liposomes. *Biomaterials,* 27**,** 271-80.

SOU, K. 2011. Electrostatics of carboxylated anionic vesicles for improving entrapment capacity. *Chemistry and physics of lipids,* 164**,** 211-215.

STOCKER, R., YAMAMOTO, Y., MCDONAGH, A. F., GLAZER, A. N. & AMES, B. N. 1987. Bilirubin is an antioxidant of possible physiological importance. *Science,* 235**,** 1043-6.

STONE, N. R. H., BICANIC, T., SALIM, R. & HOPE, W. 2016. Liposomal Amphotericin B (AmBisome(®)): A Review of the Pharmacokinetics, Pharmacodynamics, Clinical Experience and Future Directions. *Drugs,* 76**,** 485-500.

SUGAHARA, K. N., TEESALU, T., KARMALI, P. P., KOTAMRAJU, V. R., AGEMY, L., GIRARD, O. M., HANAHAN, D., MATTREY, R. F. & RUOSLAHTI, E. 2009. Tissue-penetrating delivery of compounds and nanoparticles into tumors. *Cancer cell,* 16**,** 510-520.

SUGIMOTO, H., HAMANO, Y., CHARYTAN, D., COSGROVE, D., KIERAN, M., SUDHAKAR, A. & KALLURI, R. 2003. Neutralization of circulating vascular endothelial growth factor (VEGF) by anti-VEGF antibodies and soluble VEGF receptor 1 (sFlt-1) induces proteinuria. *J Biol Chem,* 278**,** 12605-8.

SUN, H. X., ZENG, D. Y., LI, R. T., PANG, R. P., YANG, H., HU, Y. L., ZHANG, Q., JIANG, Y., HUANG, L. Y., TANG, Y. B., YAN, G. J. & ZHOU, J. G. 2012. Essential role of microRNA-155 in regulating endothelium-dependent vasorelaxation by targeting endothelial nitric oxide synthase. *Hypertension,* 60**,** 1407-14.

TACHIBANA, M., HASHINO, M., NISHIDA, T., SHIMIZU, T. & WATARAI, M. 2011. Protective role of heme oxygenase-1 in Listeria monocytogenes-induced abortion. *PloS one,* 6**,** e25046-e25046.

TACHIBANA, M., WATANABE, K., YAMASAKI, Y., SUZUKI, H. & WATARAI, M. 2008. Expression of heme oxygenase-1 is associated with abortion caused by Brucella abortus infection in pregnant mice. *Microb Pathog,* 45**,** 105-9.

TAHGHIGHI, F., PARVANEH, N. & ZIAEE, V. 2019. Post-mortem Diagnosis of Heme Oxygenase-1 Deficiency by Whole Exome Sequencing in an Iranian Child. *International journal of molecular and cellular medicine,* 8**,** 300-307.

TAKESHITA, F., PATRAWALA, L., OSAKI, M., TAKAHASHI, R.-U., YAMAMOTO, Y., KOSAKA, N., KAWAMATA, M., KELNAR, K., BADER, A. G., BROWN, D. & OCHIYA, T. 2010.

Systemic Delivery of Synthetic MicroRNA-16 Inhibits the Growth of Metastatic Prostate Tumors via Downregulation of Multiple Cell-cycle Genes. *Molecular Therapy,* 18**,** 181-187.

TANG, L. C., KWOK, A. C., WONG, A. Y., LEE, Y. Y., SUN, K. O. & SO, A. P. 1997. Critical care in obstetrical patients: an eight-year review. *Chinese medical journal,* 110**,** 936-941.

THADHANI, R., HAGMANN, H., SCHAARSCHMIDT, W., ROTH, B., CINGOEZ, T., KARUMANCHI, S. A., WENGER, J., LUCCHESI, K. J., TAMEZ, H., LINDNER, T., FRIDMAN, A., THOME, U., KRIBS, A., DANNER, M., HAMACHER, S., MALLMANN, P., STEPAN, H. & BENZING, T. 2016. Removal of Soluble Fms-Like Tyrosine Kinase-1 by Dextran Sulfate Apheresis in Preeclampsia. *J Am Soc Nephrol,* 27**,** 903-13.

THADHANI, R., KISNER, T., HAGMANN, H., BOSSUNG, V., NOACK, S., SCHAARSCHMIDT, W., JANK, A., KRIBS, A., CORNELY, O. A., KREYSSIG, C., HEMPHILL, L., RIGBY, A. C., KHEDKAR, S., LINDNER, T. H., MALLMANN, P., STEPAN, H., KARUMANCHI, S. A. & BENZING, T. 2011. Pilot study of extracorporeal removal of soluble fms-like tyrosine kinase 1 in preeclampsia. *Circulation,* 124**,** 940-50.

THOMAS, C. P., ANDREWS, J. I. & LIU, K. Z. 2007. Intronic polyadenylation signal sequences and alternate splicing generate human soluble Flt1 variants and regulate the abundance of soluble Flt1 in the placenta. *Faseb j,* 21**,** 3885-95.

THOMAS, C. P., ANDREWS, J. I., RAIKWAR, N. S., KELLEY, E. A., HERSE, F., DECHEND, R., GOLOS, T. G. & LIU, K. Z. 2009. A Recently Evolved Novel Trophoblast-Enriched Secreted Form of fms-Like Tyrosine Kinase-1 Variant Is Up-Regulated in Hypoxia and Preeclampsia. *The Journal of Clinical Endocrinology and Metabolism,* 94**,** 2524-2530.

THOMAS, C. P., RAIKWAR, N. S., KELLEY, E. A. & LIU, K. Z. 2010. Alternate processing of Flt1 transcripts is directed by conserved cis-elements within an intronic region of FLT1 that reciprocally regulates splicing and polyadenylation. *Nucleic acids research,* 38**,** 5130-5140.

TINKLE, S., MCNEIL, S. E., MÜHLEBACH, S., BAWA, R., BORCHARD, G., BARENHOLZ, Y. C., TAMARKIN, L. & DESAI, N. 2014. Nanomedicines: addressing the scientific and regulatory gap. *Ann N Y Acad Sci,* 1313**,** 35-56.

TIVNAN, A., ORR, W. S., GUBALA, V., NOONEY, R., WILLIAMS, D. E., MCDONAGH, C., PRENTER, S., HARVEY, H., DOMINGO-FERNÁNDEZ, R., BRAY, I. M., PISKAREVA, O., NG, C. Y., LODE, H. N., DAVIDOFF, A. M. & STALLINGS, R. L. 2012. Inhibition of Neuroblastoma Tumor Growth by Targeted Delivery of MicroRNA-34a Using Anti-Disialoganglioside GD2 Coated Nanoparticles. *PLOS ONE,* 7**,** e38129.

TRANG, P., WIGGINS, J. F., DAIGE, C. L., CHO, C., OMOTOLA, M., BROWN, D., WEIDHAAS, J. B., BADER, A. G. & SLACK, F. J. 2011. Systemic Delivery of Tumor Suppressor microRNA Mimics Using a Neutral Lipid Emulsion Inhibits Lung Tumors in Mice. *Molecular Therapy,* 19**,** 1116-1122.

TRANQUILLI, A. L., BROWN, M. A., ZEEMAN, G. G., DEKKER, G. & SIBAI, B. M. 2013. The definition of severe and early-onset preeclampsia. Statements from the International Society for the Study of Hypertension in Pregnancy (ISSHP).

Pregnancy Hypertension: An International Journal of Women's Cardiovascular Health, 3**,** 44-47.

TRANQUILLI, A. L., DEKKER, G., MAGEE, L., ROBERTS, J., SIBAI, B. M., STEYN, W., ZEEMAN, G. G. & BROWN, M. A. 2014. The classification, diagnosis and management of the hypertensive disorders of pregnancy: A revised statement from the ISSHP. *Pregnancy Hypertension: An International Journal of Women's Cardiovascular Health,* 4**,** 97-104.

TREIBER, T., TREIBER, N. & MEISTER, G. 2019. Regulation of microRNA biogenesis and its crosstalk with other cellular pathways. *Nat Rev Mol Cell Biol,* 20**,** 5-20.

TRUPIN, L. S., SIMON, L. P. & ESKENAZI, B. 1996. Change in paternity: a risk factor for preeclampsia in multiparas. *Epidemiology,* 7**,** 240-4.

TSAI, W.-C., HSU, P. W.-C., LAI, T.-C., CHAU, G.-Y., LIN, C.-W., CHEN, C.-M., LIN, C.-D., LIAO, Y.-L., WANG, J.-L., CHAU, Y.-P., HSU, M.-T., HSIAO, M., HUANG, H.-D. & TSOU, A.-P. 2009. MicroRNA-122, a tumor suppressor microRNA that regulates intrahepatic metastasis of hepatocellular carcinoma. *Hepatology,* 49**,** 1571-1582.

TSATSARIS, V., GOFFIN, F., MUNAUT, C., BRICHANT, J.-F. O., PIGNON, M.-R., NOEL, A., SCHAAPS, J.-P., CABROL, D., FRANKENNE, F. & FOIDART, J.-M. 2003. Overexpression of the Soluble Vascular Endothelial Growth Factor Receptor in Preeclamptic Patients: Pathophysiological Consequences. *The Journal of Clinical Endocrinology & Metabolism,* 88**,** 5555-5563.

TUBBERGEN, P., LACHMEIJER, A. M., ALTHUISIUS, S. M., VLAK, M. E., VAN GEIJN, H. P. & DEKKER, G. A. 1999. Change in paternity: a risk factor for preeclampsia in multiparous women? *J Reprod Immunol,* 45**,** 81-8.

TUFI, R., PANARETAKIS, T., BIANCHI, K., CRIOLLO, A., FAZI, B., DI SANO, F., TESNIERE, A., KEPP, O., PATERLINI-BRECHOT, P., ZITVOGEL, L., PIACENTINI, M., SZABADKAI, G. & KROEMER, G. 2008. Reduction of endoplasmic reticulum Ca2+ levels favors plasma membrane surface exposure of calreticulin. *Cell Death & Differentiation,* 15**,** 274-282.

TURANOV, A. A., LO, A., HASSLER, M. R., MAKRIS, A., ASHAR-PATEL, A., ALTERMAN, J. F., COLES, A. H., HARASZTI, R. A., ROUX, L., GODINHO, B., ECHEVERRIA, D., PEARS, S., ILIOPOULOS, J., SHANMUGALINGAM, R., OGLE, R., ZSENGELLER, Z. K., HENNESSY, A., KARUMANCHI, S. A., MOORE, M. J. & KHVOROVA, A. 2018. RNAi modulation of placental sFLT1 for the treatment of preeclampsia. *Nat Biotechnol*.

URA, B., FERIOTTO, G., MONASTA, L., BILEL, S., ZWEYER, M. & CELEGHINI, C. 2014. Potential role of circulating microRNAs as early markers of preeclampsia. *Taiwan J Obstet Gynecol,* 53**,** 232-4.

URBICH, C., KUEHBACHER, A. & DIMMELER, S. 2008. Role of microRNAs in vascular diseases, inflammation, and angiogenesis. *Cardiovasc Res,* 79**,** 581-8.

USHIDA, T., KOTANI, T., TSUDA, H., IMAI, K., NAKANO, T., HIRAKO, S., ITO, Y., LI, H., MANO, Y., WANG, J., MIKI, R., YAMAMOTO, E., IWASE, A., BANDO, Y. K., HIRAYAMA, M., OHNO, K., TOYOKUNI, S. & KIKKAWA, F. 2016. Molecular hydrogen ameliorates several characteristics of preeclampsia in the Reduced

Uterine Perfusion Pressure (RUPP) rat model. *Free Radical Biology and Medicine,* 101**,** 524-533.

UZAN, J., CARBONNEL, M., PICONNE, O., ASMAR, R. & AYOUBI, J.-M. 2011. Pre-eclampsia: pathophysiology, diagnosis, and management. *Vascular Health and Risk Management,* 7**,** 467-474.

VALENSISE, H., VASAPOLLO, B., GAGLIARDI, G. & NOVELLI, G. P. 2008. Early and late preeclampsia: two different maternal hemodynamic states in the latent phase of the disease. *Hypertension,* 52**,** 873-80.

VENDITTI, C. C., CASSELMAN, R., YOUNG, I., KARUMANCHI, S. A. & SMITH, G. N. 2014. Carbon Monoxide Prevents Hypertension and Proteinuria in an Adenovirus sFlt-1 Preeclampsia-Like Mouse Model. *PLOS ONE,* 9**,** e106502.

VUORELA, P., HELSKE, S., HORNIG, C., ALITALO, K., WEICH, H. & HALMESMAKI, E. 2000. Amniotic fluid--soluble vascular endothelial growth factor receptor-1 in preeclampsia. *Obstet Gynecol,* 95**,** 353-7.

WALSH, S. K., ENGLISH, F. A., JOHNS, E. J. & KENNY, L. C. 2009. Plasma-Mediated Vascular Dysfunction in the Reduced Uterine Perfusion Pressure Model of Preeclampsia. *Hypertension,* 54**,** 345.

WANG, H. J., ZHANG, P. J., CHEN, W. J., FENG, D., JIA, Y. H. & XIE, L. X. 2012a. Four serum microRNAs identified as diagnostic biomarkers of sepsis. *J Trauma Acute Care Surg,* 73**,** 850-4.

WANG, S., AURORA, A. B., JOHNSON, B. A., QI, X., MCANALLY, J., HILL, J. A., RICHARDSON, J. A., BASSEL-DUBY, R. & OLSON, E. N. 2008. The endothelial-specific microRNA miR-126 governs vascular integrity and angiogenesis. *Developmental cell,* 15**,** 261-271.

WANG, S., QIU, L., YAN, X., JIN, W., WANG, Y., CHEN, L., WU, E., YE, X., GAO, G. F., WANG, F., CHEN, Y., DUAN, Z. & MENG, S. 2012b. Loss of microRNA 122 expression in patients with hepatitis B enhances hepatitis B virus replication through cyclin G(1) -modulated P53 activity. *Hepatology,* 55**,** 730-41.

WANG, W., FENG, L., ZHANG, H., HACHY, S., SATOHISA, S., LAURENT, L. C., PARAST, M., ZHENG, J. & CHEN, D. B. 2012c. Preeclampsia up-regulates angiogenesis-associated microRNA (i.e., miR-17, -20a, and -20b) that target ephrin-B2 and EPHB4 in human placenta. *J Clin Endocrinol Metab,* 97**,** E1051-9.

WANG, X., LAM, E. K., ZHANG, J., JIN, H. & SUNG, J. J. 2009. MicroRNA-122a functions as a novel tumor suppressor downstream of adenomatous polyposis coli in gastrointestinal cancers. *Biochem Biophys Res Commun,* 387**,** 376-80.

WANG, Y., LIANG, H., JIN, F., YAN, X., XU, G., HU, H., LIANG, G., ZHAN, S., HU, X., ZHAO, Q., LIU, Y., JIANG, Z.-Y., ZHANG, C.-Y., CHEN, X. & ZEN, K. 2019. Injured liver-released miRNA-122 elicits acute pulmonary inflammation via activating alveolar macrophage TLR7 signaling pathway. *Proceedings of the National Academy of Sciences,* 116**,** 6162.

WARD, R. M. 1993. Drug therapy of the fetus. *The Journal of Clinical Pharmacology,* 33**,** 780-789.

WATTS, J. K., DELEAVEY, G. F. & DAMHA, M. J. 2008. Chemically modified siRNA: tools and applications. *Drug Discovery Today,* 13**,** 842-855.

WEBSTER, W. S. & FREEMAN, J. A. D. 2001. Is this drug safe in pregnancy? *Reproductive Toxicology,* 15**,** 619-629.

WICKHAM, T. J., TZENG, E., SHEARS, L. L., 2ND, ROELVINK, P. W., LI, Y., LEE, G. M., BROUGH, D. E., LIZONOVA, A. & KOVESDI, I. 1997. Increased in vitro and in vivo gene transfer by adenovirus vectors containing chimeric fiber proteins. *Journal of virology,* 71**,** 8221-8229.

WILLIAMS, P. J. & BROUGHTON PIPKIN, F. 2011. The genetics of pre-eclampsia and other hypertensive disorders of pregnancy. *Best Pract Res Clin Obstet Gynaecol,* 25**,** 405-17.

WORLD HEALTH ORGANISATION, W. 1988. Geographic variation in the incidence of hypertension in pregnancy. World Health Organization International Collaborative Study of Hypertensive Disorders of Pregnancy. *Am J Obstet Gynecol,* 158**,** 80-3.

WORLD HEALTH ORGANISATION, W. 2005. World Health Report: Make every mother and child count.

WU, L., ZHOU, H., LIN, H., QI, J., ZHU, C., GAO, Z. & WANG, H. 2012. Circulating microRNAs are elevated in plasma from severe preeclamptic pregnancies. *Reproduction,* 143**,** 389-97.

WU, Y., CRAWFORD, M., MAO, Y., LEE, R. J., DAVIS, I. C., ELTON, T. S., LEE, L. J. & NANA-SINKAM, S. P. 2013. Therapeutic Delivery of MicroRNA-29b by Cationic Lipoplexes for Lung Cancer. *Molecular Therapy - Nucleic Acids,* 2**,** e84.

WU, Y., CRAWFORD, M., YU, B., MAO, Y., NANA-SINKAM, S. P. & LEE, L. J. 2011. MicroRNA delivery by cationic lipoplexes for lung cancer therapy. *Mol Pharm,* 8**,** 1381-9.

XU, F., LIAO, J.-Z., XIANG, G.-Y., ZHAO, P.-X., YE, F., ZHAO, Q. & HE, X.-X. 2017. MiR-101 and doxorubicin codelivered by liposomes suppressing malignant properties of hepatocellular carcinoma. *Cancer Medicine,* 6**,** 651-661.

XU, H., HE, J. H., XIAO, Z. D., ZHANG, Q. Q., CHEN, Y. Q., ZHOU, H. & QU, L. H. 2010. Liver-enriched transcription factors regulate microRNA-122 that targets CUTL1 during liver development. *Hepatology,* 52**,** 1431-42.

XU, P., ZHAO, Y., LIU, M., WANG, Y., WANG, H., LI, Y. X., ZHU, X., YAO, Y., WANG, H., QIAO, J., JI, L. & WANG, Y. L. 2014. Variations of microRNAs in human placentas and plasma from preeclamptic pregnancy. *Hypertension,* 63**,** 1276-84.

YACHIE, A., NIIDA, Y., WADA, T., IGARASHI, N., KANEDA, H., TOMA, T., OHTA, K., KASAHARA, Y. & KOIZUMI, S. 1999a. Oxidative stress causes enhanced endothelial cell injury in human heme oxygenase-1 deficiency. *J Clin Invest,* 103**,** 129-35.

YACHIE, A., NIIDA, Y., WADA, T., IGARASHI, N., KANEDA, H., TOMA, T., OHTA, K., KASAHARA, Y. & KOIZUMI, S. 1999b. Oxidative stress causes enhanced endothelial cell injury in human heme oxygenase-1 deficiency. *Journal of Clinical Investigation,* 103**,** 129-135.

YADAV, S. P., THAKKAR, D., KOHLI, S., NIVARGI, S. & RASTOGI, N. 2018. Human Heme-Oxygenase-1 Deficiency Treated Successfully by Matched Sibling Donor Allogeneic Stem Cell Transplant. *Biology of Blood and Marrow Transplantation,* 24**,** S443.

YAMAMOTO, M., IKEZAKI, M., TOUJIMA, S., IWAHASHI, N., MIZOGUCHI, M., NANJO, S., MINAMI, S., IHARA, Y. & INO, K. 2017. Calreticulin Is Involved in Invasion of Human Extravillous Trophoblasts Through Functional Regulation of Integrin β1. *Endocrinology,* 158**,** 3874-3889.

YANG, J., BROWN, M. E., ZHANG, H., MARTINEZ, M., ZHAO, Z., BHUTANI, S., YIN, S., TRAC, D., XI, J. J. & DAVIS, M. E. 2017a. High-throughput screening identifies microRNAs that target Nox2 and improve function after acute myocardial infarction. *American Journal of Physiology-Heart and Circulatory Physiology,* 312**,** H1002-H1012.

YANG, X. & MENG, T. 2019. MicroRNA-431 affects trophoblast migration and invasion by targeting ZEB1 in preeclampsia. *Gene,* 683**,** 225-232.

YANG, X., ZHANG, J. & DING, Y. 2017b. Association of microRNA-155, interleukin 17A, and proteinuria in preeclampsia. *Medicine (Baltimore),* 96**,** e6509.

YANG, Y.-P., CHIEN, Y., CHIOU, G.-Y., CHERNG, J.-Y., WANG, M.-L., LO, W.-L., CHANG, Y.-L., HUANG, P.-I., CHEN, Y.-W., SHIH, Y.-H., CHEN, M.-T. & CHIOU, S.-H. 2012. Inhibition of cancer stem cell-like properties and reduced chemoradioresistance of glioblastoma using microRNA145 with cationic polyurethane-short branch PEI. *Biomaterials,* 33**,** 1462-1476.

YANG, Z., WU, L., ZHU, X., XU, J., JIN, R., LI, G. & WU, F. 2013. MiR-29a modulates the angiogenic properties of human endothelial cells. *Biochemical and biophysical research communications,* 434**,** 143-149.

YAO, X., YOSHIOKA, Y., MORISHIGE, T., ETO, Y., NARIMATSU, S., KAWAI, Y., MIZUGUCHI, H., GAO, J.-Q., MUKAI, Y., OKADA, N. & NAKAGAWA, S. 2011. Tumor vascular targeted delivery of polymer-conjugated adenovirus vector for cancer gene therapy. *Molecular therapy : the journal of the American Society of Gene Therapy,* 19**,** 1619-1625.

YAO, X., YOSHIOKA, Y., MORISHIGE, T., ETO, Y., WATANABE, H., OKADA, Y., MIZUGUCHI, H., MUKAI, Y., OKADA, N. & NAKAGAWA, S. 2009. Systemic administration of a PEGylated adenovirus vector with a cancer-specific promoter is effective in a mouse model of metastasis. *Gene Therapy,* 16**,** 1395-1404.

YAO, X.-L., YOSHIOKA, Y., RUAN, G.-X., CHEN, Y.-Z., MIZUGUCHI, H., MUKAI, Y., OKADA, N., GAO, J.-Q. & NAKAGAWA, S. 2012. Optimization and Internalization Mechanisms of PEGylated Adenovirus Vector with Targeting Peptide for Cancer Gene Therapy. *Biomacromolecules,* 13**,** 2402-2409.

YEKTA, S., SHIH, I. H. & BARTEL, D. P. 2004. MicroRNA-directed cleavage of HOXB8 mRNA. *Science,* 304**,** 594-6.

YI, R., QIN, Y., MACARA, I. G. & CULLEN, B. R. 2003. Exportin-5 mediates the nuclear export of pre-microRNAs and short hairpin RNAs. *Genes & development,* 17**,** 3011-3016.

YIN, H., KANASTY, R. L., ELTOUKHY, A. A., VEGAS, A. J., DORKIN, J. R. & ANDERSON, D. G. 2014. Non-viral vectors for gene-based therapy. *Nat Rev Genet,* 15**,** 541-55.

YOUNG, B. C., LEVINE, R. J. & KARUMANCHI, S. A. 2010. Pathogenesis of Preeclampsia. *Annual Review of Pathology-Mechanisms of Disease,* 5**,** 173-192.

ZENCLUSSEN, M. L., ANEGON, I., BERTOJA, A. Z., CHAUVEAU, C., VOGT, K., GERLOF, K., SOLLWEDEL, A., VOLK, H.-D., RITTER, T. & ZENCLUSSEN, A. C. 2006. Over-expression of heme oxygenase-1 by adenoviral gene transfer improves pregnancy outcome in a murine model of abortion. *Journal of Reproductive Immunology,* 69**,** 35-52.

ZENCLUSSEN, M. L., CASALIS, P. A., EL-MOUSLEH, T., REBELO, S., LANGWISCH, S., LINZKE, N., VOLK, H. D., FEST, S., SOARES, M. P. & ZENCLUSSEN, A. C. 2011. Haem oxygenase-1 dictates intrauterine fetal survival in mice via carbon monoxide. *J Pathol,* 225**,** 293-304.

ZENCLUSSEN, M. L., JENSEN, F., REBELO, S., EL-MOUSLEH, T., CASALIS, P. A. & ZENCLUSSEN, A. C. 2012. Heme oxygenase-1 expression in the ovary dictates a proper oocyte ovulation, fertilization, and corpora lutea maintenance. *Am J Reprod Immunol,* 67**,** 376-82.

ZENCLUSSEN, M. L., LINZKE, N., SCHUMACHER, A., FEST, S., MEYER, N., CASALIS, P. A. & ZENCLUSSEN, A. C. 2014. Heme oxygenase-1 is critically involved in placentation, spiral artery remodeling, and blood pressure regulation during murine pregnancy. *Front Pharmacol,* 5**,** 291.

ZENG, Y. & CULLEN, B. R. 2004. Structural requirements for pre-microRNA binding and nuclear export by Exportin 5. *Nucleic Acids Res,* 32**,** 4776-85.

ZHANG, B., CHENG, G., ZHENG, M., HAN, J., WANG, B., LI, M., CHEN, J., XIAO, T., ZHANG, J., CAI, L., LI, S. & FAN, X. 2018a. Targeted delivery of doxorubicin by CSA-binding nanoparticles for choriocarcinoma treatment. *Drug delivery,* 25**,** 461-471.

ZHANG, B., LIANG, R., ZHENG, M., CAI, L. & FAN, X. 2019. Surface-Functionalized Nanoparticles as Efficient Tools in Targeted Therapy of Pregnancy Complications. *International journal of molecular sciences,* 20**,** 3642.

ZHANG, B., TAN, L., YU, Y., WANG, B., CHEN, Z., HAN, J., LI, M., CHEN, J., XIAO, T., AMBATI, B. K., CAI, L., YANG, Q., NAYAK, N. R., ZHANG, J. & FAN, X. 2018b. Placenta-specific drug delivery by trophoblast-targeted nanoparticles in mice. *Theranostics,* 8**,** 2765-2781.

ZHANG, C. 2008. MicroRNomics: a newly emerging approach for disease biology. *Physiol Genomics,* 33**,** 139-47.

ZHANG, D., WANG, G., HAN, D., ZHANG, Y., XU, J., LU, J., LI, S., XIE, X., LIU, L., DONG, L. & LI, M. 2014. Activation of PPAR-γ ameliorates pulmonary arterial hypertension via inducing heme oxygenase-1 and p21WAF1: An in vivo study in rats. *Life Sciences,* 98**,** 39-43.

ZHANG, J., HU, J., CHAN, H. F., SKIBBA, M., LIANG, G. & CHEN, M. 2016a. iRGD decorated lipid-polymer hybrid nanoparticles for targeted co-delivery of doxorubicin and sorafenib to enhance anti-hepatocellular carcinoma efficacy. *Nanomedicine: Nanotechnology, Biology and Medicine,* 12**,** 1303-1311.

ZHANG, Q., RAN, R., ZHANG, L., LIU, Y., MEI, L., ZHANG, Z., GAO, H. & HE, Q. 2015. Simultaneous delivery of therapeutic antagomirs with paclitaxel for the management of metastatic tumors by a pH-responsive anti-microbial peptide-mediated liposomal delivery system. *J Control Release,* 197**,** 208-18.

ZHANG, X., LI, Y., CHEN, Y. E., CHEN, J. & MA, P. X. 2016b. Cell-free 3D scaffold with two-stage delivery of miRNA-26a to regenerate critical-sized bone defects. *Nature Communications,* 7**,** 10376.

ZHANG, Y., DIAO, Z., SU, L., SUN, H., LI, R., CUI, H. & HU, Y. 2010. MicroRNA-155 contributes to preeclampsia by down-regulating CYR61. *Am J Obstet Gynecol,* 202**,** 466.e1-7.

ZHANG, Y., FEI, M., XUE, G., ZHOU, Q., JIA, Y., LI, L., XIN, H. & SUN, S. 2012. Elevated levels of hypoxia-inducible microRNA-210 in pre-eclampsia: new insights into molecular mechanisms for the disease. *Journal of cellular and molecular medicine,* 16**,** 249-259.

ZHANG, Y., WANG, Z. & GEMEINHART, R. A. 2013. Progress in microRNA delivery. *Journal of Controlled Release,* 172**,** 962-974.

ZHAO, H., AZUMA, J., KALISH, F., WONG, R. J. & STEVENSON, D. K. 2011a. Maternal heme oxygenase 1 regulates placental vasculature development via angiogenic factors in mice. *Biology of reproduction,* 85**,** 1005-1012.

ZHAO, H., WONG, R. J., KALISH, F. S., NAYAK, N. R. & STEVENSON, D. K. 2009. Effect of heme oxygenase-1 deficiency on placental development. *Placenta,* 30**,** 861-8.

ZHAO, L., BRACKEN, M. B. & DEWAN, A. T. 2013. Genome-wide association study of pre-eclampsia detects novel maternal single nucleotide polymorphisms and copy-number variants in subsets of the Hyperglycemia and Adverse Pregnancy Outcome (HAPO) study cohort. *Annals of human genetics,* 77**,** 277-287.

ZHAO, X., HO, D., GAO, S., HONG, C., VATNER, D. E. & VATNER, S. F. 2011b. Arterial Pressure Monitoring in Mice. *Current Protocols in Mouse Biology,* 1**,** 105-122.

ZHAO, Y. & HUANG, L. 2014. Lipid nanoparticles for gene delivery. *Advances in genetics.* Elsevier.

ZHONG, Y., ZHU, F. & DING, Y. 2019. Differential microRNA expression profile in the plasma of preeclampsia and normal pregnancies. *Exp Ther Med,* 18**,** 826-832.

ZHOU, C., ZOU, Q. Y., LI, H., WANG, R. F., LIU, A. X., MAGNESS, R. R. & ZHENG, J. 2017. Preeclampsia Downregulates MicroRNAs in Fetal Endothelial Cells: Roles of miR-29a/c-3p in Endothelial Function. *J Clin Endocrinol Metab,* 102**,** 3470-3479.

ZHOU, F., JIA, X. L., YANG, Q. M., YANG, Y., ZHAO, Y. H., FAN, Y. B. & YUAN, X. Y. 2016. Targeted delivery of microRNA-126 to vascular endothelial cells via REDV peptide modified PEG-trimethyl chitosan. *Biomaterials Science,* 4**,** 849-856.

ZHOU, Y., DAMSKY, C. H., CHIU, K., ROBERTS, J. M. & FISHER, S. J. 1993. Preeclampsia is associated with abnormal expression of adhesion molecules by invasive cytotrophoblasts. *Journal of Clinical Investigation,* 91**,** 950-960.

ZHOU, Y., DAMSKY, C. H. & FISHER, S. J. 1997a. Preeclampsia is associated with failure of human cytotrophoblasts to mimic a vascular adhesion phenotype. One cause

of defective endovascular invasion in this syndrome? *The Journal of Clinical Investigation,* 99**,** 2152-2164.

ZHOU, Y., FISHER, S. J., JANATPOUR, M., GENBACEV, O., DEJANA, E., WHEELOCK, M. & DAMSKY, C. H. 1997b. Human cytotrophoblasts adopt a vascular phenotype as they differentiate. A strategy for successful endovascular invasion? *The Journal of Clinical Investigation,* 99**,** 2139-2151.

ZHU, X.-M., HAN, T., SARGENT, I. L., YIN, G.-W. & YAO, Y.-Q. 2009a. Differential expression profile of microRNAs in human placentas from preeclamptic pregnancies vs normal pregnancies. *American Journal of Obstetrics and Gynecology,* 200**,** 661.e1-661.e7.

ZHU, X. M., HAN, T., SARGENT, I. L., YIN, G. W. & YAO, Y. Q. 2009b. Differential expression profile of microRNAs in human placentas from preeclamptic pregnancies vs normal pregnancies. *Am J Obstet Gynecol,* 200**,** 661 e1-7.

ZLATEV, I., CASTORENO, A., BROWN, C. R., QIN, J., WALDRON, S., SCHLEGEL, M. K., DEGAONKAR, R., SHULGA-MORSKAYA, S., XU, H., GUPTA, S., MATSUDA, S., AKINC, A., RAJEEV, K. G., MANOHARAN, M., MAIER, M. A. & JADHAV, V. 2018. Reversal of siRNA-mediated gene silencing in vivo. *Nat Biotechnol,* 36**,** 509-511.

Published articles

[Full text of the two articles below has been redacted for copyright reasons]

Badarau, Eduard, Wang, Zhuo, Rathbone, Dan L., Costanzi, Andrea, Thibault, Thomas, Murdoch, Colin E., El Alaoui, Said, Bartkeviciute, Milda and Griffin, Martin (2015). Development of potent and selective tissue transglutaminase inhibitors:their effect on TG2 function and application in pathological conditions. Chemistry and Biology, 22 (10), pp. 1347-1361.
https://doi.org/10.1016/j.chembiol.2015.08.013

Murdoch, Colin E., Broadway-Stringer, Sophie A., Bartkeviciute, Milda, Siciliano, Camilla, Altobelli, Roberta and de Falco, Elena (2014). Stem cell therapies for ischemic cardiovascular diseases. Recent patents on regenerative medicine, 4 (3), pp. 149-167.
https://doi.org/10.2174/2210296504666141016214824